Spring 6-9-2023

LIGNOCELLULOSE CONVERSION VIA CONSOLIDATED BIOPROCESSING: HIGH SOLID LOADINGS, BIOREACTOR DEVELOPMENT, AND TECHNOECONOMIC ANALYSIS

Matthew R. Kubis
matthew.r.kubis.th@dartmouth.edu

LIGNOCELLULOSE CONVERSION VIA CONSOLIDATED BIOPROCESSING: HIGH SOLID LOADINGS, BIOREACTOR DEVELOPMENT, AND TECHNOECONOMIC ANALYSIS

A Thesis
Submitted to the Faculty
in partial fulfillment of the requirements for the

Doctor of Philosophy

in

Engineering Sciences

by Matthew R. Kubis

Thayer School of Engineering
Guarini School of Graduate and Advanced Studies
Dartmouth College
Hanover, New Hampshire

May 9th, 2023

Examining Committee:

Chair_____
Dr. Lee R. Lynd

Member_____
Dr. Evert K. Holwerda

Member_____
Dr. Mark S. Laser

Member_____
Dr. Tom L. Richard

Member_____
Dr. Daniel L. Sanchez

_____
F. Jon Kull, Ph.D.
Dean of the Guarini School of Graduate and Advanced Studies

(BLANK PAGE)

ABSTRACT

Efficient deconstruction and conversion of inedible plant biomass, i.e., lignocellulose, is critical to decarbonizing the energy system in order to meet climate stabilization objectives. However, lignocellulose biomass is recalcitrant to deconstruction, and is often augmented by energy and capital-intensive thermochemical pretreatment. Alternatively, *Clostridium thermocellum* is a thermophilic anaerobe capable of both deconstruction and conversion of lignocellulose without pretreatment. This thesis seeks to inform the deployment of cellulosic ethanol production by furthering our understanding of *C. thermocellum* mediated deconstruction, especially at industrially relevant conditions, i.e., solid loadings exceeding 100 g/L. In batch fermentations, it was observed that fractional deconstruction declines as solid loadings increase, which prompted diagnostic experiments and the inclusion of a second bacterium, *Thermoanaerobacterium thermosaccharolyticum*, to improve deconstruction. Ultimately, the bioreactors used to characterize this were unsuitable for work above 100 g/L, which necessitated a novel bioreactor system capable of high solids, semi-continuous fermentations. To our knowledge, this first-of-its-kind bioreactor will enable lab-scale characterization of lignocellulose deconstruction at high solid loadings not yet reported in literature. Lastly, a technoeconomic analysis adds another component to the thesis describing project economics and relative greenhouse gas (GHG) emissions for a 60-million gallon per year biorefinery. The impact of adopting emerging technologies such as carbon capture and storage (CCS) and biogas upgrading were evaluated in this context. Results indicate there are significant, i.e., up to 8-fold improvement, in net GHG benefits by adopting this approach, while simultaneously improving project economics.

Preface

To all those who have supported me throughout my time in the Lynd Lab, Dartmouth, and New England- I am forever grateful. As I navigated graduate school (and my mid-twenties), I have learned so much and appreciate all those who enabled this experience.

I am grateful for my mentors, Evert Holwerda and Lee Lynd. Evert, you provided the day-to-day mentorship that steadied my graduate studies. I have immense respect for you as a scientist, a mentor, and a friend, and simply cannot thank you enough. Lee, you have given me countless opportunities to succeed, and I will always appreciate your willingness to help your students grow and try new things. I have seen the Lynd Lab grow significantly over the past five years, and am truly impressed by your resolve to make cellulosic ethanol work. And to my many colleagues from the Lynd Lab, you all were essential for completing my studies and I want to thank you for keeping such an accommodating and friendly workspace.

Many thanks to the Thayer staff, in particular Mike West, David McDevitt, Scott Walker, and Gary "Hutch" Hutchins, who gave me the flexibility I needed to complete my research. Mark Laser, thank you for your patience, advice, positive reinforcement, and a being a great teacher. And thank you to Tom Richard and Daniel Sanchez for their helpful discussions and serving as my thesis committee.

A special thanks to my fellow graduate students, and to all my friends, both here and in Tennessee. There would be no doctoral thesis without you. You have kept me healthy and sane, no easy feat, I'm sure.

And to my family, especially my parents, thank you for all your support while I got to go to school for five more years. Their patience and support are unyielding, and I am truly fortunate to have them. Lastly, a special thanks to my family in Connecticut, especially my grandparents.

Table of Contents

List of Tables

List of Illustrations

1. Introduction

Climate change remains a defining challenge of our time and advancing bioenergy deployment is desirable in light of climate stabilization objectives to limit global warming to 2˚C by the end of the century (1,2). Biomass energy systems are a logical starting point for decarbonizing the transport sector as they cycle carbon between fuel combustion reactions and plant photosynthesis, effectively giving rise to the carbon-neutrality of biofuels (3). Another important contribution of biomass energy systems is the synergistic opportunity for carbon dioxide removal (CDR). Biomass energy with carbon capture and storage (BECCS) could enable large, negative emissions by drawing out carbon from the atmosphere via photosynthesis, processing biomass into useful fuels, chemicals, or electricity, and routing stationary carbon dioxide emissions towards permanent geologic sequestration (4–7). In time, it is within reason that the value of biomass energy systems for photosynthetic carbon removal may exceed that for displaced fossil fuels (8,9). Yet, 2nd generation biofuels, those made from inedible feedstocks, have fallen short of production expectations (10), and could risk forfeiting potential climate change mitigation if not realized. This thesis seeks to advance 2nd generation biofuel production technology by investigating feedstock deconstruction and conversion via *Clostridium thermocellum*-mediated consolidated bioprocessing (CBP) towards industrially relevant substrate loadings. In addition to wet-lab experiments, process design, simulation, and technoeconomics were also used to determine the cost and greenhouse gas (GHG) mitigation potential of a prospective cellulosic ethanol biorefinery including CDR at industrial scale.

The production of liquid biofuels from renewable biomass feedstocks has been an active area of research over the past several decades. In the United States, the first-generation (1G) approach towards biofuels primarily sought to convert corn kernels, a starch-based feedstock, into ethanol for gasoline fuel blending. Among biologically derived fuel molecules, ethanol distinctively combines useful features including high yield and titer, ease of separation, and can be used as a fuel by itself, blended, or serve as an intermediate for synthesis of other hydrocarbon fuels (11–13). Although starch is readily digestible, and conversion efficiencies are high, 1G liquid biofuels have struggled to provide satisfactory GHG emission reductions

(relative to petroleum gasoline) with often cited reasons being land intensification and displaced food production related to indirect land use change (14). Use of inedible cellulosic biomass, i.e., second-generation biofuels, is generally recognized as a priority in light of large potential supply (15,16), decreased competition for food resources, and lower GHG emissions compared to other edible biomass feedstocks (14,17–19).

Despite these advantages, cellulosic (or advanced) second-generation (2G) ethanol production continues to not meet production quotas set by the United State Renewable Fuel Standard by wide margins (> 95%) (10) largely due to cost inefficiency (20,21). Indeed, the technological challenges facing 2G biofuel production are steep considering that lignocellulose is a heterologous matrix consisting of insoluble cellulose, hemicellulose, and lignin, and deconstructing these components into usable substrates is naturally difficult as they natively evolved to avoid biological degradation (22–24). The most common practice to overcome this "recalcitrance barrier" is combining thermochemical pretreatment and free enzymes (e.g., fungal cellulases) to hydrolyze the carbohydrates before fermentation can occur (20,25–28). This processing paradigm has been extensively reported throughout the literature in a variety of configurations but remains cost-prohibitive largely in part to the energy and chemicals associated with pretreatment and enzyme production (20,21,29,30).

Alternatives to this processing paradigm continue to be research and developed, for instance, consolidated bioprocessing with cotreatment (C-CBP) wherein both biomass deconstruction and fermentation occur simultaneously, and without the need for thermochemical pretreatments (21,31,32). Anaerobic, thermophilic bacterium *Clostridium thermocellum* is one candidate microbe capable of solubilizing and utilizing carbohydrates from unpretreated lignocellulose (33). However, unpretreated feedstock presents challenges for handling and conversion at industrially relevant solid loadings and fractional carbohydrate solubilization remains less understood (34,35). Ultimately, high solids are required for economic recovery of ethanol to reduce fermenter capital investment and lower the energy demand for distillation depends largely on ethanol titer. In order to generate ethanol titers sufficiently high (4-6% w/w), the substrate needs

to be loaded in adequate quantity, which after accounting for carbohydrate content, is on the order of 15-20% total solids (20,36–40).

In this thesis, work was undertaken to document fractional carbohydrate solubilization at increasing solid loadings up to the limit of a conventional batch bioreactor (chapter 4), at which point a custom bioreactor was designed to further enable laboratory exploration of high solids (chapter 5). In the final chapter (6), technoeconomic analysis was used to investigate C-CBP economics pursuant to improving energy efficiency and enabling CDR. A general overview of background and literature relevant to this work is presented in the following chapter.

2. Background and Literature

2.1 Biomass Energy Systems

Plant biomass is the most abundant carbon store in the terrestrial biosphere and has long been utilized by humans as a convenient energy carrier (16). Biomass energy systems are broadly divided into two camps: traditional and non-traditional. Traditional biomass energy systems refer to the energy released via combustion of biomass in forms of wood, animal waste, charcoal, etc. while non-traditional biomass energy systems require some transformation of the biomass into useful fuels and chemicals like bioethanol, biomethane, or woody pellets before combustion occurs (41). Generally, non-traditional biomass energy systems play a key role in the decarbonization of transport and energy sectors in light of climate stabilization objectives (1,42,43). This thesis focuses exclusively on non-traditional biomass energy systems, with a primary focus on 2nd generation cellulosic ethanol.

2.2 Lignocellulose

Utilizing inedible lignocellulosic feedstocks is the major distinction between first- and second-generation biofuels, so the chemical composition and structure of lignocellulose plays a central role in realizing biofuel production. Lignocellulose is composed of several energy-rich biopolymers that are arranged into a hierarchical structure (24) that is insoluble in water and predominantly comprised of three major components: cellulose, hemicellulose, and lignin (28,30,44). The largest proportion (approximately 30-50%) is cellulose- a straight-chain homopolysaccharide made up of β-D-glucopyranosyl units linked by β-(1-4) glycosidic bonds with cellobiose as the repeating unit (28). This type of linkage contrasts with the more-easily cleaved α-(1-4) glycosidic linkages present in starch (i.e., 1G corn ethanol) and requires specific enzymatic (i.e., cellulolytic) activity to cleave into soluble oligomers (24,45). Cellulose biopolymers directionally organize into larger, longer microfibrils (18-24 chains) that can be highly compact, crystalline, and insoluble conferring plant biomass resistance to chemical and biological hydrolysis not witnessed in 1G biofuels (23,45,46). Hemicelluloses are the second largest proportion (20-

40%) of plant biomass and are classified according to the main sugar in the backbone of the polymer, e.g. xylan (β-1,4-linked xylose) or mannan (β-1,4-linked mannose) (36,47). Compared to cellulose, hemicellulose has shorter polysaccharide chains, a higher tendency for sidechains and branching, and greater carbohydrate diversity (28,47–49). Besides xylose or mannose, hemicelluloses may contain other pentoses, hexoses, and sugar acids, and those from different sources, such as grasses, cereals, softwood, hardwood, will differ in composition and linkages (47,48). Lastly, lignin is a class of organic compounds derived from phenolic precursors and is not considered carbohydrate. Lignin usually makes up 10-20% of plant biomass and together with hemicellulose covalently binds the cellulose microfibrils in place to lend stability to the plant cell wall (28). Lignin is resistant to biological degradation under anaerobic conditions, so the carbohydrates within cellulose and hemicellulose are the target substrates for ethanol fermentation. However, lignin can act as a physical barrier to prevent enzyme access and nonproductive enzymatic binding to lignin has been reported (50). Taken together, the physiochemical nature of cellulose, hemicellulose, and lignin confers a recalcitrance to lignocellulose not seen in 1G biofuel feedstocks and has remained a technological challenge for cost-effective second-generation biofuels (20,21,23,30,51).

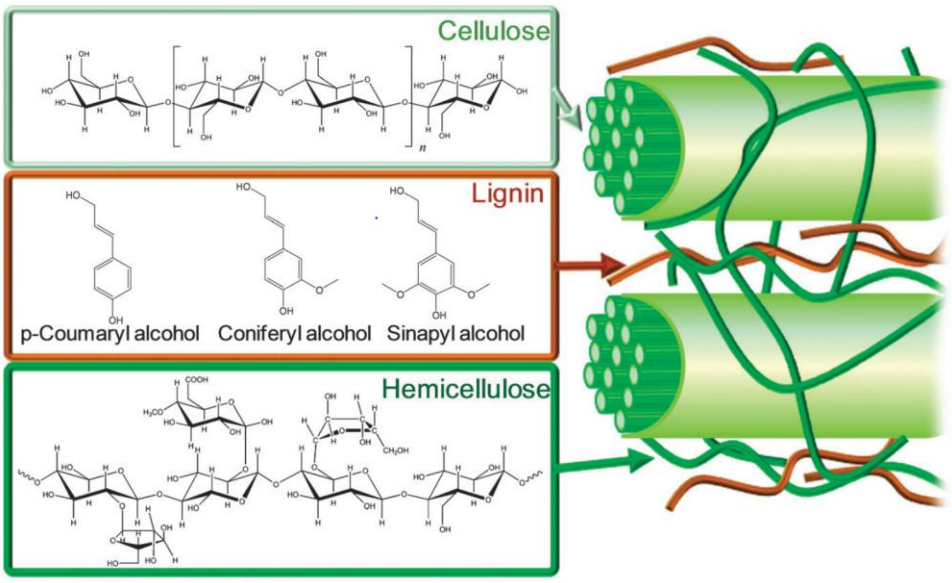

Figure 1. Compositional schematic of lignocellulose. Figure reproduced from Alonso et al. (2012) (44).

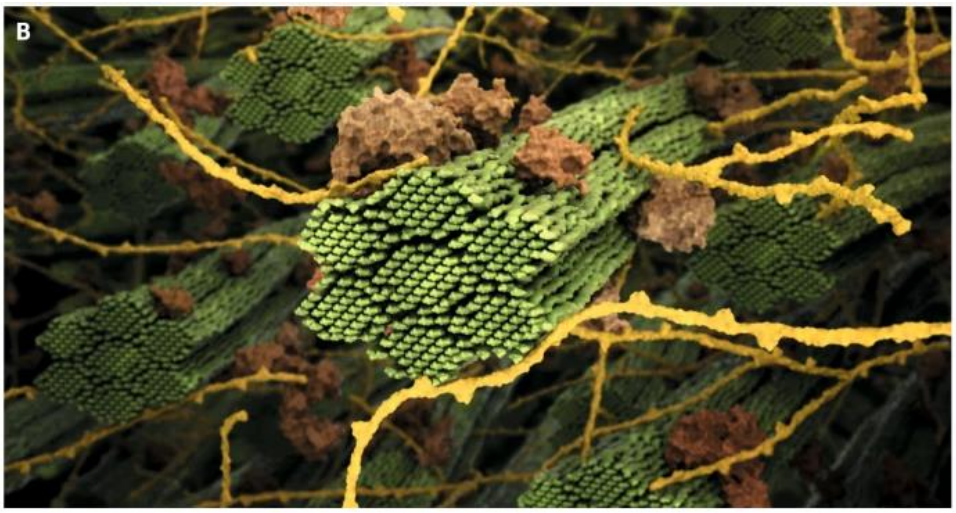

Figure 2. Illustration of lignocellulose. Figure reproduced from Petridis and Smith (2018) (46)

Water is a key factor in the processing of lignocellulose slurries as it functions as a reactant for the hydrolytic cleavage of glycosidic bonds as well as the reaction medium. Cellulose, despite having many hydroxyl groups, remains completely insoluble in water below 300˚C due to molecular-level interactions and thermodynamics related to hydrogen bonding, hydrophobicity, and entropy (46,52). In contrast, short-chain carbohydrate oligomers and monomers resulting from cellulose hydrolysis are typically soluble in water. This phenomenon gives rise to the term "carbohydrate solubilization," effectively referring to a solid-liquid phase transition for carbohydrates that occurs during lignocellulose deconstruction. For biological conversion systems, carbohydrates must be soluble in order for intracellular transport (uptake) and conversion (utilization) to occur. Because carbohydrate solubilization precedes uptake and utilization, it is a well-known bottleneck in the conversion to fuels and chemicals. The extent of carbohydrate solubilization, in addition to ethanol production, is a key performance metric for 2G biofuel production and a primary focus of this thesis. Fractional carbohydrate solubilization (FCS) ranges between 0 and 1 and can be expressed where m_c is the mass of insoluble carbohydrate present at either the beginning (t_0) or end (t_{final}) of a fermentation:

$$FCS = 1 - \frac{m_c(t_{final})}{m_c(t_0)}$$

Solid loading is a key parameter in 2G biofuel production, as biomass slurries contain both a solid-feedstock fraction and a liquid/aqueous/water fraction that change as biomass deconstruction proceeds. The term solid loading often refers to the initial mass of solid substrate added to the process divided by the total mass or volume and is often expressed in g/L, % DM (dry matter), or % TS (total solids).

2.3 Alternative Lignocellulose Conversion Pathways

Biofuels can be generated as liquids, gases, and/or solids depending on the conversion process. Lignocellulose conversion can be achieved through a variety of thermochemical or biological pathways, either alone or in combination. Thermochemical processes use high temperature and pressure and/or chemical catalysts to convert lignocellulose to fuels and chemicals (44,53) whereas biological pathways use cells or cellular components requiring lower temperatures and pressures but longer reaction times (13,54,55). Comparative studies between various thermochemical pathways have been previously reported (56–60) as well as comparisons between thermochemical and biological pathways (61–66). Depending on modeling assumptions, the cost of biological pathways is lower (62,64,65) or similar (61,63,66) to thermochemical processing. Biological processing has the potential to benefit from emergent advances in the life sciences but is less technologically mature, and there is potential advantage in hybrid processes (12,13,67). The following discussion will elaborate primarily on biological pathways since they are the most relevant to this work.

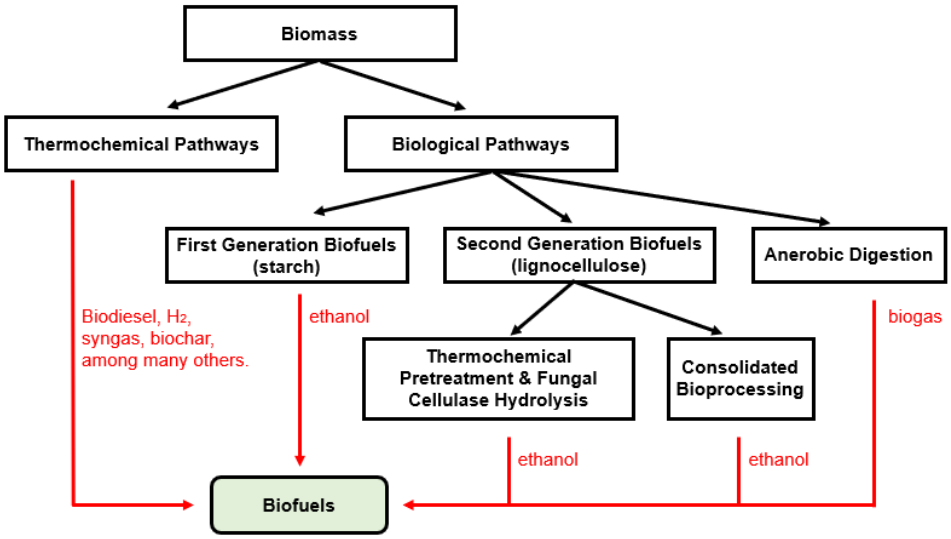

Figure 3. Simplified diagram of biomass to biofuel pathways. Note this figure was drafted to give a general overview of alternative pathways relevant to this thesis and is not considered exhaustive of all available pathways.

2.4 Biological Lignocellulose Conversion Pathways

Today, the most commonly studied process for biologically converting lignocellulose into liquid biofuel usually proceeds via 1) pretreatment, 2) hydrolysis, and 3) fermentation. Both pretreatment and hydrolysis seek to overcome biomass recalcitrance and have remained some of the most expensive unit operations in advanced (2G) biofuel production (20,29,61).

Lignocellulose has evolved to avoid deconstruction and is naturally recalcitrant towards enzymatic hydrolysis (23); hence, the need for pretreatment originally emerged (26,68). Physio-, Bio-, and thermochemical pretreatment techniques are performed to shed and/or alter lignin and hemicellulose fractions thereby making the biomass more amenable to downstream enzymatic hydrolysis (26,28,36,46). Many pretreatment techniques have been studied, including, but not limited to, acid or alkaline treatments, ammonia fiber expansion, steam explosion, mechanical grinding, and solvent extraction, among others (69–73), and comparative studies on enhancing hydrolysis have been previously reported (74–79). Thermochemical pretreatments can be costly with respect to capital investment, energy input, operational

costs, and environmental impacts (27,80–83), yet are often required for near-complete hydrolysis of lignocellulose biomass using free enzyme systems (51). However, the interactions between biomass and pretreatment are complex, and hydrolysis and fermentation inhibitors have also been reported for several biomass pretreatment techniques (28,46,77,84–87).

Hydrolysis, or solubilization, refers to the enzymatically-mediated chemical reaction responsible for cleaving long-chain carbohydrates into short-chain, soluble oligomers, and is catalyzed by a suite of carbohydrate active enzymes (CAZymes): a diverse category of enzymes that build and breakdown carbohydrates for many different biological roles (88). Commercially, high-level extracellular cellulase production by the ascomycete fungi *Trichoderma reesei* is the current gold standard for biofuel production, and enzymes are often delivered as blends composed of several functional classes (89–93). For example, *T. reesei* secretes Endo-β-(1,4)-glucanases, Exo-β-(1,4)-d-glucanases, and β-d-glucosidases in addition to hemicellulose-specific CAZymes, such as xylanases (45,94).

Fermenting hydrolysate is commonly accomplished using *Saccharomyces cerevisiae,* or brewer's yeast. Alternatively, ethanologenic bacteria of industrial interest include *Zymomonas mobilis* (95,96), *Thermoanaerobacterium saccharolyticum* (97,98), and *Escherichia coli* (96,99), among others. Native *S. cerevisiae* is a well-characterized facultative anaerobe, has high ethanol productivity and tolerance, and a large suite of genetic engineering tools (100–103). One potential drawback associated with *T. reesei* cellulase is that hydrolysis performs optimally between 45-50˚C (20,104), different from the optimal growth temperature of ethanologenic yeast (30-35 ˚C), and consequently, alternative process design configurations and biocatalysts have been studied to optimize parameters related to pretreatment, hydrolysis, and fermentation, e.g., separate hydrolysis and fermentation (SHF), simultaneous saccharification and fermentation (SSF), and Simultaneous Saccharification and co-fermentation (SSCF).

SHF allows process conditions (e.g., temperature and pH) to be optimized individually but leads to hydrolysis inhibition due to the accumulation of hydrolysate products. SSF utilizes hydrolysis products before they can accumulate but also requires a suitable process condition for both steps and may lead to

ethanol feedback inhibition (105). In comparative studies, SSF is found to be more energy efficient (106) and will outperform SHF in higher ethanol yields (39) and titers (107). Utilizing hemicellulose-derived carbohydrates is featured in many processes as it comprises about one-third of the total carbohydrate sugars in lignocellulose biomass (108) and thus improves ethanol yield per unit biomass. Hemicellulose utilization can either be a dedicated unit operation or combined with cellulose fermentation, in which case it is denoted as co-fermentation within SSCF. Utilizing both cellulose and hemicellulose is likely an economic prerequisite for large-scale production of ethanol from lignocellulose (106,109–111). Avoiding the accumulation of pentose sugars and oligomers is another important element of SSCF, as they have been known to cause deleterious effects on hydrolysis and fermentation (112–119).

Collectively, thermochemical pretreatment and added fungal cellulase featured prominently in pioneer cellulosic ethanol facilities, despite the eventual closing of many such ventures (21,30,120,121). A failure to sustain cost-effective cellulosic ethanol production (10) has motivated studying alternative bioprocesses without thermochemical pretreatment and added fungal cellulase-mediated hydrolysis, as these remain two of the largest cost factors in cellulosic ethanol production (20,21,29,30,61). With the exception of procuring feedstock, pretreatment is the single largest cost contributor to cellulosic ethanol production (20,61,122,123) followed by cellulase production costs (20,29,61,124,125), although cellulase costs are much higher in some reports (126). Operationally, fungal cellulases need to be produced onsite or purchased from a third-party for biomass hydrolysis in SHF and SSF (20,104), whereas consolidated bioprocessing (CBP) combines cellulase production, hydrolysis, and fermentation into a single vessel, eliminating a wide range of capital and operating costs (21). In nature, many organisms can synthesize and excrete cellulases to hydrolyze cellulose to support their growth and metabolism which CBP seeks to leverage using either pure or mixed culture conditions (32,33,90,104,127).

Although proof of concept for CBP has been firmly established, commercialization has been limited due to the low conversion efficiency of the technology (90). However, several cultures of thermophilic anaerobic bacteria, and in particular *Clostridium thermocellum* (128), are more effective at deconstructing

unpretreated cellulosic biomass than industry standard fungal cellulase under a broad range of conditions (21). As with SHF or SSF, thermochemically pretreating biomass prior to CBP enhances conversion efficiency (129–131) but requires additional energy and chemicals thereby increasing costs and life-cycle emissions. Milling during fermentation, i.e., consolidated bioprocessing with cotreatment (C-CBP), has been suggested as a substitute for thermochemical pretreatment (131–133). By eliminating both thermochemical pretreatment and enzymatic hydrolysis, C-CBP has the potential to significantly reduce the cost of overcoming plant recalcitrance (21).

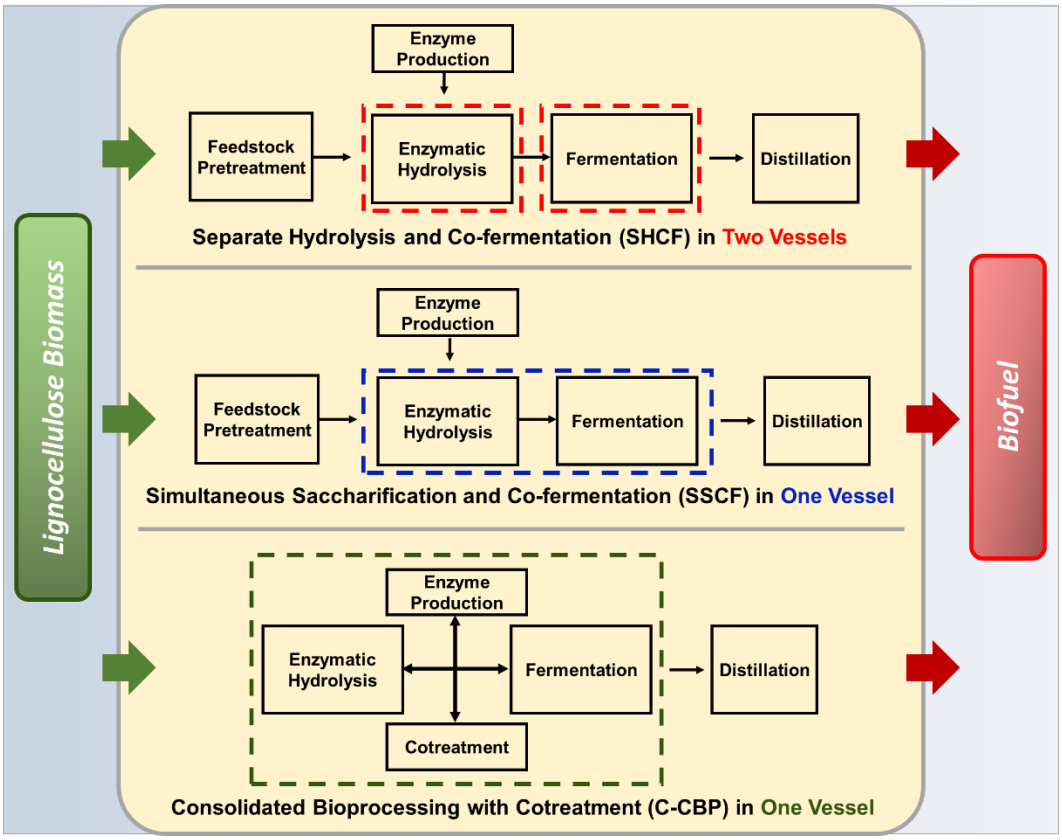

Figure 4. Lignocellulose biofuel production – alternative biological pathways.

2.5 Consolidated Bioprocessing with *Clostridium thermocellum*

A CBP approach requires biocatalysts capable of lignocellulose deconstruction and product formation, and both roles present technical challenges. An industrially relevant system would need to solubilize the majority (>85%) of carbohydrates at high solid loadings (>150 g/L) (20,37) in addition to converting solubilized sugars to ethanol at >90% of theoretical yield, a titer of at least 40 g/L, and a rate of production >1 g/L/h (134). These are reasonable targets but not hard requirements and thus can be traded off in some circumstances. However, currently, no natural microorganisms are fully capable of all attributes leading to considerable research in the last decade (90,127,134). The strategy to develop CBP biocatalysts usually proceeds according to one of two approaches: #1) The native cellulase strategy seeks to engineer cellulase produces to improve ethanol production, #2) the recombinant cellulase strategy seeks to engineer ethanologens to conger or improve cellulase production. As an alternative variant to the native strategy, consortia or defined cocultures have also been studied to divide the cellulolytic and ethanologenic responsibilities between two (or more) microorganisms (135,136).

To date, anaerobes have received the most attention as hosts pursuant to the native cellulase strategy and yeasts have most often been considered as hosts for the recombinant cellulase strategy (128). The type of cellulase envisioned for CBP is a distinguishing factor between various CBP systems, with cellulases generally categorized as free and monofunctional enzymes, free and multifunctional enzymes, or complex multiple-enzyme systems known as cellulosomes (45). Cellulosomes are larger, multi-protein complexes comprised of carbohydrate binding domains, catalytic domains, and noncatalytic scaffolding (32). Differences in enzymatic synergy, localization, and rates of hydrolysis have been reported between monofunctional, multifunctional, and cellulosomes (45,128). It has been reported that fungal cellulases and cellulosomes exhibit synergistic behavior attributed to varying modes of deconstruction enhancing substrate surface area availability (137,138). To date, a variety of microbial and fungal biocatalysts have been investigated for CBP, including *Bacillus subtilis* (139,140), *E. coli* (141), *Clostridium cellulolyticum*

(142–144), *Caldicellulosiruptor bescii* (145,146), *S. cerevisiae* (147), and *Z. mobilis* (148), among others (90,93,127).

Clostridium thermocellum (a.k.a. *Ruminiclostridium thermocellum, Hungateiclostridium thermocellum, Acetivibrio thermocellus*) is one of the leading candidates for CBP due to its remarkable solubilization efficiency compared to fungal cellulases (128,132) and native ability to produce ethanol, albeit at lower titers (134). As a thermophilic anaerobe, it also combines several desirable biocatalyst qualities including thermostable enzymes, lower contamination risk, lower cell yield, eliminated oxygen transfer costs, and facilitated ethanol recovery (32,33,134). *C. thermocellum* continues to be researched for improvement (149–153) regarding its ethanol tolerance, yield, titer, and productivity (154,155). *C. thermocellum's* cellulosome contains a diverse enzymatic suite and wide range of co-localized cellulase modalities (156,157), and is one of the most efficient cellulose degraders to date (128,132). Although the biomass deconstruction apparatus of native *C. thermocellum* equally solubilizes pentose-rich hemicellulose as well as cellulose, wild-type strains do not ferment pentose sugars (33,158,159). Recently, there has been some effort to genetically engineer a recombinant strain of *C. thermocellum* capable of hemicellulose utilization (159,160), while another approach seeks to co-culture this microbe alongside with pentose-fermenting microorganisms (161,162). On both microcrystalline cellulose and lignocellulose, enhanced substrate utilization and ethanol yield have long been reported for C. *thermocellum* cocultures with hemicellulose utilizing microbes (163,164). The *Thermoanaerobacter spp.* in particular has been studied for its innate abilities to produce comparatively high ethanol yields from hemicellulose fractions (161,165,166), and comparative studies with *Thermoanaerobacter spp.* have demonstrated enhanced product formation relative to *C. thermocellum* monocultures (165,167–170). There are also reports of possible effects related to hemicellulose for cultures of *C. thermocellum* and its cellulosome preparations (49,171), and hemicellulose utilizing cocultures have been linked to enhanced carbohydrate solubilization (48,49,172,173).

2.6 High Solid Loadings

The use of high solid loadings benefits the economics of lignocellulose conversion by decreasing both the capital and operating costs. Solid loadings on the order of 15% DM will be required in order to reach economical titers of ethanol, (4-6% w/v) prior to distillation (20,37–40) in addition decreasing fermenter investment. However, lignocellulose presents several handling challenges at high solid loadings due to its fibrous nature, high viscosity, and non-Newtonian flow characteristics related to particles that tend to be cohesive, entangled, and non-uniform in shape and size (174). Free water is a critical parameter in defining bioprocessing regimes, however, there is no firm boundary between submerged (excess free water) and solid-state (limited free water) as mixing is highly dependent on several feedstock characteristics including substrate, particle size, and pretreatment conditions (175–179). Generally, around 15% DM is considered a transitionary zone, and there are advantages and disadvantages related to operating in either processing regime (180,181). In a submerged system, the presence of excess free water increases mass and heat transfer and a homogenized broth, i.e., well-mixed, offers superior pH and temperature control. On the other hand, solid state fermentations are also of industrial interest, as diluting and mixing submerged systems require water and energy, though process control and product separation remain challenges for solid-state to overcome (182,183).

High solid loadings are understood to impede mass transfer and to increase viscosity, mixing energy, and potential inhibitors related to deconstruction (179). For lignocellulose conversion via fungal cellulase, a decrease in carbohydrate solubilization has been observed with increasing solid loadings (37,38,184–186). Kristensen et al., (2009) describe a roughly linear correlation from 5-30% solid loadings for fungal enzyme hydrolysis and review yield determining factors (38). No single factor describing this decrease was found, though there was a strong correlation between the decreasing adsorption and conversion between cellulose and cellulase. In these systems, several causative factors have also been reported including, but not limited to, the presence and/or accumulation of ethanol (85,105), glucose (105,187), cellobiose (105,187), xylan (112–116), xylose (117), xylo-oligomers (114,118,119), lignin (85,188), and inhibitors

related to thermochemical pretreatment (85,86). Only at very high solid loadings (>15-20%DM) do mass transfer limitations due to lack of free water begin to affect yield (38,184,185).

Among literature examples, a different trend is observed for undefined cultivations. Liang et al., 2018 documented fermentation of 30 g/L switchgrass using a thermophilic methanogenic mixed microbiome (i.e., non-sterile) and measured a decline in fractional carbohydrate from 0.711 to 0.538 as a result of shortened residence times (189). However, at constant residence times, Chirania et al., (2022) observed no decline in fractional carbohydrate solubilization by thermophilic and methanogenic microbiomes between 7.5 and 15% total solids on switchgrass (190). Several studies have investigated the impact of total solids on anaerobic digestion systems and have found no significant differences in the specific methane yield or volatile solid reduction between 1 and 15% total solids with a decrease at 20–30% total solids. At this condition, mass transfer limitations due to lack of free and/or organic overfeeding was also cited as possible explanations (191–196).

To date, most publications regarding *C. thermocellum* physiology use substrate concentrations <10 g/L (197,198). There are some exceptions at high substrate loadings, though these usually involve the model substrate, e.g., Avicel® PH105, a microcrystalline cellulose substrate containing negligible amounts of both lignin and hemicellulose. Argyros et al. (2011) fermented 92.2 g/L Avicel into 38.1 g/L ethanol by coculturing engineered strains of *C. thermocellum* with *Thermoanaerobacterium saccharolyticum* (199). Of note, *T. saccharolyticum* is a thermophilic, ethanologenic, hemicellulose-fermenting bacterium, but is not cellulolytic. So, while it will convert carbohydrates into ethanol, *C. thermocellum* remains responsible for all the cellulolytic enzymes and hydrolysis. Thompson and Trinh (2017) report approximately 80% utilization for 100 g/L cellulose loadings in batch fermentations (198). Holwerda et al., (2014) reported utilization of 93 g/L Avicel at 100 g/L loading in defined medium and monoculture *C. thermocellum* (197). These results held constant after genetic engineering attempts to enhance ethanol production with four different modified *C. thermocellum* strains retaining the ability to utilize >100 g/L cellulose at 120 g/L loadings reported in Holwerda et al., (2020) (153).

Only a handful of studies have characterized *C. thermocellum* mediated deconstruction at high substrate loadings of lignocellulose rather than model cellulose (34,35). In contrast to cellulose fermentations, a diminishing fraction of lignocellulose is solubilized as solid loadings increase. On switchgrass, Verbeke et al. (2017) observed a 1.72-fold decline in solubilization extent between 50 and 10 g/L and Shao et al., (2020) report a 1.31-fold decline between 92 and 9.2 g/L in mid-season switchgrass glucan solubilization (34,35).

Research pertaining to high solid loadings is inevitably limited by mixability concerns in standard, benchtop bioreactors, especially when operated in batch configuration. When there is limited free water, lignocellulose slurries behave more like a paste than a liquid, and sterilization, temperature, and pH become difficult to control. In addition to process control, mixing is essential for robust bioconversion of solids as it reduces sedimentation and increases interactions between biocatalysts and substrate (200,201). It follows that custom vessels intended to study high solids lignocellulose conversion are often designed to enhance mixability using various mechanical agitation strategies. For example, Jorgensen et al., (2007) employed free-falling mixing in a horizontal drum with paddlers for batch enzymatic hydrolysis or simultaneous saccharification and fermentation (SSF) for wheat straw up to 40% (w/w) (37). X. Zhang et al., (2009) used a peg-mixer to carry out high solids (up to 30% w/w) enzymatic hydrolysis batches and fermentations on pretreated pulp and poplar lignocellulose feedstocks (202). J. Zhang et al., (2009) explored custom-helical impeller designs for SSF of pretreated corn stover up to 30% (w/w) (203). Dasari et al., (2009) designed a scraped-surface horizontal bioreactor for batch enzymatic hydrolysis of pretreated corn stover up to 25% (w/w) (204). These studies report remarkably high solid loadings (20 to 40% w/w), hydrolysis yield (resulting in 158 g/L glucose in one scenario), ethanol titers (4.8 to 6.3% w/w) (38,202), and offer insight towards viscosity and agitation dynamics (203,204).

2.7 Semi-Continuous Processing

Semi-continuous is another configuration of interest to researchers seeking to take advantage of decreasing solids concentration and slurry viscosity as lignocellulose conversion proceeds (205). Continuous processing is characterized by constant adding and removing material from the process, whereas semi-continuous feeding does so at discrete time intervals and is easier to implement and without performance tradeoffs (206). Compared to batch configuration, semi-continuous feeding has several foreseeable advantages including:

A) Reduced viscosity: it has been previously reported that conversion processes such as pretreatment (176–178,207,208) and enzymatic hydrolysis (175) cause dramatic reductions in apparent viscosity in a process referred to as liquefaction, and a similar result was observed by Ghosh et al., (2018) for *C. thermocellum* mediated deconstruction and fermentation (209). Operationally, representative delivery of high solid slurry is far more challenging than removing fermentation broth, owing to this liquefaction.

B) Discharge of accumulating inhibitors: discharging potential inhibitors related to hydrolysis (114,119), or fermentation (105,210) could enable additional conversion.

C) Biocatalyst to substrate ratio: maintaining a stable level of biocatalyst at steady state may improve productivity, and the steady state concentration of solids observed by the biocatalysts will be less than in the influent feed (205).

Semi-continuous cultivations require transferring solid feedstock in and out of the reactor system which, operationally, is challenging to perform aseptically, especially when moving high-solid slurries. Semi-continuous mixed culture cultivation, e.g., anaerobic digestion, of lignocellulose has been investigated at both thermophilic (189,190) and mesophilic conditions (211–215), yet these studies are largely enabled by non-sterile processing. As is often the case in laboratory research, aseptic conditions are usually necessary to properly determine how a defined culture will perform under specific circumstances. However, papers

addressing high solids, semi-continuous, and sterile processing, are rare. South et al., (1993, 1994) used a fixed-volume piston sampler to intermittently feed a SSF reactor from a mixed-carboy using approximately 10% (w/w) of pretreated poplar and hardwood feedstocks (216,217). Fan et al., (2003) performed semi-continuous fermentations feeding 12% (w/w) paper sludge by slowly advancing a horizontal plug-flow towards a chopper such that it shears and falls into the fermentation vessel below (205). Notably, in both Fan et al., (2003) and South et al., (1993, 1994), the authors describe sterilizing the high solids feedstock by autoclaving their feed for >12 hours, in addition to the material being already pretreated (205,216,217). Different rheological properties exist between unpretreated and pretreated lignocellulose (178,207), and most novel high solid bioreactor designs can take advantage of upstream pretreatment to enhance sterility and alter the rheology of biomass (179,218,219). Still, considering the substantial cost factor associated with thermochemical pretreatment and added fungal cellulase (20,21,29,30,61,121) there is motivation to look beyond the industry standard for lignocellulose biofuel production. Meanwhile, CBP remains technologically immature, and additional research is necessary to inform development, especially at high solids loadings of lignocellulose substrates.

In 2021, a fixed-volume piston delivery system was developed in Galen Moynihan's Master Thesis (Lynd lab) to representative transferring of switchgrass (up to 15% TS) provided it was milled sufficiently (220). However, Galen's work did not extend to cultivating microorganisms. In this thesis, Chapter 5 describes the development and operation of a high solids reactor capable of defined biological characterization using high solid slurries in a semi-continuous configuration.

2.8 Technoeconomics of Cellulosic Ethanol

Technoeconomic analysis (TEA) is a method to evaluate the economic performance of a proposed manufacturing process or technology by leveraging elements of process design, equipment sizing, capital and operating cost estimation, and project financing. TEA features prominently within the chemical engineering discipline as it assesses profitability for novel processes or changes to existing processes. TEAs

often combine chemical process design simulations software (e.g., ASPEN PLUS, HYSYS, BioSTEAM) and economic spreadsheets to inform project economics.

For project economics, a minimum fuel selling price (MFSP) is a useful quantitative metric that reflects the levelized (per unit) cost of production. This is most often approached using a discounted cash flow return on investment analysis (DCFROI) which requires defining the project year, project lifespan, debt/equity financing ratio, depreciation schedule, taxes, and an internal rate of return. Economic estimates range in their level of detail and uncertainty, and it is not uncommon for an anticipated cost estimate to vary up to an order of magnitude in starting estimations and shrinking to +/- 10% by the time a detailed analysis is prepared (221,222). Speaking generally, most technoeconomic analyses in the academic literature are of proposed, novel, or burgeoning technologies, and thus entertain a high degree of uncertainty. Studies in literature are usually intended to explore feasibility and thus usually fall within +/- 30-50% of fully formalized estimate (221,222).

Early TEA studies studying biofuel production were primarily concerned with converting pretreated woody biomass via fungal cellulase and yeast fermentation (110,223–225). Since then, many iterations have been proposed to investigate various aspects of feedstocks, conversion pathways, coproducts, and scalability (27,80,226,227). Corn stover is a cellulosic feedstock that has holds particular value and attention in the United States due to preexisting availability. Corn stover is a residue of corn grain production consisting of stalks, cobs, and husks, one of the most abundant cellulosic biomass resources in the United States, and is projected to play a central role in emergent cellulosic biofuel deployment (15,20,227). Industrial-scale conversion of corn stover to ethanol via fermentation has been studied in a variety of configurations summarized in appendix table A.9. Many studies involve thermochemical dilute-acid pretreatment with added fungal cellulase, with widely cited studies by the National Renewable Energy Laboratory (NREL) providing detailed design and cost estimation (20,25,80,223,224). Humbird et al., 2011 is NREL's most recent technical report modeling cellulosic ethanol, which was adapted to pilot-scale tests in Tao et al.,

(2014), and an updated combination of these two studies is reflected in the 2022 GREET® pathway for estimating life cycle emissions from corn stover ethanol (228,229).

Regarding NREL technical reports, having culminated 15 years of research towards cellulosic ethanol, NREL is now focused on advancing technology for lignocellulose biomass to hydrocarbon fuels. First reported in 2013, Davis et al., simulated corn stover conversion using alkaline deacetylation before dilute acid pretreatment (DAP) followed by solid-liquid separation for aerobic conversion of hydrolysate into free fatty acids (230). In 2015, Chen et al., modeled deacetylation and mechanical disk refining (DMR) in lieu of DAP, and Davis et al., (2018) simulated DMR corn stover to hydrocarbons introducing catalytic upgrading of ethanol and lignin coproduct bioconversion while importing natural gas to compensate for lacking solids combustion (67,231,232).

Products other than biofuel, otherwise known as coproducts, are often produced in biofuel plants (233,234). For example, distillers' grains and solubles (DGS) originating from corn ethanol production is commonly sold as animal feed (235). For lignocellulose conversion, researchers have sought to leverage coproduct revenue to bolster the economics behind cellulosic ethanol production, e.g., renewable natural gas (236), succinic acid (237), hydrogen (238), pentanediols (239,240), adipic acid (241), furfural (65,242,243), xylitol (244), high-purity lignin (242), among others (245,246). Perhaps the most notable example being the coproduction of electricity, i.e., cogeneration or combined heat and power (CHP) (20,234,247). In the corn-stover-to-ethanol process design modeled by Humbird et al. (2011), all solid process residues and biogas are combusted onsite to generate steam for processing heat and electricity. Roughly two-thirds of the electricity generated onsite is consumed with the remaining one-third sold to the grid (20). In the intervening decade, it remains possible that the common assumption of solid process residues or biogas being combusted onsite for heat and electricity is based on outdated market conditions (236,248–250). Lastly, CO_2 originating from fermentation, biogas, or flue gas has recently emerged as a feasible coproduction strategy for permanent geologic sequestration, with assistance from government supports for carbon tax credits (251,252).

2.8.1 Carbon Capture and Storage

Among the thousands of climate stabilization scenarios aggregated by the IPCC, the level of carbon dioxide removal (CDR) changes depending on the extent of mitigation, but there remains extensive use of CDR in all scenarios meeting climate stabilization objectives to remain below 2˚C by the end of the century (1). According to the IPCC, CDR is "dominated by BECCS and sequestration on land, with relatively few scenarios using direct air capture with carbon storage (DACCS) and even less with enhanced weathering and other technologies" (1) (IPCC_AR6_WGIII, e-page 458). For climate stabilization pathways, the necessary scale of CDR needing to be realized is immense: a median cumulative reduction (between 2020-2100) on the order of 569 Gt CO_2eq. is required to likely remain below 2˚C by 2100 (1) (IPCC_AR6_WGIII, table 3.4, e-page 492).

In the United States, the potential for realizing value from carbon dioxide continues to gain momentum in light of continued government support and increased incentives (Internal Revenue Service Title 26 U.S. Code § section 45Q) (252–254). For liquid biofuel production, this is particularly relevant because CDR incentives can be stacked with renewable fuel incentives e.g., Renewable Fuel Standard (RFS) (10,255–257) and/or California's Low Carbon Fuel Standard (LCFS) (258–260). Thus, there is strong motivation for informing the deployment of CDR systems within the context of cellulosic ethanol production.

Historically, literature assessments of the GHG mitigation potential of cellulosic biofuels have primarily focused on displaced fossil fuel emissions rather than capturable CO_2 emissions, although in time the value of biomass energy systems for photosynthetic carbon removal may exceed that for fossil fuel displacement (8,9). Only more recently, studies have begun to leverage carbon capture and storage (CCS) to enable net negative emissions for GHG mitigation at the point of cellulose ethanol production (table 1) (66,236,261–263).

Study	Ref.	Year	Cellulosic Ethanol GHG Mitigation (g CO_2eq / MJ ethanol)		levelized cost of capture for high purity fermentation streams ($/Mg CO_2)
			No CCS	With CCS	
Yang et al.	(236)	2020	24	-111	22
Gefland et al.	(262)	2020	20.3	-98.0	52
Kim et al.	(261)	2020	67.2	-45.5	25-30
Geissler and Maravelias	(263)	2021	(23-26.4)	-22.6	34
Geissler and Maravelias	(74)	2022			24-33

Table 1. Estimated GHG mitigation of cellulosic ethanol facilities with carbon capture and storage.

It has been previously reported that CO_2 separation costs scale inversely to the CO_2 concentration in the target stream (264,265) and generally accounts for roughly 60-80% of the total levelized cost. Comprehensive reviews of the levelized cost of capture across various industries have been compiled (264,266–268), and highlight ethanol fermentation as a high-purity low-cost CO_2 source (267,269). The economic feasibility of CCS is often determined weighing the incentive available, e.g., $85/ton per 45Q, against the total levelized cost of capture and geologic storage (253). This requires accounting for the entire carbon storage supply chain which generally consists of 1) purification, 2) compression, 3) transport, 4) injection, and 5) monitoring. Annualized capital and operating costs are determined for each step and compiled into a single levelized estimate often in units $ per ton (or Mg) CO_2. Collectively, the total levelized cost of sequestration for high-purity and dilute flue gas sources are generally around $30-50 and $70−$120/ton CO_2, respectively (66,236,263,264,266,267,269).

2.8.2 Anaerobic Digestion and Renewable Natural Gas

Anaerobic digestion converts organic materials into biogas, a 50/50 (v/v) gaseous mixture of CH_4 and CO_2, and has received considerable attention as a biomass energy system in several applications including landfill, municipal solid waste (MSW), wastewater treatment (WWT), and agriculture (270–272). Anaerobic digestion is featured in many TEAs studying cellulosic biofuel production in order to realize value from remaining organic material in distillation stillage (20).

Biogas can be used as a fuel, usually after desulphurization (273), for heat and/or power generation either to be used onsite or exported to the grid. Turbines are the most common biogas conversion technology and operate similarly to their natural gas turbine counterparts except for the presence of CO_2 in the fuel stream (274). Comparing gas and biogas turbines, it has been previously reported that biogas turbines demonstrate higher heat recovery and turbine efficiency, but overall lower net efficiency due to power requirements in fuel compression. However, the net power output is nearly constant regardless of fuel composition after accounting for fuel compression and overall performance is not expected to differ significantly (275,276).

Alternatively, biomethane can be purified, commonly referred to as biogas upgrading, into renewable natural gas (RNG). This is often done to increase energy content, improve fuel characteristics, and to become compatible with existing natural gas equipment (277). Furthermore, purified carbon dioxide, resulting from biogas upgrading, would enable additional CCS deployment. For CO_2 separation technology, biogas represents an intermediate target (~50%) between fermentation off gas (>99%) and dilute post-combustion flue gas sources (<15%) (278). Direct methanation of biogas-CO_2 into CH_4 also being studied but is generally outside the scope of this thesis (279–282). RNG applications are generally categorized as either a substitute for conventional heating and cooking natural gas applications, gas-to-power, or vehicle fuel (236,270,271,283–285).

In gas-to-power applications, RNG has been suggested as a possible energy storage tool to offset fluctuations in weather-based (i.e., wind and solar) renewable electricity generation (286,287). In vehicle fuel applications, both light-duty and heavy-duty natural gas vehicles (NGVs) are a topic of continued research (283–285,288–291), most often with applications in the public transport sector (292) and with generally limited deployment worldwide (<1% of vehicles) (285). In the United States, RNG used for transportation fuel is incentivized by the RFS cellulosic biofuel credits (D3 RIN) (https://www.epa.gov/renewable-fuel-standard-program/approved-pathways-renewable-fuel) and possibly California's LCFS (270,271). Although the market-pull for RNG transportation fuel is limited in California

where RNG gross potential is greater than 5 times that currently being used notwithstanding potential contributions from other states' markets (271).

Today, biogas upgrading is a popular, well-developed, and commercially available technology (293). Several alternative processes are available to separate biogas, including water scrubbing, organic solvents, absorption (MEA), adsorption (PSA), membrane separation, and cryogenic distillation (293–296). The advantages and disadvantages of each system are considered in light of operational parameters such as the quality of incoming gas, separation efficiency, technological maturity, investment and operating costs, energy demand, consumables, RNG and CO_2 purity, recovery and losses, and environmental sustainability (297). Membrane based separation (298,299) is an attractive technology due to its high CH_4 recovery and low or no heat and chemical requirements, although drawbacks include comparatively higher capital costs and power demand (293–296). Today, membrane separation is becoming increasingly utilized compared to its alternatives (297,300,301), and is prominently featured in process design simulations evaluated in chapter 6.

3. Motivation and Objectives

In order to advance cellulosic ethanol deployment, technological innovations will be necessary to enable cost-effective production. Lignocellulose is widely available and cost competitive with petroleum on a $/GJ basis (21,31), although, its recalcitrant nature has led to thermochemical pretreatment and added fungal cellulase as the dominant processing paradigm. Despite many successes in researching and developing this approach, experience with commercial-scale cellulosic ethanol over the past decade suggests this paradigm is operationally problematic and cost prohibitive (10,21,120). In the US, there is a need for technological innovation if cellulosic ethanol is to ever become commercially deployable.

As an alternative, the Lynd Lab has proposed a C-CBP approach, mediated by *C. thermocellum*, which has several intrinsic advantages but remains technologically immature and today an object of study in the lab. Both high solids and continuous processing are characteristics found in industrial settings, but rarely in

laboratory settings investigating CBP. This thesis seeks to bridge this divide by documenting, characterizing, and enabling industrially relevant conditions for defined and controlled fermentations of *C. thermocellum* and cocultivation with a hemicellulose utilizing bacterium. Particular focus was given to the fraction of carbohydrates solubilized as a key performance metric. This was first carried out using conventional benchtop bioreactors in Chapter 4 and extended using a custom bioreactor described in Chapter 5.

This thesis coincided with two notable items which had an outsized influence on research objectives. First, measures related to the Coronavirus-19 pandemic encouraged modeling and simulation-based research in lieu of wet lab research. Second, continued awareness regarding carbon emissions has increased the social cost of carbon and incentivized its capture. For example, the US 45Q tax credit for sequestering CO_2 has increased 3-fold ($28 to $85/ton) since my graduate studies began in 2018 (252), in addition to continued renewable fuel supports, e.g., the RFS and LCFS. Taken together, there was motivation to undertake technoeconomic and GHG mitigation studies regarding liquid biofuel production via C-CBP especially as it pertains to carbon dioxide removal. Enhancing heat integration, alongside biogas upgrading and gas turbine simulation were also design targets for a revised C-CBP technoeconomic analysis in Chapter 6.

The specific objectives of this thesis are:

1) To Inform and Enable High Solid Loading fermentations

- Using batch cultures in conventional equipment, characterize solubilization performance and its potential effectors at increasing solid loadings.
    - Published in Biotechnology for Biofuels and Bioproducts February 2022. https://doi.org/10.1186/s13068-022-02110-4.
- Demonstrate operability of a bioreactor capable of semi-continuous, high solids, with defined cultures and validate performance.
    - See manuscript template in chapter 5.

2) Inform cellulosic ethanol deployment via technoeconomic analysis of a revised, projected C-CBP 60-million-gallons-per-year facility.

- Update the C-CBP process simulation originally published in Lynd et al., (2017) (21), and improve overall energy efficiency via heat integration.
- Investigate the impact of adopting emerging technologies such carbon capture and storage, biogas upgrading, and electricity generation via gas turbines.
- Evaluate Minimum Ethanol Selling Prices and GHG mitigation potential of the revised scenarios.
    - Manuscript recently accepted for publication in Sustainable Energy and Fuels

4. Declining Carbohydrate Solubilization with Increasing Solids Loading During Fermentation of Cellulosic Feedstocks by *Clostridium thermocellum*: Documentation and Diagnostic Tests.

The main text is presented below in section 4.2, with supplementary materials and data appearing in the appendix.

This work has been published in the journal Biotechnology for Biofuels and Bioproducts (previously Biotechnology for Biofuels) and can be cited as:

Kubis, M.R., Holwerda, E.K. & Lynd, L.R. Declining carbohydrate solubilization with increasing solids loading during fermentation of cellulosic feedstocks by Clostridium thermocellum: documentation and diagnostic tests. Biotechnol Biofuels 15, 12 (2022). https://doi.org/10.1186/s13068-022-02110-4

4.1 Contributions

MRK, EKH, and LRL conceived the initial study and designed experiments. MRK performed experiments and prepared data. EKH evaluated data and with MRK designed follow-up experiments. MRK, EKH, and LRL wrote the manuscript, and MRK and EKH prepared the submission.

4.2 Declining Carbohydrate Solubilization with Increasing Solids Loading During Fermentation of Cellulosic Feedstocks by *Clostridium thermocellum*: Documentation and Diagnostic Tests

Abstract

Background

For economically viable 2nd generation biofuels, processing of high solid lignocellulosic substrate concentrations is a necessity. The cellulolytic thermophilic anaerobe *Clostridium thermocellum* is one of the most effective biocatalysts for solubilization of carbohydrate harbored in lignocellulose. This study aims to document the solubilization performance of *Clostridium thermocellum* at increasing solids concentrations for two lignocellulosic feedstocks, corn stover and switchgrass, and explore potential effectors of solubilization performance.

Results

Monocultures of *Clostridium thermocellum* show high levels of carbohydrate solubilization for both unpretreated corn stover and switchgrass. However, fractional carbohydrate solubilization decreases with increasing solid loadings. Fermentation of model insoluble substrate (cellulose) in the presence of high solids lignocellulosic spent broth is temporarily affected but not model soluble substrate (cellobiose) fermentations. Mid-fermentation addition of cells (*C. thermocellum*) or model substrates did not significantly enhance overall corn stover solubilization loaded at 80 g/L, however cultures utilized the model substrates in the presence of high concentrations of corn stover. An increase in corn stover solubilization was observed when water was added, effectively diluting the solids concentration mid-fermentation. Introduction of a hemicellulose utilizing coculture partner, *Thermoanaerobacterium thermosaccharolyticum,* increased the fractional carbohydrate solubilization at both high and low solid loadings. Residual solubilized carbohydrates diminished significantly in the presence of *T.*

thermosaccharolyticum compared to monocultures of *C. thermocellum,* yet a small fraction of solubilized oligosaccharides of both C_5 and C_6 sugars remained unutilized.

Conclusion

Diminishing fractional carbohydrate solubilization with increasing substrate loading was observed for *C. thermocellum* mediated-solubilization and fermentation of unpretreated lignocellulose feedstocks. Results of experiments involving spent broth addition do not support a major role for inhibitors present in the liquid phase. Mid-fermentation addition experiments confirm that *C. thermocellum* and its enzymes remain capable of converting model substrates during the middle of high solids lignocellulose fermentation. An increase in fractional carbohydrate solubilization was made possible by 1) mid-fermentation solid loading dilutions and 2) coculturing *C. thermocellum* with *T. thermosaccharolyticum*, which ferments solubilized hemicellulose. Incomplete utilization of solubilized carbohydrates suggests that a small fraction of the carbohydrates is unaffected by the extracellular carbohydrate active enzymes present in the culture.

Keywords (3-10): corn stover, switchgrass, high solid loading, biomass deconstruction, lignocellulose, cellulose, hemicellulose, biofuels, *Clostridium thermocellum*, *Thermoanaerobacterium thermosaccharolyticum*, coculture

Background

Conversion of lignocellulose feedstocks has attracted global interest as a sustainable source of transportation fuels. Biologically mediated events in lignocellulose conversion include production of carbohydrate-active enzymes (CAZymes), enzymatically mediated carbohydrate solubilization, and fermentation of soluble sugars (23). Plants have evolved to be resistant to biological attack, and overcoming this recalcitrance is responsible for the high cost of current conversion technology (21). The most widely studied strategy for solubilizing the carbohydrate fraction of cellulosic biomass involves thermochemical pretreatment and added enzymes produced by aerobic fungi (20,26,28). Alternatively, some thermophilic anaerobes are natively capable of producing cellulases and other CAZymes and then fermenting the solubilized carbohydrates to a desired product in a one-step approach called consolidated bioprocessing (CBP) (32). Mechanical disruption during fermentation (cotreatment) has also been proposed as an alternative to thermochemical pretreatment to augment biologically mediated deconstruction (C-CBP) (131–133).

Clostridium thermocellum (Ruminiclostridium thermocellum, Hungateiclostridium thermocellum, Acetivibrio thermocellus), a cellulolytic and thermophilic anaerobic bacterium, is the most efficient microorganism at lignocellulose solubilization known (132,156), and is thus a promising candidate for CBP. Although the biomass deconstruction apparatus of *C. thermocellum* equally solubilizes pentose-rich hemicellulose as well as cellulose (141), wild-type strains do not ferment pentose sugars (33,158,159). As a result, xylo-oligomers accumulate when lignocellulose is fermented by *C. thermocellum* monocultures. Pentose sugars and oligomers originating from hemicellulose have a deleterious effect on lignocellulose deconstruction by fungal cellulase preparations (112,117–119). There have been reports of possible effects of soluble hemicellulose for cultures of *C. thermocellum* and cell free cellulase preparations on switchgrass (34,171) and corn fiber (49).

In addition to potentially affecting cellulolytic activity, failure to utilize C_5 sugars decreases the product yield per unit biomass. To avoid these undesired effects, defined cocultures of *C. thermocellum* with a

compatible hemicellulose-fermenting strain have been studied, and identifying synergistic coculture partners is important in the context of biofuel production by CBP (161). On both microcrystalline cellulose and lignocellulose, Ng et al. (1981) reported that cocultures with the hemicellulose utilizing *Clostridium thermohydrosulfuricum (renamed as Thermoanaerobacter thermohydrosulfuricus)* enhanced substrate consumption and ethanol yield (163). Saddler and Chan (1984) had similar observations for *C. thermocellum* NRCC 2688 cocultured with *Clostridium thermosaccharolyticum* on pretreated wheat straw (164). Coculture studies with *Thermoanaerobacterium* spp. on microcrystalline cellulose demonstrated increased product formation on crystalline cellulose in comparison to *C. thermocellum* monocultures (165,167,170). Recently, Froese et al. (2018) reported 2 g/L wheat straw cocultures with either *Ruminiclostridium stercorarium* or *Thermoanaerobacter thermohydrosulfuricus* improved carbohydrate solubilization by 30% relative to the monoculture as determined by measuring end products and soluble oligosaccharides (173). Beri et al. (2021) showed cocultures with hemicellulose utilizing *Herbinix spp.* and *Thermoanaerobacterium thermosaccharolyticum* on 40 g/L corn fiber resulted in a 1.39-fold increase (67% to 93%) in overall solubilization relative to the monoculture. In another study, Beri et al. described an inhibitory effect relating to a hemicellulose component of corn fiber, glucuronoarabinoxylan (GAX) (49). Supplementation of enzymes capable of disrupting the GAX-linkages alleviated inhibition and improved carbohydrate solubilization from 33 to 63% for 40 g/L corn fiber solids loading (48).

High loadings of lignocellulosic feedstocks are required for industrial feasibility in order to avoid high costs for product recovery (e.g. steam for distillation) as well as high capital costs for bioreactors (20,21). For lignocellulose solubilization mediated by fungal cellulase preparations, a decrease in solubilization has been observed with increasing solid loadings (37,38,184–186). In these systems, mass transfer and free water limitations arise as solid loadings approach 15-20% dry matter (184,185), yet several other causative factors have also been reported including, but not limited to, the presence and/or accumulation of ethanol (85,105), glucose (105,187), cellobiose (105,187), xylan (122–126), xylose (117), xylooligomers (114,118,119), lignin (85,188), and inhibitors related to thermochemical pretreatment (85,86). For mixed anaerobic

consortia cultivated during anaerobic digestion (AD), It has been observed that no significant differences in the specific methane yield occur between 1-15% total solids with a decrease eventually observed at 20-30% total solids (191–196). In these studies, mass transfer limitations due to lack of free water and/or organic overfeeding are cited as possible explanations.

For defined cultures of thermophilic anaerobes aimed at lignocellulose solubilization, most studies have targeted documenting and understanding capability at solids loadings ≤ 20 g/L. At carbohydrate loadings up to 120 g/L, *C. thermocellum* cultures solubilize 80-93% of the cellulose present in Avicel® PH105, a model microcrystalline cellulose substrate containing negligible amounts of both lignin and hemicellulose (153,197,199). However, declining solubilization with increasing loading has been observed for such cultures when fermenting unpretreated lignocellulose. Verbeke et al. (2017b) observed a 1.72-fold decline in solubilization extent between 50 and 10 g/L on mid-season switchgrass that could not be solely explained by either recalcitrance or inhibition by fermentation products (35), and Shao et al. (2020) also reports diminishing solubilization at increasing loadings of mid-season switchgrass (34). Both authors describe a deleterious effect to lignocellulose deconstruction in the presence of C_5 sugars, either in monomeric or oligomeric forms. Similarly for corn fiber, Beri et al. (2021) observed declining solubilization (90% to 67%) between 20 and 40 g/L which was largely overcome by coculturing *C. thermocellum* with a hemicellulose utilizing thermophile (57).

Here we extend the work of Verbeke, Shao, Beri et al. by documenting solubilization as a function of solids concentration by *C. thermocellum* for corn stover and senescent switchgrass with and without *T. thermosaccharolyticum,* and present experiments aimed at evaluating potential causal mechanisms.

Results

Fermentation of *C. thermocellum* with increasing solids loading.

We aimed to document the impact of solids loading on fractional carbohydrate solubilization (FCS) of corn stover and senescent switchgrass in batch, pH-controlled monocultures of *Clostridium thermocellum*

DSM1313 incubated for 7 days at 55ºC. For both of these substrates with no pretreatment other than autoclaving, FCS decreases roughly linearly as the initial substrate loading is increased from 20 g/L to 80 g/L (figure 5A). Total gas production increased with increasing substrate loading and indicated that fermentative activity stopped at about 100-120 hours (figure 5B).

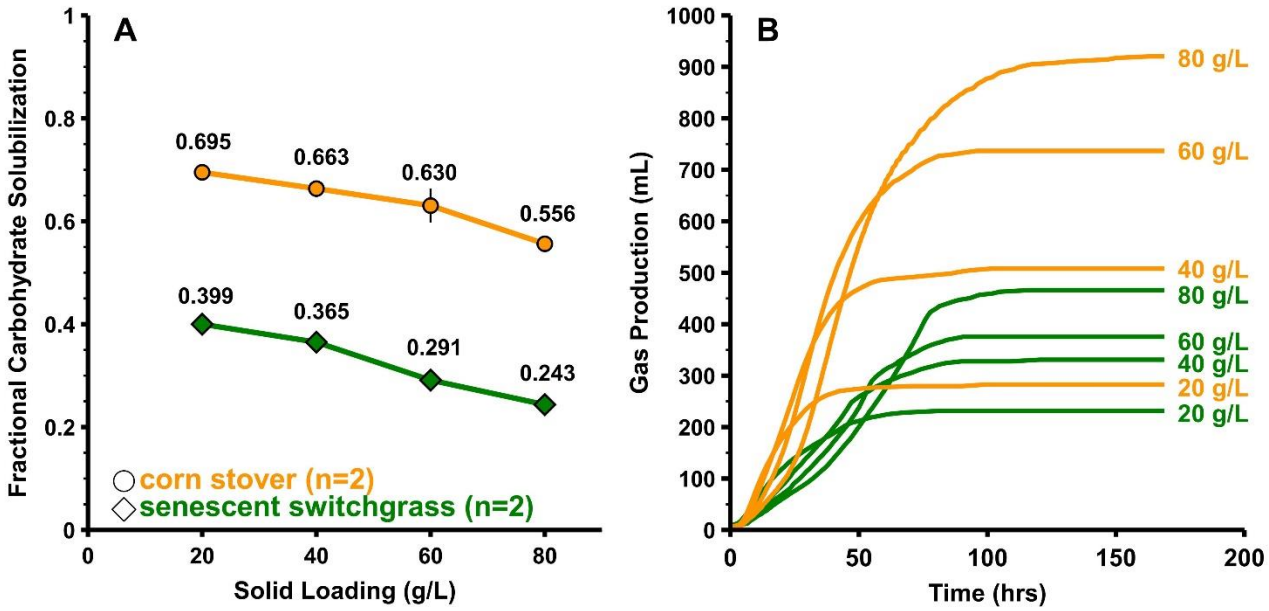

Figure 5. Fermentation of corn stover and senescent switchgrass by monocultures of Clostridium thermocellum at various solid loadings (n=2). (A) Fractional carbohydrate solubilization with error bars representing 1 standard deviation shown (n=2). (B) Representative total gas production (cumulative CO_2 and H_2) for one of the duplicate reactors.

As may be observed from figure 5, FCS decreased by similar absolute amounts for corn stover (0.139 = 0.695 – 0. 556) and for senescent switchgrass (0.156 = 0.399 – 0.243), corresponding to a 20% decrease for corn stover and a 39% decrease for switchgrass. FCS at each solids loading was higher for corn stover than for switchgrass by a factor of approximately two. The total fraction of carbohydrate per solids was

different for corn stover (0.676) and switchgrass (0.725), therefore the carbohydrate loading at equal solid loadings varied slightly for the two feedstocks.

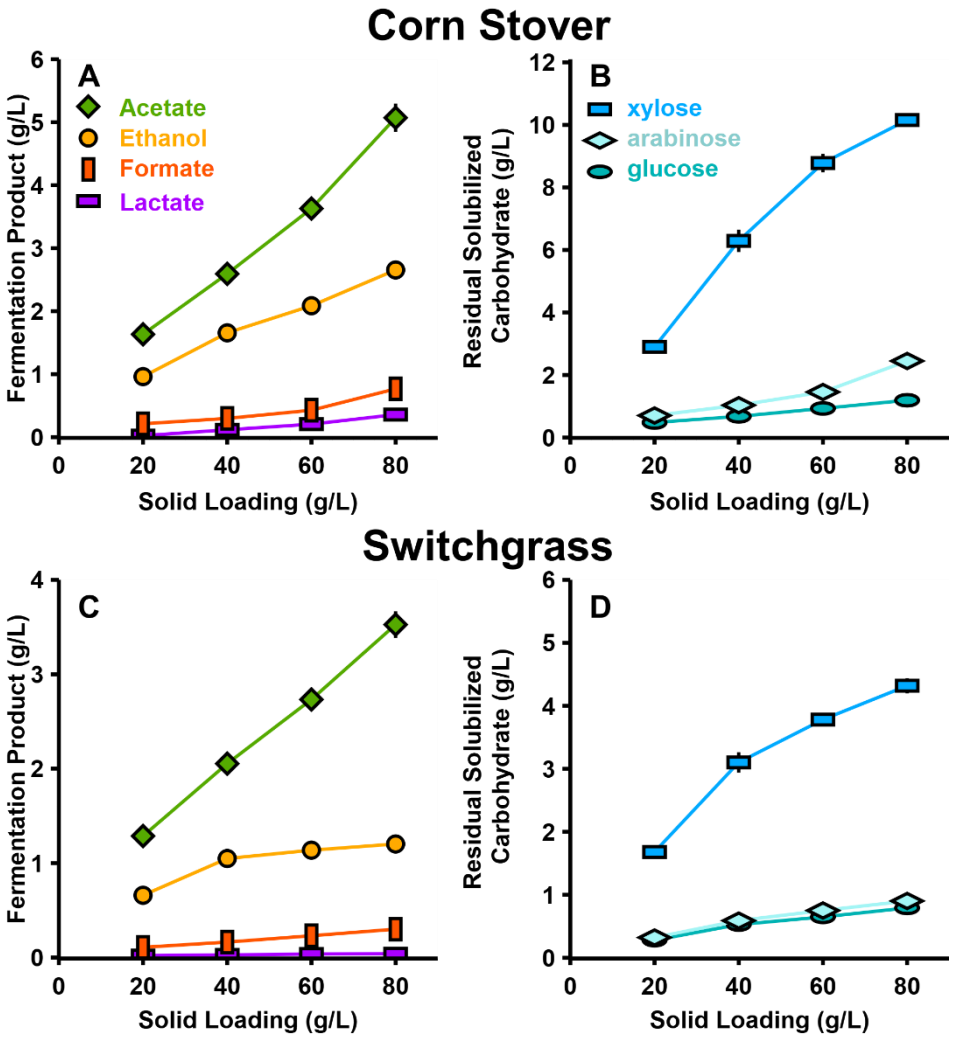

Figure 6. Fermentation products and residual solubilized carbohydrates at various solid loadings for monocultures of Clostridium thermocellum. Panels (A) corn stover and (C) senescent switchgrass fermentation products ethanol, acetate, formate, and lactate. Panels (B) corn stover and (D) senescent switchgrass residual xylose, arabinose, and glucose in the fermentation broth quantified in monomeric form via mild acid hydrolysis of the supernatant. Error bars represent 1 standard deviation for all data points in all panels (n=2). *Note that acetate originates from both the deconstruction of lignocellulosic bonds and microbial metabolism.*

With increasing solid loadings, final concentrations of fermentation products (ethanol, acetate, formate, and lactate shown in figure 6, panels A and C) increased. Note that acetate can originate as a product of fermentation or a product of the solubilization process as it is present in the feedstock as acetyl bonds. Molar ratios of the various fermentative products did not significantly change as solid loadings increased, with the exception of decreasing ethanol production in switchgrass fermentations (appendix table A.2).

Solubilized and unutilized carbohydrates exist as a mixture of complex oligomers in fermentation broth (48) but were measured in monomeric form after a mild acid hydrolysis step (see Methods), and residual solubilized carbohydrates increased with solid loadings (figure 6, panels B and D). While *C. thermocellum* strictly utilizes C_6 carbon sugars in the form of dimers and homo-oligomers of glucose linked by β–glycosidic bonds (302), a small fraction of the residual unutilized soluble carbohydrates appears to contain glucose. The other sugars present in the unutilized solubilized carbohydrates were xylose and arabinose, which is consistent with the inability of wild-type *C. thermocellum* to utilize C_5 sugars.

Testing spent broth for inhibitory effects

Spent fermentation broth from the aforementioned 80 (high) and 20 (low) g/L fermentations was collected and examined for inhibitory effects in subsequent bottle fermentations with fresh media and fresh substrate. The spent broth was centrifuged and filtered at 0.2 µm to remove cells and any remaining solids. Additional filtered spent broth was generated by fermenting 12.1 g/L cellobiose and cellulose, corresponding to the amount of glucan solubilized in an 80 g/L corn stover fermentation. The spent media then was aseptically added in 75% volumetric amounts to a 20 mL working volume serum bottle containing fresh media and either 5 g/L microcrystalline cellulose (Avicel® PH-105) or 5 g/L cellobiose (final concentration) as carbon and energy source (figure 7). Bottles with 75% v/v water instead of spent broth served as internal controls. To see if the spent broth had any transient or permanent effects on the solubilization and utilization processes, the net product formation was measured every 24 hours for a total of 5 days (product concentration measured minus product concentration present at start of incubation). As shown in figure 7, net product formation at the end of bottle incubation was comparable for those with and without spent broth,

suggesting the spent broth has limited effects towards the final utilization of model substrates for *C. thermocellum*. However, there was a temporary lag in product formation of up to 50-75 hours in the bottles containing cellulose and spent broth from high solid loadings (80 g/L). This delay was not observed for fermentation with cellobiose or at low solid loadings (20 g/L).

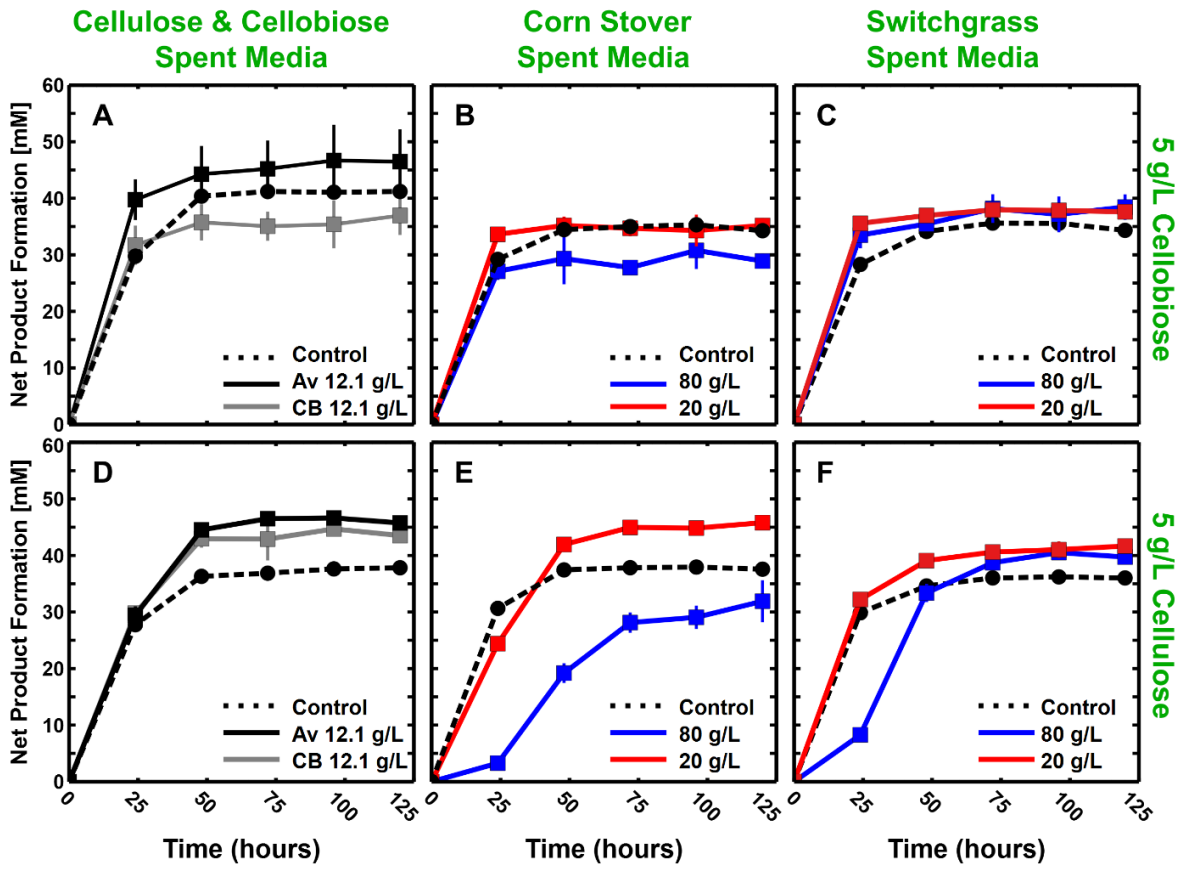

Figure 7. Spent media inhibition tests. The effect of added spent media on net cumulative product formation (acetate+ethanol+formate+lactate in [mM]) during fermentation of 5 g/L cellobiose (panels A, B, C) or cellulose (panels D, E, F) for monocultures of Clostridium thermocellum. Panels B and E show the effect of spent media from corn stover fermentations by C. thermocellum at two different initial solid loadings, and panels C and F show the effect of spent media at two different senescent switchgrass loadings. Panels A and D show results for addition of spent media from a cellobiose (A) and cellulose (D) fermentations with carbohydrate utilization equal to that of 80 g/L corn stover utilization (12.1 g/L cellobiose (CB) or cellulose (Av)). Individual controls (n=1, dashed lines) with water in lieu of spent broth were included for each condition, whereas all other datapoints represent the average of triplicate bottle fermentations (n=3). Error bars represent 1 standard deviation.

Addition of cells and substrates during fermentation of 80 g/L corn stover

In order to gain diagnostic insights into declining solubilization with increasing substrate loading, model substrates and cells were added 48 hours after inoculating duplicate 300 ml batch cultures of *C. thermocellum* in pH-controlled bioreactors with an initial corn stover loading of 80 g/L. Corn stover was chosen as it gave higher solubilization results compared to switchgrass in the previous experiment. Several additions were made including 60 ml solutions of microcrystalline cellulose (Avicel® PH-105), cellobiose, cellobiose-grown cells concentrated by centrifugation, and water which served as an internal control. Additions of cellobiose and cellulose increased the total carbohydrate loading by 32% (from 54.1 g/L to 71.5 g/L) and were intended to be approximately equal to the observed amount of glucan solubilized in a previous 80 g/L corn stover fermentation. The amount of cellobiose-grown cells added could theoretically represent an increase in cell concentration by 4 g/L, but the overall cell concentration or increase thereof was not measured.

As can be seen in figure 8, panel A, mid-fermentation addition of cellulose or cellobiose did not enhance solubilization relative to the water control. For the addition of cellulose, fractional carbohydrate solubilization was calculated based on the initial quantity of carbohydrate in the corn stover and the recovered carbohydrate after fermentation, with added cellulose not included in the initial amount of carbohydrate. An immediate increase in gas production accompanied both substrate additions (figure 8, panel B), from which we infer that the culture was active and substrate-limited in the absence of added substrate. This is mirrored by an increase in product formation in amounts expected if all added cellobiose and cellulose were utilized (see appendix figure A.2). Essentially complete fermentation of added substrate is also indicated by low amounts of residual sugars in cultures with and without added substrate (see appendix figure A.1). Extensive utilization of added substrates also suggests that limitation of media components and fermentation product inhibition are not in effect.

Although the highest FCS value was obtained with the mid-fermentation addition of 60 mL concentrated cell suspension, this was not determined to have a significant ($p > 0.05$) effect on carbohydrate

solubilization compared to the water addition control (figure 8, panel A), and gas production was very similar to added water (figure 8, panel B). The added cell culture proved to be viable as witnessed by normal growth on cellobiose or cellulose in serum bottle incubations inoculated at the same time with the same cell suspension as the addition experiment. We infer from these results that the presence of biocatalyst did not limit solubilization of the carbohydrate present in corn stover at a substrate loading of 80 g/L.

Whereas the fraction of corn stover carbohydrate solubilized was 0.556 ± 0.011 without added cells or substrate, this increased to 0.619 ± 0.005 for the water control. The difference between these values was statistically significant ($p = 0.020$). The addition of water brought the solids loading from 80 g/L to 67 g/L based on initial solids loaded, while the FCS value can be found between 40-60 g/L initial solids loading as shown in figure 5.

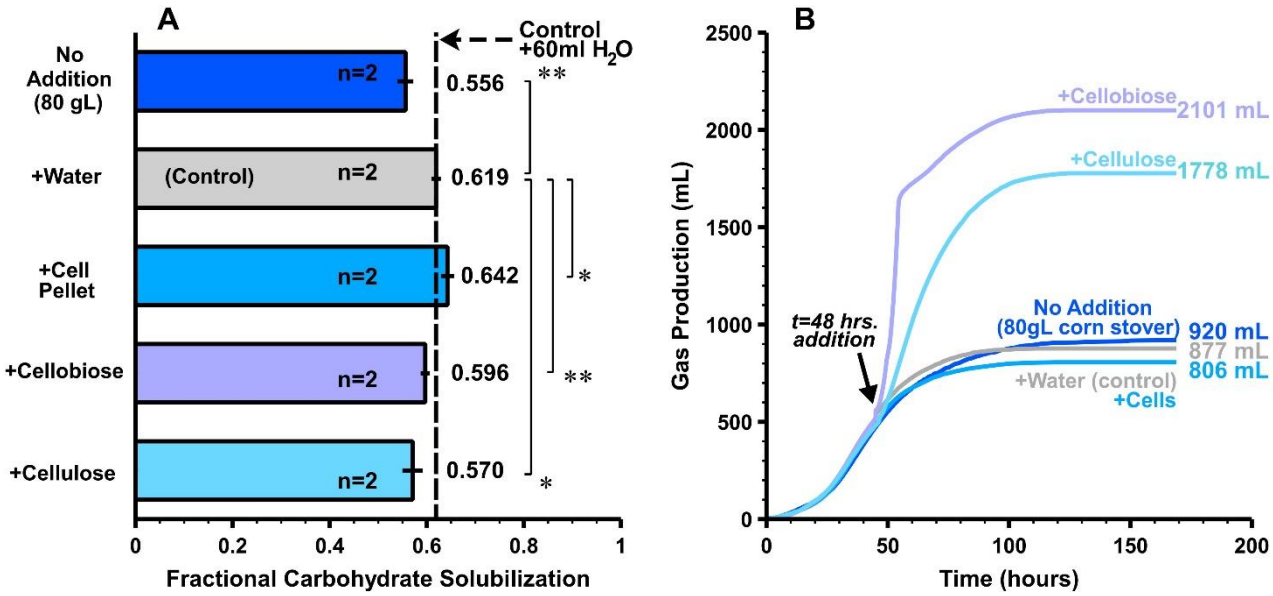

Figure 8. Fermentation addition tests. Panel (A) Fractional carbohydrate solubilization for 80 g/L corn stover with addition of cells (cellobiose-grown & centrifuged cell pellet), cellobiose solution, and suspended Avicel slurry at 48 hours after inoculation versus a control (water only) or no addition (n=2). Panel (B) Representative total gas production (cumulative CO_2 and H_2) for one of the duplicate reactors. Solubilization bars are averages of duplicate bioreactor runs, error bars represent 1 standard deviation. A single asterisk denotes a significance level of 0.1, and double asterisks denote a significance level of 0.05 between different runs as indicated in the figure. The statistical analyses were performed using t-tests for two-samples assuming unequal variance, and the results are available as supplemental files.

Coculture experiments with low and high loadings of corn stover and switchgrass

We next examined the effect of culturing *C. thermocellum* with a hemicellulose utilizing coculture partner, *Thermoanaerobacterium saccharolyticum* HG-8 ATCC 31960 for both high (80 g/L) and low (20 g/L) loadings of corn stover and switchgrass. For corn stover fermentations by monocultures and cocultures, FCS data is presented in figure 9 panel A and gas production data in panel B. Panels C and D present the same data for switchgrass. The coculture demonstrated higher solubilization (9A and 9C) and gas production (9B and 9D) for both feedstocks at low and high solid loadings. While the coculture showed

higher solubilization than the monoculture, it still exhibited diminishing solubilization as with increasing solid loadings.

Two-way ANOVA results indicate that the solids loading effect is significant at $p < 0.001$ for both substrates, while the coculture effect is significant at < 0.001 for corn stover and 0.063 for switchgrass. The net increase in FCS due to the coculture was roughly twice as large for corn stover than for switchgrass, though the relative increases are consistent with the lower fractional solubilization observed for switchgrass monocultures throughout this study. Higher standard deviations were observed for switchgrass than for corn stover, consistent with the lower significance level per ANOVA testing.

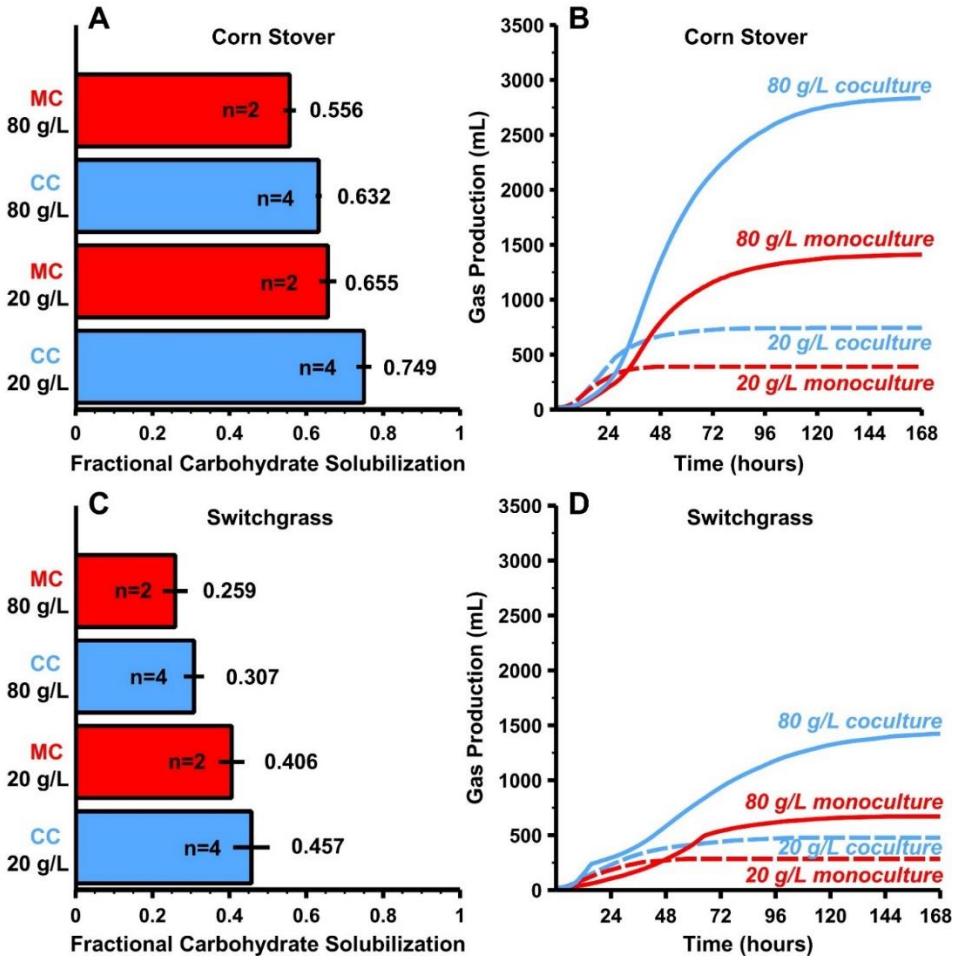

Figure 9. Monocultures and cocultures solubilization and gas production. Panels (A) and (C) Fractional carbohydrate solubilization of 20 g/L and 80 g/L corn stover (A) and senescent switchgrass (C) by monocultures of Clostridium thermocellum and cocultures of Thermoanaerobacterium saccharolyticum at pH 6.5. Panels (B) and (D) Representative total gas (cumulative CO_2 and H_2) production for one of the duplicate reactors of 20 and 80 g/L corn stover (B) and senescent switchgrass (D) fermentations at pH 6.5. Solubilization bars are averages of duplicate bioreactors runs, and error bars represent 1 standard deviation.

The operating pH during cultivation for coculture experiments was lowered from 7.0 to 6.5 for this set of experiments to better accommodate growth of *T. thermosaccharolyticum* (appendix figure A.3.). For 80 g/L substrate loadings, this was determined to have a non-significant effect on the FCS by the monoculture (figure 10).

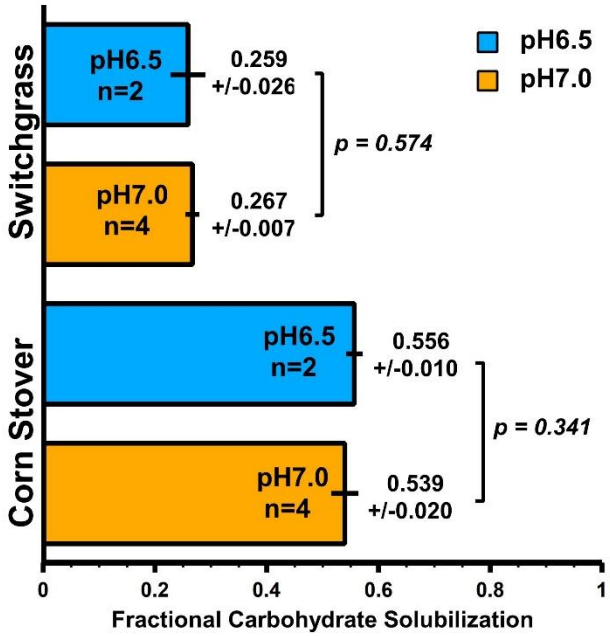

Figure 10. Monoculture solubilization at two pH levels. Fractional Carbohydrate Solubilization for 7-day Clostridium thermocellum monoculture fermentations of 80 g/L senescent switchgrass and corn stover at pH 6.5 and pH 7.0. The statistical analyses were performed using t-tests for two-samples assuming unequal variance.

Figures 11 and 12 illustrate the effect of adding *T. thermosaccharolyticum* as a hemicellulose utilizing coculture partner to cultures of *C. thermocellum*. Under the chosen conditions, the coculture partner fermented most but not all of the soluble pentose-rich oligosaccharides made available by *C. thermocellum*-mediated lignocellulose deconstruction. Fractional carbohydrate solubilization and utilization data are presented in table 2 for the experiments depicted in figures 9-12.

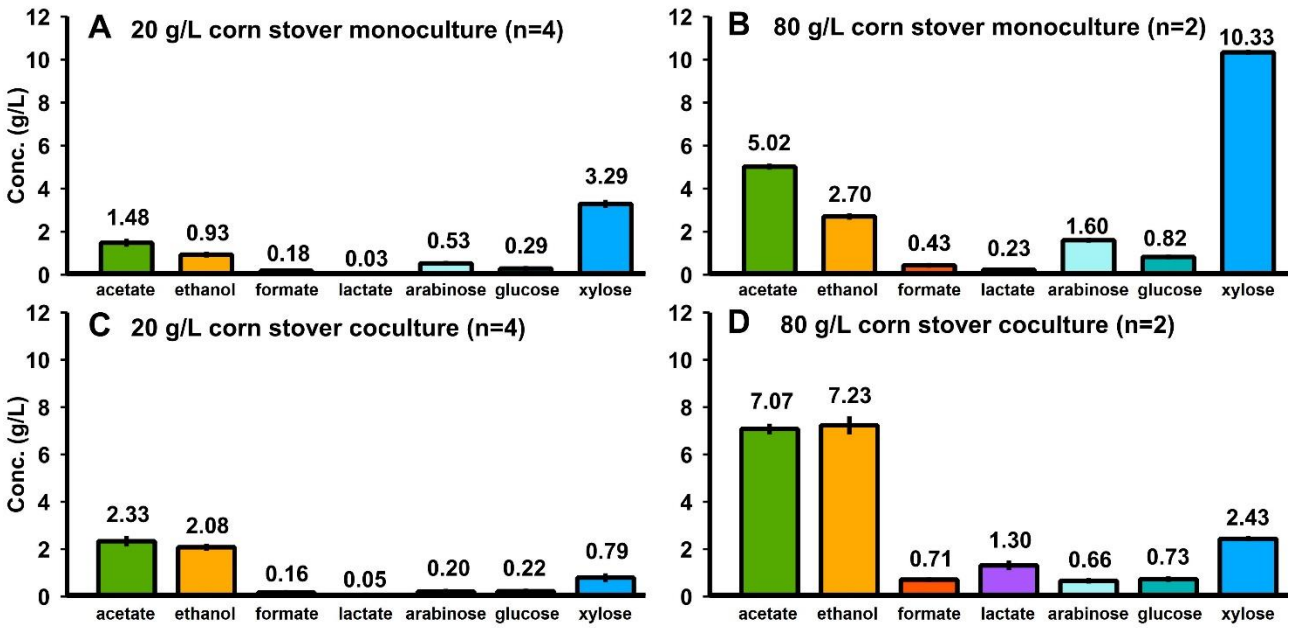

Figure 11. Monocultures and cocultures fermentation products and residual soluble carbohydrate for corn stover. 7-day fermentations of corn stover by monocultures at loadings of 20 g/L (A) and 80 g/L (B) and cocultures at loadings of 20 g/L (C) and 80 g/L (D). Residual soluble carbohydrate was quantified in monomeric form after mild acid hydrolysis of the supernatant. Note that acetate originates from both the deconstruction of lignocellulosic bonds and microbial metabolism.

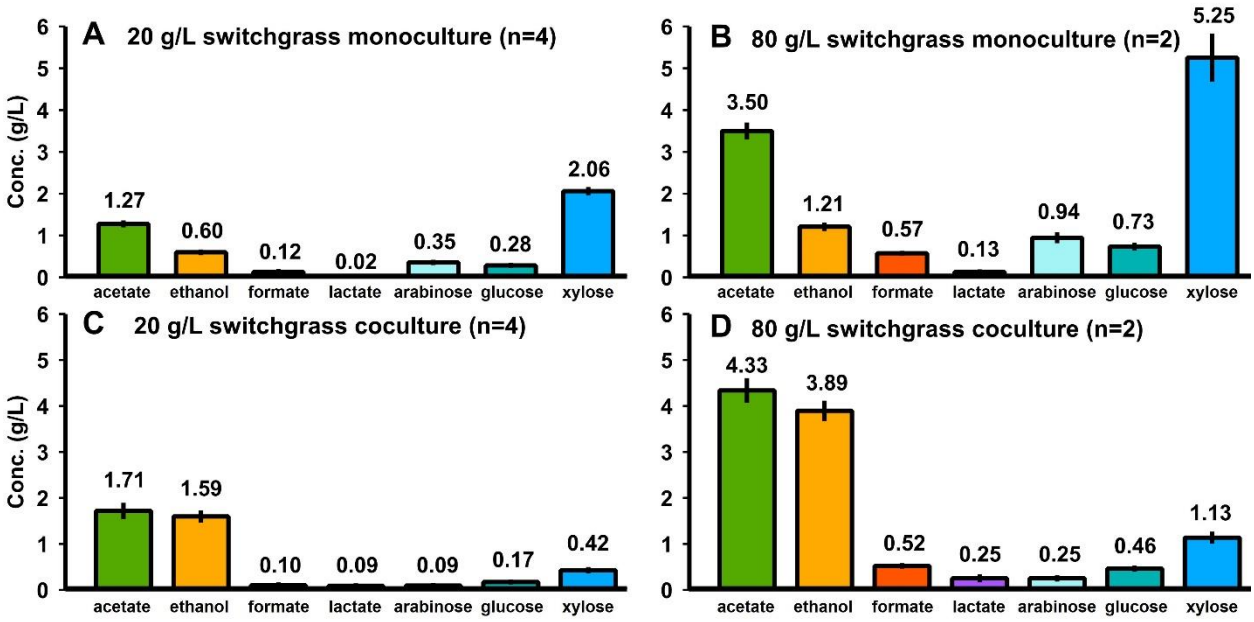

Figure 12. Monocultures and cocultures fermentation products and residual soluble carbohydrate for switchgrass. 7-day fermentations of senescent switchgrass by monocultures at loadings of 20 g/L (A) and 80 g/L (B) and cocultures at loadings of 20 g/L (C) and 80 g/L (D). Residual soluble carbohydrate was quantified in monomeric form after mild acid hydrolysis of the supernatant. Note that acetate originates from both the deconstruction of lignocellulosic bonds and microbial metabolism.

	Solid Loading	Fractional Carbohydrate Solubilization	Fractional Utilization of Solubilized Glucose	Fractional Utilization of Solubilized Xylose
Corn Stover				
Monoculture	*20 g/L*	*0.656 ±0.017*	*0.938 ± 0.002*	-
	80 g/L	*0.557 ± 0.010*	*0.946 ± 0.001*	-
Coculture	*20 g/L*	*0.749 ± 0.014*	*0.957 ± 0.001*	*0.779 ± 0.027*
	80 g/L	*0.632 ± 0.002*	*0.958 ± 0.001*	*0.798 ± 0.002*
Switchgrass				
Monoculture	*20 g/L*	*0.406 ± 0.028*	*0.904 ± 0.015*	-
	80 g/L	*0.259 ± 0.026*	*0.910 ± 0.003*	-
Coculture	*20 g/L*	*0.457 ± 0.042*	*0.952 ± 0.002*	*0.817 ± 0.002*
	80 g/L	*0.308 ± 0.021*	*0.954 ± 0.000*	*0.821 ± 0.002*

Table 2: Comparison of carbohydrate solubilization and utilization for mono- and cocultures. Fractional sugar utilization calculated as one minus the mass of sugars found in the fermentation broth over the theoretical mass of sugars that have been solubilized based on fermented and unfermented solids. Sugar concentrations in the fermentation broth quantified in monomeric form via mild acid hydrolysis of the supernatant. No fractional utilization of xylose was detected in the monocultures.

It may be observed that fractional carbohydrate solubilization is sensitive to solid loading whereas the fractional utilization of solubilized carbohydrates is not. For cocultures on either feedstock, roughly 5% and 20% of the solubilized glucose- and xylose-oligomers, respectively, are not utilized.

A linear relationship is observed for fractional solubilization of xylan and glucan for monocultures and cocultures fermenting both corn stover and switchgrass at various substrate loadings (figure 13). This relationship is largely maintained across solid loadings and culture type. This would suggest that solid loading and culture type does not bias the solubilization activity either towards or away from glucose (or xylose).

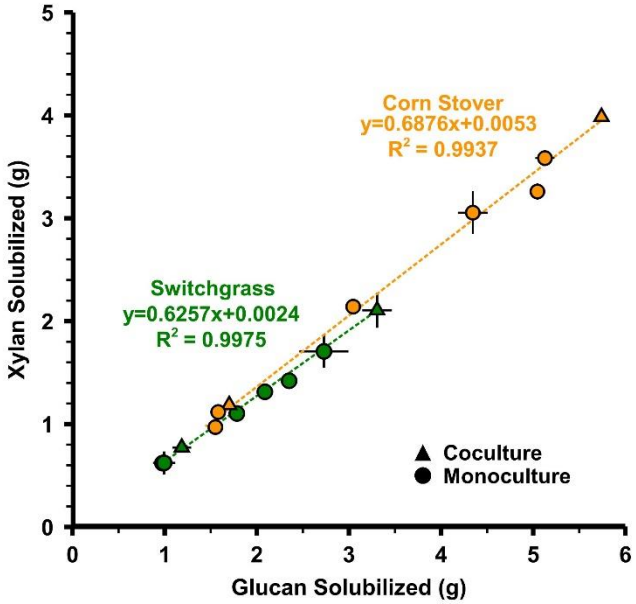

Figure 13. Linear solubilization ratio between xylan and glucan for different cultivation conditions. Datapoints are averages of the duplicate fermentations depicted in figure 5 and figure 9 and error bars represent one standard deviation. Trendlines are calculated using combined datasets for each feedstock which represent two culture types (mono- and cocultures) and multiple solid loadings (20, 40, 60, 80 g/L).

Discussion

Here we document declining solubilization with increasing solids loading over a range of 20 to 80 g/L for batch monocultures of *C. thermocellum* fermenting either corn stover or senescent switchgrass. Our observation of this trend is consistent with results of both Verbeke et al. (2017b) and Shao et al. (2020) on mid-season switchgrass at various solids loadings (34,35). Comparing monocultures with 80 g/L and 20 g/L substrate loadings with no pretreatment other than autoclaving, final total carbohydrate solubilization declined from 0.695 to 0.565 for corn stover and from 0.399 to 0.243 for switchgrass. Data at intermediate solids loading indicate a roughly linear declining solubilization trend for both substrates. Remediation of this effect is likely necessary for commercial application acknowledging that substrate loadings about 2-fold higher than the maximum studied herein are generally envisioned for economically viable production

of ethanol from lignocellulose (20,21). Such remediation would be greatly informed, and likely require, understanding the factor(s) responsible for the declining fractional solubilization trend observed here.

As reported previously, we routinely observe near-complete utilization of Avicel-cellulose up to 120 g/L by *C. thermocellum* cultures (153,197,199), which is accompanied by concentrations of fermentation products over twice those observed herein with corn stover or switchgrass at 80 g/L. In light of these results, both inhibition by fermentation products and limitation by inadequate amounts of growth medium components seem unlikely to explain the declining fractional solubilization trend. Several alternative hypotheses for the basis of this phenomenon were tested but did not confirm specific factors. Accumulation of liquid phase inhibitors is a common explanation for cellulase inhibition, yet in this study, *C. thermocellum* was able to overcome a transient delay in cellulose utilization in the presence of spent broth from high lignocellulose loadings. Addition of spent-broth from fermentation of 20 and 80 g/L corn stover and switchgrass (figure 7) resulted in little to no impact on cellobiose fermentation, indicating that fermentation of glucan solubilization products was not inhibited, and little if any long-term impact on the generation of fermentation products from cellulose, suggesting that cellulase activity is not irreversibly inhibited. In this respect, our results differ from those of Beri et al. (2021), who observed inhibition from corn fiber spent broth on cellobiose incubations by *C. thermocellum* monocultures (57). It should be noted that there are several compounding factors that obscure comparisons between spent broth experiments, including cultivation conditions and spent broth preparation, and similar results for corn stover and corn fiber would not necessarily be expected considering the markedly different feedstock composition and experimental design (56,57). For cellulose incubations in the presence of switchgrass spent broth, Verbeke et al. (2017b) observed reductions in solubilization for 17.5 g/L cellulose but showed little difference in net-end product concentrations, as we also observed (41). Shao et al. (2020) observed decreased cellulose conversion due to added spent broth measured at 24 hours, however measurements were not taken at longer times to determine if conversion with added broth eventually equaled the controls as was observed in figure 7 (42).

Mid-fermentation addition of cellobiose or cellulose to 80 g/L corn stover *C. thermocellum* monocultures resulted in a dramatic increase in gas formation compared to controls without substrate added, but no significant increase in FCS. This suggests that the culture and its cellulases were active and not limited in utilizing additional (model) substrate, but rather had stopped solubilizing additional substrate from lignocellulose. Note that the additional utilization of cellobiose and cellulose could have resulted in an increase in cellular biomass or posed an opportunity for new cellular biomass to be generated. Furthermore, no significant increase in solubilization was observed for additions of biocatalyst (concentrated cells) suggesting limitations in solubilization could be more closely related to the lignocellulosic substrate rather than *C. thermocellum's* enzymatic machinery. An increase in FCS was observed for an addition of 60 ml water to a 300 ml culture which effectively diluted the initial substrate loading at 80 to 66.7 g/L. Linear interpolation of carbohydrate solubilization at 60 and 80 g/L from figure 5 gives an expected solubilization of 0.606 at a substrate loading of 66.7 g/L, which is very close to the observed value of 0.619. Thus, results with different initial substrate loadings are very nearly recapitulated by a water dilution during active fermentation.

To be consistent with the observations reported herein, a proposed mechanism for declining fractional carbohydrate solubilization with increasing solids would need to be lignocellulose-specific, involve factors other than nutrient limitation and inhibition by liquid-phase products of fermentation or deconstruction, not be due to inactive microbial cells or CAZymes, be reversed by liquid-phase dilution, and partially reversed by addition of a hemicellulose-fermenting coculture partner. In general, a mechanism involving decreasing lignocellulose accessibility with increasing substrate loading seems mostly likely to us. It has been previously reported that xylan and pentose-rich oligosaccharides adsorb onto cellulose surfaces (113,303–306), and cellulase performance is generally enhanced in the presence of hemicellulolytic enzymes (123–126). Noting that dilution of the liquid phase would be expected to cause adsorbed oligosaccharides to enter solution by Le Chatelier's principle, impediment of deconstruction by adsorbed oligosaccharides would appear to be a plausible mechanism for *C. thermocellum*. This remains to be definitively proven, however.

Co-culturing *C. thermocellum* with the hemicellulose-fermenting *Thermoanaerobacterium thermosaccharolyticum* increased solubilization compared to monocultures at both 20 g/L and 80 g/L substrate loadings for corn stover ($p < 0.001$) and switchgrass ($p = 0.063$). Inclusion of *T. thermosaccharolyticum* as a coculture partner did not, however, ameliorate declining solubilization as was observed at 40 g/L corn fiber by Beri et al. (2021) (from 67% to 93%) although the absolute amount of carbohydrates solubilized and utilized is much higher for corn stover (57). For each feedstock we observed a consistent fraction of hemicellulose sugars are being solubilized but not utilized regardless of solid loadings (table 2). Our results are consistent with certain linkages present in soluble products of *Clostridium thermocellum*-mediated hemicellulose deconstruction being inaccessible to the array of carbohydrate active enzymes of *T. thermosaccharolyticum,* as had been previously observed by Beri et al. for corn fiber (56).

Conclusions

Decreasing fractional carbohydrate solubilization with increasing substrate loading was observed for monocultures of *C. thermocellum* and coculture fermentations of *C. thermocellum* and *T. thermosaccharolyticum* fermenting corn stover and senescent switchgrass with no pretreatment other than autoclaving. Results of experiments involving spent media addition do not support a major role for inhibitors present in the liquid phase. Substrate addition experiments confirm that *C. thermocellum* and its CAZymes remain capable of converting model substrates during the middle of lignocellulose fermentation at the maximum substrate loading tested (80 g/L). Substrate dilution reverses the observed decrease in fractional carbohydrate solubilization at increasing substrate loading, and coculture of *C. thermocellum* with *T. thermosaccharolyticum*, which ferments hemicellulose, increases fractional carbohydrate solubilization compared to *C. thermocellum* monocultures at both lower (20 g/L) and higher (80 g/L) loadings of both corn stover and switchgrass. For both monocultures and cocultures, regardless of solid loading, there remains a consistent fraction of carbohydrates that undergo solubilization, but not utilization. This suggests that some carbohydrates are unaffected by the existing suite of CAZymes present in the culture. Impediment of deconstruction by adsorbed oligosaccharides would appear to be a plausible

mechanism for the observed trend of declining solubilization with increasing substrate loading, although this remains to be conclusively shown.

Methods

Substrates

Carbohydrate solubilization of two lignocellulosic feedstocks were characterized across various solid loadings. Corn stover was a gift from POET Research Inc (Sioux Falls, SD) premilled at 1/8" size material, and senescent switchgrass was a gift from Ernst Seeds at 1/4" size (Meadville PA, USA). Due to material limitations, a separate batch of corn stover (also from POET Research Inc) was used for experiments comparing monocultures and cocultures. Prior to characterization and use in experiments, both feedstocks were milled to pass through a 0.5 mm sieve on a Retsch ZM 200 centrifugal mill (Verder Scientific, Newton PA) (132). Carbohydrate content was determined by quantitative saccharification (QS) with 72% (w/w) H_2SO_4 (Fisher, Waltham MA), as described in Sluiter et al (307). Acid-hydrolyzed monomeric sugars (arabinose, glucose, xylose) were quantified by refractive index detection and separated via HPLC (Waters, Milford MA) with an Aminex® HPX-87H column (Bio-Rad, Hercules CA) operating at 60˚ C, 2.5 mM H_2SO_4 eluent, at a flowrate of 0.6 mL/min (132).

Microbial strains and growth media

Clostridium thermocellum DSM1313 (LL1004) was obtained from the Deutsche Sammlung von Mikroorganismen und Zellkulturen GmbH (DSMZ, Liebnitz, Ger.). *Thermoanaerobacterium thermosaccharolyticum* HG-8 ATCC 31960 (LL1244) was obtained from the American Type Culture Collection (ATCC, Manassas, VA). Inocula were prepared by culturing *C. thermocellum* on MTC (308) and 50 g/L microcrystalline cellulose (Avicel® PH105, FMC biopolymers, Philadelphia PA) in a pH-controlled 1.2 L Sartorius bioreactor. During mid-log growth, 30 mL cell culture aliquots were transferred to 50 mL serum bottles. Cell culture aliquots were stored at -80˚C and were slowly thawed several hours before bioreactor inoculation. *T. thermosaccharolyticum* inoculum was cultured on modified CTFüD

medium substituted with D-xylose for cellobiose (309). Inoculum was re-seeded several hours prior to bioreactor inoculation in order to ensure culture viability, which was added to bioreactors at 4%(v/v). Defined Medium for Thermophilic Clostridia (MTC) was prepared as described prior(308); solution B had final concentrations of 2.12 g/L potassium citrate monohydrate ($C_6H_7O_8K_3$), 1.25 g/L $C_6H_8O_7 \cdot H_2O$, 1.0 g/L Na_2SO_4, 1 g/L KH_2PO_4, 2.5 g/L $NaHCO_3$, and was added at 4%(v/v). Solution C had final concentrations of 2.0 g/L CH_4N_2O and was added at 2%(v/v). Solution D had working concentrations of 1.0 g/L $MgCl_2 \cdot 6H_2O$, 0.2 g/L $CaCl_2$, 0.1 g/L $FeCl_2 \cdot 4H_2O$, 1.0 g/L L-cysteine HCL monohydrate ($C_3H_7NO_2S \cdot HCl \cdot H_2O$), and was added at 2%(v/v). Solution E had final concentrations of 0.02 g/L pyridoxamine dihydrochloride, 0.004 g/L 4-aminobenzoic acid, 0.002 g/L D-biotin, 0.002 g/L vitamin B_{12}, and was added at 2%(v/v). Solution TE had final concentrations of 0.00625 g/L $MnCl_2 \cdot 4H_2O$, 0.0025 g/L $ZnCl_2$, 0.000625 g/L $CoCl_2 \cdot 6H_2O$, 0.000625 g/L $NiCl_2 \cdot 6H_2O$, 0.000625 g/L $CuSO_4 \cdot 5H_2O$, 0.000625 g/L H_3BO_3, 0.000625 g/L $Na_2MoO_4 \cdot 2H_2O$, and was added at 0.5%(v/v). Each MTC solution was purged by 20 cycles of alternating N_2 gas and Vacuum for 45 seconds each. After purging, solution D was autoclaved for 30 minutes on liquid cycle.

Monoculture Fermentations at Various Solid Loadings

All lignocellulose fermentations were performed at 300 mL working volume in 0.5 L Sartorius Qplus bioreactors (Sartorius, Bohemia NY). Each solids loading was run at least in duplicate (n=2). Lignocellulosic feedstocks were suspended in Milli-Q water (MilliporeSigma, Burlington MA) and autoclaved for 90 minutes on a liquid/slow exhaust cycle. Overnight, the bioreactor's headspace was sparged with 'ultra pure' N_2 gas (Airgas, White River Junction VT) while being stirred at 300 RPM at 55˚C. After sparging the bioreactors, media solutions were added to the lignocellulose slurry via a 0.2 μm polyethersulfone (PES) sterile syringe filter (Corning, Corning NY).

Prior to inoculation, the pH was controlled at 7.0 or 6.5 using a gel-filled pH probe (Mettler-Toledo, Billerica MA) and automatic addition of 4 N KOH (Fisher, Waltham MA) via a peristaltic pump in the Sartorius control tower. Online gas production was monitored with a milligas flow meter (Ritter, Hawthrone

NY) filled with 0.5 N HCl. Total volumetric gas production data was recorded by the accompanying Rigamo software. *C. thermocellum* inoculum was added at 2% (v/v), and the fermentations proceeded for 168 hours.

Harvesting residual solids and determination of carbohydrate solubilization and fermentation products

After fermentation, the bioreactor contents were harvested as a whole and centrifuged for 15 minutes at 16,000 x *g* at 4 ºC on an Avanti J-26S XP centrifuge using rotor JA-10. Both the residual solids and supernatant were collected to determine their respective carbohydrate concentrations. Fractional carbohydrate solubilization is calculated as the difference between carbohydrate mass in the unfermented feedstock versus the residual solids. Carbohydrate content in the residual solids were determined via QS as described in the feedstock material section. Similarly, the carbohydrate content of the supernatant was determined using a mild-acid hydrolysis step named liquid quantitative saccharification (LQS) adjusted from Sluiter et al. (307). Analysis of fermentation products (acetate, ethanol, formate, lactate) was performed by mixing 35 µL 10% (v/v) H_2SO_4 and 700 µL fermentation supernatant and allowing the solution to sit for >5 minutes to denature proteins. The acidified solution was spun down in the microcentrifuge at 21,130 x g and the supernatant was filtered via Spin-X centrifuge tubes (0.22 µm nylon) (Corning, Corning NY). The filtrate was quantified for products via HPLC and quantified by comparison to standard solutions.

Bottle fermentations with lignocellulose fermentation spent media

Serum bottles (30 mL) were prepared by adding either D+ cellobiose (MilliporeSigma, Burlington MA), or microcrystalline cellulose (Avicel® PH105, FMC biopolymers, Philadelphia PA) to MilliQ water, purged with nitrogen gas, and autoclaved for 30 minutes on liquid cycle. Carbon substrates were concentrated such that the final concentration was either 5.0 g/L cellulose or cellobiose. The final volume (20 mL) consisted of 75% spent media (or sterile and anaerobic water for controls) and 25% fresh substrate and MTC media.

To buffer pH, solution A was also included at a final concentration of 5.0 g/L morpholinopropane sulfonic acid (MOPS) and was added at 2% (v/v). MTC was added to each bottle as described above. However, for bottle fermentations solutions A, B, and C were autoclaved for 30 minutes on liquid cycle, and not filter-sterilized.

Supernatant was collected from the high solids monoculture batch fermentations described above. Harvesting the residual solids, collecting and preparing the supernatant, and inoculating bottle fermentations were all performed on the same day. The liquid phase from 80 g/L corn stover, 20 g/L corn stover, 80 g/L switchgrass and 20 g/L switchgrass fermentations were used for bottle experiments. The supernatant was subject to a second centrifugation for 10 minutes at 50,000 x *g* on an Avanti J-26S XP centrifuge using a JA-25.50 rotor. The supernatant was then vacuum filtered with a glass fiber membrane prefilter (MilliporeSigma, Burlington MA) and then vacuum filtered with a 0.45 um nylon membrane filter (MilliporeSigma, Burlington MA). Lastly, the supernatant was added through a 0.2 um PES syringe sterile filter into an empty and autoclaved serum bottle and was aseptically purged for 20 cycles as previously described.

In addition to collecting lignocellulosic supernatant, supernatant from batch fermentations on model substrates, cellobiose and cellulose, were collected for bottle experiments. Monoculture batch fermentations of cellobiose and cellulose were performed as described above for 0.5 L final volume in 1.2 L Sartorius bioreactors. Both substrates were loaded at a final concentration of 12.1 g/L, which is approximately equal to the amount of glucan utilized in an 80 g/L corn stover fermentation as determined results in prior experiments. The model substrate cultures were harvested at 48 hours which corresponded to approximately 24 hours after base addition had stopped. Supernatant was collected and filtered in the same procedure described above for lignocellulosic supernatant.

A one-way release valve was used aseptically to equilibrate pressure before inoculation. Bottles, ran in triplicate (n=3), were inoculated 2% (v/v) with a -80˚C bottle of *C. thermocellum* as described above. Bottles were cultivated at 55˚C in a shaking incubator and sampled for product formation every 24 hours

for five days, with net product formation equal to the product concentration at the timepoint of inquiry, minus the product concentration at time zero. To serve as a control (n=1), a bottle with 75% (v/v) water instead of supernatant was included for each experimental condition totaling three individual controls for cellulose with water and three for cellobiose with water.

Monoculture fermentations with substrate and biocatalyst additions

Bioreactor fermentations at 80 g/L corn stover were prepared in the same manner described above. During growth phase, determined to be approximately t=48 h by monitoring gas production, respective solutions were added to the fermentations. Based on prior experiments, 60 ml cellulose (n=2) and cellobiose (n=2) solutions were added at a concentration that effectively doubled the observed amount of glucan solubilized (5.524 g) in an uninterrupted 80 g/L corn stover fermentation. Biocatalyst was obtained by culturing *C. thermocellum* on MTC containing 25 g/L cellobiose in a 1.2 L Sartorius bioreactor with a 1.0 L working volume. The fermentation broth was anaerobically and aseptically transferred out of the bioreactor during mid-growth phase (t=24 h) by a peristaltic pump, and further processed in an anaerobic glovebag, (Coy Laboratory Products, Grass Lakes, MI). The broth was aseptically transferred into centrifuge bottles and the cell mass pelleted at 16,000 x g for 5 minutes. The cell pellet was anaerobically resuspended in 200 mL (water), and 60 mL was immediately added to each bioreactor via syringe (n=2). As a control, 60 ml of anaerobic and autoclaved MilliQ water was added at the same timepoint (t=48 h) to an otherwise unaltered 80 g/L corn stover fermentations (n=2). Bioreactors proceeded until t = 168 h, where they are harvested as described above.

Co-culture batch fermentations with low and high solids loadings

Two additional media solutions were added to support co-culture batch fermentations of *C. thermocellum* and *T. thermosaccharolyticum.* First, a 2% (v/v) NH_4Cl solution was added with a final concentration of 2 g/L. Second, a 4% (v/v) vitamin solution was added with final concentrations of 0.004 g/L thiamine and 0.004 g/L thioctic acid. For experiments comparing monocultures and cocultures, these two additional

solutions were also given to monocultures to ensure an identical media background. Additionally, a third solution of xylose-less CTFüD was added in place of *T. thermosaccharolyticm* inoculum (4% v/v) for monocultures. The xylose-less CTFüD is identical to the aforementioned CTFüD medium, except does not include the primary carbon substrate, D-xylose. This was done to control for the presence of yeast extract persisting in the *T. thermosaccharolyticum* inoculum in the coculture runs. Fractional utilization of solubilized carbohydrates was determined based on concentrations in the unfermented feedstock, fermented solids, and spent broth as determined by quantitative saccharification protocols. Sugar utilization was calculated as one minus the mass of sugars found in the liquid phase over the theoretical mass of sugars that have been solubilized based on fermented and unfermented solids.

Declarations

Abbreviations

CBP: consolidated bioprocessing

C-CBP: consolidated bioprocessing with cotreatment

FCS: fractional carbohydrate solubilization

AD: anaerobic digestion

Av: Avicel

CB: cellobiose

QS: quantitative saccharification

LQS: liquid quantitative saccharification

CBI: Center for Bioenergy Innovation

MTC: media for thermophilic *Clostridia*

PES: polyethersulfone

MOPS: morpholinopropane sulfonic acid

CAZymes: carbohydrate-active enzymes

Authors' contributions

MRK, EKH, and LRL conceived the initial study and designed experiments. MRK performed experiments and prepared data. EKH evaluated data and with MRK designed follow-up experiments. MRK, EKH, and LRL wrote the manuscript, and MRK and EKH prepared the submission.

Acknowledgements

The authors want acknowledge POET research Inc. and Ernst Conservation Seeds for providing feedstock materials.

Competing interests

LRL is a shareholder in a start-up company focusing on cellulosic biofuel production and conversion. There are no other competing interests.

Availability of data and materials

All data generated and reported during this study is included in the published article and its additional files.

Consent for publication

All authors have read the manuscript and consent for its publication.

Ethics approval and consent to participate

Not applicable.

Funding

This work was supported by the Center for Bioenergy Innovation, a US Department of Energy Bioenergy Research Center supported by the Office of Biological and Environmental Research in the DOE Office of Science.

5. Enabling High-Solids, Aseptic, Semi-Continuous Lab-Scale Fermentation of Unpretreated Lignocellulose by Consolidated Bioprocessing

The following work has been formatted as a thesis chapter with the intent of publishing it at a later date. The tentative manuscript is presented in section 5.4 with supplementary materials appearing in the appendix.

5.1 Contributions

This project began as a master student's thesis which successfully demonstrated representative delivery of high solids in an abiotic setting. I inherited the task of realizing biological cultivations around January 2021, which took approximately two years. In this thesis, both hardware and procedures were developed to enable biological characterization, with a series of experiments aimed at validating 1) semi-continuous, 2) aseptic, and 3) high solid loading operation. Significant time and effort was spent on improving hardware, controlling fermentation conditions, formalizing data acquistion, and developing strerilization procedures. The last 6 months have been spent validating the system with a set of preliminary experiments, very much enabled with the help of a postdoctoral researcher, Annamalai Neelamegam, with follow up experiments in the near future.

5.2 Significance

In providing equipment to enable 1) semi-continuous feeding, 2) aseptic operation and 3) high solids delivery, this high solids reactor overcomes several limitations in defined cultivation at high solid loadings in conventional benchtop reactors. First, in high solids batch operation, sterilization and process control are difficult due to poor mixing. Second, in semi-continuous operation, slurry transfers using the approach reported in Liang et al., (2018) were performed by manually opening the reactor and adding slurry which is not feasible for defined cultures (189). Thus, this high solid reactor would be, to our knowledge, a first-of-its-kind lab-scale demonstration for semi-continuous bioprocessing of high solids loading of

unpretreated lignocellulose for the production of ethanol using *C. thermocellum* or defined cocultures, and a valuable tool for future strain adaptation experiments.

5.3 Highlights

- Physical operation is working well (code, electronics, pneumatics, level control, etc.).
- Controlled fermentation conditions have been enabled (pH, temperature, stirring, media).
- Data acquisition pipeline is working regularly (online data recording and offline sampling).
- Data analysis pipeline is formalized (arriving at defensible calculations/determinations).
- Ran four 15+ day semi-continuous cultivations at 30 and 120 g/L and prepared tentative manuscript for peer-review publication.
- Developed custom steam-in-place sterilization equipment and onboarded a used 30-L Sartorius steam-jacketed bioreactor.
- Weathered a laboratory move/stay hybrid workspace.
- Postdoctoral researcher is remaining on project and has finely milled corn stover available for future experiments.

5.4 Enabling High-Solids, Aseptic, Semi-Continuous Lab-Scale Fermentation of Unpretreated Lignocellulose by *Clostridium thermocellum*

Matthew R. Kubis[a,b], Galen Moynihan[a,b], Annamalai Neelamegam[a,b], Evert K. Holwerda[a,b]*, Lee R. Lynd[a,b]

a. Thayer School of Engineering, Dartmouth College, 14 Engineering Drive, Hanover, NH 03755 USA.

b. The Center for Bioenergy Innovation, Oak Ridge National Laboratory, Oak Ridge, TN 37831 USA.

*Correspondence: Evert.K.Holwerda@dartmouth.edu

Abstract

Efficient deconstruction and conversion of lignocellulose is critical to decarbonizing the current energy system. However, lignocellulosic biomass is recalcitrant to deconstruction, which is often augmented by energy and capital-intensive thermochemical pretreatment. Consolidated bioprocessing (CBP) using a native cellulolytic biocatalyst like *Clostridium thermocellum* enables both deconstruction and conversion of lignocellulose without pretreatment, yet is less technologically mature. One of the hurdles for CBP is bioprocessing at solid substrate concentrations of 150 g/L. This study aims to enable future research by developing and demonstrating operability of a custom bioreactor for conducting lab-scale CBP fermentations under industrially relevant substrate loadings. To our knowledge, this high solids reactor (HSR) would be a first-of-its-kind lab-scale demonstration for semi-continuous, aseptic bioprocessing of high solids loading of unpretreated lignocellulose. To validate the HSR performance, experiments were aimed at confirming representative solids delivery and performing semi-continuous fermentations at different solid loadings. Results demonstrated that representative delivery of solids was possible at 150 g/L switchgrass, the highest loading tested, and the system was able to cultivate defined cocultures of *Clostridium thermocellum* and *Thermoanaerobacterium thermosaccharolyticum* in a semi-continuous configuration for several weeks at low (30 g/L) and high (120 g/L) solid loadings. Using a 72-hour residence time, the steady-state fractional carbohydrate solubilization of corn stover was measured at 0.63 +/- 0.01

and 0.0.55 +/- 0.084 for 30 and 120 g/L, respectively. Lower reproducibility at higher solid loadings was generally attributed to inconsistent C_5 utilization among biological replicates.

Introduction

Climate change remains a defining challenge of our time and advancing bioenergy deployment is considered desirable to limit global warming to 2˚C by the end of the century (1,2). Biomass energy systems are effective tools for decarbonizing the fuel and transport sectors as they cycle carbon between fuel combustion reactions and plant photosynthesis (10), and enable removal of biogenic carbon dioxide (8). The use of inedible, lignocellulosic biomass is generally recognized as a target because of large potential supply and lower GHG emissions compared to edible biomass feedstocks (18). Fuels derived from lignocellulose can be generated as liquids, gases, and/or solids depending on the process. Biological conversion to liquid fuels often features ethanol fermentation in combination with thermochemical pretreatment (70–72). In order for ethanol distillation to be economically feasible, it likely requires ethanol titers in the range of 4-6% (w/w). With lignocellulose being around 2/3rd carbohydrate, required solid loadings would have to be near 150 g/L (i.e., 15% w/w solids or 15% DM) (20,38–40). However, lignocellulose presents several handling challenges at high solid loadings due to its fibrous nature, high viscosity, and non-Newtonian flow characteristics related to particles that tend to be cohesive, entangled, and non-uniform in shape and size (174). Free water is an important parameter in defining lignocellulose slurries, although there is no firm boundary between submerged (excess free water) and solid-state (limited free water), as mixing is highly dependent on several feedstock characteristics. Generally, biomass slurries will exhibit unique rheological properties depending on substrate choice, solid loading, particle size, and pretreatments (or lack thereof) (176–179,208).

There is motivation to look beyond the industry standard for lignocellulose biofuel production involving thermochemical pretreatment, added fungal cellulase, and yeast fermentation (27,37,114). Consolidated bioprocessing (CBP) with *Clostridium thermocellum* is a potentially cost-disruptive alternative technology that eliminates cellulase production costs (28,38). In comparative studies, *C. thermocellum* has been shown

to be more effective at solubilizing unpretreated lignocellulose than the industry standard fungal cellulase (128,132), and enhanced solubilization and product formation have also been reported for defined cocultures containing *C. thermocellum* and hemicellulose utilizing *Thermoanaerobacterium spp.* (49,172,173). CBP has several intrinsic advantages but remains technologically immature. Both high solids and continuous processing are characteristics found in industrial settings, but rarely in laboratory investigation of CBP.

Research pertaining to high solid loadings is inevitably limited by mixability concerns in laboratory scale bioreactors, especially in batch configuration. When there is limited free water, lignocellulose slurries behave more like a paste than a liquid, and sterilization, temperature, and pH become difficult to control. In addition to process control, mixing is essential for robust bioconversion of solids as it reduces sedimentation and increases interactions between biocatalysts and substrate (200,201). To enable research at high solid loadings, custom vessels are often designed to enhance mixability using various mechanical agitation strategies. For example, Jorgensen et al., (2007) employed free-fall mixing in a rotating horizontal drum with paddles for batch enzymatic hydrolysis or simultaneous saccharification and fermentation (SSF) of pretreated wheat straw up to 40% (w/w) (37). X. Zhang et al., (2009) used a peg-mixer to carry out high solids (up to 30% w/w) enzymatic hydrolysis batches and fermentations on pretreated pulp and poplar lignocellulose feedstocks (202). J. Zhang et al., (2009) explored custom-helical impeller designs for SSF of pretreated corn stover up to 30% (w/w) (203). Dasari et al., (2009) designed a scraped-surface horizontal bioreactor for batch enzymatic hydrolysis of pretreated corn stover up to 25% (w/w) (204). These studies report remarkably high solid loadings (20 to 40% w/w), hydrolysis yield (resulting in 158 g/L glucose in one scenario), ethanol titers (4.8 to 6.3% w/w) (37,202), and offer insight towards viscosity and agitation dynamics (203,204).

Alternative to batch, semi-continuous is another mode of operation that is of interest to researchers seeking to take advantage of decreasing solids concentration and viscosity as lignocellulose conversion proceeds (205). There are several advantages to semi-continuous operation including, but not limited to, A) reduced

viscosity: it has been previously reported that conversion processes such as pretreatment (176–178,207,208) and enzymatic hydrolysis (175) cause dramatic reductions in apparent viscosity in a process referred to as liquefaction, and a similar result was observed in Ghosh et al., (2018) for *C. thermocellum* mediated deconstruction and fermentation (209). B) Discharge of accumulating inhibitors: discharging potential inhibitors related to pretreatment (93,94), hydrolysis (124,129), or fermentation (105,210), could enable additional conversion. C) Biocatalyst to substrate ratio: maintaining a stable biocatalyst population at steady state may improve productivity as the steady state concentration of solids observed by the biocatalyst(s) will be less than in the influent feed (205).

Semi-continuous cultivations require transferring mass in and out of the reactor system which, operationally, is challenging to perform aseptically, especially for high solid loadings. In general, representative delivery of high solids slurry is far more challenging than removing fermentation broth, because of conversion-mediated liquefaction in the latter. Semi-continuous mixed culture cultivation (e.g., anaerobic digestion) of lignocellulose has been investigated at both thermophilic (189,190) and mesophilic conditions (211–215), although these studies are largely enabled by non-sterile processing. For laboratory scale research, aseptic conditions are usually necessary to properly determine how a defined culture will perform under specific circumstances. However, papers addressing high solids, semi-continuous, and sterile processing, are rare. South et al., (1993, 1994) used a fixed-volume piston sampler to intermittently feed a SSF reactor from a mixed-carboy using approximately 10% (w/w) of pretreated poplar and hardwood feedstocks (216,217). Fan et al., (2003) performed semi-continuous fermentations feeding 12% (w/w) paper sludge by slowly advancing a horizontal plug-flow towards a chopper such that the paper feed would shear and fall into the fermentation vessel placed below (205). Notably, in both Fan et al., (2003) and South et al., (1993, 1994), the authors describe sterilizing the high solids feedstock by autoclaving their feed for >12 hours, in addition to the material being already pretreated (205,216,217). Different rheological properties exist between unpretreated and pretreated lignocellulose (178,207), and most novel high solid bioreactor

designs can take advantage of upstream pretreatment to enhance sterility and alter the rheology of biomass (179,218,219).

In this study, we report a novel bioreactor system designed to enable CBP using *C. thermocellum* at high solid loadings (120 g/L), semi-continuously. In a previous study, we characterized CBP solubilization performance in batch operation from 20 to 80 g/L, beyond which mixing and sterilization became impractical in a conventional batch fermenter (43). Development of the system reported herein was primarily motivated by a desire to study defined cultures at higher solid loadings then can be operated in batch mode. Two limitations in conventional benchtop reactors needed to be overcame. First, in high solids batch operation, sterilization and process control are difficult due to mixing concerns. Second, in a semi-continuous operation, slurry transfers using the approach reported in Liang et al., (2018) were performed by manually opening the reactor and adding slurry which is not feasible using defined cultures (189). This custom bioreactor seeks to overcome those limitations using steam-in-place sterilization and a fixed-volume piston sampler and combines 1) semi-continuous feeding, 2) aseptic operation and 3) high solids delivery. This high solid reactor would be, to our knowledge, a first-of-its-kind lab-scale demonstration for semi-continuous bioprocessing of high solids loading of unpretreated lignocellulose for the production of ethanol using defined cocultures of *C. thermocellum* and *T. thermosaccharolyticum* and a valuable tool for future strain adaptation experiments.

Methods

Substrate

Abiotic representative delivery of solids was validated using switchgrass and corn stover was used for biological testing in semi-continuous cultivation experiments. Senescent season switchgrass was supplied by Ernst Biomass (Meadville, PA) at approximately 2” particle size. The switchgrass was milled via an ACM (air-classifier mill) hammer mill to 80 mesh (0.177 mm) by Particle Control Inc. (Albertville Minnesota). The corn stover was a gift from POET Research Center, LLC (Sioux Falls, SD) originally

shredded to 1” and then refined to 1/8” using a hammer mill. To aid in transferring high solids slurry, the corn stover was further milled via an ACM hammer mill to 80 mesh (0.177 mm) by Particle Control Inc. (Albertville, MN).

Microbial Strains and Growth Media

Clostridium thermocellum DSM1313 (LL1004) was obtained from the Deutsche Sammlung von Mikroorganismen und Zellkulturen GmbH (DSMZ, Liebniz, Ger.). *Thermoanaerobacterium thermosaccharolyticum* HG-8 ATCC 31960 (LL1244) was obtained from the American Type Culture Collection (ATCC, Manassas, VA). Inocula were prepared by culturing *C. thermocellum* on MTC medium (Holwerda et al., 2012) and 50 g/L microcrystalline cellulose (Avicel® PH105, FMC biopolymers, Philadelphia PA) in a pH-controlled 1.2-Liter Sartorius bioreactor. During mid-growth phase, 30-mL cell culture aliquots were transferred to 50-mL serum bottles. Cell culture aliquots were stored at -80˚C and were slowly thawed several hours prior to use as bioreactor inoculation at 2% (v/v). *T. thermosaccharolyticum* inoculum was cultured overnight on modified CTFüD medium substituted with D-xylose for cellobiose (309), re-seeded several hours prior to bioreactor inoculation in order to ensure culture viability and added to the bioreactor at 2% (v/v).

Defined Medium for Thermophilic Clostridia (MTC) was prepared as described previously (308); solution B had bioreactor concentrations of 2.12 g/L potassium citrate monohydrate ($C_6H_7O_8K_3$), 1.25 g/L citric acid monohydrate ($C_6H_8O_7 \cdot H_2O$), 1.0 g/L Na_2SO_4, 1 g/L KH_2PO_4, 2.5 g/L $NaHCO_3$, and was added at 4% (v/v). Solution C had a bioreactor concentration of 2.0 g/L urea (CH_4N_2O) and was added at 2% (v/v). An additional Solution C was added to support coculture growth and had a bioreactor concentration of 2.0 g/L ammonium chloride (NH_4Cl) added at 2%(v/v). Solution D had bioreactor concentrations of 1.0 g/L $MgCl_2 \cdot 6H_2O$, 0.2 g/L $CaCl_2$, 0.1 g/L $FeCl_2 \cdot 4H_2O$, 1.0 g/L L-cysteine HCL monohydrate ($C_3H_7NO_2S \cdot HCl \cdot H_2O$), and was added at 2% (v/v). Solution E had bioreactor concentrations of 0.02 g/L pyridoxamine dihydrochloride, 0.004 g/L 4-aminobenzoic acid, 0.002 g/L D-biotin, 0.002 g/L vitamin B12, and was added at 2% (v/v). Solution E had two additional vitamins to support coculture growth with bioreactor

concentrations of 0.004 g/L thiamine and 0.004 g/L thioctic acid. Solution TE had bioreactor concentrations of 0.00625 g/L $MnCl_2 \cdot 4H_2O$, 0.0025 g/L $ZnCl_2$, 0.000625 g/L $CoCl_2 \cdot 6H_2O$, 0.000625 g/L $NiCl_2 \cdot 6H_2O$, 0.000625 g/L $CuSO_4 \cdot 5H_2O$, 0.000625 g/L H_3BO_3, 0.000625 g/L $Na_2MoO_4 \cdot 2H_2O$, and was added at 0.5% (v/v). Each MTC solution was purged by 20 cycles of alternating N_2 gas and vacuum for 45 seconds each. After purging, solution D was sterilized for 30 min on a liquid autoclave cycle. All media solutions totaled 2.4 L, which were added using a peristatic pump and sterilizing via liquid filter (Millex®-GP, 0.22 um) (MilliporeSigma, Burlington, MA). The final volume in the holding tank is estimated at 14.0 $L_{initial}$ + 1.4 L_{steam} + 2.4 L_{media} = 17.8 L and solids are loaded corresponding to 30 and 120 g/L corn stover.

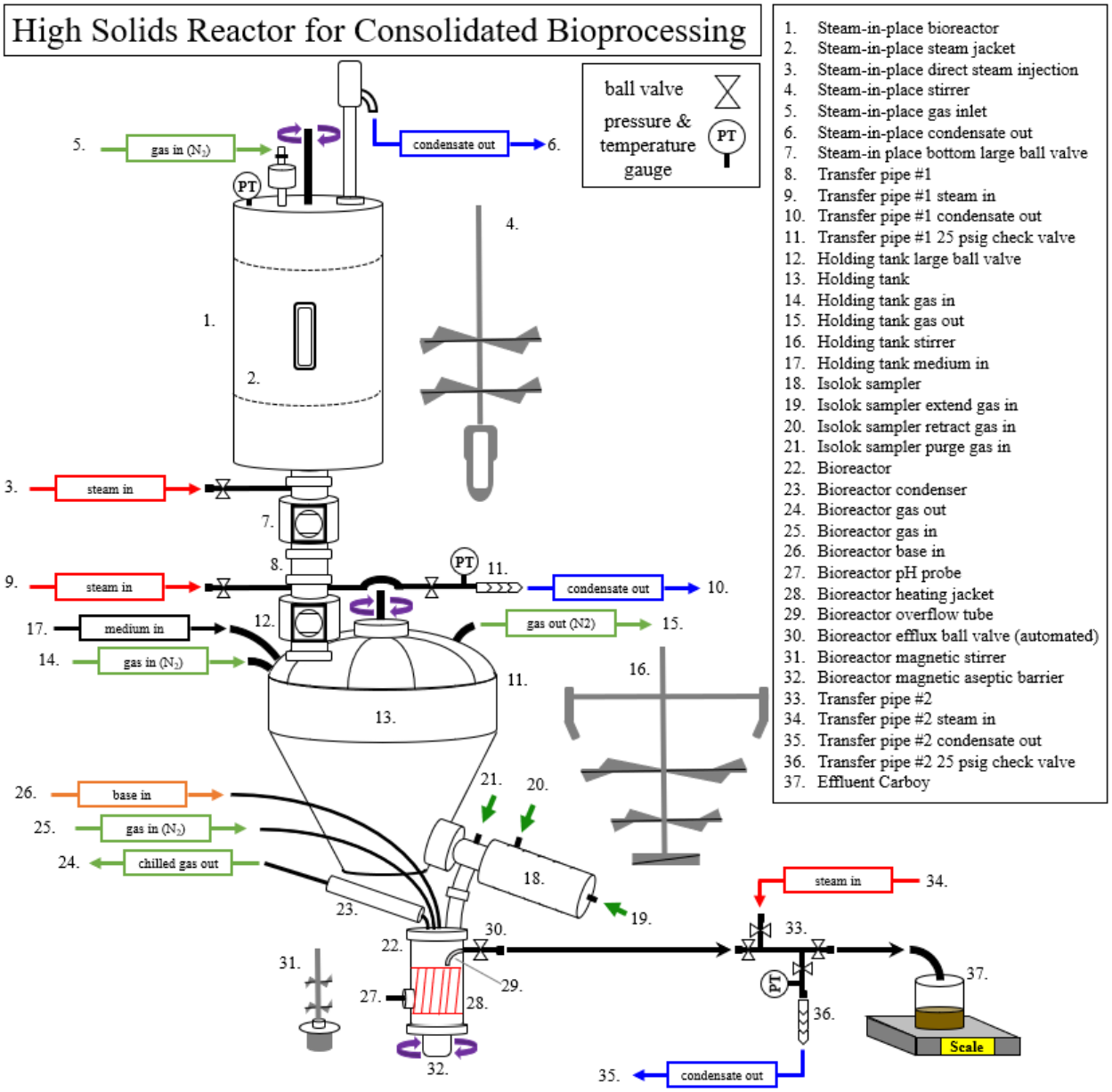

Figure 14. High solids reactor for consolidated bioprocessing with C. thermocellum. Schematic is not necessarily drawn to scale or exhaustive of all details.

Sterilization Procedure The high solids reactor described herein has four sections which are sterilized individually. The top section, a steam-jacketed Sartorius Stedim C20-2 bioreactor was used to sterilize the corn stover slurry. The assembled bottom section consisting of the holding tank, Isolok® sampler, and bioreactor and were sterilized via autoclaving. The middle section (transfer pipe #1) connects the other two sections and was steam-in-place sterilized. Lastly, another transfer pipe (#2) connecting the bioreactor to a

sterilized carboy for effluent collection was also steam-in-place sterilized. A schematic of the system is presented in figure 14.

As previously mentioned, sterilizing corn stover slurries (without media components) was accomplished using a steam-jacketed Sartorius Stedim Biotech C20-2 bioreactor. After gradually increasing the internal temperature beyond 100˚C (to avoid rapid frothing), the slurry is held for 120 minutes at 121˚C and 0.121 MPaG for complete sterilization. For the first 30 minutes only, steam is directly injected into the slurry causing a temporary increase in temperature and pressure. For the remaining 90 minutes, the slurry is held at 121˚C.. As an additional measure, 6' of constant wattage BriskHeat® (Columbus, OH) rubber heat tape was wrapped around the bottom ball valve to improve sterilization. The slurry was cooled to 55 ˚C using the jacket and an overpressure of ~0.8 MPa was manually maintained by intermittently feeding N_2 to compensate for the cooling-induced vacuum. Corn stover sterilization was initiated at 14 L and increased to 15.4 L due to direct steam injection. Continuous mixing was performed during and after sterilization of 30 and 120 g/L corn stover slurries at 100 and 150 RPM, respectively.

The bottom section, comprised of the holding tank, Isolok® sampler, and bioreactor, is autoclaved for 150 minutes at 121˚C and 0.121 MpaG. Roughly 750 mL of water is added to the bioreactor prior to autoclaving to avoid autoclaving the pH probe in a dry environment. After removing the vessel from the autoclave, sterile liquid media filters (Millex®-GP, 0.22 um) (MilliporeSigma, Burlington, MA) are attached to the holding tank for later addition of media components. Both the bioreactor and holding tank were sparged with N_2 overnight, and connected to the Sartorius vessel the next day for transfer pipe #1 sterilization. The bottom assembly was vertically aligned and lifted using a Southworth Lift-Tool™ aluminum scissor lift table with 300 lbs. capacity (Portland, ME).

Sterilizing transfer pipe #1 was accomplished by passing steam through the transfer pipe cordoned off by two ball valves. Steam, at 136˚C and 0.22 MpaG, is fed into the interior of the transfer pipe and exits through a Swagelok™ stainless steel 1-Piece check valve rated at 25 psi (Cambridge, MA) into a condensate drain for 180 minutes. Simultaneously, both of the ball valves are wrapped in constant wattage

rubber heat tape to further enable sterilization. Subsequently, the slurry was transferred from the top vessel into the holding tank below by manually opening the ball valves.

Transfer pipe #2 functions as a steam-in-place connection between the bioreactor and the effluent carboy (both autoclaved individually) to maintain culture sterility. Initial designs envisioned making this connection sterile by flame, but was replaced by steam-in-place as transfer pipe #1 was being developed-primarily to ensure culture integrity for multiple weeks or month-long experiments. Sterilization proceeded similarly to transfer pipe #1, but with smaller pipe diameters. Ball valves were manually opened and closed to perform steam-in-place sterilization.

High Solids Delivery Equipment and Tests

A Sentry Isolok® SAA automatic fixed-volume sampler was chosen to transfer high solid slurries because of its applications in chemical process slurry sampling, rugged stainless-steel body, wear-resistant seals for abrasive materials, and prior laboratory experience published in South et al. (1993, 1994) (216,217).

The holding tank was agitated using a Baldor Reliance Washdown Duty CWDM3542 motor (3/4 HP) and Toledo Gearmotor Company inline reducer M164-B (Sylvania, OH) controlled by a M-Max Series adjustable frequency drive (MMX11AA3D7) (EATON, Beachwood, OH). The controller frequency was set to 15.00 Hz (approximately 80 RPM), as any higher would cause overheating.

Abiotic feeding tests were performed starting with 20 L of slurry at 15% w/w (approx. 150 g/L) switchgrass (220). The Isolok® sampler was programmed to perform fixed-volume transfers (i.e., pumps) in quick succession for 180 samples, at which point 3 samples are manually collected to analyze mass and solids concentration. This process was repeated until the failure, i.e., when volume in the holding tank drops below the sampling port.

Semi-Continuous Feeding Cycle

Well-mixed samples of slurry were intermittently transferred from the holding tank to the bioreactor using a Sentry Isolok® SAA automatic fixed-volume sampler (Oconomowoc, WI). Individually, the slurry samples are approximately 25 mL and are successively added to the bioreactor until the required level is reached via electronic level control sensors. A simplified schematic of the feeding cycle loop can be found in figure 15 and a description of the feeding control cycle is as follows:

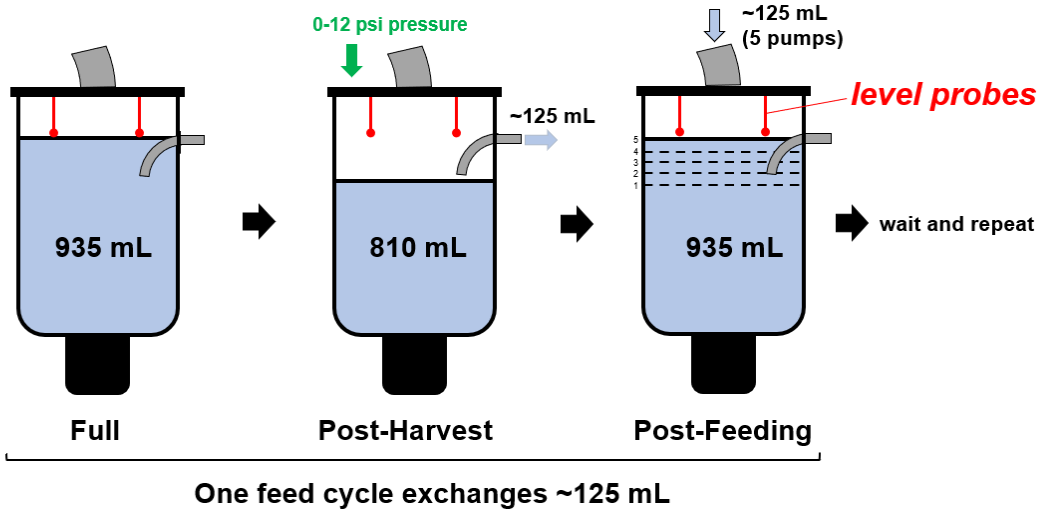

Figure 15. Bioreactor semi-continuous slurry feeding cycle loop.

Effluent Removal: Efflux ball valve (automated) (Assured Automation EVS1V) (Roselle, NJ) opens and N_2 gas is fed to the bioreactor at 12 psi, pushing fermentation broth through the overflow tube out of the bioreactor. Volume ejected depends on the distance between the level probes and overflow tube, as well as the bioreactor stir intensity related to the surface level profile. The bioreactor ejects 125 mL per feeding loop, on average.

Level Check: After ejecting spent fermentation broth, level probes measurements confirm if the bioreactor is harvested.

Feed Cycle: Actuates the piston sampler once, extending into the holding tank and retracting, delivering approximately 25 mL to the bioreactor. A short blast (0.5 seconds) of high pressure (55 psi) N_2 is intended to dislodge any solids that might not free-fall into the bioreactor below. CYTIVA WHATMAN Filter

Capsules (polypropylene, 36 mm Dia, 0.2 um pore size) (Marlborough, MA) were used filter sterilize high pressure N_2. After 1 piston cycle, a three-tier level check takes place to infer 'empty' or 'full.' All three signals need to infer 'full' in order to break out of the feeding loop. Generally, five pumps, or 125 mL, are required to achieve a 'full' signal.

Wait: With the current hardware configuration constraints, the bioreactor was considered 'full' and 'empty' at 935 and 810 mL, respectively. One feed cycle consists of 125 mL, and 935 mL / 125 mL = 7.48 feed cycles per reactor volume. For a 72-hour residence time, feed cycles were separated by 72 / 7.48 = 9.62 hours. As the holding tank is emptied over the course of an experiment, the volume transfer potentially draws a vacuum inside, which is problematic for maintaining sterility. To compensate, the headspace was trickle sparged with 'ultra pure' N_2 gas (Airgas, White River Junction VT) during whole duration of the experiment.

An Arduino Mega 2560 microcontroller board with an endless loop code structure (appendix figure A.4) was used to control the feeding regiment's electric (appendix figure A.5) and pneumatic controls (appendix A.6). Within this loop are several Boolean logic gates that automate operation using feedback from level control probes. Conductive level detection was implemented using Sartorius BIOSTAT® level/foam 80x6 mm sensor probes (BB-8844463/ BB-8844461) using digitalWrite() and analogRead() Arduino functions to transmit 5V signal between the two probes. To improve signal reliability, grounded 12 kΩ resistors were added to the level control circuit (appendix figure A.5.3).

Bioreactor Control

The bioreactor was designed to control fermentation conditions including pH, temperature, and agitation. The pH was controlled at 6.5 using a 150 mm gel-filled pH probe (Mettler-Toledo, Columbus OH) and automatic addition of 4 N KOH (Fisher, Waltham MA) via a peristaltic pump in a Sartorius Stedim Biotech BIOSTAT® A plus tower, while an A & D Company (Tokyo, Japan) EJ-6100 scale was used to record the weight of the base bottle during the experiment (see appendix A.8.2 for one example). Temperature was

monitored using the same Sartorius A plus tower, although the temperature probe only contacted the outside of the vessel. Temperature control was implemented using a BriskHeat® silicone rubber heating jacket with an SDC digital on/off k-type thermocouple automatic controller. Since both temperature probes are on the outside of the vessel, the setpoint was calibrated heuristically using an OMEGA™ OM-CP-HITEMP140 wireless autoclave temperature data logger (Norwalk, CT) for the interior to remain at (or near) 55°C (appendix A.7). To stir the bioreactor, it was assumed that bottom-entry stirring was implemented because the headplate was primarily occupied by the Isolok® sampler. Accordingly, coaxial-type magnetic couplings MTC-10-021 (Magnetic Technologies Ltd, Putnam, CT) separated by a customized stainless steel aseptic barrier were used to mix the bioreactor. An electric DC Motor (1/4 HP) (M1135045.00) with a right-angle shaft (Leeson Direct, Santa Fe, CA) rotated the outer magnetic coupling, and was controlled using a Minarik Corp. Motor Master XL C4XL3200A speed controller at 40% capacity (Minarik Drives, South Beloit, IL) which correlated to approximately 90 RPM. To avoid unintended evaporation or product loss, the bioreactor off gas was chilled using custom stainless-steel shell and tube condenser cooled with 4ºC circulating water from a VWR/PolyScience 1140A (Radnor, PA) circulating chiller.

Initializing Semi-Continuous Feeding

After the bioreactor was inoculated, it was initially run as a 24-hour batch to allow the culture to develop before semi-continuous feeding started. As described in the sterilization procedure section, the bioreactor was initially autoclaved containing water. Prior to inoculating the bioreactor, a quick succession of feeding cycles was used to flush out the water and replace it with corn stover slurry. The initial water volume slightly diluted the solid loading of corn stover during the beginning residence times (RTs) but eventually washes out. This was performed before the reactor was inoculated, at which point it is run as a 24-hour batch to allow the culture to develop before semi-continuous feeding starts. Measurements taken at 0.00 RT correspond to the end of the startup batch and start of the regular semi-continuous feeding intervals. At 120 g/L, however, additional considerations became necessary to initialize semi-continuous feeding. At this

solid loading, flushing the initial reactor water volume away with slurry is not feasible due to unreacted lignocellulose's propensity to clog, particularly at transfer pipe #2, and a more staggered approach was necessary for high solid loadings. First, the bioreactor was fed fixed-volume transfers until the level probes were reached, which generally yielded a bioreactor environment between 35 and 45 g/L solids. At this point, the bioreactor was inoculated and ran in controlled batch-mode for 24-hours. After, a quick succession of feeding cycles was used to raise the solid loading to 70-80 g/L, however, feeding cycles are well-mixed, so the system does not separate unreacted solids, reacted solids, and biocatalyst quantities when removing broth from the bioreactor. Still, this approach benefits from hydrolysis-mediated liquification taking place during the 24-hour batch. This method presents some irregularities for earlier solid loading assumptions and data acquisition but comes to steady-state along with carbohydrate solubilization. Results from a dilution spreadsheet are available in appendix tables A.8.5 and A.8.6 to estimate solids loadings during this window, and was used to calculate FCS for samples taken in the first RT during 120 g/L semi-continuous cultivations.

Sample Collection and Analysis

Samples were taken every 48 hours by attaching an autoclaved & empty 1-Liter carboy to transfer pipe #2, sterilizing for 90 minutes, waiting for bioreactor effluent removal, and removing the carboy containing approximately 125 mL of spent fermentation broth. It is replaced by another autoclaved & empty carboy is attached, and transfer pipe #2 is re-sterilized for another 90 minutes.

Three well-mixed 25 mL aliquots were transferred from the carboy to Corning Falcon® 50 mL polypropylene conical tubes (Corning, NY) to recover solids for quantitative saccharification (QS). Aliquots were spun down for 10 minutes at max speed (7,197 x g) using a benchtop eppendorf centrifuge 5430 rotor F-35-6-30 (Enfield, CT). The supernatant was decanted and saved for liquid quantitative saccharification (LQS) and fermentation product analysis. Pelleted solids were resuspended in 25 mL fresh water and spun down a second time. The supernatant was discarded, and the solids transferred to a pre-weighed aluminum dish for drying in a 55-60°C for at least 7 days.

Carbohydrate content in the residual solids was determined via QS with 72% (w/w) H_2SO_4 (Fisher, Waltham MA), as described in Sluiter et al. (307). Post-QS-sample supernatant was filtered via Spin-X microcentrifuge tubes (0.22 µm nylon) (Corning, Corning NY) before HPLC analysis. The acid-hydrolyzed monomeric sugars arabinose, glucose, and xylose were quantified by refractive index detection and separated via HPLC (Waters, Milford MA) with an Aminex® HPX-87H column (Bio-Rad, Hercules CA) operating at 60°C , 2.5 mM H_2SO_4 eluent, at a flowrate of 0.6 mL/min. Similarly, the carbohydrate content of the supernatant was determined using a mild-acid hydrolysis (i.e., liquid quantitative saccharification or LQS) adjusted from Sluiter et al. (307). Analysis of fermentation products (acetate, ethanol, formate, lactate) was performed by mixing 35 µL 10% (v/v) H_2SO_4 and 700 µL fermentation supernatant and allowing the solution to sit for > 5 min to denature proteins. The acidified solution was pelleted in a microcentrifuge (Eppendorf, Enfield, CT) at 21,130 × g for three minutes and the supernatant was filtered via Spin-X microcentrifuge tubes (0.22 µm nylon) (Corning, Corning NY). The filtrate was quantified for products via HPLC and quantified by comparison to standard solutions.

Carbohydrate solubilization was calculated relative to the carbohydrate content measured in the holding tank at the end of the experiment (appendix tables A.8.1-A.8.4). Although, for the first RT at 120 g/L, a solid loading estimation was used to determine fractional carbohydrate solubilization (see methods section on ‘Initializing Semi-Continuous Feeding’ for more details).

Results and Discussion

Representative Solids Delivery

A Sentry Isolok® SAA automatic fixed-volume sampler was chosen to transfer high solid slurries due to its applications in chemical process slurry sampling, rugged stainless-steel body, wear-resistant seals for abrasive slurries, and prior in-laboratory experience reported in South et al. (1993, 1994) (216,217). To confirm representative delivery of high solid slurries, abiotic feeding tests using 0.177 mm milled switchgrass were conducted. Smaller particle sizes were observed to have advantageous effect on

representative delivery (1.6, 0.5, and 0.177 mm tested, and 0.177 mm particle size was used for both representative delivery tests and biological testing (220). Considerable attention was given to impeller design to maintain well-mixed solids suspension in the holding tank. Notably, a custom designed wiper impeller was a necessary inclusion for representative delivery in light of solids accumulating on the holding tank walls. The results of the abiotic feeding tests are shown in figure 16.

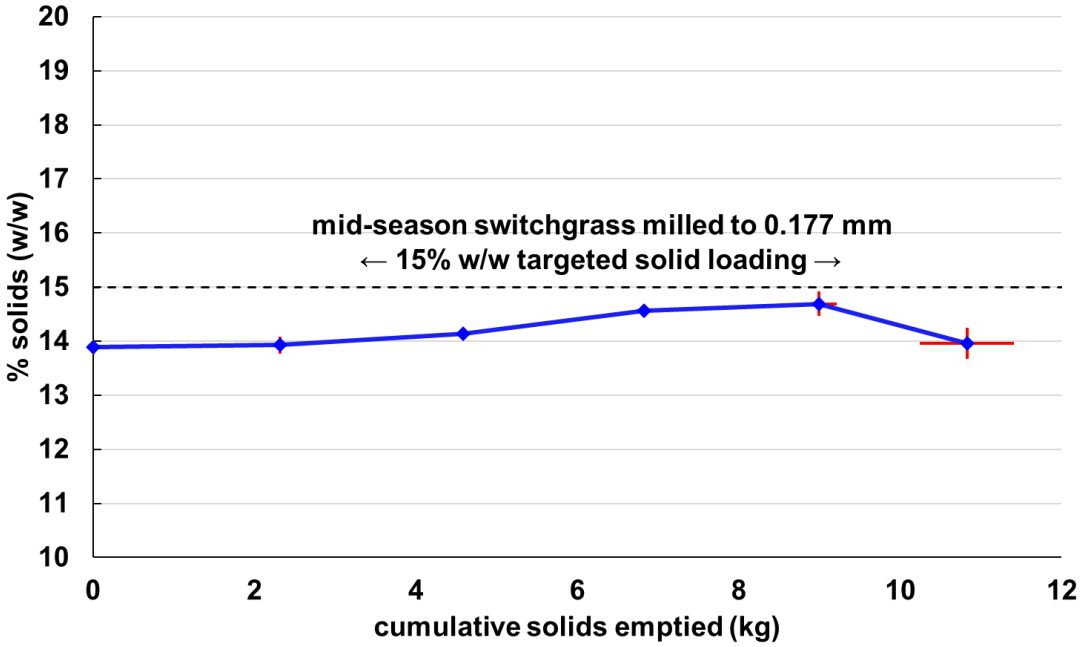

Figure 16. Representative delivery feeding tests. Delivery of high solid slurries (15% w/w) did not deviate more than 1% from the feed concentration. Datapoints represent the average of two separate feeding tests (n=2), while individual samples were taken in triplicate. Vertical error bars (red) represent one standard deviation between the measured solids concentration collected in each feeding test (n=2) and horizontal error bars (red) are included here to accommodate for differences in sample timing between the two feeding tests and represent one standard deviation with respect to the average sampling time. Figure reproduced from Moynihan MS thesis (2021) (220).

Tests demonstrated that delivery of high solid slurries did not deviate more than 1% from the feed concentration and this endured for over ten residence times, assuming a 1 L reactor volume. These initial

tests were promising in light of the apparent phase transition of 0.177 switchgrass between 50 and 200 g/kg solid loadings, displayed in several pictures available in appendix figure A.9. While measured solids were closer to 14 than 15% w/w solid loading, this deviation was both small and consistent.

Biological Testing and Validation

The high solids reactor (HSR) system was validated by performing a series of experiments at 30 g/L (low) and 120 g/L (high) corn stover loadings. We aimed to document the fractional carbohydrate solubilization (FCS) in semi-continuous controlled fermentations using a coculture of *Clostridium thermocellum* DSM1313 and *Thermoanaerobacterium thermosaccharolyticum* HG-8 ATCC 31960. Corn stover was milled to 0.177 mm particle size and underwent no pretreatment other than sterilization.

Maintaining aseptic conditions for semi-continuous fermentation initially proved a difficult task, and significant time and effort was dedicated to identifying and troubleshooting sterilization failures. As a general procedure, the HSR was divided into sub-sections to isolate sterilization failures. Confirming sterile conditions was validated using several approaches including OMEGA™ wireless temperature data logging, SPORDEX® SCBI Ampoules containing *Geobacillus stearothermophilus* spores (STERIS Corporation, Mentor, OH), transferring rich medium throughout the various subsystems without inoculation, and examining the uninoculated feed under a microscope.

Sterilizing corn stover slurry in a steam-jacketed Sartorius Stedim Biotech C20-2 bioreactor proved more difficult than anticipated. This was largely related to the presence of lignocellulosic solids, as operation was relatively straightforward using soluble substrates or model solid substrates like crystalline cellulose (Avicel® PH105). The steam-jacketed bioreactor was modified with a bottom outlet (2.21” inner diameter) terminating in a large ball valve for transferring the slurry downwards into another vessel. Mixing is advantageous, if not required, for sterilizing slurries at higher solid loadings, however, due to the modifications made to for the bottom outlet, there was functionally a 5” pipe that behaved as an isolatedregion where solids could settle. As a result, a PTFE-fitted custom impeller was designed to stir the

pocketed region above the ball valve (see figure 14). This region was also modified to allow for direct steam injection (147.5˚C and 0.35 MPa) into the slurry. This, however, was not the full extent of the problem, as the sterilization procedure for lignocellulose solids, regardless of solid loading, proved susceptible to rapid frothing or foaming when the measured internal temperature approached 100˚C. This required close monitoring and manually increasing the temperature setpoint by small (~0.3˚C) increments to avoid froth from rapidly evolving and thereby clogging the headplate with solids. Once past the boiling point (~100˚C), the overhead pressure increases, and the slurry was no longer susceptible to rapid frothing and could be sterilized. Additional details for the sterilization processes are available in the methods section.

As may be observed in figure 17, steady-state behavior with respect to FCS at 30 g/L develops quickly in the experiment, i.e., within one RT. A different result is observed at 120 g/L wherein steady-state develops closer to the third residence time. Results were more variable at 120 g/L which is possibly attributable to variable coculture behavior. Of note, fractional carbohydrate solubilization was determined relative to measured solid loading in the holding tank at the end of the experiment, except for the first residence time at 120 g/L (see methods section for additional details) when there is more uncertainty in solid loadings. Using datapoints >3 RTs (i.e., steady-state), 30 g/L corn stover yielded an average FCS of 0.632 +/- 0.009 and 120 g/L yielded 0.55 +/- 0.084.

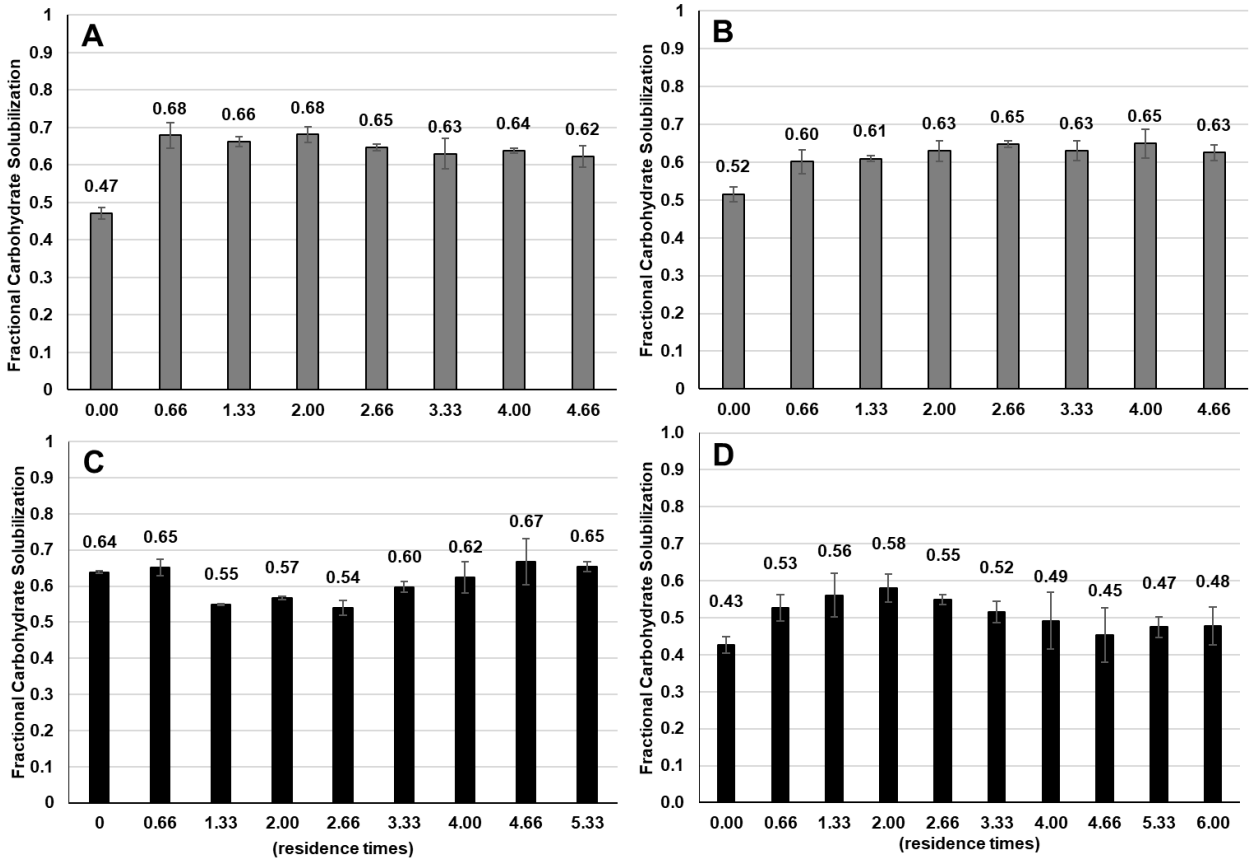

Figure 17. Fractional carbohydrate solubilization during semi-continuous fermentations. Panels depict 30 g/L (gray) (A and B) and 120 g/L (black) (C and D) corn stover cultivations at a 72-hour residence time using defined bacterial cocultures. Samples were collected every 48 hours by attaching an empty carboy to the bioreactor efflux (via transfer pipe #2). Error bars represent one standard deviation from technical triplicates. Fractional carbohydrate solubilization was determined using quantitative saccharification.

It is known that *C. thermocellum* strictly utilizes C_6 sugars and does not utilize C_5 sugars while *T. thermosaccharolyticum* utilizes both C_6 and C_5's. However, *C. thermocellum* provides the majority of cellulolytic capabilities and *T. thermocsaccharolyticum* provides primarily hemicellulose fermentation. Thus, a defined coculture provides a commensal association where *C. thermocellum* is mostly responsible for solubilizing C_5's and C_6's, both bacteria utilize C_6's, and *T. thermosaccharolyticum* exclusively utilizes C_5's. As a result, the soluble sugar utilization profiles, i.e., the degree to which solubilized sugars are taken up and converted, is heavily dependent on both coculture members growing which was not consistent across

biological duplicates in these experiments (see figure 18 below). In figure 18 panel A, we observed more glucose than expected, whereas figure 18 panel B looks very similar to previously reported cocultures (prior observations were generally arabinose ≈ glucose < xylose g/L, as measured by mild acid hydrolysis, see chapter 4). In figure 18 panel C, the xylose concentrations found in the fermentation broth are emblematic of a *C. thermocellum* monoculture, and suggests that *T. thermosaccharolyticum* hemicellulose utilization did not persist. The opposite is occurring in figure 18 panel D, which looks like a successful coculture with high and consistent xylose utilization. However, much like figure 18 panel A, figure 18 panel D also has more glucose than expected.

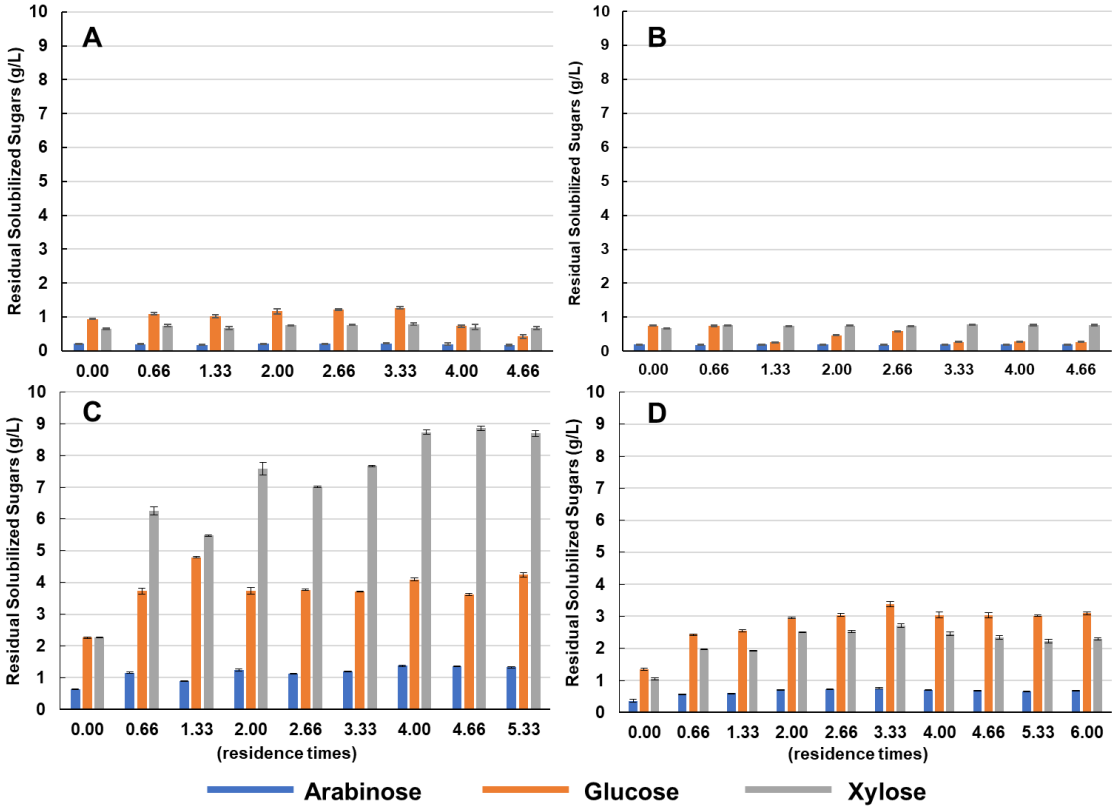

Figure 18. Residual solubilized sugars during semi-continuous fermentations. Residual arabinose, glucose, and xylose are measured in monomeric form via mild acid hydrolysis of the supernatant. Error bars represent one standard deviation from technical triplicates.

Essentially, the soluble sugar utilization problem is twofold. The first and most obvious dilemma is that seemingly no C_5 sugar utilization took place in figure 18, panel C. The second issue is that in spite of thriving cocultures, the final titers in residual solubilized glucose and xylose remain inconsistent between runs. It is probable that these two concerns are related, and as we continue to develop our methods for performing semi-continuous high solids fermentations, optimizing the conditions for hemicellulose utilization remains a top priority. The presence of a hemicellulose utilizing coculture partner has been previously reported to improve carbohydrate solubilization, however it is difficult to disentangle the effect of a coculture partner when it's survivability is not completely guaranteed. Possible explanations include, but are not limited to, non-optimum temperature and pH, growth medium, physical disruptions related to feeding (sheer forces, pressure swings, etc.), or inoculum. Although, we had implemented measures to

ensure optimal conditions were applied during these experiments. Nevertheless, we have repeatedly observed that *C. thermocellum* cultivation is not problematic, which has been a significant step towards validating HSR performance.

Fermentation product profiles are presented in figure 19. While there are many variables that influence the relative amounts of fermentation products, perhaps the two most impactful (at least from a material balance point of view) will be carbohydrate solubilization and soluble carbohydrate utilization. Thus, the fermentation product profiles reported here are heavily influenced by the data presented in figures 17 and 18. Fermentation product profiles remain fairly constant across timepoints, with the exception of figure 19 panel D. It is not immediately clear why the ethanol titers in this panel linearly tapered off past the third RT, or where that carbon could have gone. Unfortunately, the duplicate run functionally behaved as a *C. thermocellum* monoculture (figure 18, panel C), so meaningful comparisons cannot yet be made. This monoculture-like behavior observation was consistent with previous reports for monocultures of wild-type *C. thermocellum* having higher titers of acetate than ethanol (chapter 4). Also observed during only this particular experiment (120 g/L, panel C) were temporally increasing citrate and phosphate signals on the HPLC (data not shown). Low concentrations of fermentation products were measured in the holding tank at the end of each experiment. Yet, there was not overwhelming evidence that contamination took hold (see appendix figures A.10.1 and A.10.2 for additional discussion).

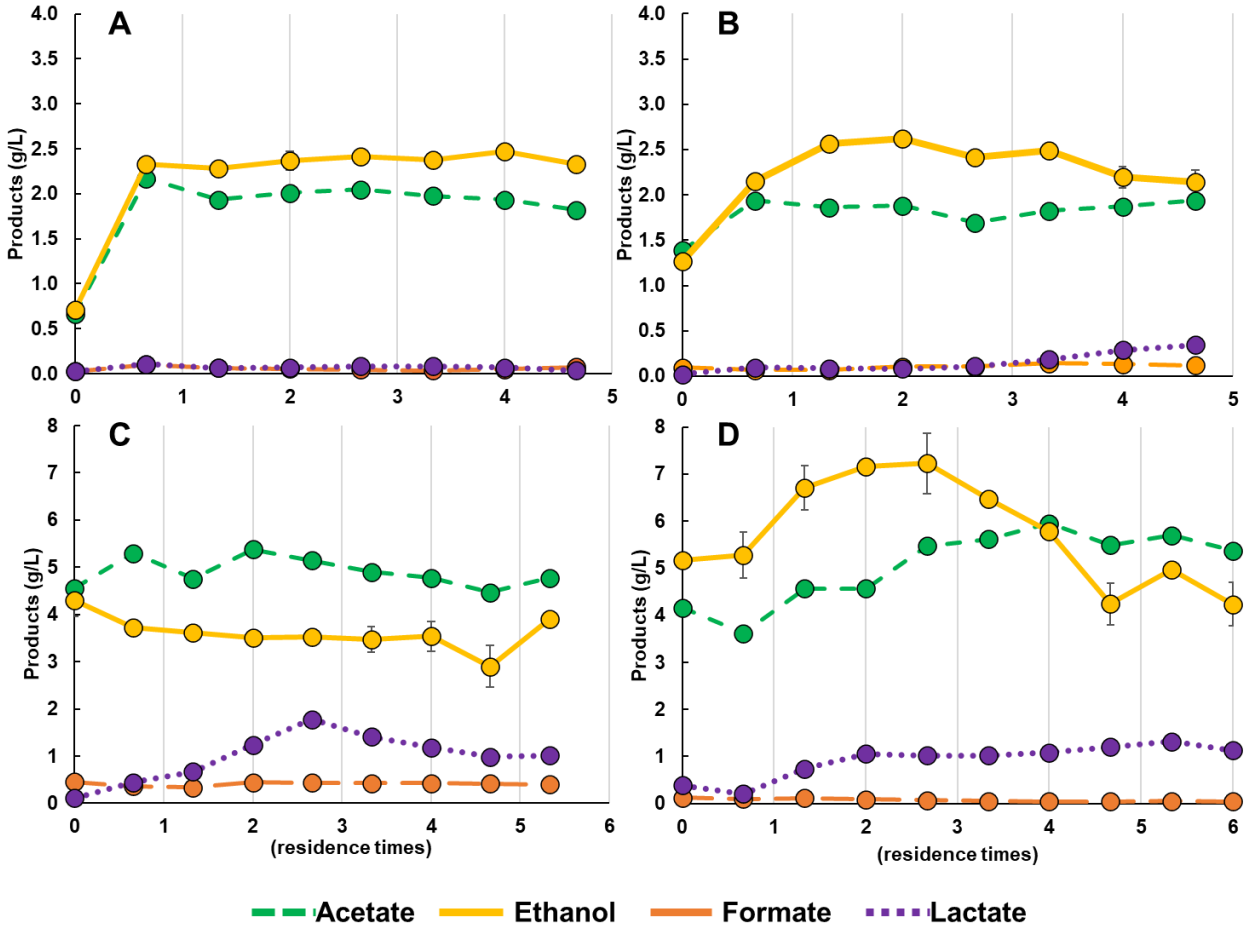

Figure 19. Fermentation product profiles during semi-continuous fermentations. Panels depict 30 g/L (A and B) and 120 g/L (C and D) corn stover at a 72-hour residence time using defined bacterial cocultures. samples were collected every 48 hours by attaching an empty carboy to the bioreactor efflux (via transfer pipe #2). Error bars represent one standard deviation from technical duplicates. Note acetate can originate as a product of fermentation or a product of the solubilization process as it is present in the feedstock as acetyl bonds.

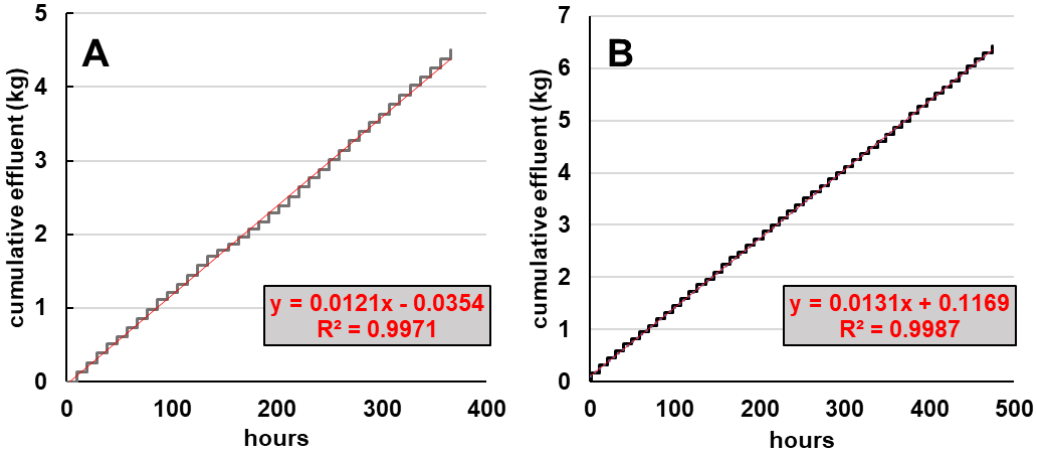

Figure 20. Cumulative effluent carboy weight during semi-continuous fermentations. Measured during biological testing at (A) 30 g/L and (B) 120 g/L.

The weight of fermentation broth harvested was monitored throughout the biological tests to validate semi-continuous behavior. The cumulative effluent weight measured in the outgoing carboy during biological testing are presented in figure 20 at both (panel A) 30 g/L and (panel B) 120 g/L. Results underscore semi-continuous feeding regularity and is a reasonable proxy for volumetric throughput assuming slurry density is similar to water at 1 kg/L. It is possible that variable slurry density could be contributing to the small differences in slope (i.e., feed rate in kg/hr) between 30 and 120 g/L experiments. These measurements, however, are subject to some fluctuations as a result of the sampling protocol which required exchanging effluent carboys every 48 hours.

Conclusions

A custom high solids reactor (HSR) system was developed to enable conducting lab-scale CBP fermentations at higher solid loadings than can be accommodated in a conventional bioreactor. The assembly combines steam-in-place sterilization, a fixed-volume sampler for slurry transfers, and automated feeding controls to enable long-term semi-continuous cultivations at high solid loadings of lignocellulose. A series of tests were used to validate the HSR performance, including experiments aimed at confirming representative solids delivery and semi-continuous cultivation. Representative delivery using the pneumatic

sampler demonstrated up to 150 g/L switchgrass with less than 10 g/L deviation. Biological testing was successfully conducted using a defined coculture (*C. thermocellum* and *T. thermosaccharolyticum*) at both 30 and 120 g/L corn stover and a 72-hour residence time. Under these conditions, steady state behavior with respect to carbohydrate solubilization was consistent between biological duplicate runs, although soluble sugar utilization and fermentation products were variable due to poor coculture reproducibility, especially at 120 g/L. Nevertheless, cultivating *C. thermocellum* was possible which remains a significant milestone towards the HSR enabling future research and development at industrially relevant conditions. In this study, the steady-state fractional carbohydrate solubilization of corn stover was measured at 0.63 +/- 0.01 and 0.55 +/- 0.084 for 30 and 120 g/L, respectively.

Acknowledgements

Fabrication: Gary “Hutch” Hutchins, Mike West, Trevor Marsh, Joseph Poissant, Dwayne Adams, Scott Ramsay, Miles Duncanson. *Electronics:* Mike West, Ali Hamlin. *Building services:* Mike West, David McDevitt, Scott Walker.

Funding

The Center for Bioenergy Innovation (CBI), which is a U.S. Department of Energy Bioenergy Research Center supported by the Office of Biological and Environmental Research in the DOE Office of Science. Oak Ridge National Laboratory is managed by UT-Battelle, LLC for the US DOE under Contract Number DE-AC05-00OR22725.

The HSR (including construction, custom manufacturing and purchasing of fabricated parts) was supported by a supplemental funding allocation from CBI to E.K. Holwerda.

6. Carbon Capture from Corn Stover Ethanol Production via Mature Consolidated Bioprocessing Enables Large Negative Biorefinery GHG emissions and Fossil Fuel-Competitive Economics

This study was recently (April 24th) accepted (with minor revisions) for publication at Sustainable Energy & Fuels. The main text is presented below in section 6.2, with supplementary materials and data appearing in the appendix. A table of contents entry, submitted with manuscript, appears below.

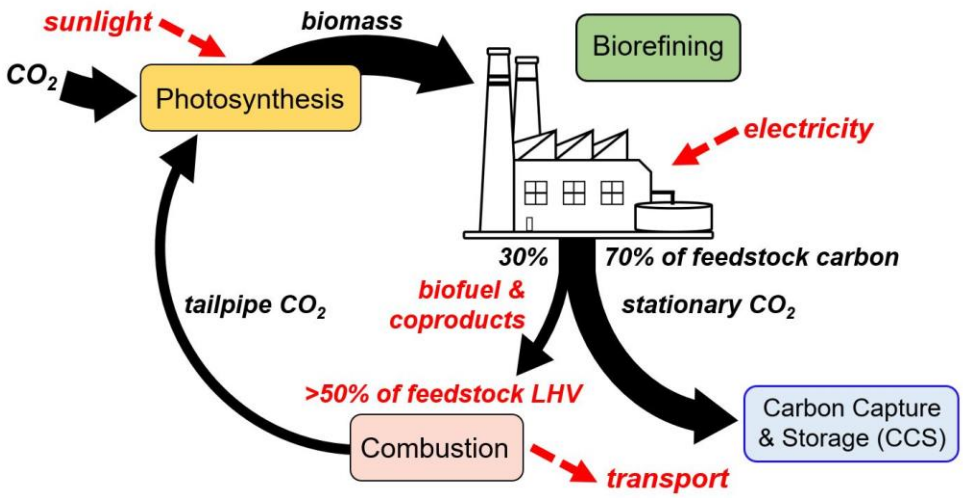

Figure 21. Biorefinery carbon and energy schematic. Illustration depicts a revised C-CBP biorefinery exporting >50% of feedstock lower heating value (LHV) while permanently sequestering nearly 70% of feedstock carbon thus reinforcing the role liquid biofuel production can play in climate mitigation stratagies. Above image submitted as table of contents entry with manuscript.

6.1 Contributions

Matthew R. Kubis: Conceptualization, Methodology, Investigation, Formal analysis, Writing – Original Draft, Writing – Review & Editing. Lee R. Lynd: Conceptualization, Writing – Review & Editing, Supervision, Funding acquisition.

With special thanks to Tom L. Richard, Dan L. Sanchez, and Mark S. Laser for useful discussions.

The entire body of work, including supplementary materials, is presented below.

6.2 Carbon Capture from Corn Stover Ethanol Production via Mature Consolidated Bioprocessing Enables Large Negative Biorefinery GHG emissions and Fossil Fuel-Competitive Economics

Matthew R. Kubis[a,b], Lee R. Lynd[a,b]*

a .Thayer School of Engineering, Dartmouth College, 14 Engineering Drive, Hanover, NH 03755 USA.

b. The Center for Bioenergy Innovation, Oak Ridge National Laboratory, Oak Ridge, TN 37831 USA.

*Correspondence: Lee.R.Lynd@Dartmouth.edu

Abstract

Process simulation and technoeconomic analysis was used to evaluate corn stover conversion to ethanol via mature consolidated bioprocessing and cotreatment (C-CBP) technology with carbon capture and storage (CCS). Process design was explored pursuant to increasing energy efficiency and greenhouse gas (GHG) emission reductions for a 60 million gallon per year facility featuring coproduction of fuel pellets, electricity, CO_2, and renewable natural gas (RNG) in various combinations. After performing heat integration for C-CBP, process heat was able to be met entirely from onsite biogas production and without any solid process residue combustion. When compared to its reference case, incorporating high-purity CCS and biogas upgrading led to a 4.3-fold improvement in net negative biorefinery GHG emissions (-85 gCO_2eq/MJ ethanol) while also lowering the minimum ethanol selling price (MESP). Recovering CO_2 from high-purity streams had a levelized cost of capture estimated between 14 to 15 \$/ton CO_2, well below current estimates for lowest-cost capture systems projected at fossil energy plants. Cellulosic ethanol production via C-CBP with high-purity CCS was generally cost-competitive with wholesale gasoline prices on an energy equivalent basis. Total carbon capture, including all potential emissions from onsite flue gas and fuel pellet coproduct combustion in addition to high-purity streams, led to net negative biorefinery GHG emissions of -157 gCO_2eq/MJ ethanol. Because C-CBP remains configurationally distinct from other biological conversion pathways with thermochemical pretreatment and added fungal cellulase, it enables a

dramatically lower cost of production while simultaneously achieving negative carbon emissions. To our knowledge, this is the first analysis of CCS for cellulosic ethanol produced by routes not involving thermochemical pretreatment and added enzymes, and the GHG mitigation potential values reported here are the highest to date for cellulosic ethanol with CCS.

Introduction

Primary energy annually supplied by non-traditional biomass energy systems is projected to expand 5-fold (from 25 to 128 EJ) by 2060 to meet climate stabilization objectives (2). Use of inedible cellulosic biomass is generally recognized as a priority in light of large potential supply, decreased competition for food resources, and lower GHG emissions compared to edible biomass feedstocks (25). Corn stover is a residue of corn grain production consisting of stalks, cobs, and husks, one of the most abundant cellulosic biomass resources in the United States, and is projected to play a central role in emergent cellulosic biofuel deployment (15,20,227). Among biologically derived fuels or fuel intermediates, ethanol distinctively combines desired features including high yield and titer, ease of separation, anaerobic production, and can be used as a fuel or as an intermediate for synthesis of higher molecular weight hydrocarbon fuels (18–20).

Determining the climate change mitigation potential of bioethanol is most often approached using a well-to-wheels life-cycle analysis in terms of CO_2 equivalent emissions per MJ ethanol (3,261,311). Net life-cycle emissions result from the sum of positive and negative emission contributions in the supply chain, biorefinery, and coproduct utilization. Positive contributions are typically feedstock production and transport, product distribution, and biorefinery emissions associated with process energy and chemical inputs. Biorefinery emissions are the largest contributor to emissions in most studies, with chemical inputs being on the order of a third of total biorefinery emissions (3,311). Land use change for corn stover production has been estimated at -0.7 gCO_2eq/MJ ethanol, corresponding to <1% of a gasoline base case (312). Net emissions are decreased as a result of avoided fossil fuel emissions (AFFE) via coproducts such as electricity generated from lignin-rich solid process residues. The chemical combustion of bioethanol is usually considered to be carbon neutral (10).

Industrial-scale conversion of corn stover to ethanol via fermentation has been studied in a variety of configurations summarized in appendix table A.9. Many studies involve thermochemical dilute-

acid pretreatment with added fungal cellulase, with widely cited studies by the National Renewable Energy Laboratory (NREL) providing detailed design and cost estimation (20,25,80,223,224). Alternative, less- developed processing innovations with potential for lower costs and emissions continue to be investigated (31,313,314). One alternative is consolidated bioprocessing (CBP) with mechanical disruption during fermentation (cotreatment) in lieu of thermochemical pretreatment (21), thereby avoiding emissions and costs related to chemical inputs and enzyme production. In this direction, Lynd et al. (2017) analyzed production via C-CBP with projected bioconversion efficiencies enabled by future research and development. This scenario eliminated thermochemical pretreatment as well as added cellulase, substituted a gas boiler for a solids boiler, and converted solid process residues into a fuel pellet coproduct rather than being burned on-site to generate electricity. As a result of lowering capital investment and increasing coproduct revenue, the authors report significantly reduced payback periods and improved GHG emission reductions per ton feedstock compared to a base-case featuring thermochemical pretreatment and added fungal cellulase.

Published assessments of GHG mitigation with biofuels have focused primarily on displaced fossil fuel emissions rather than CO_2 capture (315,316). It has been suggested that in time the value of biomass energy systems for photosynthetic carbon removal may exceed that for energy supply (15,16). Studies have recently begun to leverage carbon capture and storage (CCS) technologies to enable net negative life-cycle emissions for biofuel production (236,261–263). Yang et al. (2020) demonstrated net negative life-cycle emissions for cellulosic sorghum ethanol at -21.3 and -109 gCO_2eq/MJ ethanol for recovery of high purity CO_2 and all CO_2 emitted, respectively. In Kim et al (2020), CCS from all production emissions improved the average life cycle GHG mitigation from 67.2 to -43.8 gCO_2eq/MJ. Gelfand et al., (2020) focused primarily on impact of biomass supply chain on soil carbon stocks and report that corn stover ethanol emission intensity improved from 19.8 to -98.7 gCO_2eq/MJ with CCS inclusion. Geissler and Maravelias (2021) have also shown

CCS to enable negative GHG emissions, e.g., from 24.7 to -22.6 gCO_2eq/MJ and that only capture from fermentation was required to achieve net negative emissions. All analyses known to us of CCS applied towards cellulosic ethanol were based on processes featuring thermochemical pretreatment and added enzymes.

Commercial bioethanol production is a logical starting point technologies because of high-purity CO_2 streams (produced via fermentation or anaerobic digestion) compared to more-dilute onsite flue gas. It has been reported that the levelized cost of CO_2 capture scales inversely with concentration (264). The cost of separating CO_2 from dilute flue gas (< 20% CO_2) is projected to be between \$30-\$70/ton before compression can be performed (5,263,264,266,267,317,318), whereas during ethanol fermentation, nearly pure CO_2 is generated as a saturated gas at low to atmospheric pressure (319). Largely related to separation costs, capturing CO_2 from combustion diluted flue gas requires around 10-fold more energy than from fermentation sources (263). Onsite biogas, an intermediate stream generated during anaerobic digestion (AD) of thin stillage, consists of roughly 50/50 (v/v) CH_4 and CO_2. Biogas upgrading via membrane separation is a promising technology that can deliver high-purity streams of both methane (i.e., renewable natural gas or RNG) and CO_2 (236,320,321). Collectively, the total levelized cost of sequestration for high-purity and dilute flue gas sources are generally around \$30-50/t CO_2 and \$70−\$120/t CO_2, respectively (236,259,267,269,318).

To date, there have been numerous studies investigating the CCS potential at fossil energy plants (317,318,322), industrial sectors (264,266,267), and corn ethanol production (251,267,269,319,323–325). Prior studies of CCS applied to cellulosic biofuel production have been limited to processes involving thermochemical pretreatment and added fungal cellulase (236,261–263). A knowledge gap thus exists with respect to evaluating the CCS potential of other process concepts, which we address here for C-CBP. Specifically, we present an updated technoeconomic evaluation of corn stover ethanol via C-CBP aimed at increasing energy efficiency

and leveraging alternative coproduction strategies including CCS for revenue and climate stabilization benefits. Minimum ethanol selling price (MESP) and net biorefinery GHG emission reductions are evaluated and presented.

Methodology

Scenario Definitions and Methods

This study builds on the previous report of Lynd et al. (2017) that described the performance and cost of a simulated cellulosic ethanol biorefinery featuring C-CBP intended to represent long-term potential (21). Material and energy flows were modeled using ASPEN PLUS^{tm} (V10) process simulations and economic analyses were adapted from the NREL study of corn stover-to-ethanol by Humbird et al. (2011). In the updated technoeconomic analysis presented here, changes were made to the process simulation without changing major conversion parameters related to ethanol bioconversion efficiency, e.g., solid loading (19.5 wt.%), carbohydrate solubilization (88%), fermentation yield (0.46 g/g solubilized carbohydrate or 85.6 gallons per dry metric ton feedstock), and ethanol throughput (60 million gallon per year). A summary table of fermentation conditions and conversion parameters is available in appendix table A.9.

New scenarios were analyzed stepwise incorporating the following design features: 1) enhanced heat integration, 2) biogas surplus to electricity generation using a gas turbine, 3) fermentation-CO_2 capture for carbon capture and storage, 4) biogas membrane upgrading with biogas-CO_2 capture and surplus RNG sales and lastly, 5) an RNG turbine to generate electricity instead of selling surplus RNG. These scenarios were evaluated with respect to greenhouse gas emissions, minimum ethanol selling prices (MESPs), and CO_2 levelized costs of capture. A summary description of scenario inputs, outputs, and GHG benefits are presented in appendix table A.13. Technical details regarding the scenario modifications are described in the sections immediately below.

Scenario I – Enhanced Heat Recovery

Increasing the operating pressure of the distillation train (both the beer and rectification columns) from 1 to 3.2 atm was implemented to recover the latent heat in overhead vapor condensation via heat exchange

and generated saturated steam to inject during feedstock pasteurization. In the advanced case described in Lynd et al. (2017) (21), referred to herein as the reference case, process steam supplied the heat duty both to distillation (38.5 MMkcal/hr) and feedstock pasteurization (23.4 MMkcal/hr) while a distillation-related heat duty of similar magnitude (-20.3 MMkcal/hr) was lost to the ambient environment by an air-cooled rectification column condenser. Redirecting the air-cooled condenser duty for pasteurization was the primary source of heat recovery in this study. A summary diagram for enhancing recovery is depicted below in figure 22.

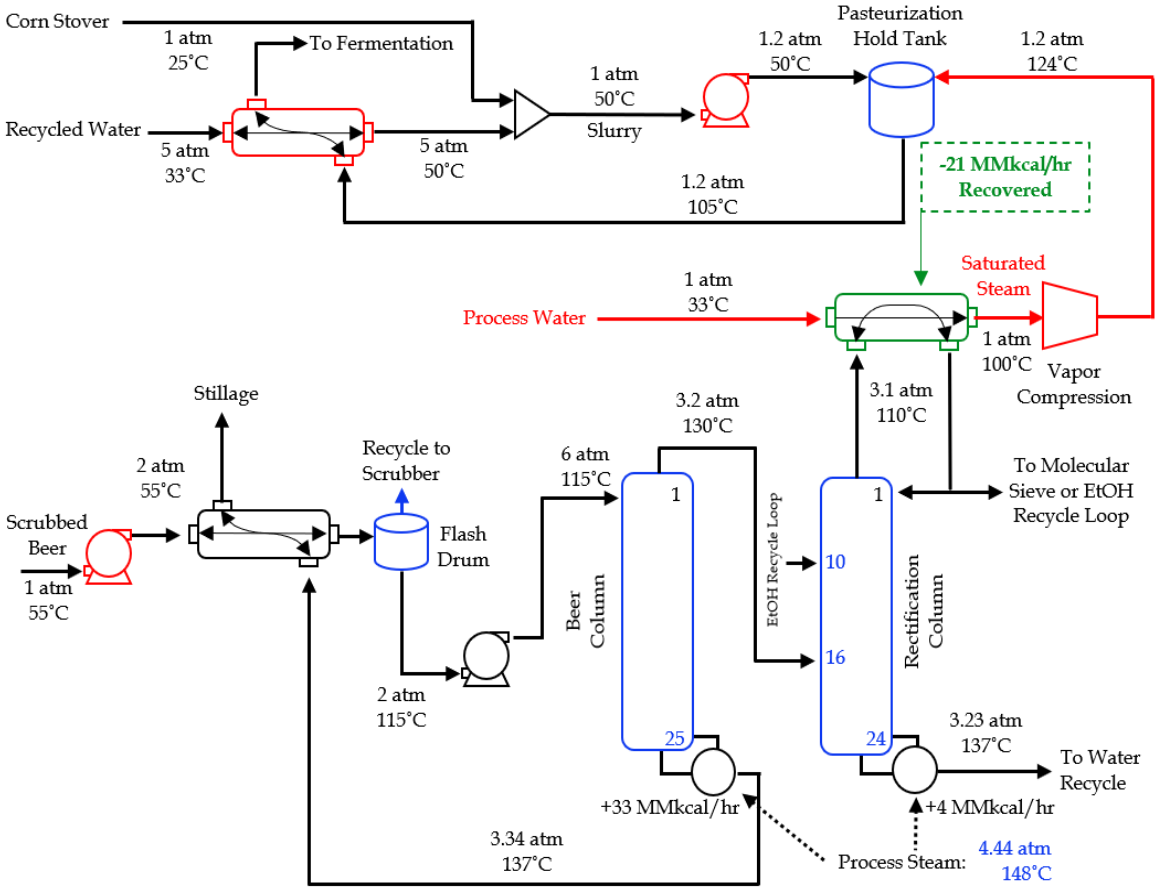

Figure 22. Heat recovery diagram. Modifications made to the existing equipment are depicted in blue and newly installed equipment in red. Exchanging the air-cooled condenser with a shell-and-tube heat exchanger (in green) enabled low-grade steam generation which was compressed and injected for pasteurization. Distillation operating pressure was increased from 1 to 3.2 atm to enable waste heat recovery.

In the revised beer column, the overhead vapor condenser was omitted with wet ethanol vapor leaving the top stage instead of a vapor side draw, resulting in a conventional stripping column. A pump discharging the beer stream at 2 atm was added to the upstream scrubber recycling loop to promote CO_2 separation prior to distillation. The beer stream was then preheated to 114˚C using a beer stillage economizer, and an adiabatic vapor-liquid separation at 2 atm and 114˚C was performed to recycle CO_2 back to the water scrubber. The CO_2 removal by the upstream scrubber/recycle loop was > 99.9%, with less CO_2 remaining in the distillation feed than in the Humbird et al. design (20). Ethanol leaving in the bottoms was fixed at 0.05% mass fraction by varying reboiler duty. The operating pressure was set at 3.2 atm, and the stage number was increased from 16 to 25. In the revised rectifying column: operating pressure was also increased to 3.1 atm, and the stage number was reduced from 35 to 24. A pressure drop of 0.006 atm per stage was assumed. Across both columns, the total number of stages was kept constant relative to the reference case, though stages were moved from the rectification column to the beer column. In the revised rectification column, the feed stages for the wet ethanol vapor and molecular sieve recycle loop were set to stages 16 and 10, respectively. Ethanol leaving in the bottoms was fixed at 0.05% mass fraction by varying the distillate rate. The ethanol-rich vapor was fixed at 92.5% mass fraction by varying the reflux ratio. In both columns, stage number and feed stages were decided heuristically based on separation performance and heat demand. The low-pressure saturated steam was compressed (75% isentropic efficiency) to 1.2 atm and 124˚C to inject into pasteurization. Saturated process steam (generated via the gas boiler) was changed from 2.1 to 4.44 atm to fire the distillation columns at elevated pressure (3.2 atm).

The pasteurization procedure was revised to reflect anticipated operating conditions of a cellulosic ethanol facility. Holding of the unfermented corn stover slurry was changed from 100℃ & 1 atm for an hour in the reference case to 105℃ & 1.2 atm for thirty minutes in the revised scenarios (I-V). An additional pump discharging the slurry at 1.2 atm was used to feed the pasteurization tank. Injection of the steam generated by condensing distillation vapor as described above was the primary supply of heat; however, it became necessary to feed the recycled water at 50℃ instead of 33℃ to reach pasteurization temperature. A spiral

plate heat exchanger was included to recycle heat from the hot stream leaving pasteurization (105˚C), and roughly a quarter of available heat remaining in the pasteurized, hot corn stover slurry was used in feed water preheating (33˚ to 50˚C) with the remaining heat duty chilled by the cooling tower.

The purchase cost for the distillation train at elevated pressure was adapted from Humbird et al. (2011), as the original cost estimate was designed for an operating pressure of 2 atm and the pressure cost factor is not expected to change significantly from 2 atm to 3.2 atm (221). Some equipment changes were made to reflect the new design. The purchase cost for a beer column condenser was deducted, and the purchase cost for the air-cooled condenser was replaced with a water-cooled shell-and-tube condenser. A compressor was added for mechanical steam compression. For pasteurization, an additional pump and spiral plate heat exchanger was included and the capital cost for the tank was calculated using the revised hold time. A summary of all revised capital equipment purchase costs can be found in appendix B (online supplementary materials).

Scenario II – Biogas Electricity Generation

Partial on-site electricity production was investigated to realize value from the excess biogas made available by the enhanced heat integration strategy described above. Biogas turbine systems operate similarly to their natural gas turbine counterparts except for the presence of CO_2 in the fuel stream (274–276). Comparing gas and biogas turbines, it has been previously reported that biogas turbines demonstrate higher heat recovery and turbine efficiency, but overall lower net efficiency due to power requirements in fuel compression. However, the net power output is nearly constant regardless of fuel composition after accounting for fuel compression and overall performance is not expected to differ significantly (275,276).

Gas turbine performance parameters were adapted from the literature as specified in appendix table A.11 (276,321,326,327). Heat recovery from turbine exhaust is common in combined cycle gas turbine platforms, and heat-to-process-steam was implemented here rather than generating additional electricity via steam turbines. Hot turbine exhaust (675-698°C) was used to partially vaporize process condensate (148°C) from distillation in a spiral plate heat exchanger using a hot/cold outlet temperature approach of 10 ˚C, and the cooled exhaust (158°C) was vented to the environment. Capital cost estimation for the turbine and heat

exchanger are available in appendix B (online supplementary materials). An iron-oxide sponge for biogas desulphurization was adapted from Abatzoflou and Boivin (2008) but not expressly simulated (273). Capital costs for desulphurization equipment were also applied to the reference case.

Scenario III- Biogas Electricity & Fermentation CCS

Design parameters and capital costs for on-site CO_2 compression were adapted from the NETL technical report *Cost of Capturing CO_2 from Industrial Sources (2014) DOE/NETL-2013/1602*. A reciprocating compressor delivers fermentation CO_2 at 15.3 MPa and 49˚C, conditions suitable for pipeline transportation (264,267). Pipeline instead of truck transport was assumed to be more cost effective considering the annual estimated CO_2 production would be well above >0.1 million tons of CO_2 per year, i.e., an approximate cut-off for truck transport (264).

Interstage cooling and dehydration was simulated to reduce water content in the CO_2 stream (264,328). In the reference case, fermentation off-gas underwent water-scrubbing to capture any volatilized ethanol which results in a CO_2 stream with 2.4% water content by mass, above the specified conditions for transport: 50-840 ppmv (12). A five-stage compressor with interstage cooling was simulated where low pressure CO_2 (0.101 MPa) was first compressed to moderate pressure (3.8 MPa) using three stages, cooled to 28˚C for vapor-liquid separation and compressed to high pressure (15.3 MPa) using the remaining two stages (328). Vapor-liquid separation flash drums were intended to simulate various interstage coolers and knockout vessels used to decrease temperature and remove moisture. High pressure CO_2 was cooled to 49˚C for vapor-liquid separation removing a cumulative of 98.8% of H_2O and leaves the CO_2 stream with 74 ppmv water content at 15.3 MPa. The electricity demand for CO_2 compression was determined in ASPEN using compressor isentropic and mechanical efficiencies of 88% and 99%, respectively.

Scenario IV – RNG & High-Purity CCS

Biogas upgrading via membrane separation into renewable natural gas (RNG) which was assumed necessary to sell surplus biogas/methane generated as described in Scenario I. Biogas upgrading performance parameters were adapted from Deng and Hägg (2010) (320) to purify CO_2 and upgrade CH_4

in a 2-stage configuration with symmetric cascade recycling using polyvinylamine/polyvinylalcohol (PVAm/PVA) blend membranes and are recapitulated in appendix table A.12. Capital costs were also adapted, and electricity demand was determined using ASPEN simulations. The module lifetime was increased from 20 to 30 years by including two additional hollow fiber membranes each with a 5-year lifetime. Equipment cost estimates were scaled in proportion to the biogas feed rate (appendix table A.12, shown in brackets). Compressors were sized using a six-tenths exponent (20)and membrane modules were scaled linearly. Capital costs are presented in appendix B (online supplementary materials).

Scenario V – RNG Electricity and High-Purity CCS

The biogas turbine from scenario II was placed downstream from the biogas upgrading described in scenario IV. As with surplus biogas, only a fraction of the total RNG (i.e., the surplus) was routed to the turbine (approximately 38%) whereas the remainder was combusted specifically for process heat. Because RNG is delivered from the biogas membrane upgrading module at 20 bar, no additional fuel compression is required for gas turbine operation, which improved the modular thermal efficiency relative to firing-biogas (appendix table A.11).

Solids Combustion, Electricity Generation, and Flue Gas Capture

The following adjustments were made to Scenario V to study the differences between fuel pellet and electricity coproduction regarding MESP and GHG reductions. Fuel pellets revenue, capital expense, and electricity consumption were removed from project economics. The gas boiler (2.5 MM$) was replaced with a solids boiler (46.2 MM$), and a 42.2 MW steam turbogenerator was added to the project (18.2 MM$) (27). Capital costs associated with capturing CO_2 from flue gas were adapted assuming amine-based absorption and stripping (including compression) as reported in Kim et al., (2012) (329). The direct cost estimate was assumed to scale linearly (4.4-fold to 35 MM$). Operating costs associated with capturing CO_2 from flue gas were adapted from Geissler and Maravelias (2021) (263). Heat required to capture flue gas was provided by natural gas at a rate of 325 kg/hr. Electricity required to capture flue gas totaled 9.0 MWh and was deducted from the electricity produced onsite. The steam turbogenerator loop reported in

Humbird et al., 2011 generates 41.37 MWh electricity, but also includes extracting steam at high-pressure (12%) for thermochemical pretreatment and at low-pressure (35%) for distillation (27). Considering ethanol throughput is nearly equal, distillation duty should remain similar while the generated electricity was adjusted to 47.0 MWh to compensate for absence of high-pressure steam extraction. Exported electricity revenue was determined assuming a selling price of 0.0681 $/KWh (EIA, 2019 US total average). Solid residue combustion was adapted from Humbird et al., (2011), which produced flue gas at 20% CO2 by mass (27). Flue gas CO_2 capture yield was assumed to equal 85% (329), generating approximately 0.524-million-ton CO_2 per year.

Economic Analysis

Project economics were determined using the financial assumptions in Humbird et al. (2011), including 40% equity, a 10-year loan at 8% interest terms, and n^{-th} plant assumptions. Minimum ethanol selling price (MESP) was determined using a 10% discount rate over a 30-year project lifetime. A 7-year MACRS (modified accelerated cost recovery system) depreciation schedule was assumed for capital investment. Capital and operating costs were estimated for project year 2019, including the corporate tax rate of set at 21%. All scenarios were assumed to have identical indirect costs. For calculating additional direct costs, CO_2 compression and pellet production capital equipment were considered inside battery limits (ISBL).

Corn stover feedstock cost was assumed to equal $81.37/dry metric ton according to the Herbaceous Feedstock n^{th}-supply state of technology (SOT) report by the Idaho National Laboratory (INL) (330) and reflects preprocessed corn stover delivered to the reactor throat at the biorefinery. Fuel pellet price was determined using data available through the US Energy Information Agency (EIA) (331). The 2019 annual average domestic price for densified biomass fuel was selected for this analysis at $166/ton. A sensitivity analysis for fuel pellet selling prices towards MESP was included in appendix figure A.13.1. The 2019 annual average price for industrial electricity was $0.0681/kWh, (EIA) (332). No market value was assigned to excess biogas in scenario I that was not utilized or upgraded. A selling price of $50 per ton of CO_2 was chosen in light of the supply chain logistics not included in this analysis (transportation, injection,

monitoring) (236,269,333–335). The US tax credit for carbon sequestration was recently (2022) raised from $50 to $85 per ton CO_2 for geologic storage (253).

GHG Accounting

Relative biorefinery GHG emissions were determined focusing on the cellulosic ethanol manufacturing facility and MJ ethanol as the comparative metric (g CO_2 equivalent per MJ ethanol). Simulated mass and energy balances were used to determine biorefinery greenhouse gas emissions. Emissions related to the corn stover supply chain were estimated at 59.92 kg CO_2eq per metric ton (GREET® 2022 v1.3.0.13991) (18,19,229). Life-cycle emissions related to ethanol/coproduct transport and distribution were not considered in this analysis. Geologic CO_2 storage and avoided fossil fuel emissions (AFFE) for products other than ethanol were included in the GHG accounting. The carbon displacement factor for fuel pellets was determined to be 0.61 by dividing the LHV of fuel pellets (16.3 MJ./kg) by the LHV of bituminous coal (29.0 MJ/kg). Thus, for each CO_2 equivalent in fuel pellets utilized (i.e., combusted), 0.61 of CO_2 equivalents related to coal combustion are avoided. A sensitivity analysis for fuel pellet fossil fuel displacement towards net biorefinery GHG reductions was included in appendix figure A.13.2. RNG was assumed to have a 1:1 carbon displacement factor with natural gas on a CO_2 equivalent basis. Nutrient inputs to support biological growth were added in the form of corn steep liquor and urea, which were assumed to have carbon intensities equal to 0.935 and 0.878 gCO_2eq/g (GREET® 2022 V1.3.0.13991) (18,19,229). The carbon emissions related to grid electricity consumption were calculated as 0.417 kg CO_2/kWh using the 2019 national averages for CO_2 emissions related to electricity generation and emissions provided by the US EIA (appendix B) (online supplementary materials) (332).

Results and Discussion

Carbon and Energy Balances

Process design scenarios were analyzed in a stepwise fashion with the later scenarios including features from previous scenarios (appendix table A.13). The fate of feedstock carbon and energy is depicted in figures 23 and 24 respectively. Adjustments considered here did not dramatically affect fractional energy

recovery in final fuel products apart from eliminating natural gas in Scenario I. This is largely attributable to unchanged conversion parameters leading to equal production of ethanol and fuel pellets across all the scenarios.

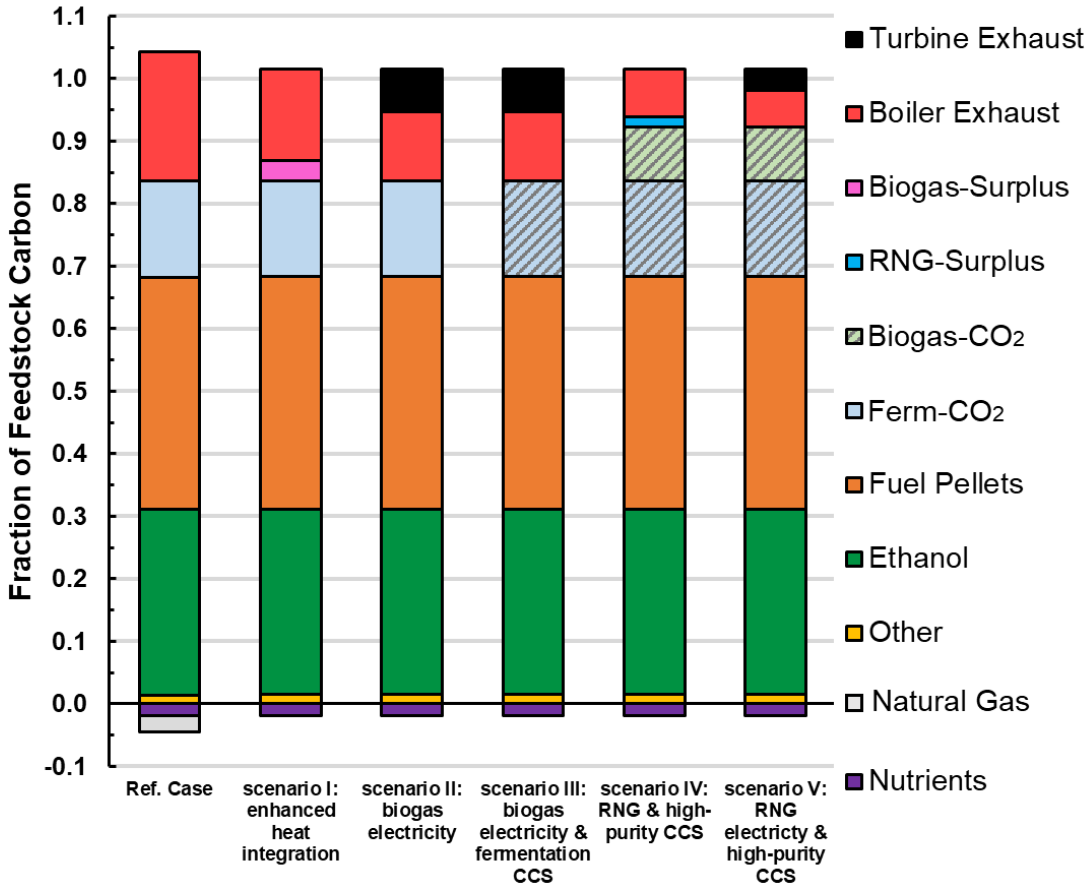

Figure 23. Carbon balances represented as terminal fraction of feedstock carbon input. Material Balances generated using ASPEN PLUS process simulations. Dashed bars represent high-purity CO_2 streams purposed for carbon capture and storage.

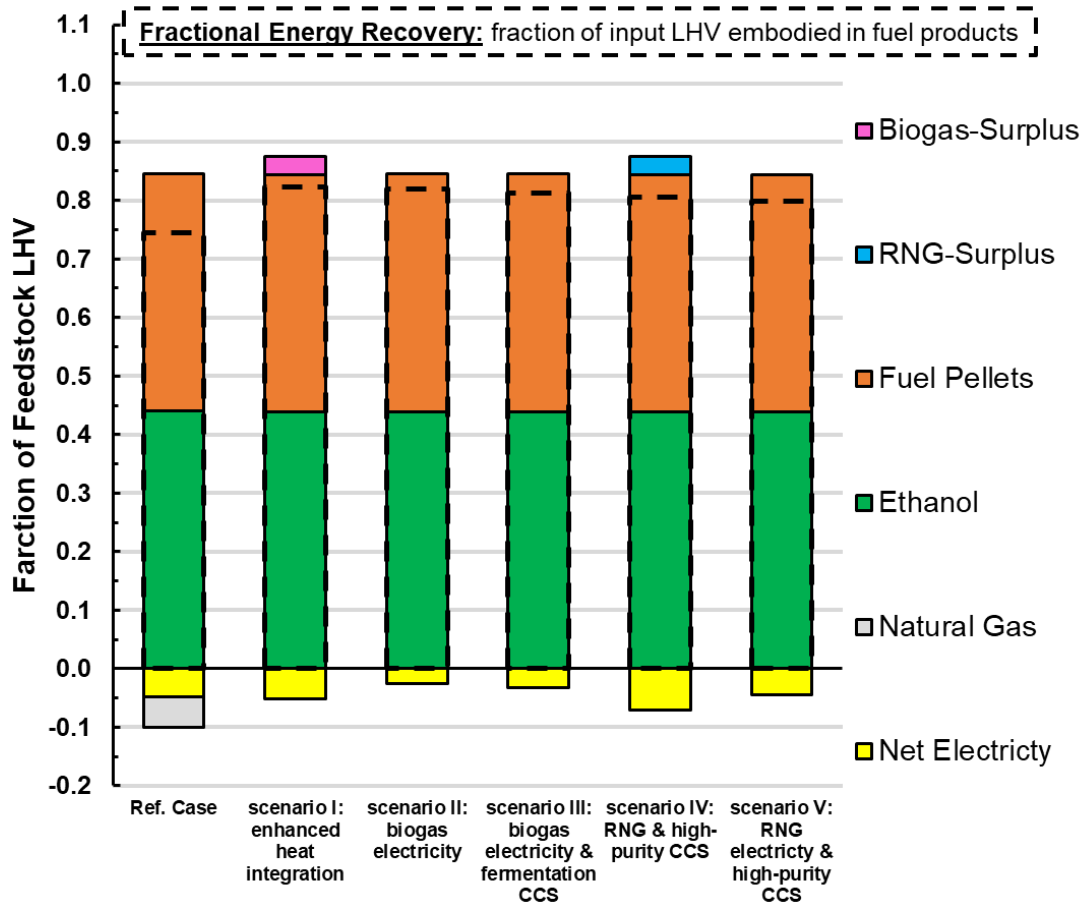

Figure 24. Energy balances represented as terminal fraction of feedstock lower heating value (LHV). Fractional energy recovery (black dashed bars) represents the fraction of feedstock energy input embodied in terminal fuel products and is the sum of positive and negative contributions seen above.

In scenario I, enhancing heat recovery completely eliminated natural gas consumption in the reference case (used for process heat) and led to a surplus of biogas available (17.5% of total). Fractional energy recovery, defined by the fraction of input LHV leaving in fuel products, increased by 8% by enhancing heat recovery in scenario I. Similarly, Pourhashem et al. (2013) also found that onsite biogas from stillage can meet steam demands without lignin/solids combustion (248). In scenario II, surplus biogas was used to generate electricity onsite via a gas turbine, with 61% of the biogas fed to the steam boiler and 39% fed to the turbine. Recovering heat from turbine exhaust enables a larger fraction of biogas (39% instead of 17.5%) to be routed towards the turbine for electricity generation. By producing electricity from surplus

biogas, externally supplied (grid) electricity consumption was reduced by 49%, relative to the reference case. In Scenario III, near-pure CO_2 produced by fermentation is compressed in advance of transportation and storage, representing 15.4% of feedstock carbon input. There was a 16.4% increase in total electricity demand for compression of fermentation CO_2, resulting in approximately 7.3 kg CO_2 compressed per kWh consumed. From a GHG perspective, this compares favorably with the current (i.e., 2019) grid carbon intensity 0.417 kg CO_2 per kWh (see methods). In scenario IV, biogas membrane upgrading was included, and the total supply of RNG was split 82.5% & 17.5% between supplying process heat and sold surplus RNG, respectively. This generated an additional fuel stream, surplus RNG, but required 43% more grid electricity consumption than the reference case due to membrane separation and CO_2 capture compression demands. Biogas membrane separation enabled an additional 8.6% of feedstock carbon to be captured from biogas. Combining the CO_2 streams from fermentation and biogas resulted in nearly of quarter of feedstock carbon (24.0%) available for permanent geologic storage. Of note, this result was obtained without any CO_2 separation from dilute flue streams, i.e., the boiler or turbine exhausts. Lastly, in scenario V, utilizing surplus-RNG onsite to generate electricity via a gas turbine (instead of selling surplus RNG) enabled biogas-CO_2 to be captured while also offsetting grid electricity consumption (figure 24). Scenario V required roughly the same amount of electricity as the starting reference case while also delivering a significant fraction (i.e., 24.0%) of feedstock carbon input to permanent geologic storage. Regarding uncaptured yet stationary exhaust emissions, in scenario V only 9% of feedstock carbon input is emitted via onsite combustion (figure 23), and the bulk of potential flue gas carbon (37%) is leaving the facility as coproduct fuel pellets.

Capital Investment, Costs, and Revenues

The installed capital investment for each scenario is depicted in figure 25. Total capital investment for a 60 million gallon per year (MMgal/yr) facility varied between 270-325 MM$. These compared favorably with the Humbird et al. (2011) total capital investment estimate of 488 MM$ (adjusted to 2019$) for a 61 MMgal/yr facility using a conventional processing paradigm involving thermochemical pretreatment and

added fungal cellulase. The gas turbine capacity was approximately 9 MW and estimated at 7.0 MM$ for scenarios II, III, and V. The capital investment for fermentation-CO_2 compression was 6.7 MM$ (scenario III) and 8.7 MM$ for scenarios with additional biogas-CO_2 compression (IV & V). Capital expenses related to biogas upgrading via membrane separation totaled $17.9 million (scenario IV and V). Generally, the capital investments that enable additional GHG reductions presented throughout this study were small compared to the 285 MM$ total capital investment required for the reference case.

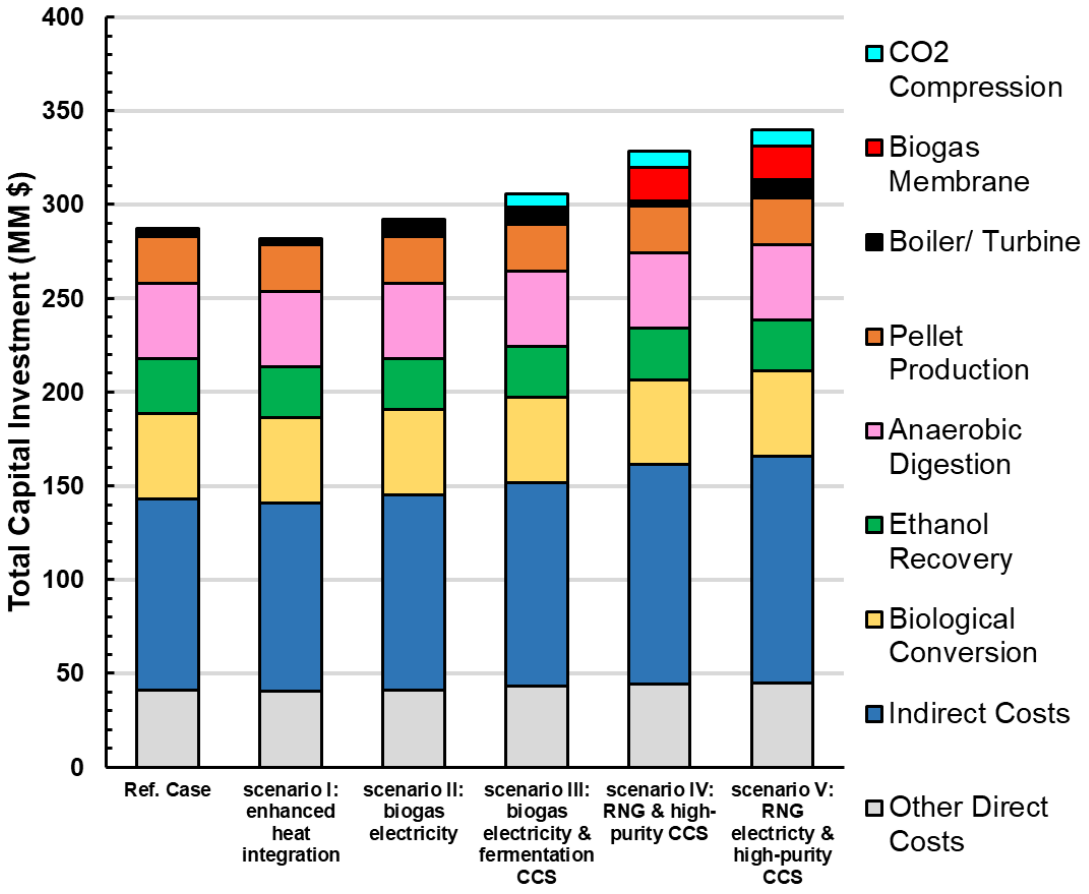

Figure 25. Total capital investment. All scenarios generate 60 million gallons per year (MMgal/yr) and processes 2,000 dry metric tons of corn stover per day. Capital equipment purchase cost estimation and a summary of total capital investment is available in appendix B (online supplementary materials).

Product revenue and operating costs for each scenario are depicted in figure 26. Note that ethanol revenue was determined by multiplying ethanol output (equal among all scenarios) by the scenario MESP, which led to different ethanol revenues in each scenario despite all the scenarios having the same profitability, i.e., 30-year project net present value equal to zero assuming a 10% discount rate. As can be observed from figure 26, feedstock dominates operating costs among all the scenarios, underscoring its importance to project economics. In Scenario I, elimination of natural gas consumption led to a small improvement in operating costs and project economics. In scenario II, grid electricity operating costs were split in half by utilizing surplus biogas onsite via gas turbine. Scenario III built on that result, but also included a small coproduct revenue from fermentation CO_2 to CCS. In scenario IV, the coproduct revenue from surplus-RNG and biogas-CO_2 was realized but was largely offset by an 115% increase in electricity operating costs relative to scenario III. When compared to the revenue from ethanol or fuel pellets, the coproduct revenue from either CO_2 or surplus-RNG was roughly an order of magnitude smaller.

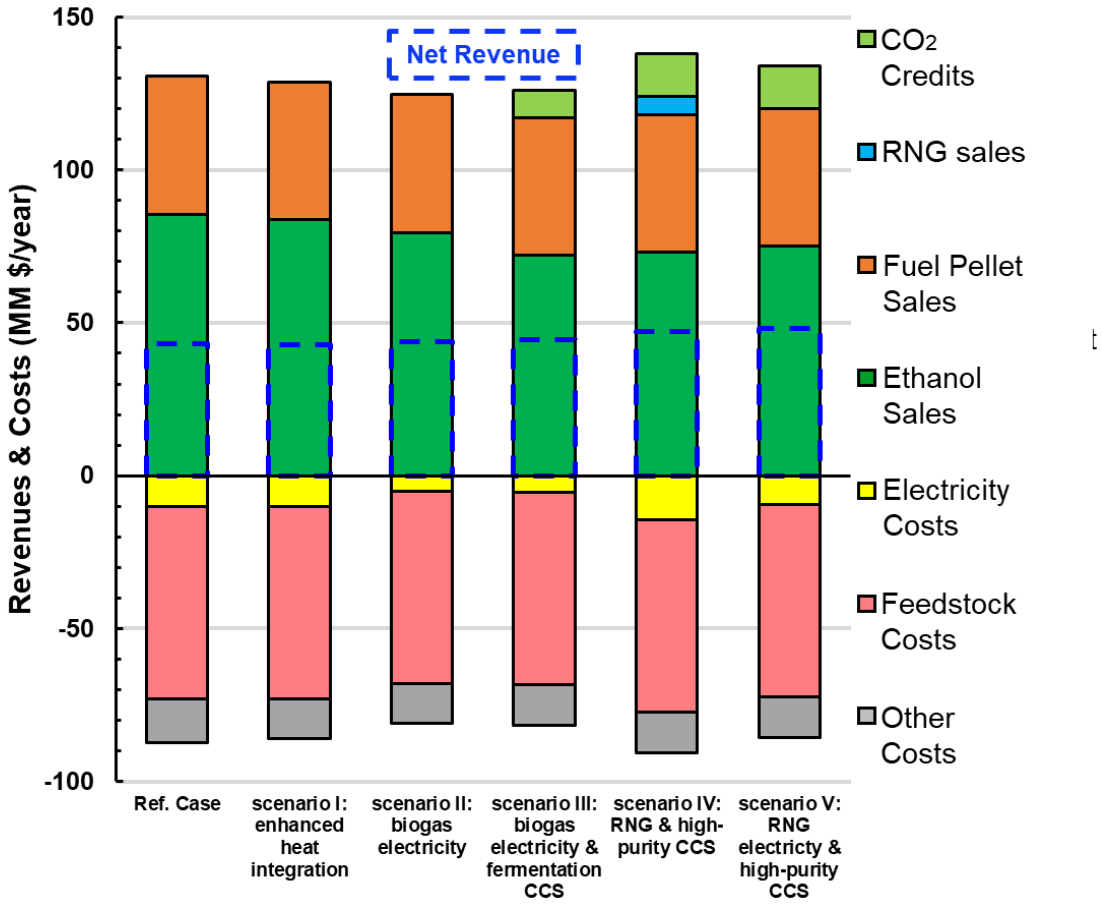

Figure 26. Revenues and costs. Minimum ethanol selling prices (MESPs) were used to determine ethanol revenue leading to variable ethanol revenues across the various scenarios despite the same throughput (60 MMgal/yr). Only the reference case includes natural gas consumption, which is included under the label other costs. Net revenue (dashed blue bars) is equal to revenues minus costs.

The CO_2 levelized cost of capture was estimated to be between \$13.7 and \$14.8/ton CO_2 depending on the scenario (appendix figure A.12). Levelized costs were lower for scenarios IV and V than III due to capturing additional biogas-CO_2 and economies of scale for compressor capital investment. Levelized costs of capture were similar to those found in the literature for cases where CCS was selectively applied to high-purity streams (236,261,336). The total levelized cost of carbon abatement, including transportation and storage, would be higher. For comparison, levelized transport costs have been reported in the range of \$5-14/ton CO_2 (261,264,269,333), storage in the range of \$6-24/ton (259,261), and monitoring \$0.1-0.3/ton (335). At

a manufacturing-gate assumed selling price of $50/metric ton, adding high-purity CCS is profitable compared to not doing so.

Scenario Comparisons: GHG reductions and MESPs

Relative GHG reductions and MESPs for each scenario are presented in figure 27. Generally, all process design scenarios presented here lowered the MESP and improved GHG reductions relative to the reference case. Many of the GHG reduction measures considered here impart only minor increases in total capital investment (figure 25) and no changes in ethanol and fuel pellet production (figure 23 and 24). Avoided fossil fuel emissions (AFFE) afforded by fuel pellets were equal in all scenarios presented here and was determined assuming coal displacement (see methods). Later scenarios, with overall larger negative emissions, were less sensitive towards fuel pellet AFFE (appendix figure A.13.2). Despite additional capital investment, decreasing MESPs ($1.43, $1.39, $1.34, $1.23, $1.27, $1.31 per gallon ethanol, respectively) indicate that the process design modifications would improve project economic outcomes overall. It should be noted that MESPs depend on financial assumptions, production scale, and project schedule, and variables assumed here align with the n^{th} plant analysis as specified by NREL (Humbird et al., 2011). Estimated MESPs here range from $1.23 to $1.43 per gallon ethanol, which is in the lower end of estimates previously reported for corn stover ethanol (especially compared to studies from the past decade) (appendix table A.9). Inclusion of high-purity CCS resulted in lower MESP values than without and enabled cost-competitive ethanol on a gasoline equivalent basis. Over the last fifteen years, the average wholesale selling price of gasoline has equaled $2.14/gal gasoline (+/- 0.59 $/gal, i.e., one standard deviation) (EIA data) whereas ethanol MESP's reported here range between $1.86 and $2.17 per gallon of gasoline equivalent (GGE) (appendix B) (online supplementary materials, underscoring the cost-competitiveness with wholesale gasoline.

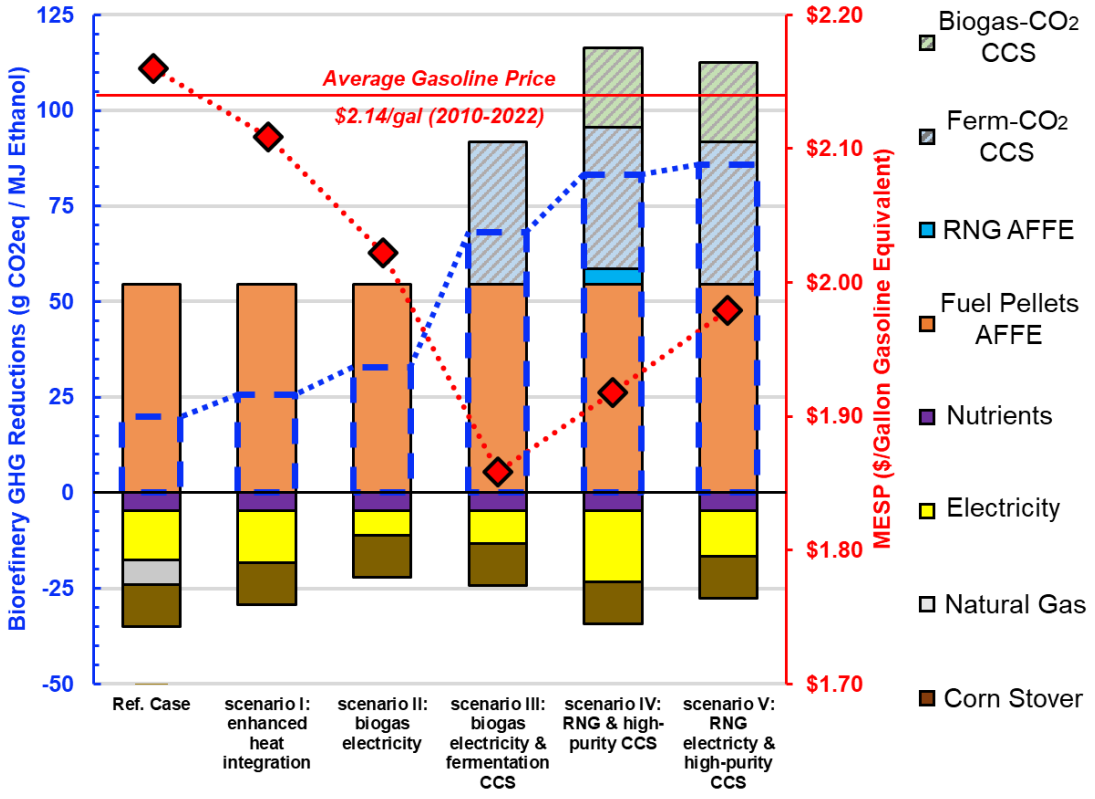

Figure 27. Greenhouse gas reductions and minimum ethanol selling prices for the reference case and scenarios I to V. AFFE: avoided fossil fuel emissions. GHG emissions determined on a gCO_2 equivalent per MJ ethanol basis for a 60 million gallon per year facility. MESP determined on gallon gasoline equivalent (GGE) basis. Average wholesale gasoline price (solid red line) reported by the EIA between 2010-2022 equaled $2.14/gal with a single standard deviation of $0.59. Minimum ethanol selling price (MESP) (red bars) was determined using the same financial assumptions as Humbird et al. (2011) for a 30-year project with a 10% discount factor. Net biorefinery GHG reductions (dashed blue bars) were determined by summing positive and negative contributions presented here.

Eliminating natural gas consumption in scenario I led to a marginal improvement in GHG reductions and leaves externally purchased (i.e., grid) electricity as the largest remaining fossil fuel input. Scenario II builds on this result, utilizing surplus biogas via gas turbine and cutting electricity imports nearly in half. Possible GHG benefits realized by minimizing grid electricity may be transient, i.e., not reflective of future low-

carbon grid technology (250), while those of CCS would persist in, and indeed help enable, a net-zero carbon economy. Compared to scenario II, deploying CCS for fermentation CO_2 in scenario III resulted in a 2.1-fold improvement in the net GHG emission reductions (an additional -35 gCO_2eq/MJ ethanol) and lowered MESP from $2.03 to $1.86 per GGE. Scenario IV introduced biogas upgrading via membrane separation to sell surplus RNG which required additional electricity and sacrificed any onsite electricity generation via RNG-turbine. Ultimately, only 17.5% of RNG is sold (i.e., the surplus, corresponding to 1.6% of feedstock carbon input) and thus the much larger contribution to GHG emission reductions is the biogas-CO_2 byproduct stream. Scenario V displaced more grid electricity CO_2 equivalents than RNG coproduct sales in scenario IV, yielding the highest GHG emission reduction among the scenarios simulated thus far. The reference scenario's net biorefinery GHG emission reduction was estimated at -19.5 gCO_2eq/MJ ethanol and --84.8 gCO_2eq/MJ for Scenario V, thus, the cumulative impact of the changes described throughout this study increased the carbon abatement by 4.3-fold while simultaneously lowering the minimum ethanol selling price.

Up to this point, the analysis has primarily focused on the energy and economic efficiencies related to capturing high-purity CO_2 streams at the biorefinery. However, it is also possible to imagine a total CCS approach which would also capture dilute flue gas CO_2. The net biorefinery GHG reductions in a total-CCS approach nearly doubled to -157 gCO2eq/MJ ethanol (figure 28). However, this increases the capital investment from 322 to 445 MM$ while reducing total revenue from 137 to 118 MM$. Despite exporting 9 MW electricity to the grid, the minimum ethanol selling price was increased 1.4-fold (1.98 to 2.82 $/GGE, respectively). This result is consistent with the prior study, Lynd et al. (2017), that demonstrated lower operational costs and project investment based on fuel pellet coproduction rather than onsite electricity production (21). Notably, the trade-off between economics and GHG reductions is not observed when capturing only high-purity streams.

In summary, it would be possible to economically recover 24% of feedstock carbon as high purity gas (fermentation off-gas and separated biogas), and an additional 46% from solids combustion for a total of

70% of feedstock carbon could be captured. These streams correspond to 0.276, 0.105, and 0.524 million tons of CO_2 annually available, respectively, all originating from a 60 MMgal/yr facility. These results demonstrate the potential for improving GHG mitigation benefits as cellulosic biofuel technology matures.

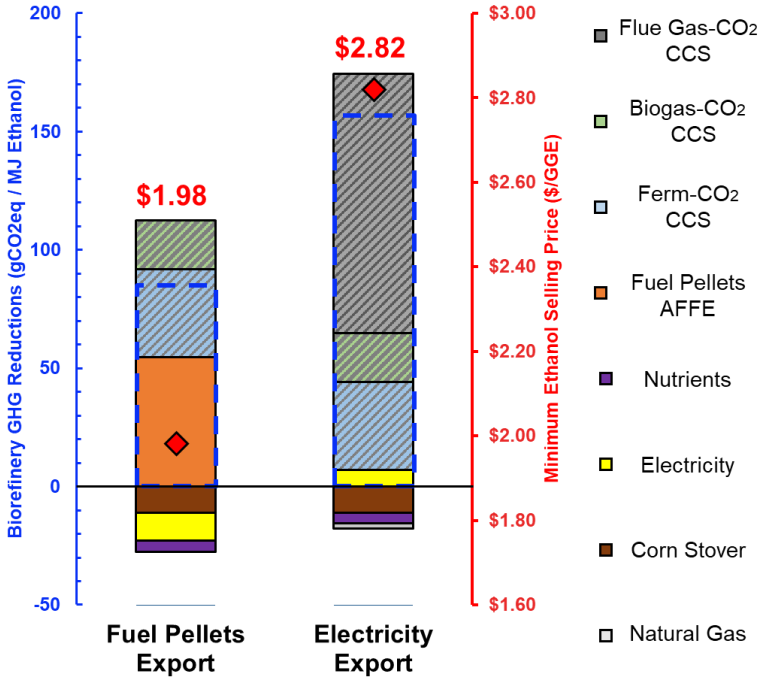

Figure 28. Greenhouse gas reductions and minimum ethanol selling prices for coproduction of fuel pellets or electricity. AFFE: avoided fossil fuel emissions. GHG emissions are determined on a gCO_2 equivalent per gallon gasoline equivalent (GGE) basis for a 60 million gallon per year facility. Scenario V is duplicated from figure 27 with no changes titled fuel pellets export.

Conclusions

This study offers an updated technoeconomic evaluation of corn stover conversion to ethanol via C-CBP at a scale of 60 million gallon per year. Compared to the reference case (Lynd et al., 2017), each of the revised scenarios presented here enables additional GHG emission reductions while simultaneously decreasing the MESP. Enhanced heat recovery eliminated natural gas input and generated surplus biogas. Increased CO_2 removal may be realized by upgrading the biogas produced onsite via membrane separation where RNG can be sold as a coproduct or combusted to offset grid electricity consumption via gas turbines.

Results indicate that carbon capture and storage (CCS) from fermentation sources is a direct and cost-effective (MESP: $1.23/gal) pathway to enabling negative carbon flux (15.4% of feedstock carbon input) and significant GHG emission reductions (an additional -35 gCO_2eq/ MJ ethanol). In another scenario (IV), Biogas membrane separation enables selling surplus RNG and captures an additional 8.6% of feedstock carbon input, or 24% combined. In the final scenario (V), GHG reductions are 4.3-fold higher while the MESP is nearly 10% lower than the starting reference case for an increase in total capital investment (+18%). These results underscore the role cellulosic ethanol can play in realizing negative carbon emissions at the biorefinery. The levelized cost of capture for fermentation CO_2, both with and without biogas CO_2, was $13.7 and $14.8/ton, respectively, both of which compare favorably with the existing price incentives for geologic storage ($85/ton overall). Overall, our analysis suggests that 1) a corn-stover-to-ethanol facility can be self-sufficient in process heat without onsite combustion of solid process residues, 2) compared to wholesale gasoline, the C-CBP platform offers cost-competitive cellulosic ethanol with MESPs ranging between $1.86 and $2.17/GGE, 3) capturing CO_2 from fermentation was a relatively straightforward path to enabling negative carbon flux (plus coproduct revenue) and when coupled with biogas upgrading, enables capture of 24% feedstock carbon input without using dilute flue streams, and 4) a total-CCS approach would enable capturing 70% of feedstock carbon with a 8-fold increase in net biorefinery GHG emission reductions, relative to the starting case.

Author Contributions

Matthew R. Kubis: Conceptualization, Methodology, Investigation, Formal analysis, Writing – Original Draft, Writing – Review & Editing. Lee R. Lynd: Conceptualization, Writing – Review & Editing, Supervision, Funding acquisition.

Conflicts of interest

MRK, none. LRL is an equity holder in a cellulosic biofuel company.

Acknowledgements

The authors acknowledge Tom L. Richard, Dan L. Sanchez, and Mark S. Laser for useful discussions, and the Center for Bioenergy Innovation, a US Department of Energy Bioenergy Research Center supported by the Office of Biological and Environmental Research in the DOE Office of Science, for financial support.

6.3 Project History

It can be useful to reflect on project trajectories, and this project took many iterations which I am now taking the chance to catalogue. I first began to incorporate process design into my research after taking the graduate level course Biomass Energy Systems instructed by Prof. Lee R. Lynd. The class project conceptualized returning high lignin fermentation byproduct (HLFB) (i.e., solid process residues) as a potentially circular coproduct cellulosic ethanol alongside sustainable agricultural practices. As a class project, my responsibilities included preparing mass and energy balances and I developed a biorefinery model using Excel. I eventually transitioned this project into my qualifications exam (a research proposal based format) proposing a self-sufficient cellulosic biorefinery that no longer combusts solid process residues using ASPEN® plus simulations and GREET® life cycle assessments. In the context of revaluating solids combustion during bioprocessing, we had initial success in enhancing heat integration (by modifying distillation/pasteurization) that eliminated onsite natural gas combustion and provided a surplus of biogas (this eventually became my Scenario I). However, at this point, the primary focus of the analysis was producing HLFB. In an effort to assign value to HLFB, I balanced nitrogen flows in the ASPEN®plus simulations to establish C:N estimates for the corn stover feed and HLFB coproduct. Nutrient inputs were overhauled specific to a CBP bioconversion process, and were applied across all process scenarios for consistency. At this point we began exploring carbon capture and storage as well as biogas upgrading and began simulating new unit processes based on literature parameters. Eventually, other projects studying HLFB took precedent, and it became clear that the HLFB coproduction scenario was more distracting then informative. Meanwhile, the incentives to capture carbon emissions were gaining momentum. For example, the US 45Q tax credit for sequestering CO_2 has increased 3-fold ($28 to $85/ton) since my graduate studies began in 2018 (252), this in addition to continued renewable fuel supports (e.g., the RFS and LCFS). Taken together, carbon capture and storage/ carbon management/ carbon dioxide removal became the primary focus. At this point the study was finalizing while focusing exclusively on

capturing high purity streams. As a final iteration, I estimated flue gas capture onsite and off, assuming contemporary or futuristic carbon intensity and displacement.

7. Conclusions

The significance of this thesis is broadly divided into three camps: wet-lab biological characterizations, bioreactor development, and process design. Thesis projects were linked by a shared goal, i.e., seeking to better understand lignocellulose conversion via CBP using *C. thermocellum* in industrial settings. Important findings from each grouping are summarized as follows:

Chapter 4 was an important foray towards industrially relevant substrate loadings. Using defined batch cultures in conventional benchtop reactors, diminishing carbohydrate solubilization was extensively documented between 20 and 80 g/L corn stover or senescent switchgrass. Follow up diagnostic experiments offered novel insights to the limits facing carbohydrate solubilization. Mid-fermentation dilutions and partnering *C.thermocellum* alongside a hemicellulose utilizing microbe, *T. thermosacccharolyticum,* were shown to improve fractional carbohydrate solubilization. Results were consistent with the hypothesis that impediment of deconstruction by adsorbed oligosaccharides could be a possible mechanism for declining solubilization with increasing substrate loading, although this remains to be further elucidated. This work served as an important milestone for our understanding of *C. thermocellum* mediated lignocellulose solubilization, and provides a solid foundation for future and ongoing research, especially at high solid loadings.

In Chapter 5, a custom bioreactor was developed to characterize CBP solubilization performance beyond 80 g/L, the point where mixing and sterilization became unreliable using conventional benchtop reactors. This work originally started as a Master's student thesis (Galen Moynihan) who successfully demonstrated representative solids delivery using a fixed-volume piston sampler (220). Described in this thesis, both hardware and standard operating procedures were developed to enable biological characterization, with a series of experiments aimed at validating aseptic, semi-continuous, and high solid loading conditions.

Significant time and effort was spent on improving hardware, formalizing data acquisition, and designing sterilization procedures for biological testing. Biological testing was successfully conducted using a defined coculture at both 30 and 120 g/L corn stover and a 72-hour residence time. Under these conditions, steady state behavior with respect to carbohydrate solubilization was observed, although soluble sugar utilization and fermentation products were variable due to poor coculture reproducibility, especially at 120 g/L. Nevertheless, cultivating *C. thermocellum* was entirely possible which remains a key milestone for the novel high solids reactor. A manuscript summarizing these results in the context of tool development has been prepared, and will likely be submitted to a journal after the thesis defense. One caveat, however, is the cohesion of the fermentation runs at 120 g/L. With only two runs complete at the submission of this thesis, it is unclear how representative the current data is for the stability of the system. There are multiple future runs planned, and the eventual paper will address this.

Chapter 6 uses simulation based methods to offer an updated technoeconomic evaluation of corn stover conversion to ethanol via C-CBP at a scale of 60 MMgal/yr. Using Lynd et al., (2017) as a simulation departure point (21), this study documents the effects incorporating heat integration, biogas upgrading, and carbon capture and storage. The revised scenarios enable additional GHG emission reductions while simultaneously decreasing the MESP. Results indicate that high-purity carbon capture and storage (CCS) is a direct pathway to enabling negative carbon flux, significant GHG emission reductions, and cellulosic ethanol production cost-competitive with average wholesale gasoline prices. In a total-CCS approach, up to 70% of feedstock carbon can be captured while exporting over 50% of feedstock LHV as fuel or electricity- reinforcing the role liquid biofuel production could play in climate mitigation strategies.

7.1 Recommendations for Future Work

High Solids Fermentation *(Independent from bioreactor development)*

- Continue to optimize coculture growth conditions/media background. (see appendix figure A.3)
- In table 2 (page 42), the calculated fractional utilization of xylose was remarkably similar between solid loadings, but changed depending on feedstock choice. Test if this trends holds consistent with additional lignocellulose feedstocks (keeping biocatalyst the same). This might offer insights into the character of residual, solubilized C_5's based on relative abundance in different feedstocks.
- Evaluating *C. thermocellum* performance at solid-state loadings. It would be interesting to perform a comparison between submerged and solid state cultivations in the Lynd lab, given our extensive experience with submerged fermentations and continued interest in high solid loadings.
- Evaluate *C. thermocellum* carbohydrate solubilization sensitivity to stirring at high solid loadings (e.g. 5, 50, 250, 500 RPM). Could be a relatively simple experiment to gain insight into mass transfer effects on carbohydrate solubilization.
- For semi-continuous cultivations at high solids, begin to determine the culture's sensitivity to residence times. We chose 72-hours for both solid loadings, although perhaps quicker residence times could be advantageous.

HSR Development

- Seeking experience with modeling software (e.g., AutoCAD, solidworks) and the machine shop will help aid in future endeavors. Similarly, perhaps to a lesser extent, coding and automated controls.
- HSR data acquisition and analysis can likely be improved. For example, I have to manually comb through data to find the feeding cycles in a dataset with 14,000+ data entries. A data analysis pipeline using e.g. python or matlab could enable quicker, and perhaps less error-prone, data analysis.

- Further evaluation of high solid slurry pumps (e.g., rotary lobe) in lieu of fixed-volume sample or augur. Perhaps revisit horizontal plugflow feeding as in South et al., (1993, 1994).
- Characterize the performance of the HSR finely milled corn stover in a benchtop reactor for as a comparison for semi-continuous fermentations.
- It is recommended to do heating control recalibration.
- Hardware: the next iteration of custom bioreactor should have headplate space for pH and temperature probes. Both the bioreactor and the holding tank need sampling lines. Future impellers should be fabricated with metal but allow for bolting-on PTFE to scrape reactor walls.
- The HSR holding frame is difficult to work with for a couple reasons: alignment is not ideal, it is heavy, and we cannot remove bioreactor without completely dismantling the system. If anyone designs another high solids reactor, do not underestimate the importance of a good frame.
- The bottom stir assembly is workable, but I would add more seals and bearings if I were to design another. (Some of these parts are already wearing down, so they will need replacement sooner rather than later.)
- Sparging needs to be optimized. In an effort to avoid contamination, we are likely sparging N_2 through the mixtank too aggressively.

Technoeconomic Analyses

- Growth media, nutrients, nitrogen etc. for *C. thermocellum* containing cocultures could be an interesting direction for technoeconomic and life cycle analysis. It would be additionally compelling if the analysis is informed by some wet-lab experiments looking at minimal media component requirements in industrial settings.
- Our technoeconomic analyses would be stronger paired with GREET life cycle analysis. It is user-friendly and I recommend lab members interested in TEA get acquainted sooner rather than later.
- There may some value in trying to publish the C:N balances / high lignin fermentation byproduct coproduction scenario described in section 6.3.

8. Appendices

8.1 Chapter 4 Appendix

Table A.1. Data from figure 5 and figure 6, fractional carbohydrate solubilization (FCS) and fermentation end product concentrations.

(n=2)	Corn Stover					Senescent Switchgrass				
Loading	FCS	Ethanol (g/L)	Acetate (g/L)	Formate (g/L)	Lactate (g/L)	FCS	Ethanol (g/L)	Acetate (g/L)	Formate (g/L)	Lactate (g/L)
20 g/L	0.695 ±0.013	0.962 ±0.007	1.634 ±0.097	0.213 ±0.028	0.063 ±0.013	0.399 ±0.001	0.658 ±0.006	1.286 ±0.018	0.108 ±0.001	0.020 ±0.001
40 g/L	0.663 ±0.006	1.657 ±0.028	2.953 ±0.169	0.299 ±0.025	0.188 ±0.008	0.365 ±0.009	1.048 ±0.070	2.053 ±0.088	0.063 ± ±0.003	0.027 ±0.003
60 g/L	0.630 ±0.033	2.087 ±0.085	3.630 ±0.029	0.428 ±0.021	0.207 ±0.000	0.291 ±0.007	1.136 ±0.046	2.732 ±0.082	0.230 ±0.007	0.036 ±0.000
80 g/L	0.556 ±0.011	2.655 ± ±0.028	5.071 ±0.224	0.767 ±0.056	0.359 ±0.010	0.2436 ±0.005	1.202 ±0.031	3.526 ±0.140	0.300 ±0.002	0.040 ±0.005

Table A.2. Molar product ratios for increasing solids (figure 5 and figure 6)

Molar Product Ratios								
(n=2)	Corn Stover				Senescent Switchgrass			
Loading	Ethanol	Acetate	Formate	Lactate	Ethanol	Acetate	Formate	Lactate
20 g/L	1.000	1.303	0.277	0.033	1.000	1.499	0.168	0.016
40 g/L	1.000	1.201	0.185	0.036	1.000	1.503	0.159	0.013
60 g/L	1.000	1.334	0.210	0.051	1.000	1.845	0.207	0.016
80 g/L	1.000	1.465	0.148	0.069	1.000	2.250	0.255	0.017

Table A.3. Data from figure 6, residual solubilized carbohydrates.

(n=2)	Corn Stover			Senescent Switchgrass		
Loading	Arabinose (g/L)	Glucose (g/L)	Xylose (g/L)	Arabinose (g/L)	Glucose (g/L)	Xylose (g/L)
20 g/L	0.704 ± 0.015	0.480 ± 0.018	2.899 ±0.172	0.322 ±0.013	0.279 ±0.007	1.680 ±0.054
40 g/L	1.034 ±0.050	0.677 ±0.020	6.292 ±0.357	0.590 ±0.031	0.527 ±0.022	3.102 ±0.033
60 g/L	1.456 ±0.054	0.931 ±0.041	8.778 ±0.298	0.751 ±0.003	0.649 ±0.000	3.781 ±0.033
80 g/L	2.448 ± 0.000	1.192 ±0.035	10.157 ± 0.087	0.902 ±0.034	0.791 ±0.030	4.318 ±0.120

Table A.4. Data from figure 7, fermentation end product ratios.

Spent Media Experiments Net Product Ratios					
Substrate	Spent Media	Ethanol (mol/L)	Acetate (mol/L)	Formate (mol/L)	Lactate (mol/L)
5 g/L Avicel	Corn Stover 80 g/L	1.000	1.101	0.070	0.089
5 g/L Avicel	Switchgrass 80 g/L	1.000	0.897	0.271	0.044
5 g/L Avicel	Corn Stover 20 g/L	1.000	1.158	0.083	0.016
5 g/L Avicel	Switchgrass 20 g/L	1.000	0.863	0.293	0.028
5 g/L Avicel	Avicel 12.1 g/L	1.000	0.732	0.322	0.218
5 g/L Avicel	Cellobiose 12.1 g/L	1.000	0.997	0.335	0.019
5 g/L Avicel	water/none	1.000	1.021	0.684	0.167
5 g/L Cellobiose	Corn Stover 80 g/L	1.000	1.089	0.350	0.055
5 g/L Cellobiose	Switchgrass 80 g/L	1.000	0.822	0.400	0.038
5 g/L Cellobiose	Corn Stover 20 g/L	1.000	1.137	0.504	0.026
5 g/L Cellobiose	Switchgrass 20 g/L	1.000	0.863	0.293	0.028
5 g/L Cellobiose	Avicel 12.1 g/L	1.000	0.814	0.464	0.095
5 g/L Cellobiose	Cellobiose 12.1 g/L	1.000	0.760	0.363	0.040
5 g/L Cellobiose	water/none	1.000	0.887	0.449	0.095

Figure A.1. Residual solubilized carbohydrates per addition.

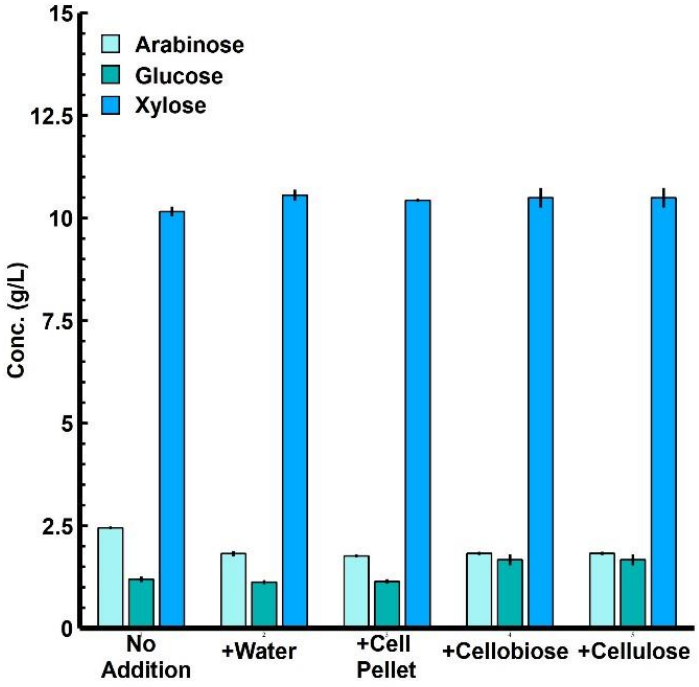

Figure A.1. Residual solubilized carbohydrate concentrations determined by mild acid hydrolysis of the supernatant for additions of model substrates and cells to 80 g/L corn stover fermentations. Concentrations are normalized to dilutions for comparison of results with and without additions. Error bars represent 1 standard deviation for duplicate bioreactor runs.

Data Summary: This data emphasizes that additions of model substrates or cells did not improve xylose solubilization, which for monocultures of *C. thermocellum*, is a reasonable proxy for overall carbohydrate solubilization. Considering the overall carbohydrate solubilization did not significantly change (see figure 8) and the xylose concentrations are similar, it can be reasoned that the additional cellulose was nearly or completely consumed, and only a marginal increase in glucose (+0.15 and +0.54 g/L) was found in the supernatant for cellulose and cellobiose additions, respectively.

Figure A.2. Fermentation products per addition.

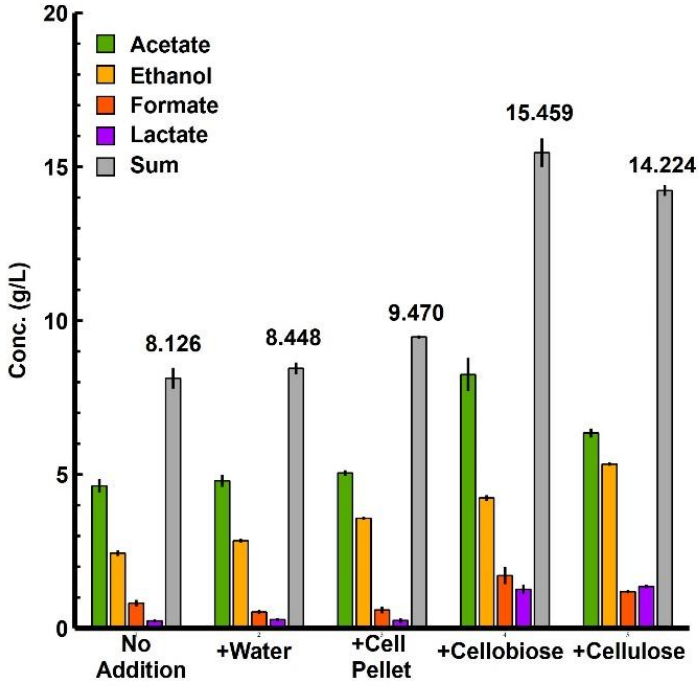

Figure A.2. Products ethanol, acetate, formate, and lactate from fermentations of 80 g/L corn stover per addition. Sum refers to the addition of the above four product concentrations in g/L. Concentrations are normalized to dilutions for comparisons between no additions and additions. Error bars represent 1 standard deviation for duplicate bioreactor runs. *Acetate originates from both lignocellulose solubilization (cleavage of acetyl groups) and microbial fermentation of carbohydrates.*

Data Summary: Higher concentrations of fermentations products were observed for additions of cellobiose and cellulose. This data, along with gas production (figure 8B), suggests that the culture readily utilized the model substrates, and cellular limitations related to medium nutrients or product inhibition were not observed.

Figure A.3. Xylose utilization by cocultures on defined medium.

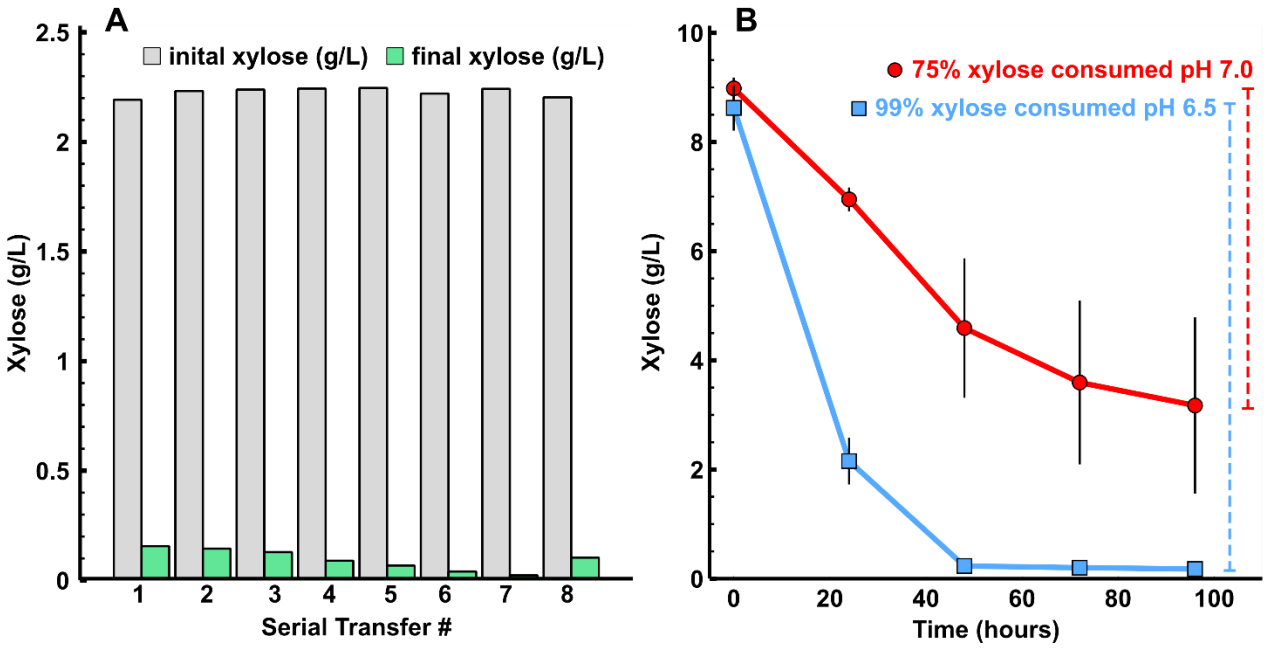

Figure A.3. Xylose utilization by cocultures. Panel (A) depicts initial (t=0 h) and final (t=24 h) xylose concentrations for a serially transferred coculture bottle fermentation. Defined MTC media with 2.5 g/L cellulose and 2.5 g/L xylose was pH buffered with 5 g/L working concentration of MOPS sodium salt. Panel (B) shows decreasing xylose concentrations across 24-hour samples for a coculture bioreactor fermentation. Defined MTC media with 20 g/L cellulose and 10 g/L xylose was pH controlled with additions of 4 N KOH. Concentration values are averages of duplicate bioreactor runs (n=2) and the error bars represent one standard deviation.

Data Summary: Preliminary experiments demonstrate that pH is an influential factor in the fractional utilization of xylose by *T. thermosaccharolyticum* on defined media. Following experiments comparing monocultures and cocultures were operated at pH 6.5 to ensure reliable coculture partner performance.

Panel (A): It should be noted that the *T. thermosaccharolyticum* inoculum is prepared on undefined CTFUD medium containing yeast extract. The inoculum containing yeast extract that enters serial transfer bottle one is serially diluted (via 2%v/v serial inoculum) such that a negligible yeast extract concentration persists

into the later serial transfers. Near-complete xylose utilization in the later serial transfers suggests that the coculture retains the ability to utilize xylose in the absence of yeast extract under defined pH-buffered MTC medium.

Panel (B): Under pH-controlled operating conditions (via additions of 4 N KOH), the coculture demonstrates near-complete utilization (~99%) of the xylose at pH 6.5 and unfinished xylose utilization (~75%) at pH 7.0. The variability is a great deal higher for the cocultures operating at pH 7.0, which could suggest that pH 7.0 is roughly the threshold for viable *T. thermosaccharolyticum* cultivations on xylose and defined medium.S8.

Table A.5. Data from figure 9 and figure 11, fractional carbohydrates solubilization and fermentation end product and residual solubilized carbohydrate concentrations for corn stover fermentations.

	Corn Stover								
Culture Type	Solid Loading (g/L)	FCS	Ethanol (g/L)	Acetate (g/L)	Formate (g/L)	Lactate (g/L)	Arabinose (g/L)	Glucose (g/L)	Xylose (g/L)
MC	20 (n=4)	0.655 ±0.016	0.932 ±0.031	1.483 ±0.078	0.188 ±0.004	0.033 ±0.003	0.530 ±0.006	0.290 ±0.006	3.293 ±0.083
CC	20 (n=4)	0.749 ±0.014	2.080 ±0.049	2.333 ±0.122	0.166 ±0.011	0.055 ±0.009	0.205 ±0.020	0.220 ±0.013	0.794 ±0.088
MC	80 (n=2)	0.556 ±0.010	2.707 ±0.044	5.020 ±0.034	0.438 ±0.007	0.234 ±0.001	1.603 ±0.006	0.824 ±0.003	10.337 ±0.016
CC	80 (n=2)	0.632± 0.002	7.232 ±0.284	7.079 ±0.127	0.710 ±0.008	1.309 ±0.105	0.660 ±0.020	0.734 ±0.022	2.438 ±0.016

Table A.6. Data from figure 9 and figure 12, fractional carbohydrates solubilization and fermentation end product and residual solubilized carbohydrate concentrations for senescent switchgrass fermentations.

	Senescent Switchgrass								
Culture Type	Solid Loading (g/L)	FCS	Ethanol (g/L)	Acetate (g/L)	Formate (g/L)	Lactate (g/L)	Arabinose (g/L)	Glucose (g/L)	Xylose (g/L)
MC	20 (n=4)	0.405 ±0.028	0.597 ±0.016	1.278 ±0.031	0.129 ±0.013	0.023 ±0.005	0.355 ±0.011	0.283 ±0.009	2.061 ±0.045
CC	20 (n=4)	0.457 ±0.042	1.597 ±0.083	1.717 ±0.127	0.100 ±0.016	0.088 ±0.009	0.093 ±0.007	0.171 ±0.008	0.428 ±0.022
MC	80 (n=2)	0.259 ±0.026	1.209 ±0.048	3.502 ±0.147	0.573 ±0.005	0.130 ±0.007	0.947 ±0.079	0.736 ±0.040	5.254 ±0.519
CC	80 (n=2)	0.307 ±0.020	3.894 ±0.172	4.338 ±0.222	0.521 ±0.011	0.250 ±0.039	0.251 ±0.023	0.462 ±0.018	1.136 ±0.080

Table A.7. Data from Figure 5, 6, 9, 11, and 12, estimated contributions towards reported acetate titers from either lignocellulose deconstruction or microbial fermentation product.

Feedstock	Culture	pH	Lignocellulose Loading			FCS	Acetyl Content [1][2]	Theoretical Acetate Solubilized		Total Acetate Titer		
			(g)	(L)	(g/L)		(dry wt. %)	(g)	(g/L)	(g/L)	(% lignocellulose)	(% microbial)
corn stover	MC	7	6	0.3	20	0.695	2.51%	0.105	0.349	1.63	21.41%	78.59%
corn stover	MC	7	12	0.3	40	0.663	2.51%	0.200	0.666	2.59	25.71%	74.29%
corn stover	MC	7	18	0.3	60	0.63	2.51%	0.285	0.949	3.63	26.15%	73.85%
corn stover	MC	7	24	0.3	80	0.556	2.51%	0.335	1.117	5.07	22.03%	77.97%
switchgrass	MC	7	6	0.3	20	0.399	3.60%	0.086	0.287	1.28	22.44%	77.56%
switchgrass	MC	7	12	0.3	40	0.365	3.60%	0.158	0.526	2.05	25.64%	74.36%
switchgrass	MC	7	18	0.3	60	0.291	3.60%	0.189	0.629	2.73	23.02%	76.98%
switchgrass	MC	7	24	0.3	80	0.243	3.60%	0.210	0.700	3.52	19.88%	80.12%
corn stover	MC	6.5	6	0.3	20	0.656	2.51%	0.099	0.329	1.46	22.56%	77.44%
corn stover	MC	6.5	24	0.3	80	0.557	2.51%	0.336	1.119	5.02	22.29%	77.71%
corn stover	CC	6.5	6	0.3	20	0.749	2.51%	0.113	0.376	2.33	16.14%	83.86%
corn stover	CC	6.5	24	0.3	80	0.632	2.51%	0.381	1.270	7.07	17.96%	82.04%
switchgrass	MC	6.5	6	0.3	20	0.406	3.60%	0.088	0.292	1.27	23.02%	76.98%
switchgrass	MC	6.5	24	0.3	80	0.259	3.60%	0.224	0.746	1.71	43.62%	56.38%
switchgrass	CC	6.5	6	0.3	20	0.457	3.60%	0.099	0.329	3.5	9.40%	90.60%
switchgrass	CC	6.5	24	0.3	80	0.308	3.60%	0.266	0.887	4.33	20.49%	79.51%

1. Kumar, R., Mago, G., Balan, V., & Wyman, C. E. (2009). Physical and chemical characterizations of corn stover and poplar solids resulting from leading pretreatment technologies. Bioresource Technology, 100(17), 3948–3962. https://doi.org/10.1016/j.biortech.2009.01.075

2. Wyman, C. E., Balan, V., Dale, B. E., Elander, R. T., Falls, M., Hames, B., Holtzapple, M. T., Ladisch, M. R., Lee, Y. Y., Mosier, N., Pallapolu, V. R., Shi, J., Thomas, S. R., & Warner, R. E. (2011). Comparative data on effects of leading pretreatments and enzyme loadings and formulations on sugar yields from different switchgrass sources. Bioresource Technology, 102(24), 11052–11062. https://doi.org/10.1016/j.biortech.2011.06.06

8.2 Chapter 6 Appendix

Figure A.4. Semi-continuous Arduino Script

```
// semi-continuous operation code
// Matt Kubis April 19th, 2023
// High Solids Reactor

// initializing variables
// defining time variable outputs
long start_time=0;
long total_time=0;
long start_cycle_time=0;
long end_cycle_time=0;

// defining time variables inputs
long ExtendTime = 12000; // includes time to extend as well as dwell
long RetractTime = 6000; // time to retract piston
long PurgeTime = 500; // how long purge valve is open
long wait_time = 34372406; // 9.626 hrs (CHANGE RTs HERE)

// defining variables for level evaluation
int TotalSamples = 101; // number of total datapoints for level probes
int DataPoints = 100; // number of kept datapoints for level probes
int LevelData[100]; // array destination for level probes kept datapoints
int nLevel = 99; // dataPoints minus 1
int P = 0;    // used to populate LevelData array
int X1 = 0;   // used to populate LevelData array
long median1 = 0; // defining a varible for the median value of the first tier level evaluation
long median2 = 0; // defining a varible for the median value of the second tier level evaluation
long median3 = 0; // defining a varible for the median value of the third tier level evaluation

// defining variables for cumulative data
int CycleNumber = 0; // cumulative number of completed feeding cycles
int PumpCount = 0; // cumulative number of isolok pumps
int beets = 0;


// defining bioreactor harvest variables
int initial_test1 = 0; // defining a variable for the median value of the first tier initial level evaluation
int initial_test2 = 0; // defining a variable for the median value of the second tier initial level evaluation
int Threshold = 125; // analog level signals needs to be greater than this value to read 'full' values range from 0 to 1023.

// defining boolean variables
bool Feeding = true;
bool T1Pass = false;
bool T2Pass = false;
bool T3Pass = false;

// Digital Arduino Pin numbers
int Extend = 2;
int Purge = 3;
int OpenBV = 4;
int CloseBV = 5;
int GasOut = 6;
```

```
int GasIn = 7;

// Analog Arduino Pin numbers for level control
int LevelProbe1 = A5;
int LevelProbe2 = A7;

// the setup routine runs once when you press reset:
void setup() {
  Serial.begin(115200); // baud rate
  delay(5000);
  Serial.println(F("0,0,0,0,0"));
  pinMode(CloseBV, OUTPUT);
  pinMode(GasOut, OUTPUT);
  pinMode(GasIn, OUTPUT);
  pinMode(OpenBV, OUTPUT);
  pinMode(LevelProbe1, OUTPUT);
  pinMode(LevelProbe2, INPUT);
  pinMode(Purge, OUTPUT);
  pinMode(Extend, OUTPUT);

  digitalWrite(CloseBV, LOW);
  digitalWrite(GasOut, LOW);
  digitalWrite(OpenBV, LOW);
  digitalWrite(GasIn, LOW);
  digitalWrite(Purge, LOW);
  digitalWrite(Extend, HIGH);
  digitalWrite(LevelProbe1, HIGH);

  start_time=millis();
}

// semi-continuous loop runs infinitely until another code is uploaded to the Arduino
// e.g., 'stop signals' code

void loop() {
  int i=0;
  start_cycle_time=millis();

  BeginHarvest(); //closes reactor gas exhaust, pressurizes for 10 secs, 5 secs dwell, open BV for 10 secs.
  EndHarvest();   //closes BV and waits 10 secs, opens reactor gas exhaust and waits 180 secs.

  initial_test1 = Initial_Harvest(); // First level probe signal to confirm successful harvest
  delay(5000);
  initial_test2 = Initial_Harvest(); // Second level probe signal to confirm successful harvest
  Serial.print(initial_test1); // prints initial level evaluation result
  Serial.print(',');
  Serial.println(initial_test2); // prints initial level evaluation result
  delay(3000);

  if ((initial_test1 >= Threshold) && (initial_test2 >= Threshold))
    Feeding = false;  // if reactor remained 'full' no feeding will happen
  else
    Feeding = true;  // else reactor is now 'empty' and feeding commences
  while (Feeding) {
    beets=FeedReactor(); // Operates ISOLOK sampler for a single pumping cycle
```

```
  delay(10000); // Allow mixing after feeding before signal collection

  long FirstSignal[DataPoints];
  CollectLevelData(); // collects 100 level measurements into 'FirstSignal' array
  for (int l = 0; l <= nLevel; l++) {
  FirstSignal[l] = LevelData[l];
  //Serial.println(FirstSignal[l]);
  }
  delay(10000);

  long SecondSignal[DataPoints];
  CollectLevelData(); // collects 100 level measurements into 'SecondSignal' array
  for (int l = 0; l <= nLevel; l++) {
  SecondSignal[l] = LevelData[l];
  //Serial.println(SecondSignal[l]);
  }
  delay(10000);

  long ThirdSignal[DataPoints];
  CollectLevelData(); // collects 100 level measurements into 'ThirdSignal' array
  for (int l = 0; l <= nLevel; l++) {
  ThirdSignal[l] = LevelData[l];
  //Serial.println(SecondSignal[l]);
  }

  bool ReactorFull = false;

  Array_sort(FirstSignal, DataPoints); // sorts 100 level measurements by numerical order
  Array_sort(SecondSignal, DataPoints); // sorts 100 level measurements by numerical order
  Array_sort(ThirdSignal, DataPoints); // sorts 100 level measurements by numerical order

  median1 = (Find_median(FirstSignal,100)); // identifies median value
  median2 = (Find_median(SecondSignal,100)); // identifies median value
  median3 = (Find_median(ThirdSignal,100)); // identifies median value

  // all three medians have to exceed threshold value to break out of feeding loop
  if ((median1 >= Threshold) && (median2 >= Threshold) && (median3 >= Threshold)) {
  ReactorFull = true;
  Feeding = false;
  }
  else {
  ReactorFull = false;
  Feeding = true;
  }
  Serial.print(median1);
  Serial.print(',');
  Serial.print(median2);
  Serial.print(',');
  Serial.println(median3);
 }

 end_cycle_time=millis()-start_cycle_time;
 total_time=millis();

// feed cycle output information
 {
```

```
    total_time=millis();
    Serial.print(total_time);
    Serial.print(',');
    Serial.print(start_cycle_time);
    Serial.print(',');
    Serial.print(end_cycle_time);
    Serial.print(',');
    Serial.print(CycleNumber);
    Serial.print(',');
    Serial.println(PumpCount);

  }

  // extends the piston to dwell in the mixtank during wait time
  delay(2000);
  digitalWrite(Extend, HIGH);
  delay(ExtendTime);
  delay(wait_time);
}

int Initial_Harvest() {
  CollectLevelData();
  long initial[DataPoints];
  int complete = 0;
  for (int l = 0; l <= nLevel; l++) {
    initial[l] = LevelData[l];
  }
  Array_sort(initial, DataPoints);
  long initial_median = (Find_median(initial, 100));
  return initial_median;
}

void BeginHarvest() {
  digitalWrite(GasOut, LOW);
  digitalWrite(OpenBV, HIGH);
  delay(2500);
  digitalWrite(GasIn, HIGH);
  delay(8000);
  digitalWrite(GasIn,LOW);
  delay(500);
}

int EndHarvest() {
  digitalWrite(OpenBV, LOW);
  delay(10);
  digitalWrite(CloseBV, HIGH);
  delay(15000);
  digitalWrite(CloseBV, LOW);
  delay(1000);
  digitalWrite(GasOut, HIGH);
  delay(5000);

  Feeding = true;
  CycleNumber = CycleNumber + 1;
  return CycleNumber;
}
```

```
// function collects 100 values for varible P using the 'CheckLevel' subfunction
void CollectLevelData() {
  for (int i = 0; i <= TotalSamples; i++) {
    CheckLevel(LevelProbe1, LevelProbe2);
  // loads  100 values for varible P into an array 'LevelData' using the 'CheckLevel' function
    if (i >= (TotalSamples - DataPoints)) {
      X1 = P;
    }
    if (i >= (TotalSamples - DataPoints)) {
      LevelData[(i - (TotalSamples - DataPoints))] = X1;
    }
  }

  //Serial.println(F("LevelDataArray")); // print to see all 100 'LevelData' array values
  for (int k = 0; k <= 99; k++) {
  //Serial.println(LevelData[k]);
  }
return LevelData;
}

// function to acquire level measurement
void CheckLevel(int t1, int t2) {
  // function to send voltage from one level probe and to measure voltage from the other probe
  // collects datapoints as varible P
  // note that this function sends and reads voltage from both probes, but the second pass overwrites the first.
  // this was found to be necessary otherwise signals diminish overtime

  //First pass
  pinMode(t1, OUTPUT);
  pinMode(t2, INPUT);
  digitalWrite(t1, HIGH); //make probe1 output 5V signal
  // P = analogRead(t2); //read voltage from probe 2
  // delay(1); //wait a millisecond
  P = analogRead(t2); //read voltage from probe 2 (overwrite previous read)
  digitalWrite(t1, LOW);// turn probe 1 signal off
  delay(1); //wait a millisecond

 //Second pass
  pinMode(t2, OUTPUT);
  pinMode(t1, INPUT);
  digitalWrite(t2, HIGH);  //make probe2 output 5V signal
  //P = analogRead(t1);
  //delay(1);
  P = analogRead(t1); // P values from first signal path are purposely overwritten, otherwise signals will diminish
overtime
  delay(1);
  digitalWrite(t2, LOW);
}

//
//function sorts array into numerical order
void Array_sort(long *thearray , long n){    //not 100%sure how the asterisk works
  int i = 0 , j = 0 , temp = 0;
  for (i = 0 ; i < n ; i++)
  {
```

```
    for (j = 0 ; j < n - 1 ; j++)
    {
      if (thearray[j] > thearray[j + 1])
      {
        temp        = thearray[j];
        thearray[j]    = thearray[j + 1];
        thearray[j + 1]  = temp;
      }
    }
  }
}

// function to determine  the median of the array
float Find_median(long array[] , long n)
{
  float median = 0;
  // if number of elements are even
  if (n % 2 == 0)
    median = (array[(n - 1) / 2] + array[n / 2]) / 2.0;
  // if number of elements are odd
  else
    median = array[n / 2];
  return median;
}

// function to feed bioreactor one isolok pump
int FeedReactor() {
  digitalWrite(Extend, HIGH);
  delay(ExtendTime);
  digitalWrite(Extend, LOW);
  delay(RetractTime);
  digitalWrite(Purge, HIGH);
  delay(PurgeTime);
  digitalWrite(Purge, LOW);
  PumpCount = PumpCount + 1;
  return PumpCount;
}
```

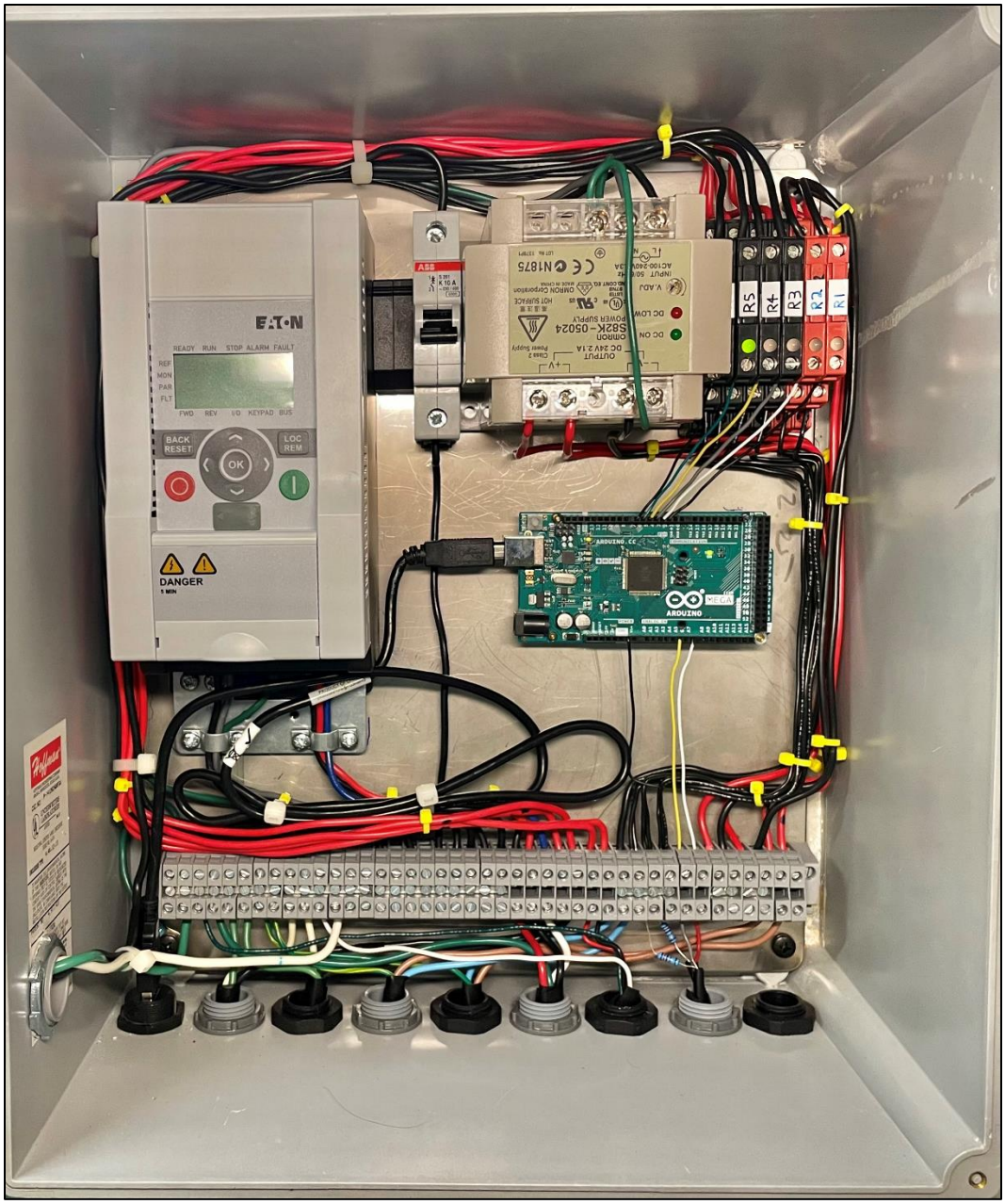

Figure A.5.1 HSR electric panel. High solids bioreactor system utilizes an Arduino microcontroller to read level probes and control pneumatics.

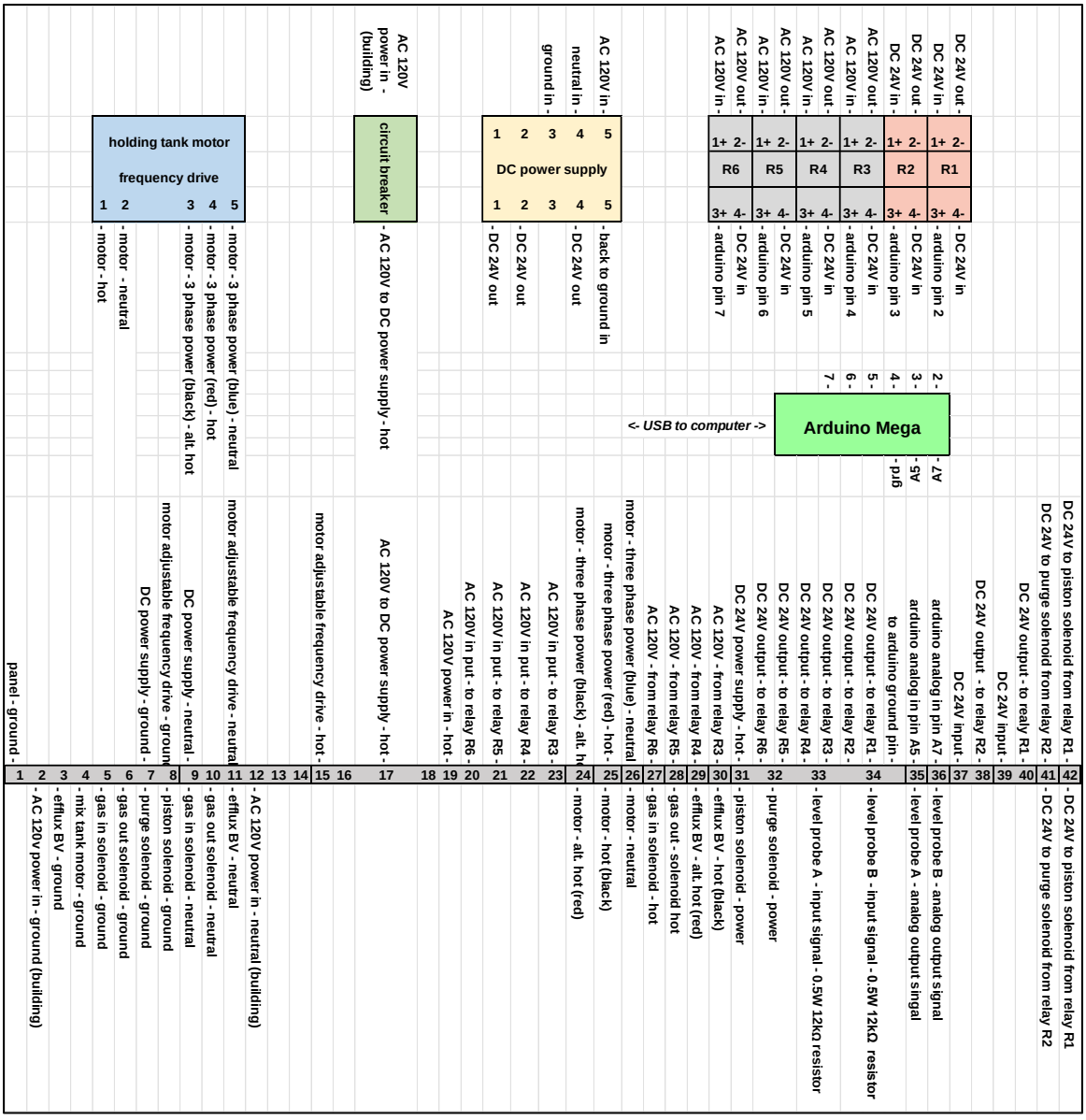

Figure A.5.2 Wiring diagram for electric panel shown figure A.5.1.

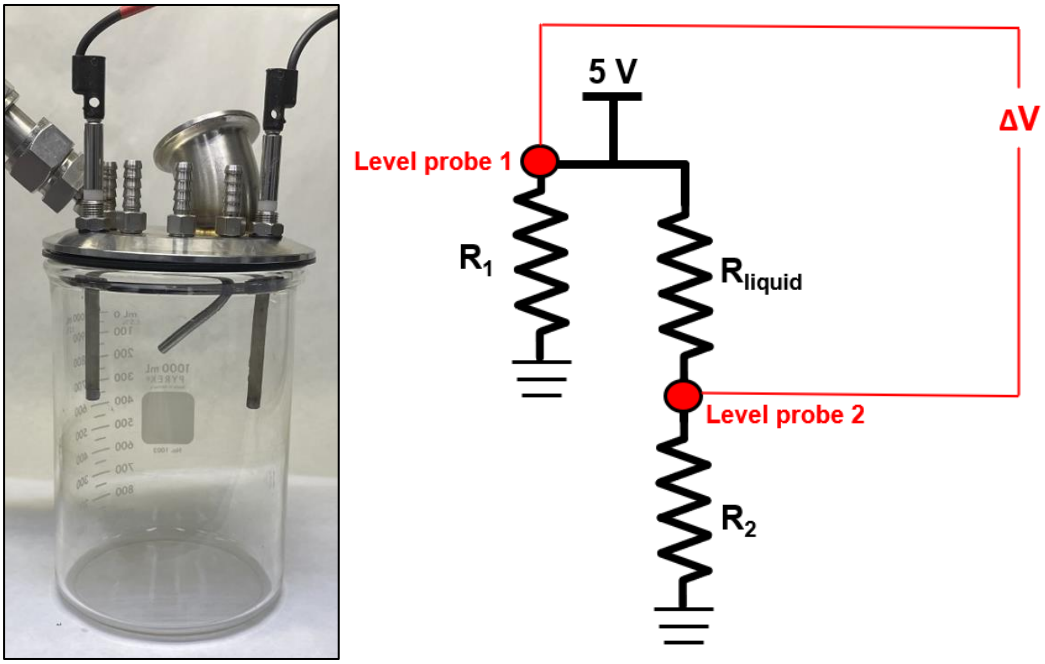

Figure A.5.3 Level control probes and circuit.

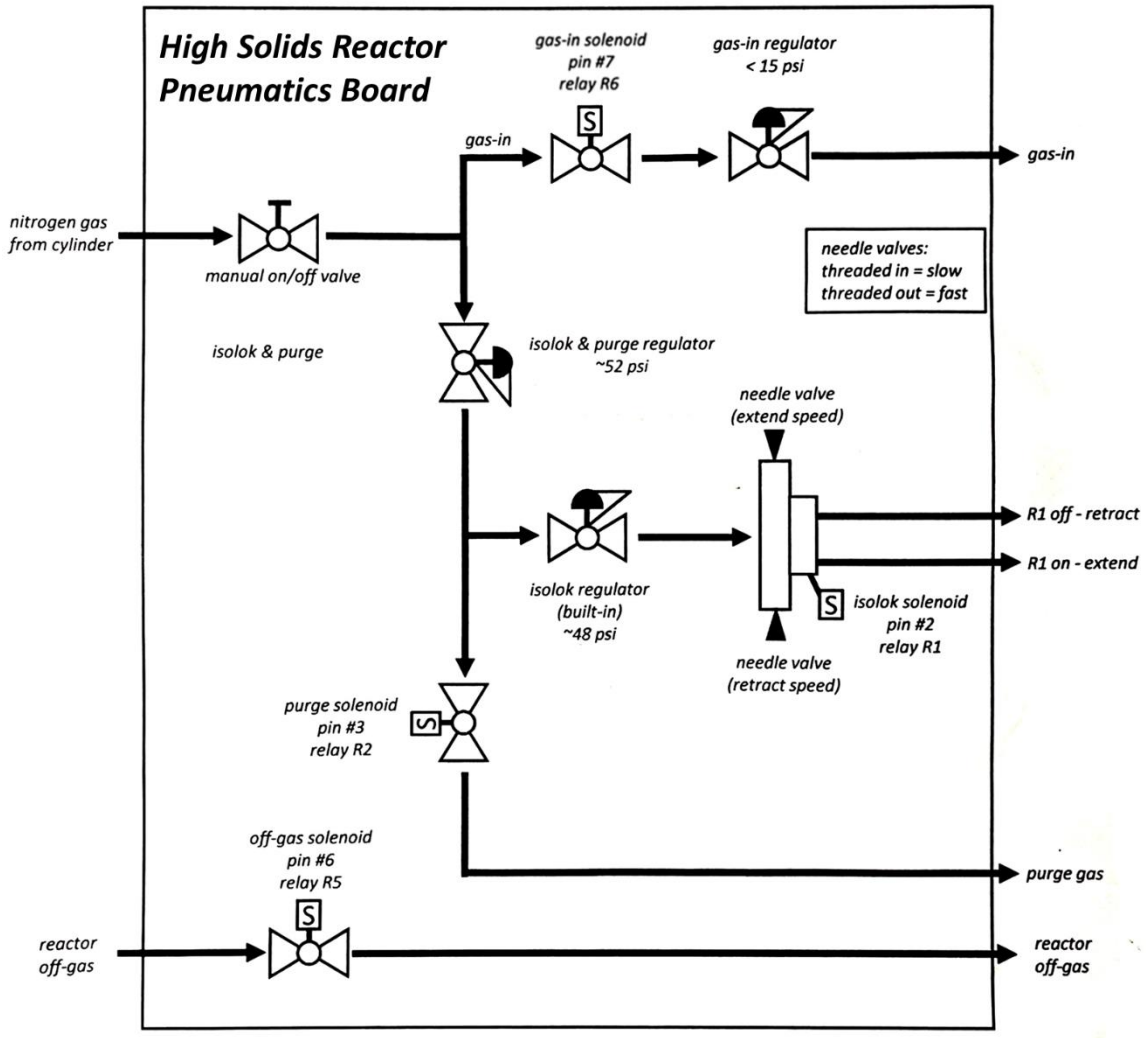

Figure A.6. Pneumatics board for the high solids reactor feeding controls.

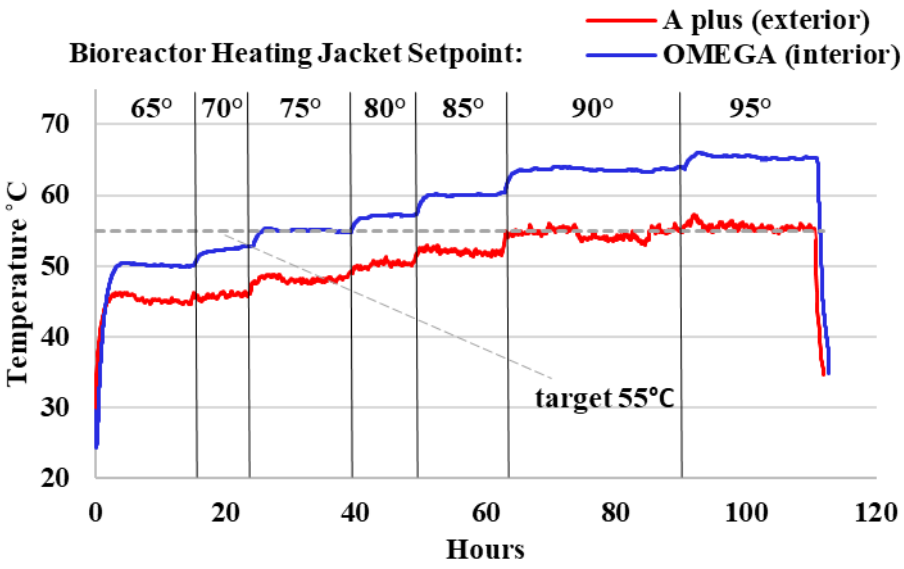

Figure A.7. Bioreactor heating jacket calibration.

Data Summary: Setpoint was determined heuristically using an OMEGA™ wireless autoclave temperature data logger inside the vessel while intermittently adjusting the heating jacket setpoint. It was determined that a setpoint at 75°C sets the bulk temperature of the interior to vessel to the target temperature, 55°C.

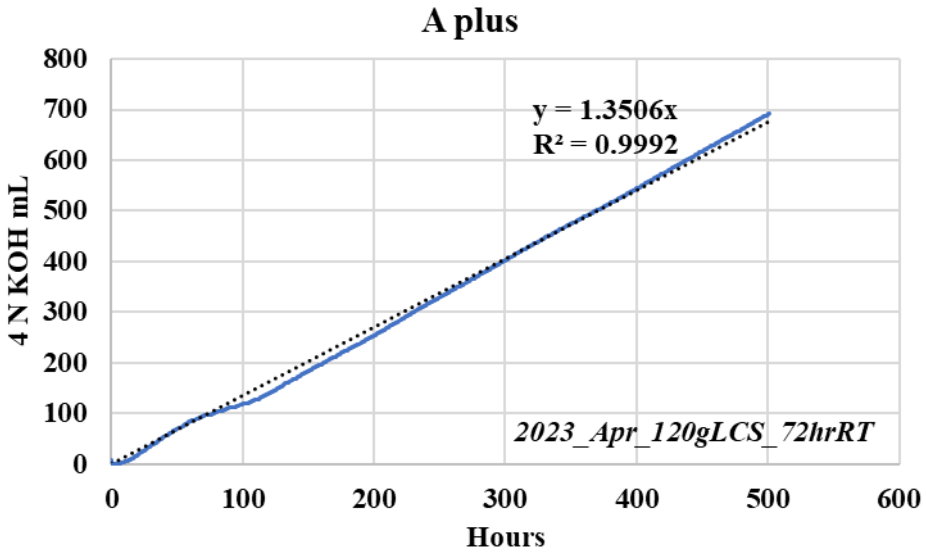

Figure A.8.1 HSR base utilization measured via A plus tower.

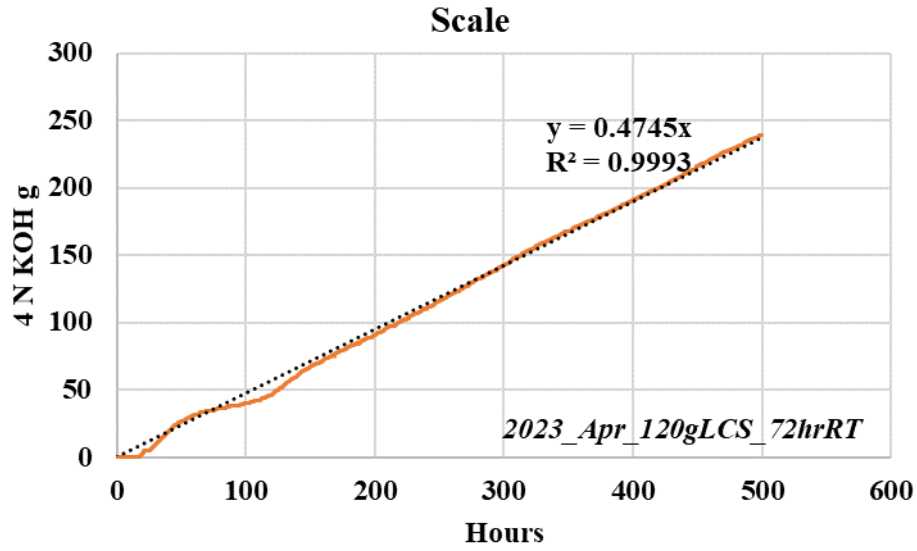

Figure A.8.2. HSR base utilization measured via weighed base jar.

Data summary: Online monitoring of base utilization for a 120 g/L corn stover for a 72-hour residence time. Base (4 N KOH) was dispensed using the Sartorius Stedim Biotech A plus tower's peristaltic pump. Volumetric data was collected by the A plus tower, but generally overestimated the volume presumably due to the elongated distance the base was forced to travel due to spatial constraints. The jar containing the base was also monitored using an A & D EJ-6100 scale, which aligned well with manually marking the base jar volume over the course of the experiment. In the event weight data is unavailable, a calibration factor of 1.35 / 0.47 = 2.85 can be used to estimate.

30 g/L Dec 2022 Run #1							
QS data							
	g ara / g solids	g glu / g solids	g xyl / g solids	g carbs / g solids	g solids / 25 ml	g carbs / 25 ml	g QS carbs / L
holding tank (endpoint) QS A	0.022	0.381	0.224	0.627	0.639	0.401	**16.032**
holding tank (endpoint) QS B	0.022	0.376	0.218	0.616	0.620	0.382	**15.285**
holding tank (endpoint) QS C	0.021	0.377	0.221	0.619	0.635	0.393	**15.717**
LQS data							
	g/L ara	g/L glu	g/L xyl	g carbs/L			
holding tank (endpoint) LQS	0.121	0.725	0.376	**1.222**			
combined QS and LQS carbohydrates							
	g QS + LQS carbs / L	**carb. Loading (g/L)**		Feedstock carb. content:		**solid loading (g/L)**	
	17.254	**16.9**	**average**	0.598		**28.3**	**average**
	16.508	**0.4**	**stdev**			**0.6**	**stdev**
	16.940						

Table A.8.1. Estimating endpoint solids loading for 30 g/L – Run #1 (Dec 2022)

30 g/L Feb 2022 Run #2							
QS data							
	g ara / g solids	g glu / g solids	g xyl / g solids	g carbs / g solids	g solids / 25 ml	g carbs / 25 ml	g QS carbs / L
holding tank (endpoint) QS A	0.028	0.395	0.233	0.656	0.621	0.407	**16.294**
holding tank (endpoint) QS B	0.026	0.375	0.224	0.626	0.587	0.367	**14.690**
holding tank (endpoint) QS C	0.028	0.403	0.239	0.670	0.563	0.377	**15.083**
LQS data							
	g/L arabin	g/L glucos	g/L xylose	g carbs/L			
holding tank (endpoint) LQS	0.122	0.238	0.376	**0.736**			
combined QS and LQS carbohydrates							
	g QS + LQS carbs / L	**carb. Loading**		Feedstock carb. content:		**solid loading**	
	17.030	**16.1**	**average**	0.598		**26.9**	**average**
	15.426	**0.8**	**stdev**			**1.4**	**stdev**
	15.820						

Table A.8.2. Estimating endpoint solids loading – Run #2 (Feb 2023)

120 g/L Mar 2023 Run #1							
QS data							
	g ara / g solids	g glu / g solids	g xyl / g solids	g carbs / g solids	g solids / 25 ml	g carbs / 25 ml	g QS carbs / L
holding tank (endpoint) QS A	0.029	0.400	0.240	0.670	2.515	1.685	**67.397**
holding tank (endpoint) QS B	0.028	0.393	0.241	0.662	2.368	1.568	**62.721**
holding tank (endpoint) QS C	0.025	0.350	0.205	0.579	2.521	1.459	**58.378**
LQS data							
	g/L ara	g/L glu	g/L xyl	g carbs/L			
holding tank (endpoint) LQS	0.496	3.621	1.594	**5.711**			
combined QS and LQS carbohydrates							
	g QS + LQS carbs / L	**carb. Loading**		Feedstock carb. content:		**solid loading**	
	73.108	**68.5**	**average**	0.598		**114.7**	**average**
	68.432	**4.5**	**stdev**			**7.5**	**stdev**
	64.089						

Table A.8.3. Estimating endpoint solids loading – Run #1 (Mar 2023)

120 g/L Apr 2023 Run #2							
QS data							
	g ara / g solids	g glu / g solids	g xyl / g solids	g carbs / g solids	g solids / 25 ml	g carbs / 25 ml	g QS carbs / L
holding tank (endpoint) QS A	0.025	0.337	0.195	0.556	2.417	1.343	**53.727**
holding tank (endpoint) QS B	0.024	0.358	0.195	0.577	2.712	1.564	**62.580**
holding tank (endpoint) QS C	0.025	0.358	0.195	0.577	2.605	1.503	**60.110**
LQS data							
	g/L ara	g/L glu	g/L xyl	g carbs/L			
holding tank (endpoint) LQS	0.512	3.168	1.600	**5.280**			
combined QS and LQS carbohydrates							
	g QS + LQS carbs / L	**carb. Loading**		Feedstock carb. content:		**solid loading**	
	59.007	**64.1**	**average**	0.598		**107.2**	**average**
	67.860	**4.6**	**stdev**			**7.6**	**stdev**
	65.390						

Table A.8.4. Estimating endpoint solids loading – Run #2 (Apr 2023)

High Solids Reactor Mar23_120gLCS_72hrRT_Run1										
Initial Reactor Fill:										
	starting volume		0.65	L			solid loading		120	g/L
	final volume		0.935	L			feed cycle volume		0.125	L
	difference		0.285	L						
	# of pumps		11							
	pump volume		0.275	L						
	# of quick cycle rest		5							
values is bold blue used to calculate FCS for early sample points.										
First Batch:										
		solids (g)	volume (L)	solids conc. (g/L)	assumed solub.					
FC	0	33	0.935	**35.29**	0					
Quick Cycles into S.C.										
		starting solids (g)	starting volume (L)	starting conc. (g/L)	post-harvest volume (L)	solids after harvest (g)	ending solids (g)	ending volume (L)	ending conc. (g/L)	assumed solub.
FC	1	33.00	0.935	35.29	0.81	28.59	43.59	0.935	46.62	0
FC	2	43.59	0.935	46.62	0.81	37.76	52.76	0.935	56.43	0
FC	3	52.76	0.935	56.43	0.81	45.71	60.71	0.935	64.93	0
FC	4	60.71	0.935	64.93	0.81	52.59	67.59	0.935	72.29	0
FC	5	67.59	0.935	72.29	0.81	58.56	73.56	0.935	**78.67**	0

Table A.8.5. Estimating solid loadings for 120 g/L first RT – Run #1 (March 2023)

High Solids Reactor		**Apr23_120gLCS_72hrRT_Run2**								
Initial Reactor Fill:										
	starting volume			0.6	L		solid loading		120	g/L
	final volume			0.935	L		feed cycle volume		0.125	L
	difference			0.335	L					
	# of pumps			13						
	pump volume			0.325	L					
	# of quick cycle restarts			5						
values is bold blue used to calculate FCS for early sample points.										
First Batch:										
		solids (g)	volume (L)	solids conc. (g/L)	assumed solub.					
FC	0	39	0.935	**41.71**	0					
Quick Cycles into S.C.										
		starting solids (g)	starting volume (L)	starting conc. (g/L)	post-harvest volume (L)	solids after harvest (g)	ending solids (g)	ending volume (L)	ending conc. (g/L)	assumed solub.
FC	1	39.00	0.935	41.71	0.81	33.79	48.79	0.935	52.18	0
FC	2	48.79	0.935	52.18	0.81	42.26	57.26	0.935	61.24	0
FC	3	57.26	0.935	61.24	0.81	49.61	64.61	0.935	69.10	0
FC	4	64.61	0.935	69.10	0.81	55.97	70.97	0.935	75.90	0
FC	5	70.97	0.935	75.90	0.81	61.48	76.48	0.935	**81.80**	0

Table A.8.6. Estimating solid loadings for 120 g/L first RT – Run #2 (April 2023)

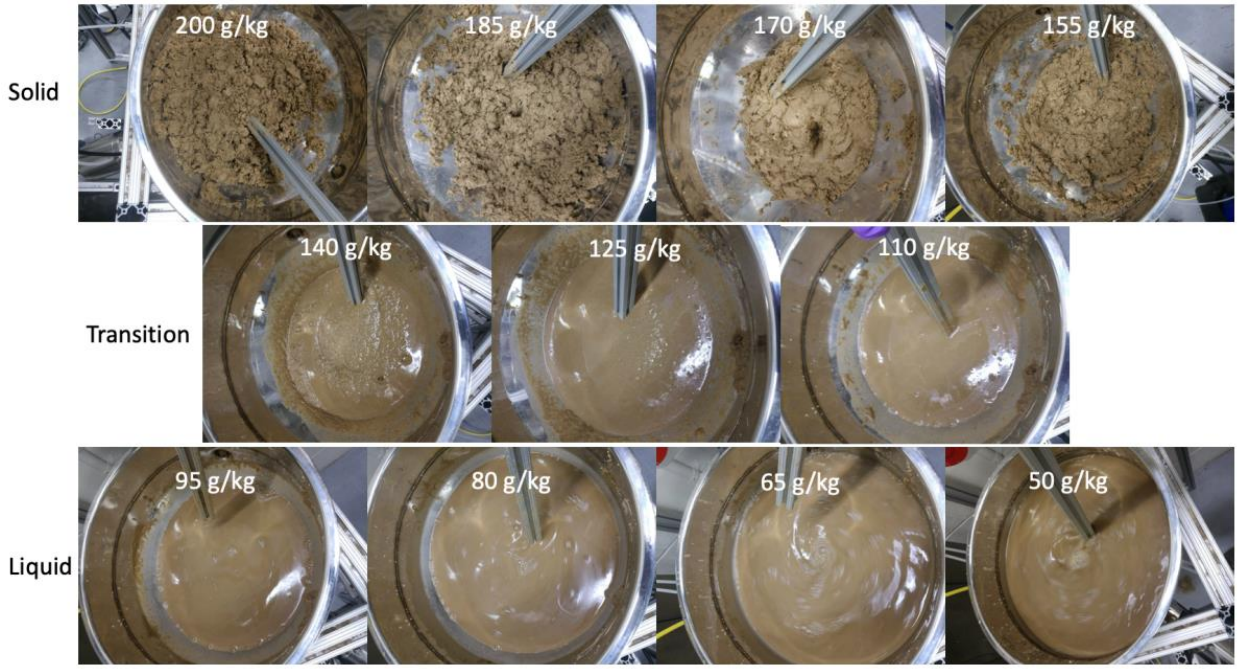

Figure A.9. Switchgrass (0.177 mm) slurry at various solid loadings.

Data summary: The slurry began at 200 g/kg solids and was diluted 10 times until the concentration was 50 g/kg. Since the agitation system was not being used, stirring could be conducted manually. Presented visually, it is quite clear that there is a significant physical change in the quality of the slurry between 155 and 125 g/kg solids. Figure reproduced from Moynihan MS thesis (2021).

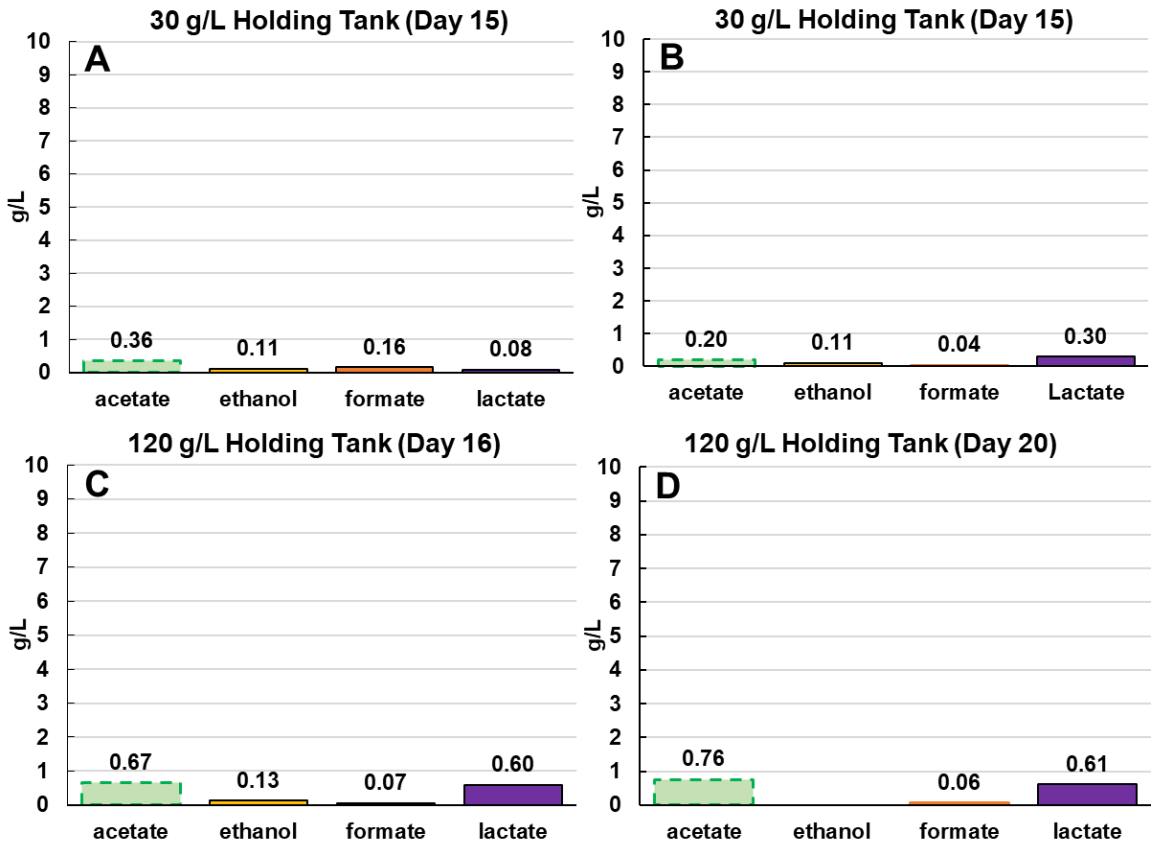

Figure A.10.1. Acetate, ethanol, formate, and lactate were measured in the holding tank at the end of each experiment. Note acetate can originate from both deconstruction of feedstock containing acetyl bonds and/or microbial production.

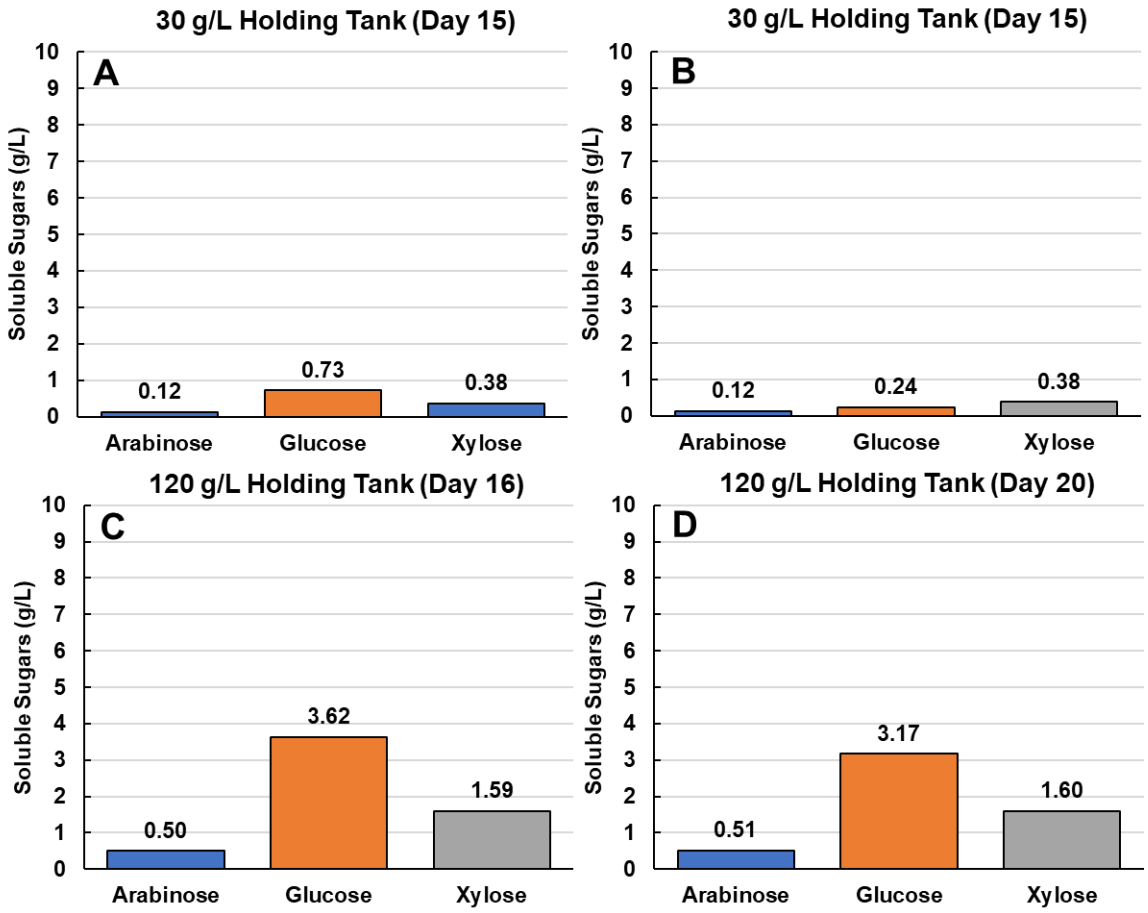

Figure A.10.2. Soluble sugars measured in the holding tank at the end of each experiment. Sugar concentrations were determined in monomeric form using a mild acid hydrolysis. Sugars were likely solubilized during the feedstock sterilization process.

Data Summary: As previously mentioned in the methods and results section, maintaining aseptic conditions for semi-continuous fermentation initially proved a difficult task, and significant time and effort was dedicated to identifying and troubleshooting sterilization failures. At first glance fermentation products in the holding would imply contamination/growth in uninoculated slurry/medium, but this was not consistent with experimental observations.

For example, biological contamination was not detected when examining a sample from the holding tank under a microscope at the end of each experiment. Furthermore, a biological contamination would likely consume solubilized C_5's which accumulated to high concentrations in figure 18 panel C. Lastly, FCS was relatively consistent across both timepoints and biological duplicates (figure 17), which is not characteristic

of a developing biological contaminant. Taken together, there was not overwhelming evidence that contamination took hold, but there is also no definitive explanation why fermentation products can be detected in the holding tank.

We now know that solids can accumulate on the piston sampler, and thus cross feeding between the bioreactor and holding tank is technically possible. While this concern came up during the initial design, it was assumed that the holding tank at room temperature would prohibit any activity by *C. thermocellum* or *T. thermosaccharolyticum*.

To further investigate this result, we began to analyze these samples using HPLC-UV absorbance to confirm the HPLC-RI (refractive index) measured concentrations. For example, lactate standards, independent of concentration, have a specific UV/RI ratio, which was not seen in our fermentation or holding tank samples. This work is still ongoing but preliminary data suggests that these samples contain both lactate and something that is not lactate. However, this interpretation is based on UV chromatograms at 210 and 250 nm that contain noisy background signals. In contrast, HPLC-refractive indices generated clean peaks. In a follow-up bottle experiment, we compared several substrates (5 g/L carbohydrate corn stover, Avicel, Avicel and xylose, xylose, and cellobiose) and media backgrounds (MTC, CTFüD) in an attempt to isolate the conditions that contain noisy background UV signals. Interestingly, uninoculated bottles of corn stover (+MTC) were the only ones that generated a similar UV profile, which disappeared for inoculated bottles of corn stover (+MTC). It is possible that the explanation for disappearance is related to relatively low substrate loading of 7.5 g/L corn stover, but warrants further experimentation. We have recently ordered and received a colorimetric enzyme-based lactate assay to cross reference these HPLC results with.

A.11 Bioreactor Data

A Sartorius A-Plus tower was used to monitor the temperature and control the pH inside the bioreactor. This is the raw data output from the A-plus tower, and not entirely representative of actual fermentation conditions inside the bioreactor. **See figures A.7 and A.8 for calibrated data.**

*The A-plus erroneously records 2.5X more base utilization than we physically observe, see appendix figure A.8 for additional details.

**A-plus measures temperature from outside the vessel walls, with a heating jacket setpoint determined heuristically, see appendix figure A.7 for additional details.

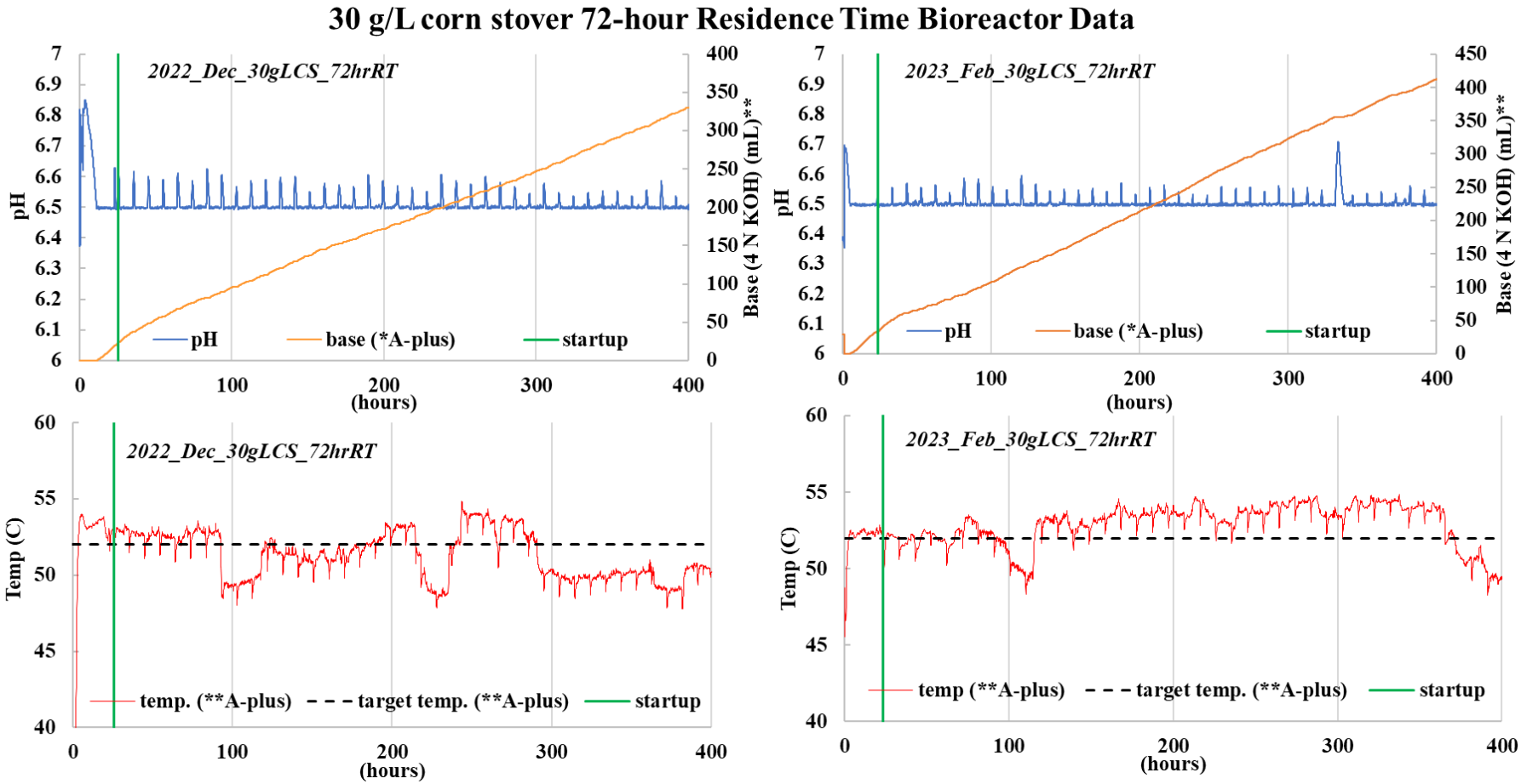

Figure A.11.1. Online bioreactor data at 30 g/L collected using Sartorius A-Plus tower. See figures A.7 and A.8 for calibrated data.

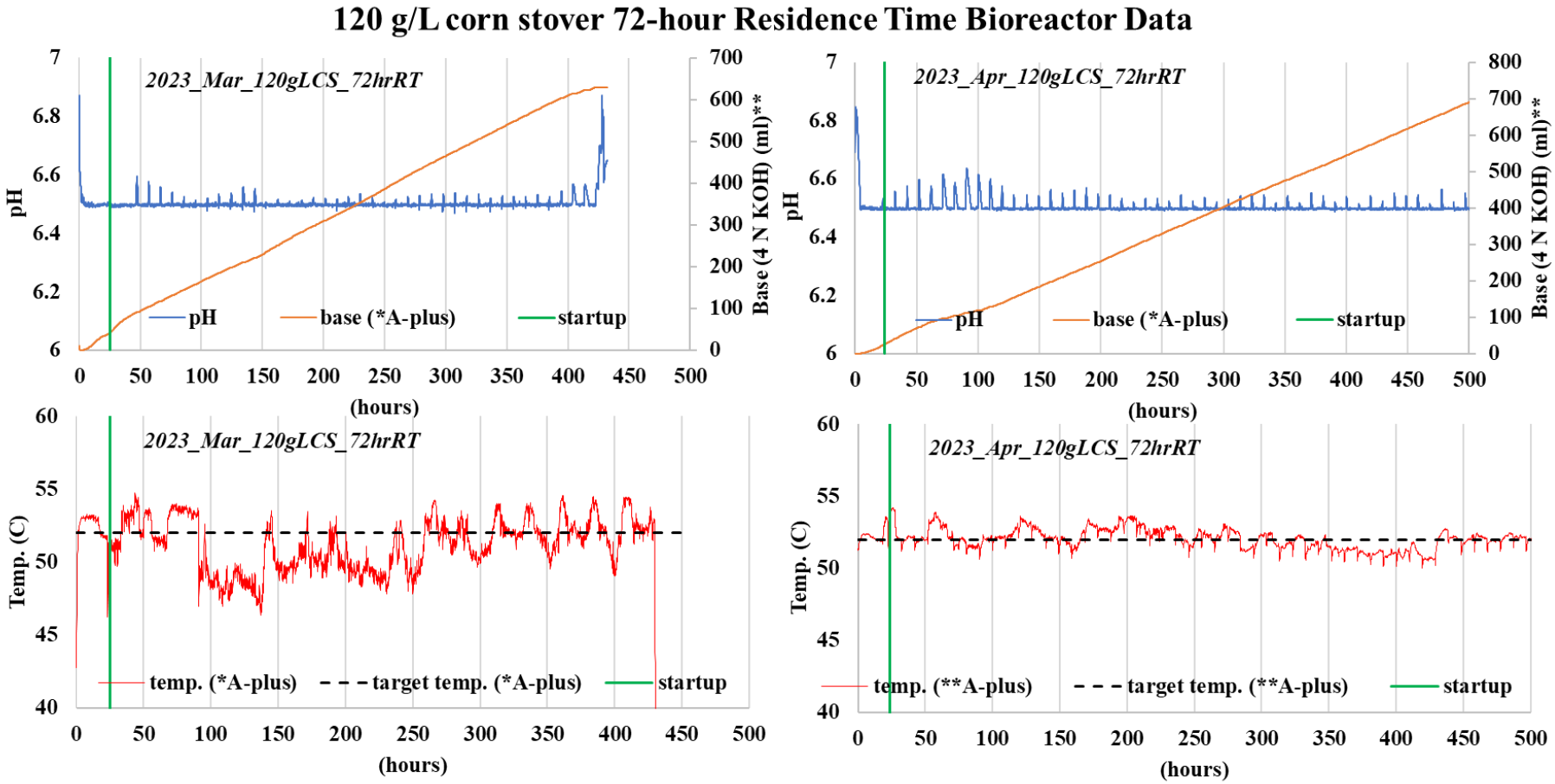

Figure A.11.2. Online bioreactor data at 120 g/L collected using Sartorius A-Plus tower. See figures A.7 and A.8 for calibrated data.

8.3 Chapter 6 Appendix

Table A.9. Survey of technoeconomic studies for cellulosic ethanol production

	Study		Published (Project Year)	Feedstock	Process	Feed Cost ($/dry metric ton)	Ethanol (MGY)	MESP ($)	Notes
NREL /TP-580-26157	Wooley et al.	(224)	1999 (1997)	yellow poplar	DAP	27.5	52.2	1.44	Biomass-to-ethanol
NREL /TP-580-28893	McAloon et al.	(223)	2000 (1999)	corn stover	DAP	38.5	25	1.50	Compares corn starch and stover
NREL /TP-510-32438	Aden et al.	(32)	2002 (2000)	corn stover	DAP	33.1	69.3	1.07	Stover-to-ethanol
NREL /TP-6A2-46588	Kazi et al.	(88)	2010 (2007)	corn stover	DAP	83.0	53.4	3.40	Compares four pretreatments, seven scenarios, and estimates pioneer plant
NREL /TP-5100-47764	Humbird et al.	(27)	2011 (2007)	corn stover	DAP	64.5	61.0	2.15	Stover-to-ethanol update
	Eggeman and Elander	(34)	2005	corn stover	DAP	35.0	56.1	1.34	Compares pretreatments and concludes DAP has best performance
	Sendich et al.	(337)	2008	corn stover	AFEX	40.0	53.8	1.03 (SSCF)	Varies CBP and SSCF, AFEX parameters
	Huang et al.	(227)	2009	corn stover	DAP	63.8	67.4	1.42	Varies biomass type and throughput
	Klien-Marcuschamer et al.	(134)	2010 (2009)	corn stover	DAP	70.5	30.9	4.58	Wiki-based biorefinery platform
	Bals et al.	(338)	2011 (2008)	corn stover	AFEX	50	23	1.86	Optimizes AFEX conditions
	Meyer et al.	(339)	2013 (2007)	corn stover	HW	64.5	47.4	2.51	Varies yeast processes
	Tao et al.	(340)	2013 (2007)	corn stover	DAP	64.5	59.0	2.21	Varies corn stover composition
	Chen et al.	(231)	2015 (2007)	corn stover	DDR	64.5	64	2.24	Varies deacetylation and

									disk refining (DDR) technique
	Yang and Rosentrater	(341)	2015	corn stover	LMAA	36.3	50	3.86	Low Moisture Anhydrous Ammonia pretreatment
	Zhao et al.	(342)	2015	corn stover	DAP	59.2	60.5	2.86	China specific economic data, compares NREL and Chinese status quo (NREL-CN-1 data shown here)
	Liu and Bao	(90)	2017 (2013)	corn stover	DryPB		60.1	1.79	Dry acid pretreatment and several others
	Lynd et al.	(21)	2017 (2014)	corn stover	CBP	84.5	60.0	1.88	Forecasted C-CBP (reference case for this study)
	Stoklosa et al.	(343)	2017 (2012)	corn stover	AFEX	60		2.09	Centralized v. decentralized corn stover processing depots
	Huang et al.	(240)	2018 (2007)	corn stover	DAP	58.5	38.1	2.16	Modeled to breakeven while coproducing 1,5-PDO
	Shen, Tao, and Yang	(344)	2018 (2014)	corn stover	DAP	85.0	57.2	2.83	Modeled to breakeven while coproducing jet fuel from lignin
	Yang et al.	(236)	2020 (2019)	sorghum	DAP	95.0		3.40	Concerns RNG and CO_2 capture with onsite solids combustion
	Das et al.	(316)	2022 (2018)	corn stover	DAP	64.5	61.4	2.47	Compares Humbird et al., 2011 model (updated to 2018) to Py-ECH

DAP = Dilute Acid Pretreatment, AFEX = Ammonia Fiber Expansion, DryPB = Dry Acid Pretreatment, LMAA = Low Moisture Anhydrous Ammonia, CBP = Consolidated Bioprocessing, HW = Hot Water, DDR = Deacetylation and Disk Refining. Py-ECH = pyrolysis with electrocatalytic hydrogenation.

Table A.10. Fermentation conditions and assumed conversions

Fermentation Conditions and Assumed Conversions			
Parameter		**Original**	**Revised**
Temperature (°C)		55	
Initial Solid Loading (wt.%)		19.5% total (59.7% carbohydrates, 23.8% insolubles, 16.5% extractives)	
Residence Time (days)		6	
Corn Steep Liquor (CSL)	Loading (wt.%)	0.155	0.64
Inorganic Nitrogen Loading	Loading (g/L)	0.261 (DAP)	0.387 (urea)
Carbohydrate Solubilization (%)		88	
Solubilized Carbohydrates	Total Conversion (%)	98.06	
	Conversion to Products (%)	85.55	
	Conversion to Cells (%)	4.75	
	Conversion to Byproducts (%)	4.75	
	Losses to Contamination (%)	3	
Ethanol	Titer (g/L)	50.26	
	Productivity (g/L-day)	8.36	
	Annual Production (MGY)	60.03	

Table A.11. Gas turbine performance parameters

Gas Turbine Conditions and Assumptions				
Parameters		**References**	**This Study**	
			Biogas Turbine	**RNG Turbine**
Scenarios		(this study)	II & III	V
Ambient Conditions	Temperature (°C)	15 (276,321,326)	25	
	Pressure (bar)	1.013 (276,321,326,327)	1.013	
Fuel Conditions	Temperature (°C)	10 (326)	28	
	Pressure (bar)	30 (326)	1.2	20
Inlet	Air Feed Rate (kg/s)	635 (326) 651 (327)	18.1	17.6
	Fuel Feed Rate (kg/s)	14.74 (326) 0.38 (276) 6.0 (321)	0.48	0.46
Compressor	Pressure Ratio	15.4 (326) 15.6 (276) 18 (321) 17 .03 (327)	15.4	
	Mechanical Efficiency (%)	99 (326) 99.5 (276)	99	
	Isentropic Efficiency (%)	88 (321,326) 85.28 (276) 89.5 (327)	88	
Combustor	Combustion Efficiency (%)	99.5 (326) 99 (321) 99.1 (327)	99.5	
Turbine	Inlet Temperature (°C)	1328.0 (326) 1286 (276) 1232 (321) 1480 (327)	1342	1400
	Exhaust Temperature (°C)	615.0 (326) 548.5 (276) 566 (321) 597.4 (327)	675	698
	Exhaust Gas Rate (kg/s)	21.09 (276) 70.5 (321)	18.6	18.1
	Isentropic Efficiency (%)	84.66 (276)	90	

		87 (321) 90 (327)		
Generator	Generator Efficiency (%)	98.5 (326) 98 (276)	98.5	
Performance	Net Power Generation (kWh)	253,200 (326) 6,327 (276) 25,060 (321) 270,494 (327)	8,830	8,922
	Thermal Efficiency (%)	36.17 (326) 33.13 (276) 36.0 (321) 38.2 (327)	37.0	38.6

Table A.12. Biogas membrane upgrading performance parameters

Parameters	**Deng & Hägg** (320) **[scaled]**	**This Study**
Raw Biogas Feed (Nm^3/h)	1,000 [13,714]	13,714
Feed pressure (bar)	1.2	1.2
Feed CO_2 concentration (vol.%)	35	47.8
Feed T and P at 1st and 2nd stage (°C, bar)	25, 20	28, 20
Permeate T and P at 1st and 2nd stage (°C, bar)	25, 1	28, 1
CH_4 purity (vol.%)	98	98
CH_4 recovery (%)	99.7	99.7
CO_2 purity (vol.%)	98.1	99.4
Recycle Ratio	0.24	0.23
Compression duty (kWh)	220 [3,017]	3,043
Compressor Isentropic Efficiency (%)	0.75	0.88
Upgraded biomethane delivery pressure (bar)	40	20

Table A.13. Scenario results summary

Scenario		Process design parameters: Enhanced heat integration	Biogas surplus to turbine	Fermentation CO_2 to CCS	Biogas membrane upgrade to RNG	RNG surplus to turbine	Additional Inputs			Exports			GHG benefits
Reference case		no	no	no	no	no	17,463	kWh	electricity	7,137	gal/hr	ethanol	fuel pellets displace fossil fuels
							3,028	kg/hr	nutrients	32,278	kg/hr	fuel pellets	
							1,351	kg/hr	natural gas				
I	Enhanced heat integration	yes	no	no	no	no	17,463	kWh	electricity	7,132	gal/hr	ethanol	no longer consumes natural gas
							3,028	kg/hr	nutrients	32,300	kg/hr	fuel pellets	
II	Biogas electricity	yes	yes	no	no	no	8,845	kWh	electricity	7,132	gal/hr	ethanol	Net electricity demand reduced 49%
							3,028	kg/hr	nutrients	32,300	kg/hr	fuel pellets	
III	Biogas electricity and fermentation CO_2 to CCS	yes	yes	yes	no	no	11,746	kWh	electricity	7,132	gal/hr	ethanol	Fermentation CO2 is now captured
							3,028	kg/hr	nutrients	32,300	kg/hr	fuel pellets	
										21,080	kg/hr	CO_2	
IV	RNG and high-purity CCS	yes	no	yes	yes	no	11,746	kWh	electricity	7,132	gal/hr	ethanol	Biogas CO2 is now captured
										32,300	kg/hr	fuel pellets	RNG surplus displaces fossil fuels
							3,028	kg/hr	nutrients	32,907	kg/hr	CO_2	
										830	kg/hr	RNG	
V	RNG electricity and high-purity CCS	yes	no	yes	yes	yes	11,746	kWh	electricity	7,132	gal/hr	ethanol	Net electricity demand reduced 7%
							3,028	kg/hr	nutrients	32,300	kg/hr	fuel pellets	
										32,907	kg/hr	CO_2	

Figure A.12 Calculations for levelized cost of CO_2 capture

CO_2 (fermentation only)

Equipment Contribution: 1) CO_2 compressor

$$6.68\ MM\$_{CO2\ compressor} \times 0.15_{capital\ charge\ factor} = 1.00\ MM\$_{annualized\ capital\ cost}$$

Electricity Contribution:

$$2{,}841\ kWh_{CO2\ compressor\ demand} \times 0.0681 \frac{\$}{kWh} = 193.47 \frac{\$}{hour}$$

$$193.5 \frac{\$}{hour} \times 8{,}410 \frac{hours}{year} = 1.62\ MM\$_{annual\ electric\ demand}$$

Sum of Contributions:

$$1.00\ MM\$_{annualized\ capital\ cost} + 1.62\ MM\$_{annual\ electric\ demand} = 2.62\ MM\$_{\ annualized\ cost}$$

Annual CO_2 Production: 177,209 ton/year

$$2.12\ MM\$_{annualized\ cost} \div 177{,}209 \frac{ton}{year} = 14.78 \frac{\$}{ton}\ CO_2$$

CO_2 (fermentation & biogas combined)

Equipment Contribution: 1) CO_2 compressor

$$8.68\ MM\$_{CO2\ compressor} \times 0.15_{capital\ charge\ factor} = 1.30\ MM\$_{annualized\ capital\ cost}$$

Electricity Contribution:

$$4{,}364\ kWh_{CO2\ compressor\ demand} \times 0.0681 \frac{\$}{kWh} = 297.18 \frac{\$}{hour}$$

$$297.18 \frac{\$}{hour} \times 8{,}410 \frac{hours}{year} = 2.50\ MM\$_{annual\ electric\ demand}$$

Sum of Contributions:

$$1.30\ MM\$_{annualized\ capital\ cost} + 2.50\ MM\$_{annual\ electric\ demand} = 3.80\ MM\$_{\ annualized\ cost}$$

Annual CO_2 Production: 276,659 ton/year

$$3.80\ MM\$_{annualized\ cost} \div 276{,}659 \frac{ton}{year} = 13.74 \frac{\$}{ton}\ CO_2$$

Figure A.13. Fuel pellet production sensitivity analysis.

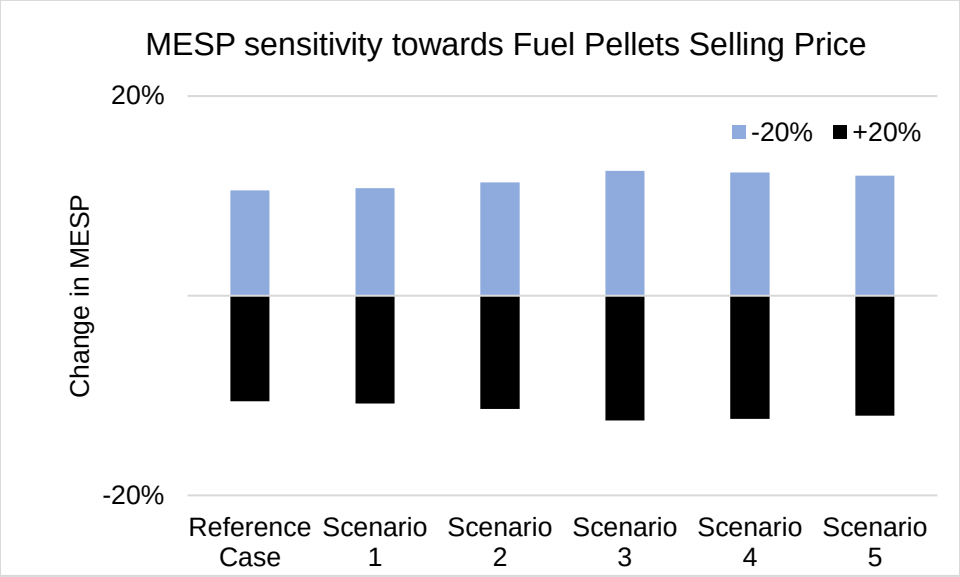

Figure A.13.1 Fuel pellet sensitivity analysis towards minimum ethanol selling price.

Data summary: It was observed that increasing or decreasing fuel pellet selling prices has a uniform effect on the MESP related to equal fuel pellet throughput amongst the scenarios. To put it another way, the modifications made to improve the biorefinery GHG balance did not change the MESP's sensitivity towards fuel pellet selling prices. A 20% change (+ or -) in fuel pellet price (baseline $166/ton) did not change the MESP by 20% which is consistent with fuel pellet revenue making up less than half of total revenue in figure 26.

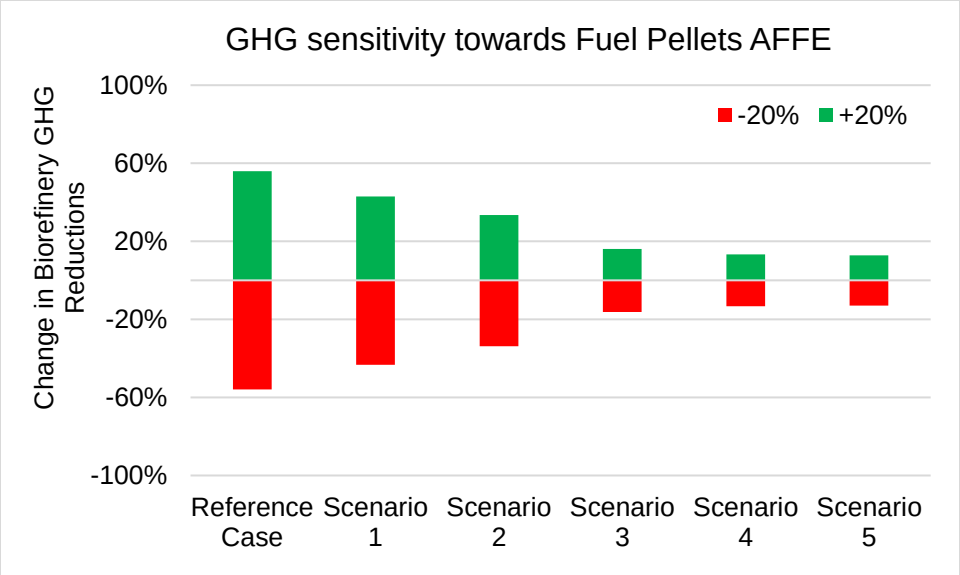

Figure A.13.2. Fuel pellet sensitivity analysis towards biorefinery GHG reductions.

Data summary: In a second sensitivity analysis, the fuel pellet contribution to avoided fossil fuel emissions (AFFE) in figure 27 are subject to + or – 20%. Since the later scenarios have greater negative carbon flux overall, any perturbation to the fuel pellet AFFE (consistent amongst all scenarios) will be effectively diluted out by the larger contributions enabled by CCS. Thus, later scenarios are less sensitive to the fuel pellet AFFE than those without CCS.

9. Bibliography

1. IPCC. Climate Change 2022 Mitigation of Climate Change: Working Group III Contribution to the Sixth Assessment Report (AR6) of the IPCC. 2022.
2. International Energy Agency. Technology Roadmap: Delivering Sustainable Bioenergy. 2017. Available from: https://www.iea.org/reports/technology-roadmap-delivering-sustainable-bioenergy
3. McKechnie J, Pourbafrani M, Saville BA, MacLean HL. Exploring impacts of process technology development and regional factors on life cycle greenhouse gas emissions of corn stover ethanol. Renew Energy. 2015 Apr 1;76:726–34.
4. IPCC. Carbon Dioxide Capture and Storage. 2005.
5. International Energy Agency. Technology Roadmap: Carbon Capture and Storage. Paris; 2013. Available from: https://www.iea.org/reports/technology-roadmap-carbon-capture-and-storage-2013
6. Leung DYC, Caramanna G, Maroto-Valer MM. An overview of current status of carbon dioxide capture and storage technologies. Vol. 39, Renewable and Sustainable Energy Reviews. Elsevier Ltd; 2014. p. 426–43.
7. Haszeldine RS, Flude S, Johnson G, Scott V. Negative emissions technologies and carbon capture and storage to achieve the Paris Agreement commitments. Vol. 376, Philosophical Transactions of the Royal Society A: Mathematical, Physical and Engineering Sciences. Royal Society Publishing; 2018.
8. Sandalow D, Aines R, Friedmann J, Mccormick C, Sanchez DL. Biomass Carbon Removal and Storage (BiCRS) Roadmap. Livermore, CA; 2021 Jan. Available from: https://www.osti.gov/biblio/1763937
9. Rosa L, Sanchez DL, Mazzotti M. Assessment of carbon dioxide removal potential: Via BECCS in a carbon-neutral Europe. Energy Environ Sci. 2021 May 1;14(5):3086–97.
10. Congressional Research Service. The Renewable Fuel Standard (RFS): An Overview. 2022. Available from: https://crsreports.congress.gov/product/pdf/R/R43325/49
11. Tao L, Markham JN, Haq Z, Biddy MJ. Techno-economic analysis for upgrading the biomass-derived ethanol-to-jet blendstocks. Green Chemistry. 2017;19(4):1082–101.
12. Hannon JR, Lynd LR, Andrade O, Benavides PT, Beckham GT, Biddy MJ, et al. Technoeconomic and life-cycle analysis of single-step catalytic conversion of wet ethanol into fungible fuel blendstocks. PNAS. 2019;117(23):12576–83.
13. Lynd LR, Beckham GT, Guss AM, Jayakody LN, Karp EM, Maranas C, et al. Toward low-cost biological and hybrid biological/catalytic conversion of cellulosic biomass to fuels†. Vol. 15, Energy and Environmental Science. Royal Society of Chemistry; 2022. p. 938–90.
14. Sheehan J, Aden A, Paustian K, Killian K, Brenner J, Walsh M, et al. Energy and environmental aspects of using corn stover for fuel ethanol. Vol. 7, Journal of Industrial Ecology. Blackwell Publishing; 2003. p. 117–46.
15. Langholtz MH, Stokes BJ, Eaton LM. 2016 Billion-Ton Report: Advancing Domestic Resources for a Thriving Bioeconomy, Volume 1: Economic Availability of Feedstocks. 2016 Jul. Available from: http://www.osti.gov/servlets/purl/1271651/

16. Bar-On YM, Phillips R, Milo R. The biomass distribution on Earth. Proc Natl Acad Sci U S A. 2018 Jun 19;115(25):6506–11.

17. Wang M, Saricks C, Wu M. Fuel-Cycle Fossil Energy Use and Greenhouse Gas Emissions of Fuel Ethanol Produced from U.S. Midwest Corn. Argonne, Illinois; 1997 Dec. Available from: https://greet.es.anl.gov/publication-oofq1amb

18. Wang M, Han J, Dunn JB, Cai H, Elgowainy A. Well-to-wheels energy use and greenhouse gas emissions of ethanol from corn, sugarcane and cellulosic biomass for US use. Efficiency and Sustainability in Biofuel Production: Environmental and Land-Use Research. 2012;7(045905).

19. Lampert D, Cai H, Wang Z, Wu M, Han J, Dunn J, et al. Development of a Life Cycle Inventory of Water Consumption Associated with the Production of Transportation Fuels. Argonne, Illinois; 2015 Oct. Available from: https://greet.es.anl.gov/publication-water-lca

20. Humbird D, Davis R, Tao L, Kinchin C, Hsu D, Aden A, et al. Process Design and Economics for Biochemical Conversion of Lignocellulosic Biomass to Ethanol: Dilute-Acid Pretreatment and Enzymatic Hydrolysis of Corn Stover. Golden, CO; 2011 May. Available from: https://www.osti.gov/biblio/1013269

21. Lynd LR, Liang X, Biddy MJ, Allee A, Cai H, Foust T, et al. Cellulosic ethanol: status and innovation. Vol. 45, Current Opinion in Biotechnology. Elsevier Ltd; 2017. p. 202–11.

22. Chundawat SPS, Beckham GT, Himmel ME, Dale BE. Deconstruction of lignocellulosic biomass to fuels and chemicals. Annu Rev Chem Biomol Eng. 2011 Jul 15;2:121–45.

23. Himmel ME, Ding SY, Johnson DK, Adney WS, Nimlos MR, Brady JW, et al. Biomass Recalcitrance: Engineering Plants and Enzymes for Biofuels Production. Vol. 315, Science. 2007. p. 804–7.

24. Bomble YJ, Lin CY, Amore A, Wei H, Holwerda EK, Ciesielski PN, et al. Lignocellulose deconstruction in the biosphere. Vol. 41, Current Opinion in Chemical Biology. Elsevier Ltd; 2017. p. 61–70.

25. Aden A, Ruth M, Ibsen K, Jechura J, Neeves K, Sheehan J, et al. Lignocellulosic Biomass to Ethanol Process Design and Economics Utilizing Co-Current Dilute Acid Prehydrolysis and Enzymatic Hydrolysis for Corn Stover. Golden, CO; 2002 Jun. Available from: https://www.osti.gov/biblio/1218326

26. Mosier N, Wyman C, Dale B, Elander R, Lee YY, Holtzapple M, et al. Features of promising technologies for pretreatment of lignocellulosic biomass. Bioresour Technol. 2005;96(6):673–86.

27. Eggeman T, Elander RT. Process and economic analysis of pretreatment technologies. Bioresour Technol. 2005;96(18 SPEC. ISS.):2019–25.

28. Hu F, Ragauskas A. Pretreatment and Lignocellulosic Chemistry. Vol. 5, Bioenergy Research. 2012. p. 1043–66.

29. Johnson E. Integrated enzyme production lowers the cost of cellulosic ethanol. Biofuels, Bioproducts and Biorefining. 2016 Mar 1;10(2):164–74.

30. Raj T, Chandrasekhar K, Naresh Kumar A, Rajesh Banu J, Yoon JJ, Kant Bhatia S, et al. Recent advances in commercial biorefineries for lignocellulosic ethanol production: Current status, challenges and future perspectives. Vol. 344, Bioresource Technology. Elsevier Ltd; 2022.

31. Lynd LR. The grand challenge of cellulosic biofuels. Vol. 35, Nature Biotechnology. Nature Publishing Group; 2017. p. 912–5.

32. Lynd LR, Weimer PJ, van Zyl WH, Pretorius IS. Microbial Cellulose Utilization: Fundamentals and Biotechnology. Microbiology and Molecular Biology Reviews. 2002 Sep;66(3):506–77.

33. Demain AL, Newcomb M, Wu JHD. Cellulase, *Clostridia*, and Ethanol. Microbiology and Molecular Biology Reviews. 2005 Mar;69(1):124–54.

34. Shao X, Murphy SJ, Lynd LR. Characterization of reduced carbohydrate solubilization during *Clostridium thermocellum* fermentation with high switchgrass concentrations. Biomass Bioenergy. 2020 Aug 1;139.

35. Verbeke TJ, Garcia GM, Elkins JG. The effect of switchgrass loadings on feedstock solubilization and biofuel production by *Clostridium thermocellum*. Biotechnol Biofuels. 2017 Nov 30;10(1).

36. Jørgensen H, Kristensen JB, Felby C. Enzymatic conversion of lignocellulose into fermentable sugars: Challenges and opportunities. Vol. 1, Biofuels, Bioproducts and Biorefining. 2007. p. 119–34.

37. Jørgensen H, Vibe-Pedersen J, Larsen J, Felby C. Liquefaction of lignocellulose at high-solids concentrations. Biotechnol Bioeng. 2007 Apr 1;96(5):862–70.

38. Kristensen JB, Felby C, Jørgensen H. Yield-determining factors in high-solids enzymatic hydrolysis of lignocellulose. Biotechnol Biofuels. 2009 Jun 8;2.

39. Wingren A, Galbe M, Zacchi G. Techno-economic evaluation of producing ethanol from softwood: Comparison of SSF and SHF and identification of bottlenecks. Vol. 19, Biotechnology Progress. 2003. p. 1109–17.

40. Lynd LR. OVERVIEW AND EVALUATION OF FUEL ETHANOL FROM CELLULOSIC BIOMASS: Technology, Economics, the Environment, and Policy. Vol. 9, Annual Reviews. AR016-15 Annu. Rev. Energy Environ. 1996.

41. IRENA. Bioenergy for the energy transition: Ensuring sustainability and overcoming barriers. Abu Dhabi; 2022. Available from: https://www.irena.org/publications/2022/Aug/Bioenergy-for-the-Transition

42. Gabrielli P, Gazzani M, Mazzotti M. The Role of Carbon Capture and Utilization, Carbon Capture and Storage, and Biomass to Enable a Net-Zero-CO_2 Emissions Chemical Industry. Ind Eng Chem Res. 2020 Apr 15;59(15):7033–45.

43. Oke D, Dunn JB, Hawkins TR. The contribution of biomass and waste resources to decarbonizing transportation and related energy and environmental effects. Sustain Energy Fuels. 2022 Feb 7;6(3):721–35.

44. Alonso DM, Bond JQ, Dumesic JA. Catalytic conversion of biomass to biofuels. Green Chemistry. 2010 Sep 3;12(9):1493–513.

45. Hobdey SE, Donohoe BS, Brunecky R, Himmel ME, Bomble YJ. New Insights into Microbial Strategies for Biomass Conversion. In: Direct Microbial Conversion of Biomass to Advanced Biofuels. Elsevier; 2015. p. 111–27.

46. Petridis L, Smith JC. Molecular-level driving forces in lignocellulosic biomass deconstruction for bioenergy. Vol. 2, Nature Reviews Chemistry. Nature Publishing Group; 2018. p. 382–9.

47. Saha BC. Hemicellulose bioconversion. In: Journal of Industrial Microbiology and Biotechnology. 2003. p. 279–91.

48. Beri D, York WS, Lynd LR, Peña MJ, Herring CD. Development of a thermophilic coculture for corn fiber conversion to ethanol. Nat Commun. 2020 Dec 1;11(1).

49. Beri D, Herring CD, Blahova S, Poudel S, Giannone RJ, Hettich RL, et al. Coculture with hemicellulose-fermenting microbes reverses inhibition of corn fiber solubilization by *Clostridium thermocellum* at elevated solids loadings. Biotechnol Biofuels. 2021 Dec 1;14(1).

50. Kristensen JB, Börjesson J, Bruun MH, Tjerneld F, Jørgensen H. Use of surface active additives in enzymatic hydrolysis of wheat straw lignocellulose. Enzyme Microb Technol. 2007 Mar 5;40(4):888–95.

51. Yang B, Wyman CE. Pretreatment: The key to unlocking low-cost cellulosic ethanol. Vol. 2, Biofuels, Bioproducts and Biorefining. 2008. p. 26–40.

52. Medronho B, Romano A, Miguel MG, Stigsson L, Lindman B. Rationalizing cellulose (in)solubility: Reviewing basic physicochemical aspects and role of hydrophobic interactions. Cellulose. 2012 Jun;19(3):581–7.

53. Bond JQ, Upadhye AA, Olcay H, Tompsett GA, Jae J, Xing R, et al. Production of renewable jet fuel range alkanes and commodity chemicals from integrated catalytic processing of biomass. In: Energy and Environmental Science. Royal Society of Chemistry; 2014. p. 1500–23.

54. Lee J. Biological conversion of lignocellulosic biomass to ethanol. Vol. 56, Journal of Biotechnology. 1997.

55. Willke T, Vorlop KD. Industrial bioconversion of renewable resources as an alternative to conventional chemistry. Vol. 66, Applied Microbiology and Biotechnology. 2004. p. 131–42.

56. Brown TR. A techno-economic review of thermochemical cellulosic biofuel pathways. Vol. 178, Bioresource Technology. Elsevier Ltd; 2015. p. 166–76.

57. Wright MM, Brown RC. Comparative economics of biorefineries based on the biochemical and thermochemical platforms. Vol. 1, Biofuels, Bioproducts and Biorefining. 2007. p. 49–56.

58. Faaij A. Modern biomass conversion technologies. In: Mitigation and Adaptation Strategies for Global Change. 2006. p. 343–75.

59. Atsonios K, Kougioumtzis MA, Panopoulos KD, Kakaras E. Alternative thermochemical routes for aviation biofuels via alcohols synthesis: Process modeling, techno-economic assessment and comparison. Appl Energy. 2015 Jan 5;138:346–66.

60. Patel M, Zhang X, Kumar A. Techno-economic and life cycle assessment on lignocellulosic biomass thermochemical conversion technologies: A review. Vol. 53, Renewable and Sustainable Energy Reviews. Elsevier Ltd; 2016. p. 1486–99.

61. Foust TD, Aden A, Dutta A, Phillips S. An economic and environmental comparison of a biochemical and a thermochemical lignocellulosic ethanol conversion processes. Cellulose. 2009;16(4):547–65.

62. Laser M, Larson E, Dale B, Wang M, Greene N, Lynd LR. Comparative analysis of efficiency, environmental impact, and process economics for mature biomass refining scenarios. Biofuels, Bioproducts and Biorefining. 2009;3(2):247–70.

63. Anex RP, Aden A, Kazi FK, Fortman J, Swanson RM, Wright MM, et al. Techno-economic comparison of biomass-to-transportation fuels via pyrolysis, gasification, and biochemical pathways. Fuel. 2010 Nov 1;89(SUPPL. 1).

64. García-Velásquez CA, Cardona CA. Comparison of the biochemical and thermochemical routes for bioenergy production: A techno-economic (TEA), energetic and environmental assessment. Energy. 2019 Apr 1;172:232–42.

65. Hossain MS, Theodoropoulos C, Yousuf A. Techno-economic evaluation of heat integrated second generation bioethanol and furfural coproduction. Biochem Eng J. 2019 Apr 15;144:89–103.

66. Geissler CH, Maravelias CT. Analysis of alternative bioenergy with carbon capture strategies: present and future. Energy Environ Sci. 2022 May 27;15(7):2679–89.

67. Davis R, Grundl N, Tao L, Biddy MJ, Tan ECD, Beckham GT, et al. Process Design and Economics for the Conversion of Lignocellulosic Biomass to Hydrocarbon Fuels and Coproducts: 2018 Biochemical Design Case Update: Biochemical Deconstruction and Conversion of Biomass to Fuels and Products via Integrated Biorefinery Pathways. 2018.

68. Broda M, Yelle DJ, Serwańska K. Bioethanol Production from Lignocellulosic Biomass-Challenges and Solutions. Molecules. 2022 Dec 9;27(24). Available from: http://www.ncbi.nlm.nih.gov/pubmed/36557852

69. Chen H, Liu J, Chang X, Chen D, Xue Y, Liu P, et al. A review on the pretreatment of lignocellulose for high-value chemicals. Vol. 160, Fuel Processing Technology. Elsevier B.V.; 2017. p. 196–206.

70. Galbe M, Wallberg O. Pretreatment for biorefineries: A review of common methods for efficient utilisation of lignocellulosic materials. Vol. 12, Biotechnology for Biofuels. BioMed Central Ltd.; 2019.

71. Mankar AR, Pandey A, Modak A, Pant KK. Pretreatment of lignocellulosic biomass: A review on recent advances. Vol. 334, Bioresource Technology. Elsevier Ltd; 2021.

72. Beig B, Riaz M, Raza Naqvi S, Hassan M, Zheng Z, Karimi K, et al. Current challenges and innovative developments in pretreatment of lignocellulosic residues for biofuel production: A review. Fuel. 2021 Mar 1;287.

73. Kumar AK, Sharma S. Recent updates on different methods of pretreatment of lignocellulosic feedstocks: a review. Vol. 4, Bioresources and Bioprocessing. Springer Science and Business Media Deutschland GmbH; 2017.

74. Uppugundla N, Da Costa Sousa L, Chundawat SPS, Yu X, Simmons B, Singh S, et al. A comparative study of ethanol production using dilute acid, ionic liquid and AFEXTM pretreated corn stover. Biotechnol Biofuels. 2014 May 13;7(1).

75. Wyman CE, Balan V, Dale BE, Elander RT, Falls M, Hames B, et al. Comparative data on effects of leading pretreatments and enzyme loadings and formulations on sugar yields from different switchgrass sources. Bioresour Technol. 2011 Dec;102(24):11052–62.

76. Wang F, Shi D, Han J, Zhang G, Jiang X, Yang M, et al. Comparative study on pretreatment processes for different utilization purposes of switchgrass. ACS Omega. 2020 Sep 8;5(35):21999–2007.

77. Zhu Z, Sathitsuksanoh N, Vinzant T, Schell DJ, McMillan JD, Zhang YHP. Comparative study of corn stover pretreated by dilute acid and cellulose solvent-based lignocellulose fractionation: Enzymatic hydrolysis, supramolecular structure, and substrate accessibility. Biotechnol Bioeng. 2009 Jul 1;103(4):715–24.

78. Nguyen TY, Cai CM, Kumar R, Wyman CE. Co-solvent Pretreatment Reduces Costly Enzyme Requirements for High Sugar and Ethanol Yields from Lignocellulosic Biomass. ChemSusChem. 2015 May 11;8(10):1716–25.

79. Conde-Mejía C, Jiménez-Gutiérrez A, El-Halwagi M. A comparison of pretreatment methods for bioethanol production from lignocellulosic materials. Process Safety and Environmental Protection. 2012 May;90(3):189–202.

80. Kazi KF, Fortman J, Anex R, Kothandaraman G, Hsu D, Aden A, et al. Techno-Economic Analysis of Biochemical Scenarios for Production of Cellulosic Ethanol. Golden, CO; 2007. Available from: https://www.osti.gov/biblio/982937

81. da Silva ARG, Torres Ortega CE, Rong BG. Techno-economic analysis of different pretreatment processes for lignocellulosic-based bioethanol production. Bioresour Technol. 2016 Oct 1;218:561–70.

82. Liu G, Bao J. Maximizing cellulosic ethanol potentials by minimizing wastewater generation and energy consumption: Competing with corn ethanol. Bioresour Technol. 2017;245:18–26.

83. Adom F, Dunn JB,, Han J. GREET Pretreatment Module. 2014.

84. Panagiotou G, Olsson L. Effect of compounds released during pretreatment of wheat straw on microbial growth and enzymatic hydrolysis rates. Biotechnol Bioeng. 2007 Feb 1;96(2):250–8.

85. Jing X, Zhang X, Bao J. Inhibition performance of lignocellulose degradation products on industrial cellulase enzymes during cellulose hydrolysis. In: Applied Biochemistry and Biotechnology. 2009. p. 696–707.

86. Rajan K, Carrier DJ. Effect of dilute acid pretreatment conditions and washing on the production of inhibitors and on recovery of sugars during wheat straw enzymatic hydrolysis. Biomass Bioenergy. 2014;62:222–7.

87. Singh S, Cheng G, Sathitsuksanoh N, Wu D, Varanasi P, George A, et al. Comparison of different biomass pretreatment techniques and their impact on chemistry and structure. Front Energy Res. 2015;3(FEB).

88. Drula E, Garron ML, Dogan S, Lombard V, Henrissat B, Terrapon N. The carbohydrate-active enzyme database: Functions and literature. Nucleic Acids Res. 2022 Jan 7;50(D1):D571–7.

89. Hansen GH, Lübeck M, Frisvad JC, Lübeck PS, Andersen B. Production of cellulolytic enzymes from ascomycetes: Comparison of solid state and submerged fermentation. Vol. 50, Process Biochemistry. Elsevier Ltd; 2015. p. 1327–41.

90. Singhania RR, Sukumaran RK, Patel AK, Larroche C, Pandey A. Advancement and comparative profiles in the production technologies using solid-state and submerged fermentation for microbial cellulases. Vol. 46, Enzyme and Microbial Technology. 2010. p. 541–9.

91. Peterson R, Nevalainen H. *Trichoderma reesei* RUT-C30 - Thirty years of strain improvement. Vol. 158, Microbiology. 2012. p. 58–68.

92. Bischof RH, Ramoni J, Seiboth B. Cellulases and beyond: The first 70 years of the enzyme producer *Trichoderma reesei*. Vol. 15, Microbial Cell Factories. BioMed Central Ltd.; 2016.

93. Hasunuma T, Okazaki F, Okai N, Hara KY, Ishii J, Kondo A. A review of enzymes and microbes for lignocellulosic biorefinery and the possibility of their application to consolidated bioprocessing technology. Bioresour Technol. 2013;135:513–22.

94. Sipos B, Benkő Z, Dienes D, Réczey K, Viikari L, Siika-Aho M. Characterisation of specific activities and hydrolytic properties of cell-wall-degrading enzymes produced by *Trichoderma reesei* rut C30 on different carbon sources. Appl Biochem Biotechnol. 2010;161(1–8):347–64.

95. Xia J, Yang Y, Liu CG, Yang S, Bai FW. Engineering *Zymomonas mobilis* for Robust Cellulosic Ethanol Production. Vol. 37, Trends in Biotechnology. Elsevier Ltd; 2019. p. 960–72.

96. Banerjee S, Mishra G, Roy A. Metabolic Engineering of Bacteria for Renewable Bioethanol Production from Cellulosic Biomass. Vol. 24, Biotechnology and Bioprocess Engineering. Korean Society for Biotechnology and Bioengineering; 2019. p. 713–33.

97. Shaw JA, Covalla SF, Miller BB, Firliet BT, Hogsett DA, Herring CD. Urease expression in a *Thermoanaerobacterium saccharolyticum* ethanologen allows high titer ethanol production. Metab Eng. 2012 Sep;14(5):528–32.

98. Shaw JA, Podkaminer KK, Desai SG, Bardsley JS, Rogers SR, Thorne PG, et al. Metabolic engineering of a thermophilic bacterium to produce ethanol at high yield. 2008.

99. Koppolu V, Vasigala VK. Role of *Escherichia coli* in Biofuel Production . Microbiol Insights. 2016 Jan;9:MBI.S10878.

100. Ho NWY, Chen Z, Brainard AP. Genetically Engineered *Saccharomyces* Yeast Capable of Effective Cofermentation of Glucose and Xylose. Vol. 64, APPLIED AND ENVIRONMENTAL MICROBIOLOGY. 1998.

101. Zha J, Shen M, Hu M, Song H, Yuan Y. Enhanced expression of genes involved in initial xylose metabolism and the oxidative pentose phosphate pathway in the improved xylose-utilizing *Saccharomyces cerevisiae* through evolutionary engineering. J Ind Microbiol Biotechnol. 2014 Jan 1;41(1):27–39.

102. Kim SR, Park YC, Jin YS, Seo JH. Strain engineering of *Saccharomyces cerevisiae* for enhanced xylose metabolism. Vol. 31, Biotechnology Advances. Elsevier Inc.; 2013. p. 851–61.

103. Nijland JG, Driessen AJM. Engineering of Pentose Transport in *Saccharomyces cerevisiae* for Biotechnological Applications. Vol. 7, Frontiers in Bioengineering and Biotechnology. Frontiers Media S.A.; 2020.

104. Liu CG, Xiao Y, Xia XX, Zhao XQ, Peng L, Srinophakun P, et al. Cellulosic ethanol production: Progress, challenges and strategies for solutions. Vol. 37, Biotechnology Advances. Elsevier Inc.; 2019. p. 491–504.

105. Holtzapple M, Cognata M, Shu Y, Hendrickson C. Inhibition of *Trichoderma reesei* CelIulase by Sugars and Solvents. Biotechnology and Bioengineering . 1990;36:275–87.

106. Ojeda K, Sánchez E, El-Halwagi M, Kafarov V. Exergy analysis and process integration of bioethanol production from acid pre-treated biomass: Comparison of SHF, SSF and SSCF pathways. Chemical Engineering Journal. 2011 Dec 1;176–177:195–201.

107. Tomás-Pejó E, Oliva JM, Ballesteros M, Olsson L. Comparison of SHF and SSF processes from steam-exploded wheat straw for ethanol production by xylose-fermenting and robust glucose-fermenting Saccharomyces cerevisiae strains. Biotechnol Bioeng. 2008 Aug 15;100(6):1122–31.

108. McMillan JD. Xylose Fermentation to Ethanol: A Review. Golden, CO; 1993.

109. Hinman ND, Wright JD, Hoagland W, Wyman CE. Xylose Fermentation An Economic Analysis.

110. Hinman HD, Schell DJ, Riley CJ, Bergeron PW, Walter PJ. Preliminary Estimate of the Cost of Ethanol Production for SSF Technology. 1992.

111. Ge Y, Li L, Yun L. Modeling and economic optimization of cellulosic biofuel supply chain considering multiple conversion pathways. Appl Energy. 2021 Jan 1;281.

112. Zhang J, Tang M, Viikari L. Xylans inhibit enzymatic hydrolysis of lignocellulosic materials by cellulases. Bioresour Technol. 2012 Oct;121:8–12.

113. Malgas S, Kwanya Minghe VM, Pletschke BI. The effect of hemicellulose on the binding and activity of cellobiohydrolase I, Cel7A, from *Trichoderma reesei* to cellulose. Cellulose. 2020 Jan 1;27(2):781–97.

114. Qing Q, Wyman CE. Supplementation with xylanase and β-xylosidase to reduce xylo-oligomer and xylan inhibition of enzymatic hydrolysis of cellulose and pretreated corn stover. Biotechnol Biofuels. 2011;4(1).

115. Selig MJ, Knoshaug EP, Adney WS, Himmel ME, Decker SR. Synergistic enhancement of cellobiohydrolase performance on pretreated corn stover by addition of xylanase and esterase activities. Bioresour Technol. 2008 Jul;99(11):4997–5005.

116. Öhgren K, Bura R, Saddler J, Zacchi G. Effect of hemicellulose and lignin removal on enzymatic hydrolysis of steam pretreated corn stover. Bioresour Technol. 2007 Sep;98(13):2503–10.

117. Zhai R, Hu J, Saddler JN. The inhibition of hemicellulosic sugars on cellulose hydrolysis are highly dependant on the cellulase productive binding, processivity, and substrate surface charges. Bioresour Technol. 2018 Jun 1;258:79–87.

118. Qing Q, Yang B, Wyman CE. Xylooligomers are strong inhibitors of cellulose hydrolysis by enzymes. Bioresour Technol. 2010 Dec;101(24):9624–30.

119. Xue S, Uppugundla N, Bowman MJ, Cavalier D, Da Costa Sousa L, Dale BE, et al. Sugar loss and enzyme inhibition due to oligosaccharide accumulation during high solids-loading enzymatic hydrolysis. Biotechnol Biofuels. 2015 Nov 26;8(1).

120. Padella M, O'Connell A, Prussi M. What is still limiting the deployment of cellulosic ethanol? Analysis of the current status of the sector. Vol. 9, Applied Sciences (Switzerland). MDPI AG; 2019.

121. Brown TR, Brown RC. A review of cellulosic biofuel commercial-scale projects in the United States. Biofuels, Bioproducts and Biorefining. 2013;7(3):235–45.

122. Aui A, Wang Y, Mba-Wright M. Evaluating the economic feasibility of cellulosic ethanol: A meta-analysis of techno-economic analysis studies. Renewable and Sustainable Energy Reviews. 2021 Jul 1;145.

123. Wyman CE. What is (and is not) vital to advancing cellulosic ethanol. Trends Biotechnol. 2007 Apr;25(4):153–7.

124. Barta Z, Kovacs K, Reczey K, Zacchi G. Process design and economics of on-site cellulase production on various carbon sources in a softwood-based ethanol plant. Enzyme Res. 2010;2010.

125. Klein-Marcuschamer D, Oleskowicz-Popiel P, Simmons BA, Blanch HW. Technoeconomic analysis of biofuels: A wiki-based platform for lignocellulosic biorefineries. Biomass Bioenergy. 2010 Dec;34(12):1914–21.

126. Carpio RR, Secchi SG, Barros RO, Oliveira RA, Queiroz S, Teixeira RSS, et al. Techno-economic evaluation of second-generation ethanol from sugarcane bagasse: Commercial versus on-site produced enzymes and use of the xylose liquor. J Clean Prod. 2022 Oct 1;369.

127. Periyasamy S, Beula Isabel J, Kavitha S, Karthik V, Mohamed BA, Gizaw DG, et al. Recent advances in consolidated bioprocessing for conversion of lignocellulosic biomass into bioethanol – A review. Chemical Engineering Journal. 2023 Feb 1;453.

128. Lynd LR, Guss AM, Himmel ME, Beri D, Herring C, Holwerda EK, et al. Advances in Consolidated Bioprocessing Using Clostridium thermocellum and *Thermoanaerobacter*

saccharolyticum. In: Industrial Biotechnology. Wiley-VCH Verlag GmbH & Co. KGaA; 2016. p. 365–94.

129. Thomas VA, Donohoe BS, Li M, Pu Y, Ragauskas AJ, Kumar R, et al. Adding tetrahydrofuran to dilute acid pretreatment provides new insights into substrate changes that greatly enhance biomass deconstruction by *Clostridium thermocellum* and fungal enzymes. Biotechnol Biofuels. 2017 Nov 30;10(1).

130. Kothari N, Holwerda EK, Cai CM, Kumar R, Wyman CE. Biomass augmentation through thermochemical pretreatments greatly enhances digestion of switchgrass by *Clostridium thermocellum*. Biotechnol Biofuels. 2018 Aug 4;11(1).

131. Holwerda EK, Worthen RS, Kothari N, Lasky RC, Davison BH, Fu C, et al. Multiple levers for overcoming the recalcitrance of lignocellulosic biomass. Biotechnol Biofuels. 2019 Jan 17;12(1).

132. Paye JMD, Guseva A, Hammer SK, Gjersing E, Davis MF, Davison BH, et al. Biological lignocellulose solubilization: Comparative evaluation of biocatalysts and enhancement via cotreatment. Biotechnol Biofuels. 2016 Jan 12;9(1).

133. Balch ML, Holwerda EK, Davis MF, Sykes RW, Happs RM, Kumar R, et al. Lignocellulose fermentation and residual solids characterization for senescent switchgrass fermentation by: *Clostridium thermocellum* in the presence and absence of continuous in situ ball-milling. Energy Environ Sci. 2017;10(5):1252–61.

134. Akinosho H, Yee K, Close D, Ragauskas A. The emergence of *Clostridium thermocellum* as a high utility candidate for consolidated bioprocessing applications. Vol. 2, Frontiers in Chemistry. Frontiers Media S. A; 2014.

135. Brethauer S, Studer MH. Consolidated bioprocessing of lignocellulose by a microbial consortium. In: Energy and Environmental Science. Royal Society of Chemistry; 2014. p. 1446–53.

136. Du R, Li C, Lin W, Lin CSK, Yan J. Domesticating a bacterial consortium for efficient lignocellulosic biomass conversion. Renew Energy. 2022 Apr 1;189:359–68.

137. Resch MG, Donohoe BS, Baker JO, Decker SR, Bayer EA, Beckham GT, et al. Fungal cellulases and complexed cellulosomal enzymes exhibit synergistic mechanisms in cellulose deconstruction. Energy Environ Sci. 2013 Jun;6(6):1858–67.

138. Qu XS, Hu B Bin, Zhu MJ. Enhanced saccharification of cellulose and sugarcane bagasse by: *Clostridium thermocellum* cultures with Triton X-100 and β-glucosidase/Cellic®CTec2 supplementation. RSC Adv. 2017;7(35):21360–5.

139. Zhang XZ, Sathitsuksanoh N, Zhu Z, Percival Zhang YH. One-step production of lactate from cellulose as the sole carbon source without any other organic nutrient by recombinant cellulolytic *Bacillus subtilis*. Metab Eng. 2011 Jul;13(4):364–72.

140. Maleki F, Changizian M, Zolfaghari N, Rajaei S, Noghabi KA, Zahiri HS. Consolidated bioprocessing for bioethanol production by metabolically engineered *Bacillus subtilis* strains. Sci Rep. 2021 Dec 1;11(1).

141. Bokinsky G, Peralta-Yahya PP, George A, Holmes BM, Steen EJ, Dietrich J, et al. Synthesis of three advanced biofuels from ionic liquid-pretreated switchgrass using engineered *Escherichia coli*. PNAS. 2011;108(50):19949–54.

142. Li Y, Tschaplinski TJ, Engle NL, Hamilton CY, Rodriguez M, Liao JC, et al. Combined inactivation of the *Clostridium cellulolyticum* lactate and malate dehydrogenase genes substantially increases ethanol yield from cellulose and switchgrass fermentations. Biotechnol Biofuels. 2012;5.

143. Desvaux M. *Clostridium cellulolyticum*: Model organism of mesophilic cellulolytic clostridia. Vol. 29, FEMS Microbiology Reviews. Elsevier; 2005. p. 741–64.

144. Higashide W, Li Y, Yang Y, Liao JC. Metabolic engineering of *Clostridium cellulolyticum* for production of isobutanol from cellulose. Appl Environ Microbiol. 2011 Apr;77(8):2727–33.

145. Yee KL, Rodriguez M, Tschaplinski TJ, Engle NL, Martin MZ, Fu C, et al. Evaluation of the bioconversion of genetically modified switchgrass using simultaneous saccharification and fermentation and a consolidated bioprocessing approach. Biotechnol Biofuels. 2012;5.

146. Chung D, Cha M, Snyder EN, Elkins JG, Guss AM, Westpheling J. Cellulosic ethanol production via consolidated bioprocessing at 75 °c by engineered *Caldicellulosiruptor bescii*. Biotechnol Biofuels. 2015 Oct 6;8(1).

147. den Haan R, van Rensburg E, Rose SH, Görgens JF, van Zyl WH. Progress and challenges in the engineering of non-cellulolytic microorganisms for consolidated bioprocessing. Vol. 33, Current Opinion in Biotechnology. Elsevier Ltd; 2015. p. 32–8.

148. He MX, Wu B, Qin H, Ruan ZY, Tan FR, Wang JL, et al. *Zymomonas mobilis*: A novel platform for future biorefineries. Vol. 7, Biotechnology for Biofuels. BioMed Central Ltd.; 2014.

149. Papanek B, Biswas R, Rydzak T, Guss AM. Elimination of metabolic pathways to all traditional fermentation products increases ethanol yields in *Clostridium thermocellum*. Metab Eng. 2015 Nov 1;32:49–54.

150. Tian L, Papanek B, Olson DG, Rydzak T, Holwerda EK, Zheng T, et al. Simultaneous achievement of high ethanol yield and titer in *Clostridium thermocellum*. Biotechnol Biofuels. 2016 Jun 2;9(1).

151. Tian L, Cervenka ND, Low AM, Olson DG, Lynd LR. A mutation in the AdhE alcohol dehydrogenase of *Clostridium thermocellum* increases tolerance to several primary alcohols, including isobutanol, n-butanol and ethanol. Sci Rep. 2019 Dec 1;9(1).

152. Hon S, Holwerda EK, Worthen RS, Maloney MI, Tian L, Cui J, et al. Expressing the *Thermoanaerobacterium saccharolyticum* pforA in engineered *Clostridium thermocellum* improves ethanol production. Biotechnol Biofuels. 2018 Sep 6;11(1).

153. Holwerda EK, Olson DG, Ruppertsberger NM, Stevenson DM, Murphy SJL, Maloney MI, et al. Metabolic and evolutionary responses of *Clostridium thermocellum* to genetic interventions aimed at improving ethanol production. Biotechnol Biofuels. 2020 Mar 10;13(1).

154. Yoav S, Barak Y, Shamshoum M, Borovok I, Lamed R, Dassa B, et al. How does cellulosome composition influence deconstruction of lignocellulosic substrates in *Clostridium (Ruminiclostridium) thermocellum* DSM 1313? Biotechnol Biofuels. 2017 Sep 18;10(1).

155. Olson DG, McBride JE, Joe Shaw A, Lynd LR. Recent progress in consolidated bioprocessing. Vol. 23, Current Opinion in Biotechnology. 2012. p. 396–405.

156. Xu Q, Resch MG, Podkaminer K, Yang S, Baker JO, Donohoe BS, et al. Cell Biology: Dramatic performance of *Clostridium thermocellum* explained by its wide range of cellulase modalities. Sci Adv. 2016 Feb 1;2(2).

157. Hirano K, Kurosaki M, Nihei S, Hasegawa H, Shinoda S, Haruki M, et al. Enzymatic diversity of the *Clostridium thermocellum* cellulosome is crucial for the degradation of crystalline cellulose and plant biomass. Sci Rep. 2016 Oct 19;6.

158. Izquierdo JA, Pattathil S, Guseva A, Hahn MG, Lynd LR. Comparative analysis of the ability of *Clostridium clariflavum* strains and *Clostridium thermocellum* to utilize hemicellulose and unpretreated plant material. Biotechnol Biofuels. 2014;7(1).

159. Xiong W, Reyes LH, Michener WE, Maness PC, Chou KJ. Engineering cellulolytic bacterium *Clostridium thermocellum* to co-ferment cellulose- and hemicellulose-derived sugars simultaneously. Biotechnol Bioeng. 2018 Jul 1;115(7):1755–63.

160. Tafur Rangel AE, Croft T, González Barrios AF, Reyes LH, Maness PC, Chou KJ. Transcriptomic analysis of a *Clostridium thermocellum* strain engineered to utilize xylose: responses to xylose versus cellobiose feeding. Sci Rep. 2020 Dec 1;10(1).

161. Levin DB, Verbeke TJ, Munir R, Islam R, Ramachandran U, Lal S, et al. Omics Approaches for Designing Biofuel Producing Cocultures for Enhanced Microbial Conversion of Lignocellulosic Substrates. In: Direct Microbial Conversion of Biomass to Advanced Biofuels. Elsevier; 2015. p. 335–63.

162. Verbeke TJ, Zhang X, Henrissat B, Spicer V, Rydzak T, Krokhin O V., et al. Genomic Evaluation of *Thermoanaerobacter* spp. for the Construction of Designer Co-Cultures to Improve Lignocellulosic Biofuel Production. PLoS One. 2013 Mar 26;8(3).

163. Ng TK, Ben-Bassat A, Zeikus JG. Ethanol Production by Thermophilic Bacteria: Fermentation of Cellulosic Substrates by Cocultures of *Clostridium thermocellum* and *Clostridium thermohydrosulfuricum*. APPLIED AND ENVIRONMENTAL MICROBIOLOGY. 1981.

164. Saddler JN, Chan MKH. Conversion of pretreated lignocellulosic substrates to ethanol by *Clostridium thermocellum* in mono-and co-culture with *Clostridium thermosaccharolyticum* and *Clostridium thermohydrosulphuricum*. Can J Microbiol. 1984;30:212–20.

165. He Q, Hemme CL, Jiang H, He Z, Zhou J. Mechanisms of enhanced cellulosic bioethanol fermentation by co-cultivation of *Clostridium* and *Thermoanaerobacter spp.* Bioresour Technol. 2011 Oct;102(20):9586–92.

166. Andersen RL, Jensen KM, Mikkelsen MJ. Continuous ethanol fermentation of pretreated lignocellulosic biomasses, waste biomasses, molasses and syrup using the anaerobic, thermophilic bacterium *Thermoanaerobacter italicus* pentocrobe 411. PLoS One. 2015 Aug 21;10(8).

167. Liu Y, Yu P, Song X, Qu Y. Hydrogen production from cellulose by co-culture of *Clostridium thermocellum* JN4 and *Thermoanaerobacterium thermosaccharolyticum* GD17. Int J Hydrogen Energy. 2008 Jun;33(12):2927–33.

168. Jiang HL, He Q, He Z, Hemme CL, Wu L, Zhou J. Continuous cellulosic bioethanol fermentation by cyclic fed-batch cocultivation. Appl Environ Microbiol. 2013 Mar;79(5):1580–9.

169. Pang J, Hao M, Li Y, Liu J, Lan H, Zhang Y, et al. Ethanol from corn straw. Vol. 13, BioResources. 2018.

170. Wang F, Wang M, Zhao Q, Niu K, Liu S, He D, et al. Exploring the Relationship Between *Clostridium thermocellum* JN4 and *Thermoanaerobacterium thermosaccharolyticum* GD17. Front Microbiol. 2019 Sep 10;10.

171. Verbeke TJ, Giannone RJ, Klingeman DM, Engle NL, Rydzak T, Guss AM, et al. Pentose sugars inhibit metabolism and increase expression of an AgrD-type cyclic pentapeptide in *Clostridium thermocellum*. Sci Rep. 2017 Feb 23;7.

172. Froese AG, Sparling R. Cross-feeding and wheat straw extractives enhance growth of *Clostridium thermocellum*-containing co-cultures for consolidated bioprocessing. Bioprocess Biosyst Eng. 2021 Apr 1;44(4):819–30.

173. Froese A, Schellenberg J, Sparling R. Enhanced depolymerization and utilization of raw lignocellulosic material by co-cultures of *ruminiclostridium thermocellum* with hemicellulose-utilizing partners. Can J Microbiol. 2019;65(4):296–307.

174. Berglin EJ, Enderlin CW, Schmidt AJ. Review and Assessment of Commercial Vendors/Options for Feeding and Pumping Biomass Slurries for Hydrothermal Liquefaction. 2012. Available from: https://www.osti.gov/biblio/1056168

175. Roche CM, Dibble CJ, Knutsen JS, Stickel JJ, Liberatore MW. Particle concentration and yield stress of biomass slurries during enzymatic hydrolysis at high-solids loadings. Biotechnol Bioeng. 2009 Oct 1;104(2):290–300.

176. Viamajala S, McMillan JD, Schell DJ, Elander RT. Rheology of corn stover slurries at high solids concentrations - Effects of saccharification and particle size. Bioresour Technol. 2009 Jan;100(2):925–34.

177. Dibble CJ, Shatova TA, Jorgenson JL, Stickel JJ. Particle morphology characterization and manipulation in biomass slurries and the effect on rheological properties and enzymatic conversion. Biotechnol Prog. 2011 Nov;27(6):1751–9.

178. Gu H, An R, Bao J. Pretreatment refining leads to constant particle size distribution of lignocellulose biomass in enzymatic hydrolysis. Chemical Engineering Journal. 2018 Nov 15;352:198–205.

179. Shiva, Climent Barba F, Rodríguez-Jasso RM, Sukumaran RK, Ruiz HA. High-solids loading processing for an integrated lignocellulosic biorefinery: Effects of transport phenomena and rheology – A review. Vol. 351, Bioresource Technology. Elsevier Ltd; 2022.

180. Brown D, Shi J, Li Y. Comparison of solid-state to liquid anaerobic digestion of lignocellulosic feedstocks for biogas production. Bioresour Technol. 2012 Nov;124:379–86.

181. Guendouz J, Buffière P, Cacho J, Carrère M, Delgenes JP. Dry anaerobic digestion in batch mode: Design and operation of a laboratory-scale, completely mixed reactor. Waste Management. 2010;30(10):1768–71.

182. Thomas L, Larroche C, Pandey A. Current developments in solid-state fermentation. Vol. 81, Biochemical Engineering Journal. 2013. p. 146–61.

183. Farinas CS. Developments in solid-state fermentation for the production of biomass-degrading enzymes for the bioenergy sector. Vol. 52, Renewable and Sustainable Energy Reviews. Elsevier Ltd; 2015. p. 179–88.

184. Hodge DB, Karim MN, Schell DJ, McMillan JD. Soluble and insoluble solids contributions to high-solids enzymatic hydrolysis of lignocellulose. Bioresour Technol. 2008 Dec;99(18):8940–8.

185. Weiss ND, Felby C, Thygesen LG. Enzymatic hydrolysis is limited by biomass-water interactions at high-solids: Improved performance through substrate modifications. Biotechnol Biofuels. 2019 Jan 4;12(1).

186. Mohagheghi A, Tucker M, Grohmann K, Wyman C. High Solids Simultaneous Saccharification and Fermentation of Pretreated Wheat Straw to Ethanol. Vol. 67, Applied Biochemistry and Biotechnology. 1992.

187. Andrić P, Meyer AS, Jensen PA, Dam-Johansen K. Reactor design for minimizing product inhibition during enzymatic lignocellulose hydrolysis: I. Significance and mechanism of cellobiose and glucose inhibition on cellulolytic enzymes. Vol. 28, Biotechnology Advances. 2010. p. 308–24.

188. Berlin A, Balakshin M, Gilkes N, Kadla J, Maximenko V, Kubo S, et al. Inhibition of cellulase, xylanase and β-glucosidase activities by softwood lignin preparations. J Biotechnol. 2006 Sep;125(2):198–209.

189. Liang X, Whitham JM, Holwerda EK, Shao X, Tian L, Wu YW, et al. Development and characterization of stable anaerobic thermophilic methanogenic microbiomes fermenting switchgrass at decreasing residence times. Biotechnol Biofuels. 2018 Sep 6;11(1).

190. Chirania P, Holwerda EK, Giannone RJ, Liang X, Poudel S, Ellis JC, et al. Metaproteomics reveals enzymatic strategies deployed by anaerobic microbiomes to maintain lignocellulose deconstruction at high solids. Nat Commun. 2022 Dec 1;13(1).

191. Wu G, Healy MG, Zhan X. Effect of the solid content on anaerobic digestion of meat and bone meal. Bioresour Technol. 2009 Oct;100(19):4326–31.

192. Wang Z, Jiang Y, Wang S, Zhang Y, Hu Y, Hu Z hu, et al. Impact of total solids content on anaerobic co-digestion of pig manure and food waste: Insights into shifting of the methanogenic pathway. Waste Management. 2020 Aug 1;114:96–106.

193. Forster-Carneiro T, Pérez M, Romero LI. Influence of total solid and inoculum contents on performance of anaerobic reactors treating food waste. Bioresour Technol. 2008 Oct;99(15):6994–7002.

194. Fernández J, Pérez M, Romero LI. Effect of substrate concentration on dry mesophilic anaerobic digestion of organic fraction of municipal solid waste (OFMSW). Bioresour Technol. 2008 Sep;99(14):6075–80.

195. Chen X, Yan W, Sheng K, Sanati M. Comparison of high-solids to liquid anaerobic co-digestion of food waste and green waste. Bioresour Technol. 2014;154:215–21.

196. Abbassi-Guendouz A, Brockmann D, Trably E, Dumas C, Delgenès JP, Steyer JP, et al. Total solids content drives high solid anaerobic digestion via mass transfer limitation. Bioresour Technol. 2012 May;111:55–61.

197. Holwerda EK, Thorne PG, Olson DG, Amador-Noguez D, Engle NL, Tschaplinski TJ, et al. The exometabolome of *Clostridium thermocellum* reveals overflow metabolism at high cellulose loading. Biotechnol Biofuels. 2014;7(1).

198. Thompson RA, Trinh CT. Overflow Metabolism and Growth Cessation in *Clostridium thermocellum* DSM1313 During High Cellulose Loading Fermentations. Biotechnol Bioeng. 2017;114:2592–604.

199. Argyros DA, Tripathi SA, Barrett TF, Rogers SR, Feinberg LF, Olson DG, et al. High ethanol Titers from cellulose by using metabolically engineered thermophilic, anaerobic microbes. Appl Environ Microbiol. 2011 Dec;77(23):8288–94.

200. Karim K, Hoffmann R, Klasson KT, Al-Dahhan MH. Anaerobic digestion of animal waste: Effect of mode of mixing. Water Res. 2005;39(15):3597–606.

201. Karim K, Klasson KT, Hoffmann R, Drescher SR, DePaoli DW, Al-Dahhan MH. Anaerobic digestion of animal waste: Effect of mixing. Bioresour Technol. 2005 Sep;96(14):1607–12.

202. Zhang X, Qin W, Paice MG, Saddler JN. High consistency enzymatic hydrolysis of hardwood substrates. Bioresour Technol. 2009 Dec;100(23):5890–7.

203. Zhang J, Chu D, Huang J, Yu Z, Dai G, Bao J. Simultaneous saccharification and ethanol fermentation at high corn stover solids loading in a helical stirring bioreactor. Biotechnol Bioeng. 2010 Mar 1;105(4):718–28.

204. Dasari RK, Dunaway K, Berson RE. A scraped surface bioreactor for enzymatic saccharification of pretreated corn stover slurries. Energy and Fuels. 2009 Jan 22;23(1):492–7.

205. Fan Z, South C, Lyford K, Munsie J, Van Walsum P, Lynd LR. Conversion of paper sludge to ethanol in a semicontinuous solids-fed reactor. Bioprocess Biosyst Eng. 2003 Dec;26(2):93–101.

206. Fan Z, Lynd LR. Conversion of paper sludge to ethanol. I: Impact of feeding frequency and mixing energy characterization. Bioprocess Biosyst Eng. 2007 Jan;30(1):27–34.

207. Hou W, Zhang L, Zhang J, Bao J. Rheology evolution and CFD modeling of lignocellulose biomass during extremely high solids content pretreatment. Biochem Eng J. 2016 Jan 15;105:412–9.

208. Knutsen JS, Liberatore MW. Rheology of high-solids biomass slurries for biorefinery applications. J Rheol (N Y N Y). 2009 Jul;53(4):877–92.

209. Ghosh S, Holwerda EK, Worthen RS, Lynd LR, Epps BP. Rheological properties of corn stover slurries during fermentation by *Clostridium thermocellum*. Biotechnol Biofuels. 2018 Sep 8;11(1).

210. Zhang Q, Wu D, Lin Y, Wang X, Kong H, Tanaka S. Substrate and product inhibition on yeast performance in ethanol fermentation. Energy and Fuels. 2015 Feb 19;29(2):1019–27.

211. Phuttaro C, Sawatdeenarunat C, Surendra KC, Boonsawang P, Chaiprapat S, Khanal SK. Anaerobic digestion of hydrothermally-pretreated lignocellulosic biomass: Influence of pretreatment temperatures, inhibitors and soluble organics on methane yield. Bioresour Technol. 2019 Jul 1;284:128–38.

212. Veluchamy C, Gilroyed BH, Kalamdhad AS. Process performance and biogas production optimizing of mesophilic plug flow anaerobic digestion of corn silage. Fuel. 2019 Oct 1;253:1097–103.

213. Zou X, Wang Y, Dai Y, Zhou S, Wang B, Li Y, et al. Batch and semi–continuous experiments examining the sludge mesophilic anaerobic digestive performance with different varieties of rice straw. Bioresour Technol. 2022 Feb 1;346.

214. Li Y, Zhang R, He Y, Zhang C, Liu X, Chen C, et al. Anaerobic co-digestion of chicken manure and corn stover in batch and continuously stirred tank reactor (CSTR). Bioresour Technol. 2014;156:342–7.

215. Rivard CJ, Himmel ME, Vinzant TB, Adney WS, Wyman CE, Grohmann K. Development of a Novel Laboratory Scale High Solids Reactor for Anaerobic Digestion of Processed Municipal Solid Wastes for the Production of Methane. Vol. 461, Applied Biochemistry and Biotechnology. 1989.

216. South CR, Lynd LR. Analysis of Conversion of Particulate Biomass to Ethanol in Continuous Solids Retaining and Cascade Bioreactors. Vol. 467, Applled Biochemistry and Blotechnology. 1994.

217. South CR, Hogsett DA, Lynd LR. Continuous Fermentation of Cellulosic Biomass to Ethanol. 1993.

218. Modenbach AA, Nokes SE. The use of high-solids loadings in biomass pretreatment-a review. Vol. 109, Biotechnology and Bioengineering. 2012. p. 1430–42.

219. Pino MS, Rodríguez-Jasso RM, Michelin M, Flores-Gallegos AC, Morales-Rodriguez R, Teixeira JA, et al. Bioreactor design for enzymatic hydrolysis of biomass under the biorefinery concept. Vol. 347, Chemical Engineering Journal. Elsevier B.V.; 2018. p. 119–36.

220. Moynihan G. Development of a Laboratory Scale System for Semi-continuous, Aseptic, and High Solids Fermentation of Lignocellulosic Substrates. Dartmouth College; 2021.

221. Ulrich GD, Vasudevan PT. Chemical engineering process design and economics : a practical guide. Process Pub., Durham, N.H.; 2004.

222. Christensen P, Larry Dysert CR, Jennifer Bates C, Dorothy Burton Robert C Creese CJ, CCE John Hollmann PK, CCE Kenneth Humphreys PK, et al. 18R-97: Cost Estimate Classification System - As Applied in Engineering, Procurement, and Construction for the Process Industries. 2005.

223. Mcaloon A, Taylor F, Yee W, Ibsen K, Wooley R. Determining the Cost of Producing Ethanol from Corn Starch and Lignocellulosic Feedstocks. Golden, CO; 2000 Oct. Available from: https://www.osti.gov/biblio/766198

224. Wooley R, Ruth M, Sheehan J, Ibsen K, Majdeski H, Galvez A. Lignocellulosic Biomass to Ethanol Process Design and Economics Utilizing Co-Current Dilute Acid Prehydrolysis and Enzymatic Hydrolysis Current and Futuristic Scenarios. Golden, CO; 1999 Jul. Available from: https://www.osti.gov/biblio/12150

225. Schell DJ, Torget R, Power A, Walter PJ, Grohmann K, Hinman ND. A Technical and Economic Analysis of Acid-Catalyzed Steam Explosion and Dilute Sulfuric Acid Pretreatments Using Wheat Straw or Aspen Wood Chips. Vol. 28, Applied Biochernistry and Biot echnology. 1991.

226. Seabra JEA, Tao L, Chum HL, Macedo IC. A techno-economic evaluation of the effects of centralized cellulosic ethanol and co-products refinery options with sugarcane mill clustering. Biomass Bioenergy. 2010 Aug;34(8):1065–78.

227. Huang HJ, Ramaswamy S, Al-Dajani W, Tschirner U, Cairncross RA. Effect of biomass species and plant size on cellulosic ethanol: A comparative process and economic analysis. Biomass Bioenergy. 2009 Feb;33(2):234–46.

228. Tao L, Schell D, Davis R, Tan E, Elander R, Bratis A. NREL 2012 Achievement of Ethanol Cost Targets: Biochemical Ethanol Fermentation via Dilute-Acid Pretreatment and Enzymatic Hydrolysis of Corn Stover. 2012.

229. Wang M, Elgowainy A, Lee U, Bafana A, Banerjee S, Benavides PT, et al. Summary of Expansions and Updates in GREET ® 2021 Energy Systems Division. 2021.

230. Davis R, Tao L, Tan ECD, Biddy MJ, Beckham GT, Scarlata C, et al. Process Design and Economics for the Conversion of Lignocellulosic Biomass to Hydrocarbons: Dilute-Acid and Enzymatic Deconstruction of Biomass to Sugars and Biological Conversion of Sugars to Hydrocarbons. 2013.

231. Chen X, Shekiro J, Pschorn T, Sabourin M, Tucker MP, Tao L. Techno-economic analysis of the deacetylation and disk refining process: Characterizing the effect of refining energy and enzyme usage on minimum sugar selling price and minimum ethanol selling price. Biotechnol Biofuels. 2015 Oct 29;8(1).

232. Davis R, Bartling A. Biochemical Conversion of Lignocellulosic Biomass to Hydrocarbon Fuels and Products: 2021 State of Technology and Future Research. 2022.

233. Wang M, Huo H, Arora S. Methods of dealing with co-products of biofuels in life-cycle analysis and consequent results within the U.S. context. Energy Policy. 2011 Oct;39(10):5726–36.

234. Laser M, Jin H, Jayawardhana K, Dale BE, Lynd LR. Projected mature technology scenarios for conversion of cellulosic biomass to ethanol with coproduction thermochemical fuels, power, and/or animal feed protein. Biofuels, Bioproducts and Biorefining. 2009;3(2):231–46.

235. Shad ZM, Venkitasamy C, Wen Z. Corn distillers dried grains with solubles: Production, properties, and potential uses. Vol. 98, Cereal Chemistry. John Wiley and Sons Inc; 2021. p. 999–1019.

236. Yang M, Baral NR, Anastasopoulou A, Breunig HM, Scown CD. Cost and Life-Cycle Greenhouse Gas Implications of Integrating Biogas Upgrading and Carbon Capture Technologies in Cellulosic Biorefineries. Environ Sci Technol. 2020 Oct 20;54(20):12810–9.

237. Biddy MJ, Davis R, Humbird D, Tao L, Dowe N, Guarnieri MT, et al. The Techno-Economic Basis for Coproduct Manufacturing to Enable Hydrocarbon Fuel Production from Lignocellulosic Biomass. ACS Sustain Chem Eng. 2016 Jun 6;4(6):3196–211.

238. Lopez-Hidalgo AM, Magaña G, Rodriguez F, De Leon-Rodriguez A, Sanchez A. Co-production of ethanol-hydrogen by genetically engineered Escherichia coli in sustainable biorefineries for lignocellulosic ethanol production. Chemical Engineering Journal. 2021 Feb 15;406.

239. Byun J, Han J. Economic feasible strategy of cellulosic biofuels: Co-production of pentanediols. Energy. 2020 Feb 15;193.

240. Huang K, Won W, Barnett KJ, Brentzel ZJ, Alonso DM, Huber GW, et al. Improving economics of lignocellulosic biofuels: An integrated strategy for coproducing 1,5-pentanediol and ethanol. Appl Energy. 2018 Mar 1;213:585–94.

241. Choe B, Lee S, Lee H, Lee J, Lim H, Won W. Integrated strategy for coproducing bioethanol and adipic acid from lignocellulosic biomass. J Clean Prod. 2021 Aug 15;311.

242. Zhao X, Liu D. Multi-products co-production improves the economic feasibility of cellulosic ethanol: A case of Formiline pretreatment-based biorefining. Appl Energy. 2019 Sep 15;250:229–44.

243. Ntimbani RN, Farzad S, Görgens JF. Techno-economic assessment of one-stage furfural and cellulosic ethanol co-production from sugarcane bagasse and harvest residues feedstock mixture. Ind Crops Prod. 2021 Apr 1;162.

244. Raj K, Krishnan C. Improved co-production of ethanol and xylitol from low-temperature aqueous ammonia pretreated sugarcane bagasse using two-stage high solids enzymatic hydrolysis and Candida tropicalis. Renew Energy. 2020 Jun 1;153:392–403.

245. Kammes KL, Bals BD, Dale BE, Allen MS. Grass leaf protein, a coproduct of cellulosic ethanol production, as a source of protein for livestock. Anim Feed Sci Technol. 2011 Feb 28;164(1–2):79–88.

246. Rosales-Calderon O, Arantes V. A review on commercial-scale high-value products that can be produced alongside cellulosic ethanol. Vol. 12, Biotechnology for Biofuels. BioMed Central Ltd.; 2019.

247. Laser M, Jin H, Jayawardhana K, Lynd LR. Coproduction of ethanol and power from switchgrass. Biofuels, Bioproducts and Biorefining. 2009;3(2):195–218.

248. Pourhashem G, Adler PR, McAloon AJ, Spatari S. Cost and greenhouse gas emission tradeoffs of alternative uses of lignin for second generation ethanol. Environmental Research Letters. 2013;8(2).

249. Adler PR, Mitchell JG, Pourhashem G, Spatari S, Grosso SJ Del, Parton WJ. Integrating biorefinery and farm biogeochemical cycles offsets fossil energy and mitigates soil carbon losses. Vol. 25, Ecological Applications. 2015.

250. U.S. Energy Information Agency. Annual Energy Outlook 2022 (AEO2022). 2022. Available from: https://www.eia.gov/outlooks/aeo/

251. Finley RJ. An Overview of the Illinois Basin - Decatur Project. Greenhouse Gases: Science and Technology. 2014;2(5):571–9.

252. Beck L. The US Section 45Q Tax Credit for Carbon Oxide Sequestration: An Update Global CCS Institute. 2020.

253. U.S. Internal Revenue Code. Title 26 U.S. Code § section 45Q: Credit for carbon oxide sequestration. 2022. Available from: https://uscode.house.gov/view.xhtml?req=(title:26%20section:45Q%20edition:prelim)

254. Beck L. Carbon capture and storage in the USA: The role of US innovation leadership in climate-technology commercialization. Vol. 4, Clean Energy. Oxford University Press; 2020. p. 2–11.

255. Electronic Code of Federal Regulations. Title 40 CFR Part 80 Subpart M. 2023. Available from: https://www.ecfr.gov/current/title-40/chapter-I/subchapter-C/part-80/subpart-M

256. U.S. Environmental Protection Agency. Renewable Fuel Standard Program. 2023. Available from: https://www.epa.gov/renewable-fuel-standard-program

257. U.S. Environmental Protection Agency. RIN Trades and Price Information. 2019. Available from: https://www.epa.gov/fuels-registration-reporting-and-compliance-help/rin-trades-and-price-information

258. Townsend A, Havercroft I. THE LCFS AND CCS PROTOCOL: AN OVERVIEW FOR POLICYMAKERS AND PROJECT DEVELOPERS. 2019. Available from: https://www.globalccsinstitute.com/resources/publications-reports-research/the-lcfs-and-ccs-protocol-an-overview-for-policymakers-and-project-developers/

259. Baker SE, Stolaroff JK, Peridas G, Pang SH, Goldstein HM, Lucci FR, et al. Getting to Neutral Options for Negative Carbon Emissions in California. Livermore, CA; 2020. Available from: https://www.osti.gov/biblio/1597217

260. Sanchez DL, Fingerman K, Herbert C, Uden S. Policy Options for Deep Decarbonization and Wood Utilization in California's Low Carbon Fuel Standard. Frontiers in Climate. 2021 May 14;3.

261. Kim S, Zhang X, Reddy AD, Dale BE, Thelen KD, Jones CD, et al. Carbon-Negative Biofuel Production. Environ Sci Technol. 2020 Sep 1;54(17):10797–807.

262. Gelfand I, Hamilton SK, Kravchenko AN, Jackson RD, Thelen KD, Robertson GP. Empirical Evidence for the Potential Climate Benefits of Decarbonizing Light Vehicle Transport in the U.S. With Bioenergy from Purpose-Grown Biomass with and without BECCS. Environ Sci Technol. 2020 Mar 3;54(5):2961–74.

263. Geissler CH, Maravelias CT. Economic, energetic, and environmental analysis of lignocellulosic biorefineries with carbon capture. Appl Energy. 2021 Nov 15;302.

264. Psarras PC, Comello S, Bains P, Charoensawadpong P, Reichelstein S, Wilcox J. Carbon Capture and Utilization in the Industrial Sector. Environ Sci Technol. 2017 Oct 3;51(19):11440–9.

265. House KZ, Baclig AC, Ranjan M, Van Nierop EA, Wilcox J, Herzog HJ. Economic and energetic analysis of capturing CO_2 from ambient air. 2011;

266. Leeson D, Mac Dowell N, Shah N, Petit C, Fennell PS. A Techno-economic analysis and systematic review of carbon capture and storage (CCS) applied to the iron and steel, cement, oil refining and pulp and paper industries, as well as other high purity sources. International Journal of Greenhouse Gas Control. 2017;61:71–84.

267. Herron S, Zoelle A, Summers WM. Cost of Capturing CO_2 from Industrial Sources. Pittsburgh, PA; 2014. Available from: https://www.osti.gov/biblio/1480985

268. Muratori M, Kheshgi H, Mignone B, Clarke L, McJeon H, Edmonds J. Carbon capture and storage across fuels and sectors in energy system transformation pathways. International Journal of Greenhouse Gas Control. 2017 Feb 1;57:34–41.

269. Sanchez DL, Johnson N, McCoy ST, Turner PA, Mach KJ. Near-term deployment of carbon capture and sequestration from biorefineries in the United States. Proc Natl Acad Sci U S A. 2018 May 8;115(19):4875–80.

270. Jaffe AM, Dominguez-Faus R, Parker NC, Scheitrum D, Wilcock J, Miller M. The Feasibility of Renewable Natural Gas as a Large-Scale, Low Carbon Substitute. 2016.

271. Parker N, Williams R, Dominguez-Faus R, Scheitrum D. Renewable natural gas in California: An assessment of the technical and economic potential. Energy Policy. 2017 Dec 1;111:235–45.

272. Baena-Moreno FM, le Saché E, Pastor-Pérez L, Reina TR. Membrane-based technologies for biogas upgrading: a review. Vol. 18, Environmental Chemistry Letters. Springer; 2020. p. 1649–58.

273. Abatzoglou N, Boivin S. A review of biogas purification processes. Vol. 3, Biofuels, Bioproducts and Biorefining. 2009. p. 42–71.

274. Walsh JL, Ross CC, Smith MS, Harper SR. Utilization of Biogas. Vol. 20, Biomass. 1989.

275. Kang JY, Kang DW, Kim TS, Hur KB. Comparative economic analysis of gas turbine-based power generation and combined heat and power systems using biogas fuel. Energy. 2014 Apr 1;67:309–18.

276. Kang DW, Kim TS, Hur KB, Park JK. The effect of firing biogas on the performance and operating characteristics of simple and recuperative cycle gas turbine combined heat and power systems. Appl Energy. 2012;93:215–28.

277. Budzianowski WM, Wylock CE, Marciniak PA. Power requirements of biogas upgrading by water scrubbing and biomethane compression: Comparative analysis of various plant configurations. Energy Convers Manag. 2017;141:2–19.

278. Psarras PC, Comello S, Bains P, Charoensawadpong P, Reichelstein S, Wilcox J. Carbon Capture and Utilization in the Industrial Sector. Environ Sci Technol. 2017 Oct 3;51(19):11440–9.

279. Collet P, Flottes E, Favre A, Raynal L, Pierre H, Capela S, et al. Techno-economic and Life Cycle Assessment of methane production via biogas upgrading and power to gas technology. Appl Energy. 2017;192:282–95.

280. Gutiérrez-Martín F, Rodríguez-Antón LM, Legrand M. Renewable power-to-gas by direct catalytic methanation of biogas. Renew Energy. 2020 Dec 1;162:948–59.

281. Zhang X, Witte J, Schildhauer T, Bauer C. Life cycle assessment of power-to-gas with biogas as the carbon source. Sustain Energy Fuels. 2020 Mar 1;4(3):1427–36.

282. Bedoić R, Dorotić H, Schneider DR, Čuček L, Ćosić B, Pukšec T, et al. Synergy between feedstock gate fee and power-to-gas: An energy and economic analysis of renewable methane production in a biogas plant. Renew Energy. 2021 Aug 1;173:12–23.

283. Khan MI. Identifying and addressing barriers for the sustainable development of natural gas as automotive fuel. Int J Hydrogen Energy. 2017 Oct 5;42(40):25453–73.

284. Hao H, Liu Z, Zhao F, Li W. Natural gas as vehicle fuel in China: A review. Vol. 62, Renewable and Sustainable Energy Reviews. Elsevier Ltd; 2016. p. 521–33.

285. Ammenberg C, Gustafsson J, O'shea M, Gray R, Lyng N, Eklund KA, et al. Perspectives on biomethane as a transport fuel within a circular economy, energy, and environmental system. Vol. 37, IEA Bioenergy Task. 2021. 12 p.

286. Hittinger E, Whitacre JF, Apt J. Compensating for wind variability using co-located natural gas generation and energy storage. Energy Systems. 2010 Dec;1(4):417–39.

287. Wu T, Bu S, Wei X, Wang G, Zhou B. Multitasking multi-objective operation optimization of integrated energy system considering biogas-solar-wind renewables. Energy Convers Manag. 2021 Feb 1;229.

288. Khan MI, Yasmeen T, Khan MI, Farooq M, Wakeel M. Research progress in the development of natural gas as fuel for road vehicles: A bibliographic review (1991-2016). Vol. 66, Renewable and Sustainable Energy Reviews. Elsevier Ltd; 2016. p. 702–41.

289. Li Y, Xue J, Peppers J, Kado NY, Vogel CFA, Alaimo CP, et al. Chemical and toxicological properties of emissions from a light-duty compressed natural gas vehicle fueled with renewable natural gas. Environ Sci Technol. 2021 Mar 2;55(5):2820–30.

290. He X, Wallington TJ, Anderson JE, Keoleian GA, Shen W, De Kleine R, et al. Life-Cycle Greenhouse Gas Emission Benefits of Natural Gas Vehicles. ACS Sustain Chem Eng. 2021 Jun 14;9(23):7813–23.

291. Byun J, Han J. Green Methane as a Future Fuel for Light-Duty Vehicles. Fermentation. 2022 Dec 1;8(12).

292. Dyr T, Misiurski P, Ziółkowska K. Costs and benefits of using buses fuelled by natural gas in public transport. J Clean Prod. 2019 Jul 10;225:1134–46.

293. Kapoor R, Ghosh P, Kumar M, Vijay VK. Evaluation of biogas upgrading technologies and future perspectives: a review. Environmental Science and Pollution Research. Springer Verlag; 2019.

294. Angelidaki I, Treu L, Tsapekos P, Luo G, Campanaro S, Wenzel H, et al. Biogas upgrading and utilization: Current status and perspectives. Vol. 36, Biotechnology Advances. Elsevier Inc.; 2018. p. 452–66.

295. Khan MU, Lee JTE, Bashir MA, Dissanayake PD, Ok YS, Tong YW, et al. Current status of biogas upgrading for direct biomethane use: A review. Vol. 149, Renewable and Sustainable Energy Reviews. Elsevier Ltd; 2021.

296. Aghel B, Behaein S, Wongwises S, Shadloo MS. A review of recent progress in biogas upgrading: With emphasis on carbon capture. Vol. 160, Biomass and Bioenergy. Elsevier Ltd; 2022.

297. R. C. Assunção L, A. S. Mendes P, Matos S, Borschiver S. Technology roadmap of renewable natural gas: Identifying trends for research and development to improve biogas upgrading technology management. Appl Energy. 2021 Jun 15;292.

298. Scholz M, Melin T, Wessling M. Transforming biogas into biomethane using membrane technology. Vol. 17, Renewable and Sustainable Energy Reviews. 2013. p. 199–212.

299. Chen XY, Vinh-Thang H, Ramirez AA, Rodrigue D, Kaliaguine S. Membrane gas separation technologies for biogas upgrading. Vol. 5, RSC Advances. Royal Society of Chemistry; 2015. p. 24399–448.

300. Nguyen LN, Kumar J, Vu MT, Mohammed JAH, Pathak N, Commault AS, et al. Biomethane production from anaerobic co-digestion at wastewater treatment plants: A critical review on

development and innovations in biogas upgrading techniques. Vol. 765, Science of the Total Environment. Elsevier B.V.; 2021.

301. Gkotsis P, Kougias P, Mitrakas M, Zouboulis A. Biogas upgrading technologies – Recent advances in membrane-based processes. International Journal of Hydrogen Energy. Elsevier Ltd; 2022.

302. Zhang YHP, Lynd LR. Cellulose utilization by Clostridium thermocellum: Bioenergetics and hydrolysis product assimilation. Proceedings of the National Academy of Sciences. 2005;102(20):7321–5. Available from: www.pnas.orgcgidoi10.1073pnas.0408734102

303. Shi J, Ebrik MA, Yang B, Garlock RJ, Balan V, Dale BE, et al. Application of cellulase and hemicellulase to pure xylan, pure cellulose, and switchgrass solids from leading pretreatments. Bioresour Technol. 2011 Dec;102(24):11080–8.

304. Gu J, Catchmark JM. The impact of cellulose structure on binding interactions with hemicellulose and pectin. Cellulose. 2013 Aug;20(4):1613–27.

305. Köhnke T, Östlund Å, Brelid H. Adsorption of arabinoxylan on cellulosic surfaces: Influence of degree of substitution and substitution pattern on adsorption characteristics. Biomacromolecules. 2011 Jul 11;12(7):2633–41.

306. Wang X, Li K, Yang M, Zhang J. Hydrolyzability of xylan after adsorption on cellulose: Exploration of xylan limitation on enzymatic hydrolysis of cellulose. Carbohydr Polym. 2016 Sep 5;148:362–70.

307. Sluiter A, Hames B, Ruiz R, Scarlata C, Sluiter J, Templeton D, et al. Determination of Structural Carbohydrates and Lignin in Biomass: Laboratory Analytical Procedure (LAP) (Revised July 2011). 2008.

308. Holwerda EK, Hirst KD, Lynd LR. A defined growth medium with very low background carbon for culturing Clostridium thermocellum. J Ind Microbiol Biotechnol. 2012 Jun;39(6):943–7.

309. Olson DG, Lynd LR. Transformation of clostridium thermocellum by electroporation. In: Methods in Enzymology. Academic Press Inc.; 2012. p. 317–30.

310. Kubis MR, Holwerda EK, Lynd LR. Declining carbohydrate solubilization with increasing solids loading during fermentation of cellulosic feedstocks by Clostridium thermocellum: documentation and diagnostic tests. Biotechnology for Biofuels and Bioproducts. 2022 Dec 1;15(1).

311. Zhao L, Ou X, Chang S. Life-cycle greenhouse gas emission and energy use of bioethanol produced from corn stover in China: Current perspectives and future prospectives. Energy. 2016 Nov 15;115:303–13.

312. Qin Z, Canter CE, Dunn JB, Mueller S, Kwon H, Han J, et al. Land management change greatly impacts biofuels' greenhouse gas emissions. GCB Bioenergy. 2018 Jun 1;10(6):370–81.

313. Salles-Filho SLM, Castro PFD de, Bin A, Edquist C, Ferro AFP, Corder S. Perspectives for the Brazilian bioethanol sector: The innovation driver. Energy Policy. 2017;108:70–7.

314. Salles-Filho SLM, Cortez LAB, Silveria JMFJ, Trindade SC, Fonseca MGD (Eds.). Global Bioethanol: Evolution, Risks, and Uncertainties. London, UK: Academic Press; 2016.

315. Lam CH, Das S, Erickson NC, Hyzer CD, Garedew M, Anderson JE, et al. Towards sustainable hydrocarbon fuels with biomass fast pyrolysis oil and electrocatalytic upgrading. Sustain Energy Fuels. 2017;1(2):258–66.

316. Das S, Anderson JE, De Kleine R, Wallington TJ, Jackson JE, Saffron CM. Technoeconomic analysis of corn stover conversion by decentralized pyrolysis and electrocatalysis. Sustain Energy Fuels. 2022 May 6;6(11):2823–34.

317. Yun S, Oh SY, Kim JK. Techno-economic assessment of absorption-based CO_2 capture process based on novel solvent for coal-fired power plant. Appl Energy. 2020 Jun 15;268.

318. James R, Zoelle A, Keairns D, Turner M, Woods M, Kuehn N. Cost and Performance Baseline for Fossil Energy Plants Volume 1: Bituminous Coal and Natural Gas to Electricity. 2019.

319. Xu Y, Isom L, Hanna MA. Adding value to carbon dioxide from ethanol fermentations. Vol. 101, Bioresource Technology. 2010. p. 3311–9.

320. Deng L, Hägg MB. Techno-economic evaluation of biogas upgrading process using CO_2 facilitated transport membrane. International Journal of Greenhouse Gas Control. 2010;4(4):638–46.

321. Lan W, Chen G, Zhu X, Wang X, Liu C, Xu B. Biomass gasification-gas turbine combustion for power generation system model based on ASPEN PLUS. Science of the Total Environment. 2018 Jul 1;628–629:1278–86.

322. Sgouridis S, Carbajales-Dale M, Csala D, Chiesa M, Bardi U. Comparative net energy analysis of renewable electricity and carbon capture and storage. Nat Energy. 2019 Jun 1;4(6):456–65.

323. Xu H, Lee U, Wang M. Life-cycle greenhouse gas emissions reduction potential for corn ethanol refining in the USA. Biofuels, Bioproducts and Biorefining. 2022 May 1;16(3):671–81.

324. Laude A, Ricci O, Bureau G, Royer-Adnot J, Fabbri A. CO_2 capture and storage from a bioethanol plant: Carbon and energy footprint and economic assessment. International Journal of Greenhouse Gas Control. 2011;5(5):1220–31.

325. Lee U, R Hawkins T, Yoo E, Wang M, Huang Z, Tao L. Using waste CO_2 from corn ethanol biorefineries for additional ethanol production: life-cycle analysis. Biofuels, Bioproducts and Biorefining. 2021 Mar 1;15(2):468–80.

326. Liu Z, Karimi IA. Simulating combined cycle gas turbine power plants in Aspen HYSYS. Energy Convers Manag. 2018 Sep 1;171:1213–25.

327. Niu M, Xie J, Liang S, Liu L, Wang L, Peng Y. Simulation of a new biomass integrated gasification combined cycle (BIGCC) power generation system using Aspen Plus: Performance analysis and energetic assessment. Int J Hydrogen Energy. 2021 Jun 23;46(43):22356–67.

328. Bhattacharyya D, Turton R, Zitney SE. Steady-state simulation and optimization of an integrated gasification combined cycle power plant with CO_2 capture. Ind Eng Chem Res. 2011 Feb 2;50(3):1674–90.

329. Kim J, Johnson TA, Miller JE, Stechel EB, Maravelias CT. Fuel production from CO_2 using solar-thermal energy: System level analysis. Energy Environ Sci. 2012 Sep;5(9):8417–29.

330. Lin Y, Sadekuzzaman Roni M, Thompson DN, Hartley DS, Griffel M, Cai H. Herbaceous Feedstock 2020 State of Technology Report. Idaho Falls, ID; 2020. Available from: https://www.osti.gov/biblio/1785122/

331. U.S. Energy Information Agency. Monthly Densified Biomass Fuel Report Form EIA-63C. 2019. Available from: https://www.eia.gov/biofuels/biomass/?year=2019&month=12#table_data

332. U.S. Energy Information Agency. Electricity Data Form EIA-923 Power Plant Operations Report. 2019. Available from: https://www.eia.gov/electricity/data/state/

333. Mccollum DL, Ogden JM. Techno-Economic Models for Carbon Dioxide Compression, Transport, and Storage & Correlations for Estimating Carbon Dioxide Density and Viscosity. Davis, CA; 2006. Available from: https://escholarship.org/uc/item/1zg00532

334. Bock B, Rhudy R, Herzog H, Klett M, Davison J, De La Torre Ugarte DG. Economic Evaluation of CO_2 Storage and Sink Enhancement Options. 2003. Available from: https://www.osti.gov/biblio/826435

335. Metz B, Davidson O, Connick H, Loos M, Meyer L. CARBON DIOXIDE CAPTURE AND STORAGE. New York, NY; 2005. Available from: https://www.ipcc.ch/report/carbon-dioxide-capture-and-storage/

336. Geissler CH, Maravelias CT. Economic, energetic, and environmental analysis of lignocellulosic biorefineries with carbon capture. Appl Energy. 2021 Nov 15;302.

337. Sendich E (Newton), Laser M, Kim S, Alizadeh H, Laureano-Perez L, Dale B, et al. Recent process improvements for the ammonia fiber expansion (AFEX) process and resulting reductions in minimum ethanol selling price. Bioresour Technol. 2008 Nov;99(17):8429–35.

338. Bals B, Rogers C, Jin M, Balan V, Dale B. Evaluation of ammonia fibre expansion (AFEX) pretreatment for enzymatic hydrolysis of switchgrass harvested in different seasons and locations. Biotechnol Biofuels. 2010 Dec 4;3(1):1.

339. Meyer PA, Tews IJ, Magnuson JK, Karagiosis SA, Jones SB. Techno-economic analysis of corn stover fungal fermentation to ethanol. Appl Energy. 2013;111:657–68.

340. Tao L, Templeton DW, Humbird D, Aden A. Effect of corn stover compositional variability on minimum ethanol selling price (MESP). Bioresour Technol. 2013;140:426–30.

341. Yang M, Rosentrater KA. Techno-economic analysis (TEA) of low-moisture anhydrous ammonia (LMAA) pretreatment method for corn stover. Ind Crops Prod. 2015 Dec 5;76:55–61.

342. Zhao L, Zhang X, Xu J, Ou X, Chang S, Wu M. Techno-economic analysis of bioethanol production from lignocellulosic biomass in china: Dilute-acid pretreatment and enzymatic hydrolysis of corn stover. Energies (Basel). 2015;8(5):4096–117.

343. Stoklosa RJ, del Pilar Orjuela A, da Costa Sousa L, Uppugundla N, Williams DL, Dale BE, et al. Techno-economic comparison of centralized versus decentralized biorefineries for two alkaline pretreatment processes. Bioresour Technol. 2017 Feb 1;226:9–17.

344. Shen R, Tao L, Yang B. Techno-economic analysis of jet-fuel production from biorefinery waste lignin. Biofuels, Bioproducts and Biorefining. 2019 May 1;13(3):486–501.